

NASA Contractor Report 168218

LOW-COST SINGLE-CRYSTAL TURBINE BLADES  
VOLUME 1



T. E. Strangman, B. Heath, and M. Fujii  
Garrett Turbine Engine Company  
Phoenix, Arizona 85010

(NASA-CR-168218) LOW-COST SINGLE-CRYSTAL  
TURBINE BLADES, VOLUME 1 Final Report  
(Garrett Turbine Engine Co.) 218 P  
HC A10/MF A01

N84-15247

CSCI 11F

Unclass  
18043

G3/26

November 1983

Prepared for

NATIONAL AERONAUTICS AND SPACE ADMINISTRATION

Lewis Research Center

Under Contract NAS3-20073

## FOREWORD

This Project Completion Report was prepared for the National Aeronautics and Space Administration, Lewis Research Center. It presents the results of a program conducted to establish exothermic heated casting technology for the manufacture of low-cost, single-crystal, uncooled turbine blades for gas turbine engines. The program was conducted as part of the Materials for Advanced Turbine Engines (MATE) Program under Contract NAS3-20073.

The special contribution of C. M. Phipps, the director of development casting activity at Jet-shapes, Inc. (a Division of Duradyne Technologies), is hereby acknowledged. Mr. Phipps directed the actual foundry activity, provided knowledge and expertise in developing this advanced casting process, and contributed to the description of the foundry practices in this report. The authors also wish to acknowledge the contribution of G. S. Hoppin III, who originated this project at GTEC and directed its initial phase.

## TABLE OF CONTENTS

	<u>Page</u>
SECTION I	
1.0 SUMMARY	1
SECTION II	
2.0 INTRODUCTION	7
SECTION III	
3.0 SINGLE-CRYSTAL CASTING TECHNOLOGY DEVELOPMENT	11
3.1 Mold System Modifications	12
3.1.1 Crystal Selector Evaluation	12
3.1.2 Wax Assembly Configuration	17
3.1.3 Ceramic Shell Mold Manufacture	17
3.2 Exothermic Heating Improvements	19
3.3 Casting Parameters Optimization	23
3.4 Post-Casting Treatment	25
SECTION IV	
4.0 SC MAR-M 247 PROPERTY EVALUATION	27
4.1 Tensile Tests	29
4.2 Stress-Rupture Tests	33
SECTION V	
5.0 SC ALLOY DEVELOPMENT	39
5.1 "Paper Alloy" Study	40
5.2 Microstructural Stability Study	42
5.2.1 Alloy 1	45
5.2.2 Alloy 2	48
5.2.3 Alloy 3	48
5.2.4 Alloy 4	48
5.2.5 Alloy 5	55

PRECEDING PAGE BLANK NOT FILMED

## TABLE OF CONTENTS (Contd)

	<u>Page</u>
5.3 SC Derivatives of Mar-M 247	55
5.3.1 Master Alloys	55
5.3.2 SC Casting Campaign-	55
5.3.3 Heat Treatment Study	59
5.3.4 Property Characterization	66
5.3.5 Tensile Tests	66
5.3.6 Stress-Rupture Tests	68
5.3.7 Oxidation Evaluation	80
5.3.8 Density	80
5.3.9 Improper Processing	81
5.3.10 SC Alloy Selection	84
SECTION VI	
6.0 ALLOY PROPERTY CHARACTERIZATION	87
6.1 Test Material Production	87
6.1.1 Master Alloys	87
6.1.2 Blade and Specimen Castings	87
6.2 Mechanical Properties	95
6.2.1 Tensile Properties	95
6.2.2 Creep-Rupture	102
6.2.3 Low-Cycle Fatigue	116
6.2.4 High-Cycle Fatigue	125
6.3 Environmental Tests	138
6.4 Physical Properties	144
6.4.1 Thermal Expansion	144
6.4.2 Thermal Conductivity	145
6.4.3 Elastic Modulus	145
SECTION VII	
7.0 BLADE DESIGN	151
7.1 Scope	151
7.2 Preliminary Blade Design	151
7.3 Final Blade Design	152

## TABLE OF CONTENTS (Contd)

	<u>Page</u>
7.3.1 Mechanical Design	152
7.3.1.1 Blade Life Analysis	162
7.3.1.2 Blade Vibration Analysis	167
7.3.2 Aerodynamic Design	170
7.3.3 Design Modifications	170
SECTION VIII	
8.0 COMPONENT MANUFACTURE	173
8.1 Tooling	173
8.2 Casting Campaign	173
8.3 Casting Inspection and Testing	176
8.4 Blade Machining	177
SECTION IX	
9.0 COMPONENT TESTING	179
9.1 Holographic Testing	179
9.2 Firtree Testing	182
9.3 Rig Testing	183
9.4 Post-Test Inspection	188
SECTION X	
10.0 COST ANALYSIS	195
SECTION XI	
11.0 CONCLUSIONS	199
APPENDIX A	202
APPENDIX B	203
APPENDIX C	205
REFERENCES	215

ORIGINAL PAGE IS  
OF POOR QUALITY

## SECTION I

### 1.0 SUMMARY

The demand for more efficient and economical engines continues to push the industry toward higher turbine operating temperatures. The ability to keep up with this trend is strongly tied to advancements in material technology. Single-crystal (SC) castings offer many significant advantages over turbine materials currently used in production engines, such as higher melting point and higher strength. The goals of MATE Project 3 were to develop a low-cost casting process capable of producing SC turbine blades and to demonstrate the capability of the SC blades through extensive property, rig, and engine testing.

The casting process chosen for development was a low-cost, nonproprietary modification of the exothermic directionally solidified (DS) casting process. The similarities between the DS and SC processes are shown in Figure 1. Both processes use exothermic

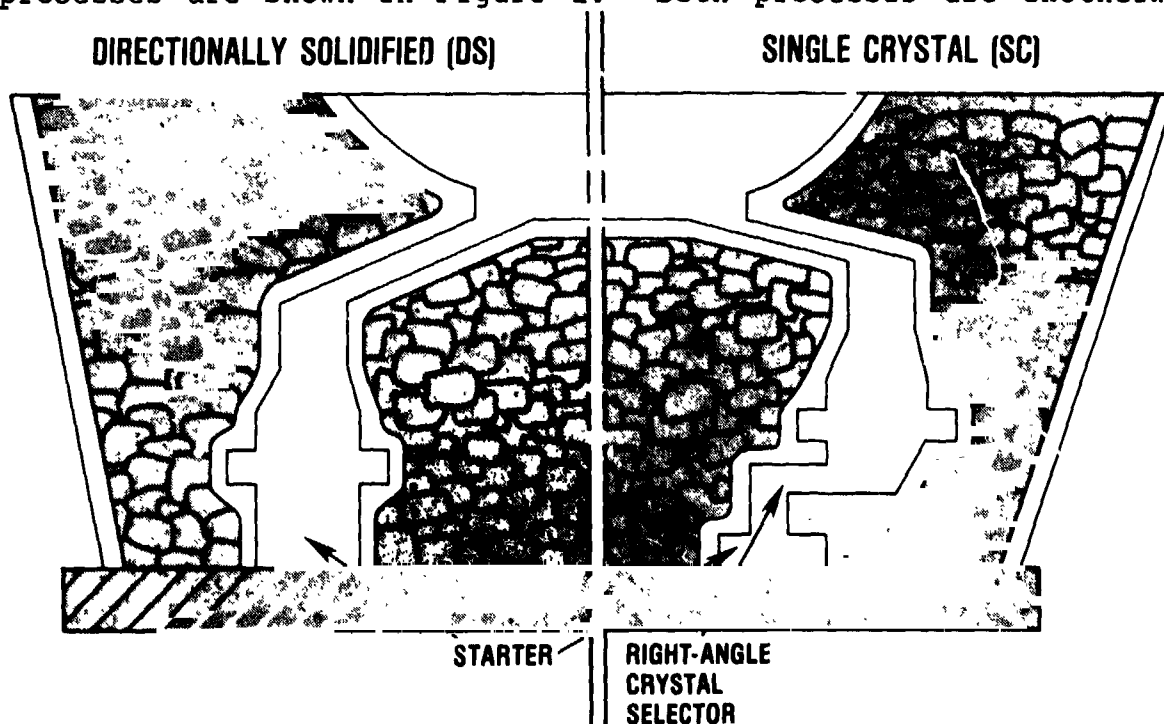


Figure 1. Exothermic Casting Process.

aluminum/iron oxide nuggets to preheat the ceramic mold above the melting point of the alloy, and both use a water-cooled copper chill plate to directionally extract heat from the mold. The major difference between the DS and SC processes is that the SC process uses a geometric crystal selector to "select" one of the DS grains from the starter and then permit this one properly oriented grain to enter and fill the blade cavity. This produces a casting without grain boundaries.

The initial work focused on characterizing the mechanical properties of SC Mar-M 247, using SC castings produced with the Project 1 final design blade mold as a source for test bars. Testing indicated that properly [001] oriented SC Mar-M 247 did not have significantly better stress-rupture properties than DS Mar-M 247. Therefore, to fully exploit the benefits of single-crystal castings, a new series of alloys specifically designed for single-crystal applications was investigated.

Since there are no grain boundaries in a "true" SC casting, the grain boundary strengthening elements such as B, Zr, and Hf can be eliminated. The benefits produced by these changes are twofold. First, by eliminating these elements, which are strong melting point depressants, the incipient melting point of the alloy is significantly increased. Second, this higher melting point allows the alloy to be heat-treated at a higher temperature where all the eutectic gamma prime can be taken into solution and subsequently reprecipitated as fine gamma prime. This significantly increases the stress-rupture strength of the alloy.

Eight single-crystal alloy modifications of Mar-M 247 were studied analytically, and five of these alloys were evaluated experimentally through a series of casting trials and screening tests. Ultimately, two of these alloys were chosen for full

property characterization: NASAIR 100 and SC Alloy 3. Figure 2 indicates the relative strengths of these two alloys.

Using the material property data generated on SC NASAIR 100 and SC Alloy 3, the final blade configuration was designed. This blade (shown in Figure 3) is essentially the same as the Project 1 final design, with the addition of a tip "winglet" and an aft platform flow discourager. Analysis of this design indicated that the single-crystal blade has significantly greater LCF and tensile strength than the DS Mar-M 247 blade and more than twice the stress-rupture life.

Vibrational response of the final blade design was evaluated on 12 single-crystal blades using holographic techniques. Results of this testing indicated that the SC blade responded in a similar fashion to the Project 1 DS blade, but at a slightly lower frequency due to the increased mass at the tip of the SC blade. Since the response of the SC blade was so similar to that of the DS blade, stress coat evaluation of the SC blades was not required.

Two complete sets of single-crystal blades were cast and machined to the final blade configuration for component and engine testing. Twelve of these blades were instrumented with dynamic strain gauges and assembled into a complete rotor for component testing (Figure 4) in the high-pressure rotor rig (HRR).

This rig allows strain-gauge monitoring of turbine components operating in an engine environment. The rig test was completed as scheduled, but during the routine post-test inspection, four Alloy 3 blades were discovered to have cracks across the leading edge at about 66-percent span. No other problems were found. Detailed examination of the cracked blades revealed previously undetected high-angle, extraneous grains in the airfoil at the crack location. It was determined that the cracks followed these extremely



ORIGINAL FILED  
OF POOR QUALITY

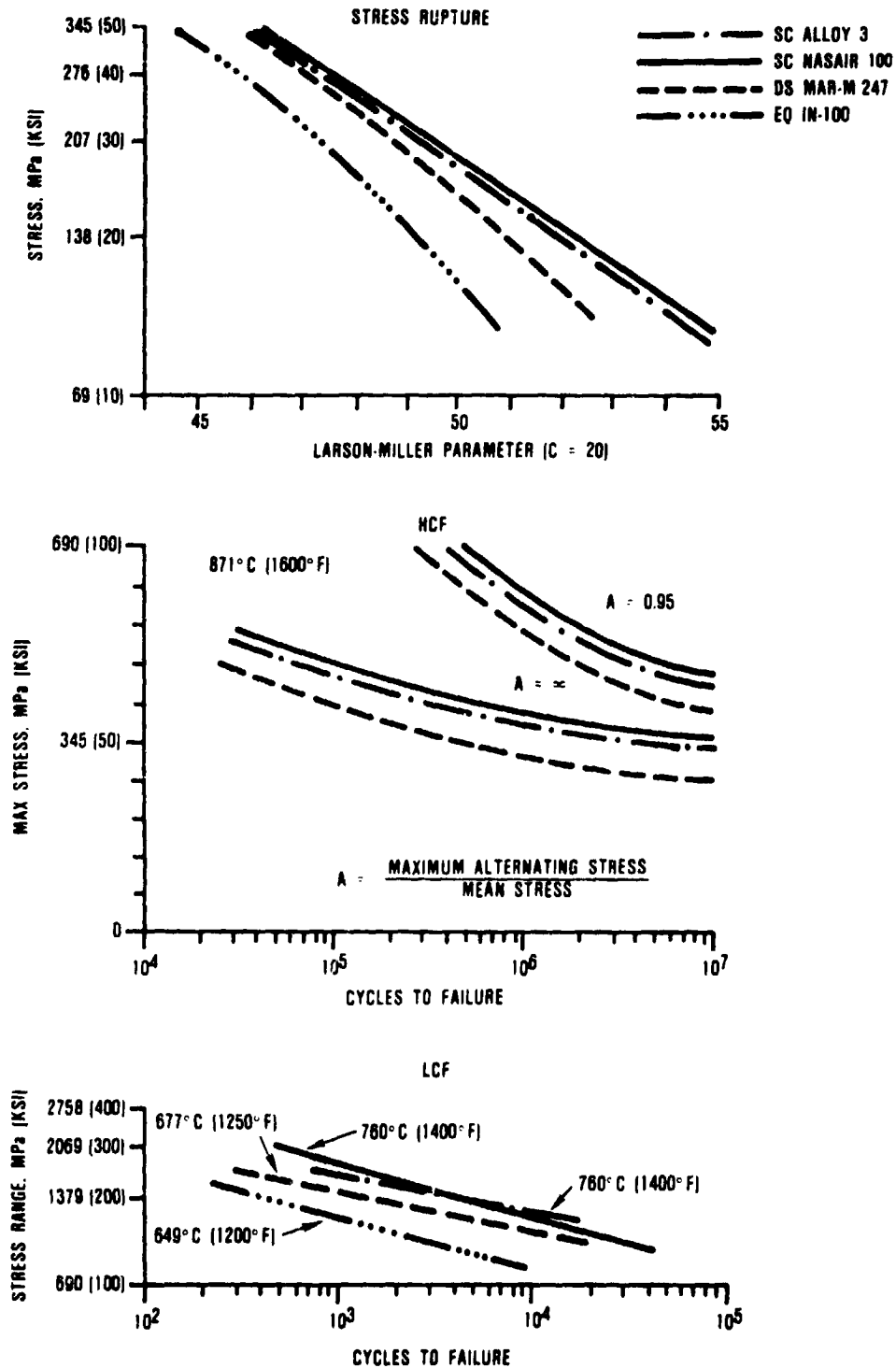


Figure 2. SC NASAIR 100 and SC Alloy 3  
Turbine Blade Alloy Properties.

ORIGINAL PAGE IS  
OF POOR QUALITY



Figure 3. MATE Project 3 SC Blade, Final Configuration.

weak grain boundaries, and they had occurred early in the test. No signs of fatigue were noted in any of the cracked blades. The remaining blades were carefully reinspected for extraneous grains, and several more were found, some of which had run in the HRR test. All of these blades were eliminated from further testing. After reinspection was completed, full-scale engine testing was initiated as scheduled. Details of engine testing are presented in Volume 2 of this report.

6

## SECTION II

### 2.0 INTRODUCTION

The NASA Materials for Advanced Turbine Engines (MATE) Program is a cooperative effort with industry to accelerate introduction of new materials into aircraft turbine engines. As part of this effort, Garrett Turbine Engine Company (GTEC) was authorized under NASA Contract NAS3-20073 to develop a new technique for manufacturing low-cost, single-crystal (SC), uncooled cast turbine blades to reduce SC casting costs and improve fuel consumption in advanced turbofan engines. The process development included those efforts required to transfer the technology from the previously demonstrated feasibility stage through component demonstration and engine test. Portions of the overall effort included process scale-up, alloy evaluations, mechanical property generation, hardware procurement, component testing, and full-scale engine testing to evaluate potential benefits.

This report constitutes Volume 1 of a two-volume Project Completion Report presenting the results of the investigations and tests performed under MATE Project 3, Low-Cost Single-Crystal Turbine Blades. This volume covers all of Project 3 except the full-scale engine testing and post-test analysis. These are the subjects of Volume 2 of this report.

The intent of Project 3 was to develop a low-cost process to produce single-crystal, uncooled turbine blades and to design and substitute this blade for the solid, directionally solidified (DS) turbine blade used in the high-pressure turbine of the GTEC TFE731 turbofan engine.

Project goals associated with this program included the following:

- o Development of a nonproprietary, low-cost SC casting process
- o Improvement of the stress-rupture capability of the SC alloys relative to DS Mar-M 247
- o Design of an uncooled HP turbine blade to use the SC material
- o Demonstration of uncooled SC turbine blades through component and engine testing.

Project 3 was subdivided into the following seven tasks:

- Task I - Casting Technology
- Task II - Alloy/Process Selection
- Task III - Property Characterization
- Task IV - Blade Design
- Task V - Component Manufacture and Testing
- Task VI - Engine Test
- Task VII - Post-Test Analysis

In Task I, the exothermic casting process was modified to consistently produce acceptable solid SC high-pressure turbine blades for the TFE731 turbofan engine. This effort focused on the castability and baseline mechanical properties of blades produced with Mar-M 247.

During Task II, SC alloy derivatives of the Mar-M 247 alloy were assessed for castability, microstructure, and improvements in mechanical properties. Two of these SC compositions, NASAIR 100 and Alloy 3, were selected for detailed characterization.

In Task III, mechanical, environmental, and physical properties of SC NASAIR 100 and Alloy 3 were quantified. Mechanical property testing included creep rupture, tensile, and high- and low-cycle fatigue, and the determination of the effects of protective coatings. Environmental characterization included coated and uncoated oxidation and hot-corrosion tests. Physical properties measured included density, elastic modulus, thermal expansion, and thermal conductivity.

The SC HPT blade was designed in Task IV to utilize the improved mechanical properties of the SC alloys (NASAIR 100 and Alloy 3).

During Task V, two full sets of SC turbine blades and the required support hardware for both rig testing and the Task VI engine testing were manufactured. Rig and bench testing were also completed in Task V.

The engine testing, test results, and post-test evaluation are described in Volume 2 of this report.

SECTION III

3.0. SINGLE-CRYSTAL CASTING TECHNOLOGY DEVELOPMENT

A primary program objective was to further develop the non-proprietary, low-cost exothermic casting process to produce uncooled single-crystal (SC) high-pressure TFE731 turbine blades of Mar-M 247 and higher strength derivative alloys. This process was selected based on success achieved in Garrett's NASA-MATE Project 1, "Low-Cost Directionally Solidified (DS) Turbine Blades,"<sup>1</sup> and work performed by Jetshapes, Inc. (Rockleigh, New Jersey). This success verified the feasibility of adapting the exothermic process to produce SC turbine components.

As illustrated schematically in Figure 5, the DS and SC exothermic processes are conceptually very similar. The casting pro-

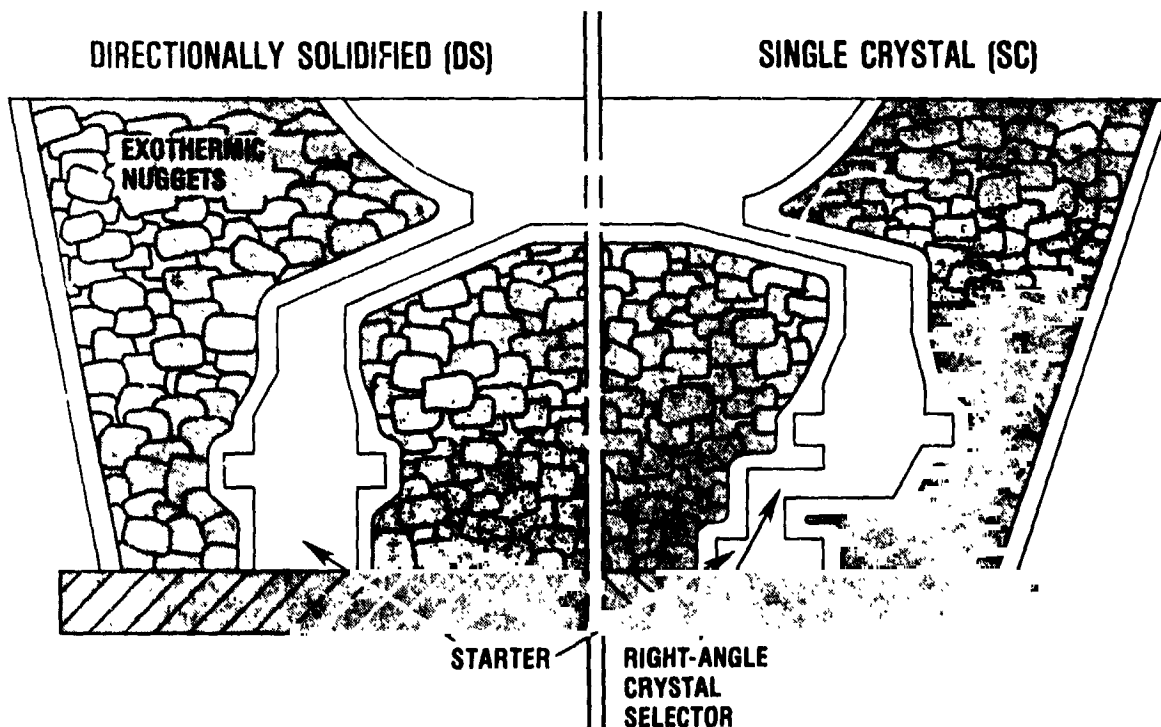


Figure 5. Exothermic Casting Process.

cess derives its name from the use of heat released during the exothermic reaction between aluminum and iron oxide finely dispersed in briquets or nuggets. This heat is used to preheat the ceramic investment casting shell mold to a temperature above the melting point of the alloy. After preheating, the mold is placed on a water-cooled copper chill to establish unidirectional heat extraction conditions. Then, the alloy is cast into the mold and directionally solidified. Figure 5 also shows that the principal modification of the process is the inclusion of a geometric crystal selector in the ceramic shell mold at a position between the starter block and the blade cavity. The crystal selector is designed to permit only one properly oriented grain to enter the blade cavity.

Although the selector geometry was an important consideration, process development included additional aspects:

- o Mold system modifications
- o Exothermic heating improvements
- o Casting parameter optimization.

### 3.1. Mold System Modifications

Development of the mold system included these areas:

- o Crystal selector evaluation
- o Wax assembly configuration
- o Ceramic shell mold manufacture.

Each aspect of tailoring the investment casting shell mold for SC castings is reviewed in the following paragraphs.

#### 3.1.1 Crystal Selector Evaluation

Based on experience, trials were run with both helical crystal selectors and selectors using several ramped right-angle turns to



ORIGINAL PAGE IS  
OF POOR QUALITY

choke off excess grains. Jetshapes worked with different helix diameters and lengths, different DS starter chamber heights, and different blade orientations to feed metal and crystal entry. The right-angle starters used one DS originating chamber, feeding grain into from one to four mold cavities. The geometries of some of the evaluated crystal selectors are shown in Figure 6.

The starter block adjacent to the chill is a 25.4 mm (1 inch) high cube. In this starter block, the casting texture transitions from essentially random to predominantly [001] parallel to the heat flow direction. Grains permitted to enter the crystal selector are taken from the central region of the selector, which best approximates the unidirectional heat flow requirement. Construction of

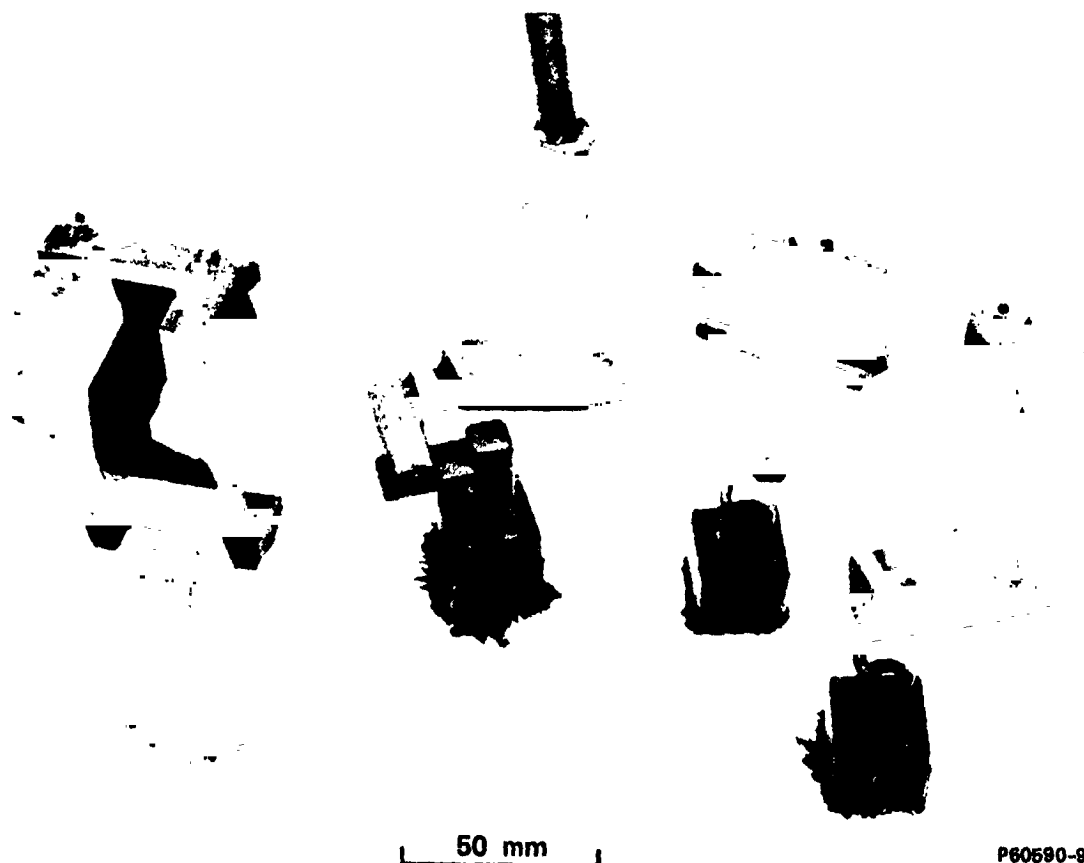


Figure 6. Single-Crystal TFE731 Turbine Blades Cast with Right-Angle Crystal Selectors (Left) and Helix Crystal Selectors (Right), One-half Size.

the starter block is consistent with observations by Gell, et al.<sup>2</sup> that grains with a  $\langle 111 \rangle$  orientation are quickly overgrown by grains with  $\langle 001 \rangle$  and  $\langle 011 \rangle$  orientations. In that study--with a similar alloy--it was found that after 20 mm (0.787 in.) of growth, more than 90 percent of the grains had the  $[001]$  direction within 15 degrees of the starter block vertical axis.

As indicated in Figure 6, the helix selector started from the center of the starter block. In contrast, the right-angle selector had an additional 20 mm (0.787 in.) long extension from the starter block before the grains entered the crystal selector.

The function of the crystal selector is to select and permit only one properly oriented SC grain to enter the blade cavity of the mold. Grain orientation results for the first 21 molds of SC Mar-M 247 TFE731 HP turbine blades are provided in Table 1. This table shows that the right-angle selector was more effective than the helix in producing SC blades. With a right-angle selector, 86 percent of the SC blades produced had the required orientation within 12 degrees of the  $[001]$ ; with the helix selector, only 42 percent of the SC blades produced had the desired orientation. This evaluation also indicated that the best single-crystal yield was generated with the blade root toward the chill plate.

Two variations in helix selector cross-section diameters were used in this evaluation: 3.2 mm (0.126 in.) and 4.0 mm (0.157 in.). Right-angle selectors also included several variations. The principal modification was growing two blades instead of one from each selector. This approach minimized the amount of metal consumed in the selector. In addition, eight other minor variations in selector geometry were evaluated to arrive at the two-blade, right-angle starter selected for the remainder of the program (Figure 7). (Productivity was expected to be increased eventually in a production process using one starter for four blades.)

TABLE 1. CRYSTAL GROWTH ORIENTATIONS\* OF TFE731-MATE 3  
SINGLE-CRYSTAL BLADES PRODUCED IN EXPERIMENTAL  
MOLDS 1-21.

Mold No.	Crystal Selector Configuration	Blades Cast	Single-Crystal Blades*		
			Within 6° of [001]	Within 12° of [001]	Unsatisfactory Other Orientations
1	Helix	16	1	1	3
2	Helix	16	0	5	8
3	Right angle	14	4	4	0
4	Right angle	16	2	0	0
5	Right angle	15	4	0	1
6	Right angle	15	6	3	0
7	Helix	16	1	1	4
8	Helix	16	2	2	2
9	Right angle	14	2	3	3
10	Helix	14	0	0	1
11	Right angle	10	5	3	2
12	Right angle	10	4	2	3
13	Right angle	12	0	4	1
14	Right angle	12	0	11	0
15	Right angle	12	0	2	0
16	Right angle	12	0	1	0
17	Right angle	12	0	4 A+R (9 A/F)	0
18	Right angle	12	0	5 A+R (11 A/F)	1
19	Right angle	12	0	8 A+R (10 A/F)	0
20	Right angle	12	0	5 A+R (7 A/F)	1
21	Right angle	12	0	8 A+R (9 A/F)	1

NOTES: (1) Determinations on Molds 1 through 9, 11, and 12 by Laue pattern; on Molds 13 through 21 by visual review.  
(2) Molds 11 and 12 also contained two 50.8 mm (2 inch) diameter bars each.  
(3) Molds 13 through 16 also contained two 38.1 mm (1.5 inch) diameter bars.  
(4) On Molds 17 through 21, "A+R" means Airfoil plus Root and "A/F" means Airfoil only.

\*Blades not included were not single crystals.

ORIGINAL PAGE IS  
OF POOR QUALITY



P67477-4

P67477-1

Figure 7. SC Blade Cast with Right-Angle Crystal Selector.

The difference in selector effectiveness is predominantly associated with exothermic process requirements. Specifically, a selector design must allow sufficient room between the mold base and its cross members in order to achieve sufficient exothermic briquette packing for proper mold preheat. In this aspect, the helix selector design was deficient. A secondary factor potentially associated with the effectiveness of the right-angle selector was the additional 20 mm (0.787 in.) length of the starter block, which may have increased the probability that only grains with the [001] primary orientation grew into the selector.

Blades with misoriented grains were frequently associated with stray grain nucleation in the right-angle starter. To minimize this problem, sharp corners and edges were rounded in the wax pattern for the starter. Another attempt to inhibit stray grain nucleation was to increase the temperature gradient by giving cross members of the starter a slight upward angle (approximately 10 degrees) with respect to the mold base.

### 3.1.2 Wax Assembly Configuration

Initially, molds that contained between 10 and 16 blades were evaluated. The evolved wax assembly arrangement, which was selected for the remainder of the program, contained 12 blades (or test bars) arranged in a 254 mm (ten inch) diameter ring (Figure 8). Two blades were attached to each single-crystal starter, around a central pouring cup for alloy reception. Each pair of blades was connected at its tip riser with a 6.4 x 9.5 mm (0.25 x 0.375 inch) runner. A feeder from the pour cup was connected to the center of this bar between the two blades (Figure 9). Thus, superheated alloy was top fed through the blade sections, flowing down through the blade roots and crystal selector into the starter chamber. Heat is transferred from the alloy throughout this path, establishing a gradient in the alloy and superheating the inner mold walls, promoting single-crystal formation and growth.

A riser was added to feed shrinkage in the thin section of the blade root platform. Later, a riser was added to the leading edge platform as well, to increase the yield of quality parts.

### 3.1.3 Ceramic Shell Mold Manufacture

Initial casting trials were conducted with investment shells of colloidal silica-bonded zircon and alumina shell systems that are standard at Jetshapes. These shells were built up to an aver-

ORIGINAL PAGE IS  
OF POOR QUALITY

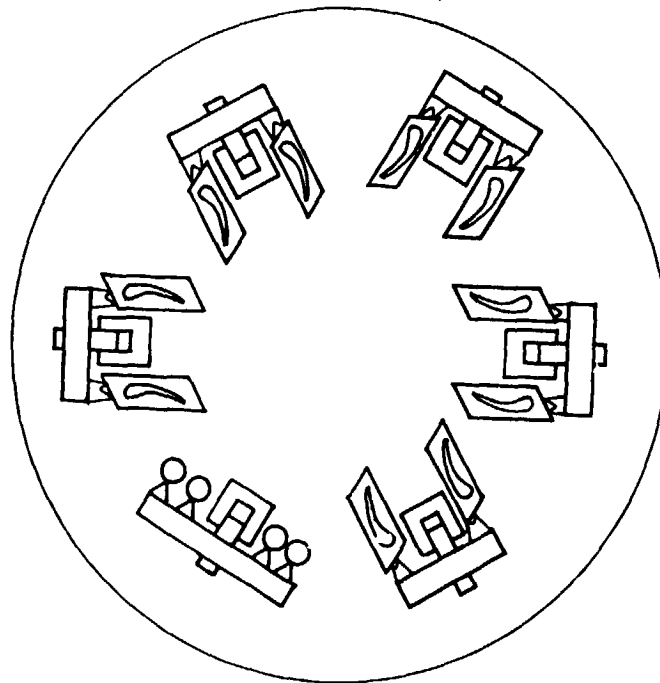
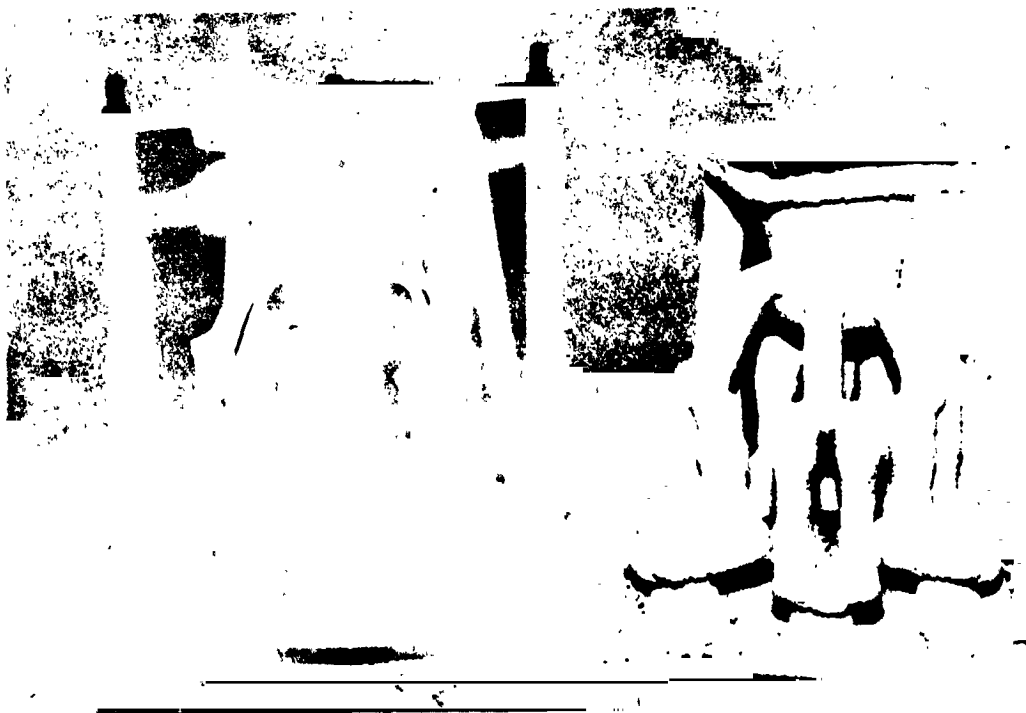


Figure 8. General Arrangement of Single-Crystal Turbine Blades and Erosion Bars within Exothermically Heated Ceramic Mold.



P67358-44

Figure 9. Wax Pattern and Ceramic Shell Mold for SC Blades.

age thickness of 6.4 to 9.5 mm (0.25 to 0.375 inch). Neither shell system showed any appreciable tendency toward excessive casting inclusions or mold deformation.

Based on the initial casting trials (which compared alumina shell results with results of a zircon shell) and exothermic process considerations, the alumina shell was selected for the mold material. The alumina shell has better fired strength, improved refractoriness, and better thermal conductivity for transfer of heat from the briquette source to the inner mold walls. The single-crystal alloy derivatives of Mar-M 247 require the lowest possible zirconium levels, which points further to the use of alumina rather than zirconium silicate to prevent mass transfer to zirconium from mold to alloy.

All molds were autoclave dewaxed, fired at 982°C (1800°F) for one hour, inspected, cleaned, and covered to prevent contamination.

### 3.2 Exothermic Heating Improvements

In preparation for casting, the fired mold was placed on a clean refractory ceramic plate in a mold handling frame. A tapered refractory fiber sleeve was placed around the mold (Figure 10). Exothermic nuggets compacted from aluminum and iron oxide powders were placed around the mold configuration to ensure heating all parts of the shell. When completely packed, the mold pour cup covering was removed, and the cup was vacuum cleaned and covered with a mullite ceramic cover. The mold was then ready for preheating.

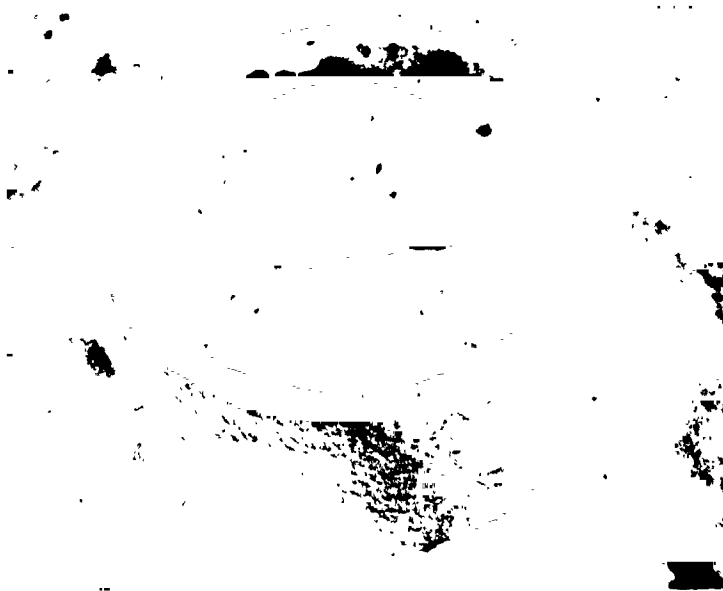
Evolution of the exothermic pack process resulted in use of a mold preheat oven for exothermic ignition and firing. Preheat temperatures between 1010° and 1093°C (1850° and 2000°F) were evaluated. Best results were obtained using an oven at 1093°C (2000°F) with an excess oxygen atmosphere. In addition to igniting the exo-

ORIGINAL PAGE IS  
OF POOR QUALITY



P67358-24

**CERAMIC SHELL AND  
MOLD INSULATION SLEEVE**



P67358-25

**MOLD PACKED WITH EXOTHERMIC  
BRIQUETS**

Figure 10. Exothermic Mold.



ORIGINAL PAGE IS  
OF POOR QUALITY

thermic reaction between the aluminum and iron oxide, preheating reduced mold stresses during the exothermic burn. Ignition and burn in the preheat oven also eliminated problems with the slight amount of smoke generated by the exothermic reaction (Figure 11). Ignition time varied from 5 to 15 minutes, depending on the condition of the nuggets. Burning was completed after another 5 to 10 minute period.

Mold temperature at the conclusion of the burn was measured to be approximately 1593°C (2900°F). At this point, the mold was transferred to the casting furnace (Figure 12).

Variations were noted using the exothermic nuggets; e.g., maximum achieved temperatures varied from 1538° to 1732°C (2800° to 3150°F). Single crystals resulted from both extremes, indicating



Figure 11. Exothermic Burn in Preheat Furnace.

ORIGINAL PAGE IS  
OF POOR QUALITY



TEMPERATURE CHECK

P67358-18



P80805

REMOVAL OF LOWER SUPPORT  
PRIOR TO PLACEMENT IN THE  
VACUUM FURNACE

Figure 12. Exothermic Mold Transfer.

an adequate heating of the mold even though the indicated temperature reading failed to positively identify the true mold temperature. Further, over a period of time using many different batches of exothermics, a zinc oxide contaminant (included in the iron ore used in exothermic preparation) was noted and continued after the supplier of the briquets changed to a different grade of ore. To avoid deleterious effect on the casting process (rapid gas evolution causing mold runout has been associated with zinc oxide deposition), the casting production phase used an oxyacetylene torching of the mold base after the exothermic burn as standard practice. This torch application eliminates the gas forming coating and reduces chances for mold runout.

Exothermic materials were purchased to a specification of  $1788^{\circ}\text{C} \pm 28^{\circ}\text{C}$  ( $3250^{\circ}\text{F} \pm 50^{\circ}\text{F}$ ) burn temperature. With either zircon or alumina shells, the molds never indicated an over-temperature condition (fusion) during the program. This indicates that for the Jetshapes mold-size sleeve-size preheat system with exothermic briquette size and packing, heat transfer to the mold is poor. Much of the heat generated is ineffective in accomplishing the purpose, and large variations between exothermic briquette and indicated temperatures are to be expected.

### 3.3 Casting Parameters Optimization

After the mold had been preheated by the exothermic reaction (burn), the mold was transferred to the chill plate of the casting unit. Alloy melting was sequenced to the burn/transfer/mold chamber pump down to be close to required temperature as the mold was raised to pouring position. Metal pouring temperatures were determined by using a two-color pyrometer. Metal was typically poured within 4 to 7 minutes after the mold was removed from the preheat furnace.

For the Mar-M 247 alloy, superheats (temperature above the freezing plateau, P) are considerably higher for directional-solidification P+236°C (P+425°F) and single-crystal castings P+278°C (P+500°F) relative to conventional equiaxed castings P+111°C (P+200°F). The optimum superheats for casting SC alloy derivatives of Mar-M 247 were still higher at P+320° to 360°C (P+575° to 650°F). High pour temperature for SC blades were used to inhibit grain nucleation on mold walls. No significant investment mold-superalloy reactions were observed as a result of the higher superheats required for SC castings.

Initial casting trials used Mar-M 247 as the alloy for experimentation. Melting was accomplished in a zirconium-oxide crucible and, as the alloy contains zirconium as an alloying element, no alloy contamination was noted. However, higher temperatures were found to be required for derivative SC alloys that had significantly reduced B, Zr, Hf, and C contents relative to the parent Mar-M 247 alloy. The higher temperature and vacuum conditions adversely affected the magnesia-stabilized zirconia crucible during melting of the derivative SC alloys. Partial decomposition of the zirconia crucible resulted in an undesirable addition (up to 0.5 percent) of zirconium to the alloy, which adversely affected heat treatability and mechanical properties (discussed in Section 5.0).

These results are consistent with the work of Barrett and Lowell that was conducted at NASA-Lewis Research Center.<sup>3</sup> Zirconium-free NiCrAl alloys were melted in zirconia crucibles and reported zirconium pickups of up to 0.6-percent weight. (Zirconium additions to their alloys were beneficial from an oxidation-resistance standpoint.)

Melting trials with both MgO and Al<sub>2</sub>O<sub>3</sub> crucibles gave acceptable results and further blade castings were made using MgO cruci-

bles, which have superior thermal shock resistance. Magnesium pickup in the SC alloys was 2 to 12 ppm, which was innocuous.

The technique for the pouring operation proved difficult for the Jetshapes furnace operator to master. A fast pour could not be accomplished due to the position of the pour cup in the center of the mold. Enlargement of the cup did not help. Finally, with a change of operators, casting of the charge within a desired time lapse (1 second) was accomplished. The more rapid pour lessened alloy heat loss and gave a more uniform filling of the mold. The more rapid filling of the mold cavity prevented differential temperatures within the mold cavity. Results were dramatic: an approximate 20-percent increase in the number of single-crystal blades generated.

#### 3.4 Post-Casting Treatment

All molds were allowed to cool overnight before shakeout. Separation of castings from mold and clinker was carefully done to avoid blade surface stresses. After knock-out, the blades were salt bath cleaned and acid etched for preliminary grain evaluation.

Blades accepted by the first inspection were solution heat treated to specification. They were then returned to Jetshapes for sand blast and grain etch and X-ray diffraction (XRD) evaluation of the crystal orientation. Acceptable blades then were processed through the usual foundry finishing operation: visual, fluorescent penetrant, and x-ray inspections.

## SECTION IV

### 4.0 SC MAR-M 247 PROPERTY EVALUATION

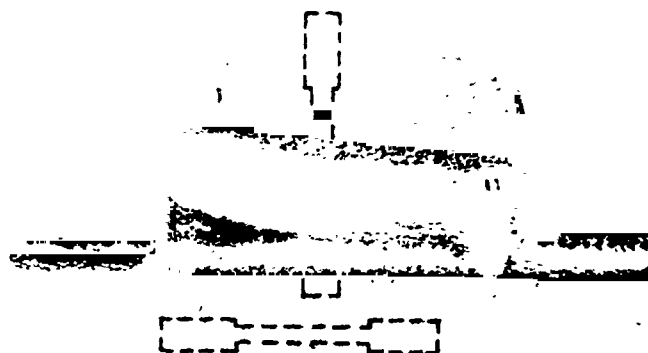
In addition to adapting the exothermic process to the manufacture of SC turbine components, the program characterized primary mechanical properties of SC Mar-M 247, providing a baseline for subsequent development of derivative alloys with improved temperature capabilities. Tensile tests were performed at room temperature and 760°C (1400°F). Stress-rupture data were obtained for SC Mar-M 247 at 760°C (1400°F), 982°C (1800°F), 1038°C (1900°F), and 1093°C (2000°F). In all cases, the test plan involved both longitudinal and transverse tests from heat-treated blades. Test specimen machining, tensile testing, and rupture testing were performed at Joliet Metallurgical Laboratories (Joliet, Illinois).

Blades were evaluated with two different solution heat treatment temperatures: 1232°C (2250°F) and 1246°C (2275°F). The first solution heat treatment was the recommended solutioning treatment for DS Mar-M 247 from Project 1.<sup>1</sup> The second (slightly higher) solution treatment was also evaluated in Project 1 and resulted in better homogenization of the matrix, slightly improved average rupture lives, and slightly increased amounts of incipient melting.

Most of the testing was performed with 1.8 mm (0.070 inch) gauge diameter minibars machined from SC blades with known orientations. Some testing was also performed with 0.51 mm (0.020 inch) thick flat specimens machined from the airfoil in order to obtain a quantitative assessment of thin-wall effects on stress-rupture properties. Machined-from-blade (MFB) specimens and their relationship to the MATE SC blade are shown in Figure 13.

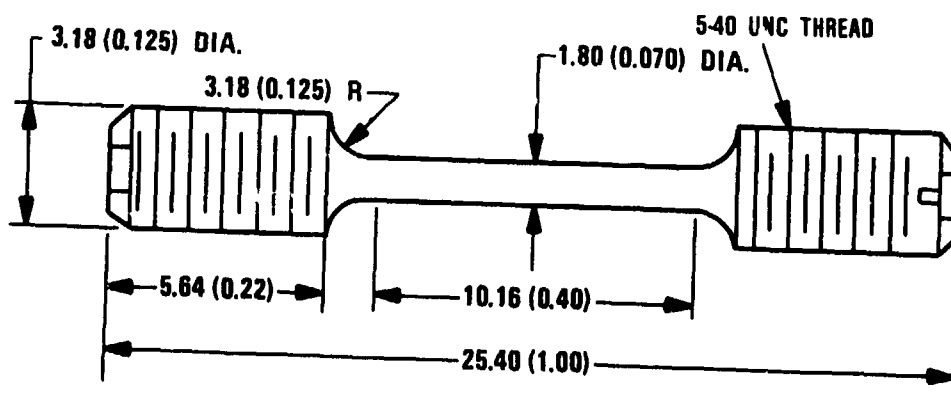
In addition to the MFB specimens, several 1.8 mm (0.070 in.) diameter minibars were also machined with a transverse orientation from small 38 mm (1.496 in.) diameter SC ingots.

ORIGINAL PAGE IS  
OF POOR QUALITY



MATE SC TURBINE BLADE

P78641



NOTE: ALL DIMENSIONS IN MM (IN.)

Figure 13. MFB Tensile and Stress-Rupture Bars.

#### 4.1 Tensile Tests

Room temperature and 760°C (1400°F) tensile test data for specimens machined from SC Mar-M 247 turbine blades are provided in Table 2 and 3. For single crystals with the [001] orientation, average tensile strengths were slightly lower and ductility was slightly higher relative to multigrained DS Mar-M 247. In contrast to stress-rupture results, 0.5 mm (0.020 inch) thick flat specimens exhibited slightly higher strengths than 1.8 mm (0.070 inch) diameter round specimens. Transverse single-crystals exhibited average tensile strengths and ductilities that were slightly higher than those of DS Mar-M 247.

Yield strength data for longitudinal MFB specimens and similar data for 6.35 mm (0.248 in.) diameter SC Mar-M 247 specimens generated by MacKay, Dreshfield, and Maier<sup>4</sup> are presented graphically in Figure 10. Substantial variation, indicated by a scatter band width of  $\pm 82.7$  MPa ( $\pm 12$  ksi), is present in these data. No obvious strength trends were present in the temperature--over the range of 23° to 760°C (73° to 1400°F)--or specimen section size. In fact, the strengths of the 0.5 mm (0.020 in.) thick flat specimens were unexpectedly higher on the average relative to the 1.8 (0.070) and 6.35 mm (0.248 in.) diameter specimens.

Inspection of Figure 14 also indicates that the yield strength is reduced by approximately 6.9 MPa (1 ksi) for each degree of deviation between the [001] crystallographic direction and the blade axis. MacKay, et al.,<sup>4</sup> indicate that this decrease is associated with the increase in the Schmid factor for the (111) [101] slip system as the specimen deviates from the [001].

Several tests were conducted at 760°C (1400°F) for orientations near the [210] and [311] specimen axes. The data in Table 3 indicates that these non-[001] orientations had significantly lower tensile strengths.



TABLE 2. ROOM-TEMPERATURE TENSILE TEST RESULTS O. TEST SPECIMENS MACHINED FROM SINGLE-CRYSTAL TURBINE BLADES OF HEAT-TREATED\* MAR-M 247.

Specimen Number	Mold No. Crystal Selector Type**	Orientation of Specimen	Specimen Type	Ultimate Tensile Strength MPa (ksi)	0.2% Yield Strength MPa (ksi)	Elongation (%)	R of A (%)
Longitudinal Orientation							
343-4	7H	4° off [001]	1.8 mm (70 mil) round	979 (142)	917 (133)	7.0	13.0
344-3	8R	6° off [001]	1.8 mm (70 mil) round	938 (136)	889 (129)	9.6	17.2
344-4	8R	5° off [001]	1.8 mm (70 mil) round	899 (129)	869 (126)	11.3	19.2
344-13	8R	8.5° off [001]	1.8 mm (70 mil) round	903 (131)	869 (126)	9.7	31.7
344-15	8R	7° off [001]	1.8 mm (70 mil) round	855 (124)	869 (126)	7.1	14.8
405-8L	18R	Visual [001]	1.8 mm (70 mil) round	924 (134)	876 (127)	13.8	19.6
405-9L	18R	Visual [001]	1.8 mm (70 mil) round	972 (141)	869 (126)	10.3	19.0
406-9L	19R	Visual [001]	1.8 mm (70 mil) round	993 (144)	869 (126)	7.7	13.9
406-11L	19R	Visual [001]	1.8 mm (70 mil) round	1014 (147)	883 (128)	9.6	13.0
343-4P	7H	4° off [001]	0.5 mm (20 mil) flat	1014 (147)	1000 (145)	4.0	---
344-3P	8R	6° off [001]	0.5 mm (20 mil) flat	938 (136)	924 (134)	16.8	---
344-4P	8R	5° off [001]	0.5 mm (20 mil) flat	993 (144)	986 (143)	12.0	---
344-9P	8R	2° off [001]	0.5 mm (20 mil) flat	1000 (145)	972 (141)	8.5	---
344-13F	8R	8.5° off [001]	0.5 mm (20 mil) flat	1055 (153)	993 (144)	6.8	---
344-15F	8R	7° off [001]	0.5 mm (20 mil) flat	972 (141)	931 (135)	27.7	---
Average 1.8 mm (70 mil) rounds				945 (137)	876 (127)	9.5	---
Average 0.5 mm (20 mil) flats				993 (144)	965 (140)	13.0	---
Average DS Blade 1.8 mm (70 mil) rounds				1062 (154)	910 (132)	5.8	---
Transverse Orientation							
397-2T	13R	Transverse	1.8 mm (70 mil) round	848 (123)	800 (116)	17.5	25.3
398-2T	14R		1.2 mm (70 mil) round	855 (124)	821 (119)	21.6	32.8
398-6T	14R		1.8 mm (70 mil) round	952 (138)	876 (127)	7.4	16.7
400-7T	15R		1.8 mm (70 mil) round	827 (120)	807 (117)	9.7	25.3
404-2T	17R		1.8 mm (70 mil) round	924 (134)	855 (124)	11.5	15.0
405-1T	18R		1.8 mm (70 mil) round	834 (121)	821 (119)	14.6	29.0
405-5T	18R		1.8 mm (70 mil) round	931 (135)	848 (123)	5.0	17.4
405-8T	18R		1.8 mm (70 mil) round	910 (132)	883 (128)	13.1	18.3
405-9T	18R		1.8 mm (70 mil) round	958 (139)	855 (124)	13.4	18.9
406-5T	19R		1.8 mm (70 mil) round	903 (131)	855 (124)	11.6	18.3
406-9T	19R		1.8 mm (70 mil) round	1014 (147)	889 (129)	6.7	14.2
406-11T	19R		1.8 mm (70 mil) round	1007 (146)	869 (126)	7.7	14.4
407-2T	20R		1.8 mm (70 mil) round	993 (144)	889 (129)	12.1	15.0
408-2T	21R		1.8 mm (70 mil) round	883 (128)	793 (115)	15.6	18.3
408-4T	21R		1.8 mm (70 mil) round	931 (135)	827 (120)	13.1	23.1
Average 1.8 mm (70 mil) round				917	(133) 848	(123)	12.0
Average DS 1.8 mm (70 mil) round				876	(127) 855	(124)	3.5

\*Heat treated at 1246°C (2275°F) for 2 hours, plus 982°C (1800°F) for 5 hours, 871°C (1600°F) for 20 hours.

\*\*R = Right-angle crystal selector; H = Helix crystal selector.

ORIGINAL PAGE IS  
OF POOR QUALITY

TABLE 3. 760°C (1400°F) TENSILE TEST RESULTS ON TEST SPECIMENS MACHINED FROM SINGLE-CRYSTAL TURBINE BLADES OF HEAT-TREATED\* MAR-M 247.

Specimen Number	Mold No. Crystal Selector Type**	Orientation of Specimen	Specimen Type	Ultimate Tensile Strength MPa (ksi)	0.2% Yield Strength MPa (ksi)	Elongation (%)	R of A (%)
Longitudinal Specimens							
322-4	5R	5° off [001]	1.8 mm (70 mil) round	1138 (165)	952 (138)	6.9	12.3
322-9	5R	5° off [001]	1.8 mm (70 mil) round	979 (142)	855 (124)	11.4	13.9
323-8	6R	2.5° off [001]	1.8 mm (70 mil) round	1083 (157)	917 (133)	3.7	10.4
343-1	7H	6° off [001]	1.8 mm (70 mil) round	1014 (147)	896 (130)	7.1	14.4
343-2	7H	12.5° off [001]	1.8 mm (70 mil) round	1062 (154)	889 (129)	9.0	15.5
344-8	8R	9.5° off [001]	1.8 mm (70 mil) round	938 (136)	931 (135)	3.6	9.7
406-8L		Visual [001]	1.8 mm (70 mil) round	1041 (151)	1000 (145)	6.0	13.7
343-3	7H	10° off [210]	1.8 mm (70 mil) round	745 (108)	717 (104)	9.4	15.0
343-9	7H	8° off [311]	1.8 mm (70 mil) round	814 (118)	814 (118)	9.5	17.6
344-2	8R	8° off [210]	1.8 mm (70 mil) round	821 (119)	772 (112)	19.9	30.8
322-4F	5R	5° off [001]	0.5 mm (20 mil) flat	993 (144)	910 (132)	7.1	---
322-9F	5R	5° off [001]	0.5 mm (20 mil) flat	1186 (172)	1020 (148)	4.0	---
323-8F	6R	2.5° off [001]	0.5 mm (20 mil) flat	1151 (167)	1000 (145)	10.0	---
343-2F	7H	12.5° off [001]	0.5 mm (20 mil) flat	903 (131)	896 (130)	4.0	---
343-6F	7H	3° off [001]	0.5 mm (20 mil) flat	993 (144)	965 (140)	7.0	---
Average 1.8 mm (70 mil) rounds within 13° of [001]				1034 (150)	903 (131)	7.0	---
Average 0.5 mm (20 mil) flats within 13° of [001]				1048 (152)	958 (139)	6.4	---
Average DS Blade 1.8 mm (70 mil) rounds				1158 (168)	965 (140)	6	---
Transverse Specimens							
322-4T	5R	Not Determined	1.8 mm (70 mil) round	1096 (159)	931 (135)	6.1	14.2
322-9T	5R	Not Determined	1.8 mm (70 mil) round	821 (119)	814 (118)	7.6	14.4
323-8T	6R	Not Determined	1.8 mm (70 mil) round	1096 (159)	883 (128)	9.2	13.9
343-1T	7H	Not Determined	1.8 mm (70 mil) round	821 (119)	793 (115)	11.3	16.5
344-8T	8R	Not Determined	1.8 mm (70 mil) round	979 (142)	848 (123)	12.4	16.3
343-3T	7H	Not Determined	1.5 mm (70 mil) round	883 (128)	752 (109)	17.6	32.4
343-9T	7H	Not Determined	1.8 mm (70 mil) round	88° (129)	779 (113)	7.4	11.8
344-2T	7H	Not Determined	1.8 mm (70 mil) round	1027 (149)	855 (124)	10.9	17.6
398-10T	14R	Not Determined	1.8 mm (70 mil) round	1041 (151)	896 (130)	8.9	17.2
404-4T	17R	Not Determined	1.8 mm (70 mil) round	993 (144)	855 (124)	12.8	18.3
404-7T	17R	Not Determined	1.8 mm (70 mil) round	1062 (154)	931 (135)	5.0	9.7
406-9T	19R	Not Determined	1.8 mm (70 mil) round	1138 (165)	945 (137)	8.3	12.9
406-12T	19R	Not Determined	1.8 mm (70 mil) round	993 (144)	848 (123)	10.0	17.0
407-9T	20R	Not Determined	1.8 mm (70 mil) round	1069 (155)	910 (132)	6.6	13.6
408-8T	21R	Not Determined	1.8 mm (70 mil) round	1014 (147)	841 (122)	11.5	18.7
Average				993 (144)	855 (124)	9.7	---
Average DS Blade 1.8 mm (70 mil) rounds				938 (136)	834 (121)	6	---

\*1246°C (2275°F) for 2 hours, plus 982°C (1800°F) for 5 hours, plus 871°C (1600°F) for 20 hours.

\*\*R = Right-angle crystal selector; H = Helix crystal selector.

ORIGINAL PAGE IS  
OF POOR QUALITY

ORIGINAL PAGE IS  
OF POOR QUALITY

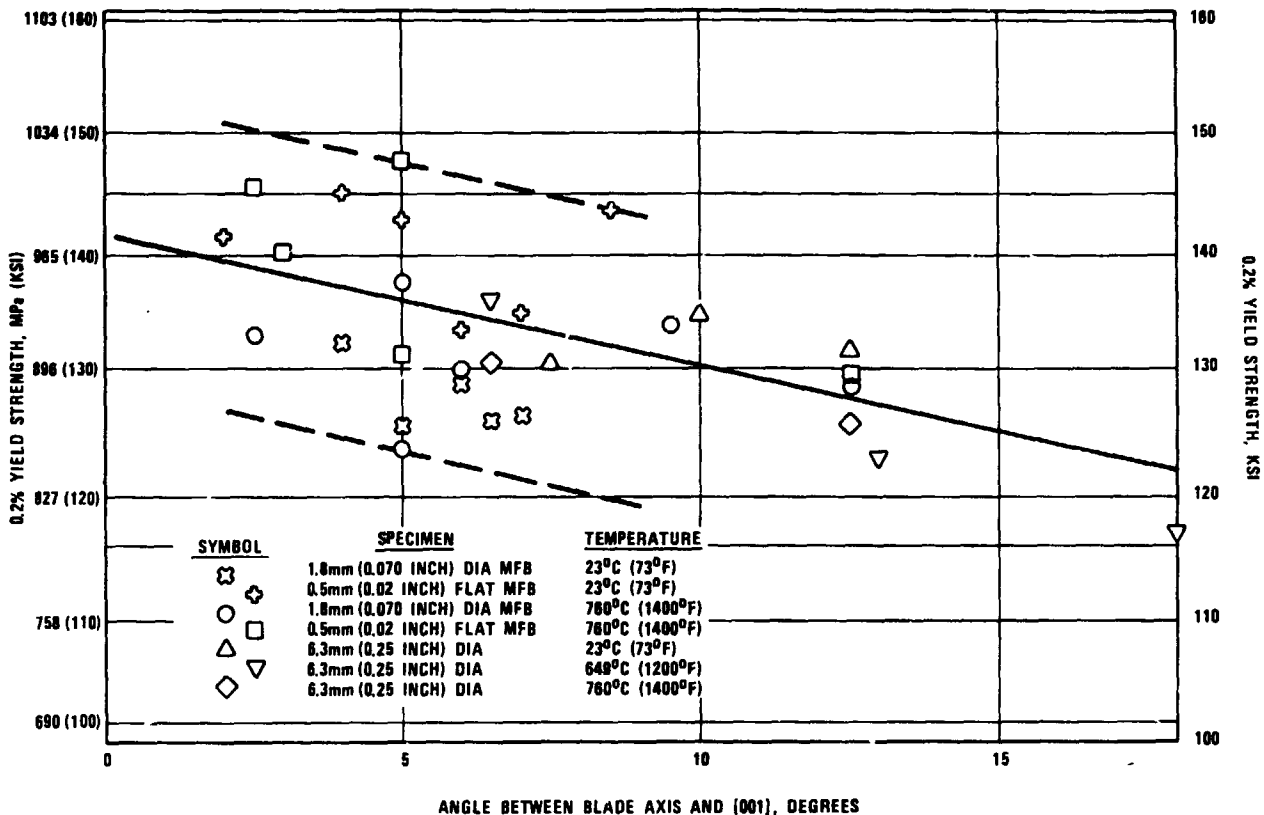


Figure 14. Yield Strength of SC Mar-M 247.

The transverse properties, where orientations were not controlled, are almost identical to average DS blade properties. The two low values at 760°C (1400°F) strongly suggest weak secondary orientations, when compared to the known orientations of the longitudinal specimens.

Elastic moduli were calculated from load-elongation curves for longitudinal and transverse orientation tensile specimens tested at room temperature and 760°C (1400°F). However, since the extensometry was attached to the grips [that is, not on the 1.8 mm (0.070 in.) diameter test specimen], the calculated values were not considered reliable and are not reported. (For a given crystallographic orientation, calculated modulus values ranged from equal to well below those reported in the literature for pure nickel and Mar-M 200.)

Transverse tensile data for controlled orientation 1.8 mm (0.070 in.) diameter minibars machined from SC Mar-M 247 ingots are provided in Table 4. This data exhibited severe scatter for the [100] orientation, but little scatter for data taken 15° from the [100]. Ignoring the two low data points at [100] gives yield strengths comparable to the longitudinal data in Figure 14.

#### 4.2 Stress-Rupture Tests

Stress-rupture testing of SC Mar-M 247 was conducted in the range of 760° to 1093°C (1400° to 2000°F). At 760°C, data was obtained using 1.8 mm (0.070 inch) diameter specimens machined from blades (Table 5) and ingots (Table 6). Both MFB 1.8 mm (0.070 inch) diameter minibars and 0.5 mm (0.020 inch) thick flat specimens were used to obtain stress-rupture data at 982° (1800°), 1038° (1900°) and 1093°C (2000°F); these data are provided in Tables 7, 8, and 9, respectively.

As expected, the greatest variation in results was observed at 760°C (1400°F), where rupture life has been shown to be highly dependent on SC orientation.

For specimen orientations within 10° of the [001], substantial scatter was observed. This variability in rupture life is similar to that reported for SC Mar-M 247 by MacKay et al.;<sup>4</sup> they concluded that the amount of crystallographic rotation associated with primary creep on the {111} <112> slip system could explain the variability in rupture life.

The effect of solutioning temperature on 760°C (1400°F) stress-rupture lives was also noticeable in the [001] orientation longitudinal specimen data; i.e., specimens solutioned at 1246°C (2275°F) had average rupture lives that were 40 percent greater than those of specimens solutioned at 1232°C (2250°F).

TABLE 4. TENSILE TEST RESULTS ON 1.8 MM (0.070 INCH) DIAMETER CONTROLLED TRANSVERSE ORIENTATION MINIBARS MACHINED FROM SINGLE-CRYSTAL INGOTS OF HEAT-TREATED\* MAR-M 247.

Specimen Number	Orientation of Specimen	Temperature °C (°F)	Ultimate Tensile Strength MPa (ksi)	0.2% Yield Strength MPa (ksi)	Elongation (%)	R of A (%)
397-21S	[100]	RT	834 (121)	821 (119)	10.6	27.9
398-21S	[100]	RT	1124 (163)	917 (133)	10.4	20.0
397-23S	15° to [100]**	RT	834 (121)	814 (118)	6.1	17.6
398-31S	15° to [100]**	RT	876 (127)	841 (122)	10.6	18.0
397-11S	[110]	RT	896 (130)	889 (129)	9.0	17.6
398-11S	[110]	RT	883 (128)	869 (126)	12.1	30.8
397-22S	[100]	760 (1400)	834 (121)	793 (115)	8.4	17.6
398-22S	[100]	760 (1400)	1193 (173)	993 (144)	8.2	13.9
398-32S	15° to [100]**	760 (1400)	931 (135)	827 (120)	11.8	18.0
398-34S	15° to [100]**	760 (1400)	889 (129)	814 (118)	9.0	17.0
397-12S	[110]	760 (1400)	972 (141)	827 (120)	11.7	13.0
398-12S	[110]	760 (1400)	848 (123)	807 (117)	14.3	27.6

\*Heat-treated at 1246°C (2275°F) for 2 hours, plus 982°C (1800°F) for 5 hours, plus 871°C (1600°F) for 20 hours.

\*\*15° rotation away from [100] toward the [110].

Limited data for SC specimens with orientations near the [311] and [111] indicated that these orientations were stronger than the [001]. The high strength of the [111] specimen was expected based on previous studies with SC Mar-M 200 and Mar-M 247.<sup>4,5</sup> On the other hand, MacKay had reported the [311] and [331] to be relatively weak.

As anticipated, based on SC Mar-M 200 and Mar-M 247 studies, single crystals with orientations near the [110] had very low stress-rupture life. This result was attributed to extensive primary creep on a single {111} <112> slip system.<sup>4</sup>

Transverse minibar stress-rupture testing at 760°C (1400°F) on specimens machined from the SC ingots indicated that specimens with an axis rotated 15 degrees away from the [001] (rotated toward the

ORIGINAL PAGE IS  
OF POOR QUALITY

TABLE 5. 760°C (1400°F) STRESS-RUPTURE TEST RESULTS ON 1.8 MM (0.070 INCH) DIAMETER BARS MACHINED FROM SINGLE-CRYSTAL TFE731-MATE TURBINE BLADES OF HEAT-TREATED\* MAR-M 247.

Specimen Number	Mold No. Crystal Selector Type**	Orientation of Specimen	Solution Treatment Temperature °C (°F)	Stress MPa (ksi)	Rupture Life (Hours)	Elongation (%)	R of A (%)	Remarks
LONGITUDINAL SPECIMENS								
304-1L	4R	0.5° off (100)	1232 (2250)	724 (105)	-	3.0	7.3	Failed on load- ing through shrink defect.
303-1L	3R	6° off (001)	1232 (2250)	724 (105)	78.2	4.4	16.6	
294-1L	1H	10° off (001)	1232 (2250)	724 (105)	165.3	15.6	19.3	
295-1L	2H	5° off (001)	1232 (2250)	724 (105)	54.5	8.5	25.3	
295-8L	2H	6° off (001)	1232 (2250)	724 (105)	13.8	14.2	19.8	
295-2L	2H	4° off (311)	1232 (2250)	724 (105)	496.5	4.7	14.2	
295-10L	2H	28° off (001)	1232 (2250)	724 (105)	31.7	11.5	21.6	
295-3L	2H	7° off (110)	1232 (2250)	724 (105)	26.9	5.9	10.2	
295-13L	2H	6° off (311)	1232 (2250)	724 (105)	214.8	9.2	15.3	
294-6L	1H	6° off (111)	1232 (2250)	724 (105)	225.1	9.5	14.9	
405-3L	18R	Visual (001)	1246 (2275)	724 (105)	245.4	13.4	16.3	
405-4L	18R	Visual (001)	1246 (2275)	724 (105)	34.0	5.9	12.1	
406-2L	19R	Visual (001)	1246 (2275)	724 (105)	66.9	11.9	25.5	Failed through shrink
406-6L	19R	Visual (001)	1246 (2275)	724 (105)	82.3	10.3	17.6	
408-9L	21R	Visual (001)	1246 (2275)	724 (105)	119.2	9.1	16.1	
(Anticipated Life - DS Castings 60 to 300 Hours)								
TRANSVERSE SPECIMENS								
303-1T	3R	***	1232 (2250)	655 (95)	276.7	8.5	21.2	
294-1T	1H	10° off (110)	1232 (2250)	655 (95)	1.0	9.3	12.6	
295-1T	2H	***	1232 (2250)	655 (95)	348.8	4.4	15.4	
295-8T	2H	***	1232 (2250)	655 (95)	20.4	2.8	10.4	Failed through shrink
295-2T	2H	4° off (311)	1232 (2250)	6.5 (95)	759.5	11.3	27.0	
295-10T	2H	***	1232 (2250)	6.5 (95)	60.1	12.7	17.0	Failed through shrink
295-3T	2H	2° off (110)	1232 (2250)	655 (95)	2.8	16.4	42.4	
295-13T	2H	***	1232 (2250)	655 (95)	501.8	3.4	10.4	
294-6T	1H	9° off (210)	1232 (2250)	655 (95)	48.8	6.5	20.8	
405-3T	18R	Visual (100)	1246 (2275)	655 (95)	1124.5	13.6	21.1	
405-4T	18R	Visual (100)	1246 (2275)	655 (95)	598.2	10.7	20.5	
406-2T	19R	Visual (100)	1246 (2275)	655 (95)	928.4	11.7	22.7	
406-6T	19R	Visual (100)	1246 (2275)	655 (95)	849.3	16.3	20.2	
408-9T	21R	Visual (100)	1246 (2275)	655 (95)	571.2	15.1	27.0	
408-11T	21R	Visual (100)	1246 (2275)	655 (95)	1145.3	12.1	18.0	
(Anticipated Life - DS Castings 100 Hours)								
* Solution treated as indicated for 2 hours with Argon Quench, plus 982°C (1800°F) for 5 hours, plus 871°C (1600°F) for 20 hours.								
** R = Right-angle crystal selector; H = Helix crystal selector.								
***Transverse orientations not determined.								

[110]) had comparable lives to [001] specimens (Table 6). This result is in agreement with MacKay's results.<sup>4</sup>

In agreement with the MFB data and studies cited earlier, machined-from-ingot specimens with the [110] orientation had rupture lives that were two orders of magnitude lower than those near the [001].

As anticipated from previous studies,<sup>4-7</sup> there was far less scatter in the higher temperature range 982° to 1093°C (1800° to 2000°F) stress-rupture lives. (See Tables 7, 8, and 9.) At these temperatures, the results for [001] oriented specimens were found

ORIGINAL PAGE  
OF POOR QUALITY

TABLE 6. 760°C (1400°F) STRESS-RUPTURE TEST RESULTS ON 1.8 MM (0.070 INCH) DIAMETER CONTROLLED TRANSVERSE ORIENTATION MINIBARS MACHINED FROM SINGLE-CRYSTAL INGOTS OF HEAT-TREATED\* MAR-M 247.

Specimen Number	Orientation of Specimen	Stress MPa (ksi)	Rupture Life (Hours)	Elongation (%)	R of A (%)
398-23S	[100]	724 (105)	227.1	10.2	20.2
398-24S	[100]	724 (105)	186.0	13.2	17.6
398-33S	15° off [100]	724 (105)	145.3	13.0	16.7
398-35S	15° off [100]	724 (105)	356.3	9.2	18.7
398-13S	[110]	724 (105)	1.3	28.8	37.8
398-14S	[110]	724 (105)	1.6	30.7	36.1
*Heat-treated at 1246°C (2275°F) for 2 hours with Argon Quench, plus 982°C (1800°F) for 5 hours, plus 871°C (1600°F) for 20 hours.					

to be at the high end of previously documented DS Mar-M 247 blade results from MATE Project 1. Scatter in the transverse specimens was dramatically reduced.

Similar results have been observed with the SC Mar-M 200 alloy.<sup>6,7</sup> In those studies, it was noted that for 857°C (1575°F) and higher temperatures, primary creep (which is associated with deformation by a single slip system) is reduced by an order of magnitude below that observed at 760°C (1400°F).

Examination of 982°C (1800°F) longitudinal and transverse SC Mar-M 247 stress-rupture data (Table 7) on <100> oriented crystals indicates that solutioning at 1246°C (2275°F) yields a small improvement in average stress-rupture life; i.e., 6 percent for longitudinal (100) and 22 percent for transverse material.

Inspection of 1038°C (1900°F) stress-rupture data (Table 8) also indicates that the higher solutioning temperature resulted in improved rupture lives. The average improvement in longitudinal properties was marginal (4 percent), but the transverse data exhibited a 44-percent improvement.

ORIGINAL PAGE IS  
OF POOR QUALITY

TABLE 7. STRESS-RUPTURE TEST RESULTS AT 982°C (1800°F) ON TEST SPECIMENS MACHINED FROM SINGLE-CRYSTAL TURBINE BLADES OF HEAT-TREATED\* MAR-M 247.

Specimen Number	Mold No. Crystal Selector Type**	Orientation of Specimen	Solution Treatment Temperature °C (°F)	Specimen Type	Stress MPa (ksi)	Rupture Life (Hours)	Elongation (%)	R of A (%)	Remarks				
Longitudinal Specimens													
304-2L	4R	6° off [001]	1232 (2250)	1.8 mm (70 mil) round	207 (30)	54.1+	--	--	Pulled from				
303-2L	3R	5° off [001]	1246 (2275)	1.8 mm (70 mil) round	207 (30)	100.5	18.9	50.1	Adapter				
295-11L	2H	8° off [001]				110.0	17.1	50.1					
295-14L	2H	4° off [001]				90.0	28.0	53.6					
303-5L	3R	6.5° off [001]				103.7	25.0	49.7					
303-6L	3R	4° off [001]				114.7	21.2	47.4					
295-4L	2H	8° off [001]				123.6	21.8	48.9					
295-7L	2H	8° off [111]				102.6	14.2	32.7					
291-9L	2H	6° off [111]				240.4	15.1	31.0					
322-13L	5R	6° off [001]				102.3	21.0	48.5					
323-12L	6R	1° off [001]				113.4	20.6	47.4					
323-14L	6R	3° off [001]				124.5	17.3	44.4					
322-13P	5R	6° off [001]		0.5 mm (20 mil) flat		82.4	36.9	--					
323-12P	6R	1° off [001]				149.3	34.0	--					
323-14P	6R	3° off [001]				49.2	13.1	--					
(Anticipated life - 1.8 mm (70 mil) rounds from DS Castings: 50-120 hours)													
(Anticipated life - 0.5 mm (20 mil) flats from DS Castings: 15-30 hours)													
Transverse Specimens													
304-2T	4R	Not Determined	1232 (2250)	1.8 mm (70 mil) round	186 (27)	120.0	17.1	26.2	Failed through shrink				
303-2T	3R	Not Determined	1246 (2275)	1.8 mm (70 mil) round	207 (30)	173.2	19.1	38.1					
295-11T	2H					21.3	2.2	5.4					
295-4T	2H					153.3	17.1	48.5					
295-7T	2H					29.4	3.7	6.2					
323-14T	6R					172.3	20.0	45.4					
343-2T	7H					134.5	16.6	51.5					
343-4T	7H					129.1	10.9	44.0					
343-6T	7H					229.7	17.3	43.8					
344-3T	8R					241.1	20.9	47.5					
398-8T	14R					107.2	19.3	38.6					
398-9T	14R					111.7	24.5	44.5					
404-5T	17R					103.8	16.5	27.8					
404-8T	17R					103.1	37.7	51.5					
407-6T	20R					87.6	27.7	43.6					
Anticipated life from DS Castings: 100 Hours at 186 MPa (27 ksi)													
*Solution treated as indicated with Argon Quench, plus 982°C (1800°F) for 5 hours, plus 871°C (1600°F) for 20 hours.													
**R = Right-Angle crystal selector; H = Helix crystal selector.													

Average 982° and 1038°C (1800° and 1900°F) rupture lives of 0.5 mm (0.020 inch) thick flat specimens [solutioned at 1246°C (2275°F)] are, respectively, 82 and 89 percent of the average lives of 1.8 mm (0.070 inch) diameter specimens solutioned at the same temperature; i.e., rupture lives of the thinner specimens are surprisingly high at these temperatures relative to equiaxed casting section-size trends. Retention of stress-rupture life in the 0.5 mm (0.020 in.) flat specimens apparently reflects the absence of grain boundaries as weak links that cause early failures. In contrast, at 1093°C (2000°F), the 0.5 mm (0.020 in.) thick flat specimens have only 20 percent of the rupture life of the 1.8 mm (70 mil) diameter specimens (see Table 9). This difference is partially attributable to the increasing effects of oxidation (reducing the effective section size) as well as the section-size effect.



ORIGINAL  
OF 2001

TABLE 8. STRESS-RUPTURE TEST RESULTS AT 1038°C (1900°F) ON TEST SPECIMENS MACHINED FROM SINGLE-CRYSTAL TURBINE BLADES OF HEAT-TREATED\* MAR-M 247.

Specimen Number	Mold No. Crystal Selector Type**	Orientation of Specimen	Solution Treatment Temperature °C (°F)	Specimen Type	Stress MPa (ksi)	Rupture Life (Hours)	Elongation (%)	R of A (%)	Remarks
Longitudinal Specimens									
295-12L	2H	9° off [001]	1232 (2250)	1.8 mm (70 mil) round	131 (19)	228.3	15.0	49.7	
295-6L	2H	6° off [001]				193.8	21.6	50.2	
303-3L	3R	4° off [001]				212.0	23.2	58.2	
303-9L	3R	2° off [001]				141.3	30.6	62.2	
303-7L	3R	9.5° off [001]				179.6	14.7	48.2	
303-11L	3R	2.5° off [001]				234.0	23.6	51.9	
323-10L	6R	2° off [001]	1246 (2275)			207.7	17.8	55.7	
344-9L	6R	2° off [001]		0.5 mm (20 mil) flat		205.9	22.1	58.9	
323-10P	6R	2° off [001]				184.3	13.4	--	
(Anticipated life-DS Castings: 55-160 hours)									
Transverse Specimens									
295-6T	2H	Not Determined	1232 (2250)	1.8 mm (70 mil) round	131 (19)	117.7	14.3	37.6	
303-3T	3R					121.4	18.9	35.5	
303-9T	3R					47.9	6.0	16.7	Failed through shrink
323-13T	6R		1246 (2275)			231.8	21.5	50.9	
323-15T	6R					209.8	20.9	50.9	
344-4T	8R					132.1	15.4	33.1	
344-15T	8R					112.7	17.9	53.6	
398-5T	14R					230.8	27.9	48.6	
407-4T	20R					115.9	15.9	43.9	
(Anticipated life - DS Castings: 100 hours)									
*Solution treated as indicated with Argon Quench, plus 982°C (1800°F) for 5 hours, plus 871°C (1600°F) for 20 hours.									
**R = Right-Angle crystal selector; H = Helix crystal selector.									

TABLE 9. STRESS-RUPTURE TEST RESULTS AT 1093°C (2000°F) ON TEST SPECIMENS MACHINED FROM SINGLE-CRYSTAL TURBINE BLADES OF HEAT-TREATED\* MAR-M 247.

Specimen Number	Mold No. Crystal Selector Type**	Orientation of Specimen	Solution Treatment Temperature °C (°F)	Specimen Type	Stress MPa (ksi)	Rupture Life (Hours)	Elongation (%)	R of A (%)	Remarks
Longitudinal Specimens									
323-13L	6R	10° off [001]	1246 (2275)	1.8 mm (70 mil) round	103 (15)	45.5	13.2	27.5	
323-15L	6R	9° off [001]			103 (15)	60.0	21.5	59.4	
343-6L	7H	3° off [001]			103 (15)	39.4	13.7	33.6	
406-1L	19R	Visual [001]			97 (14)	--	--	--	Machine Mal-function
323-13P	6R	10° off [001]		0.5 mm (20 mil) flat	103 (15)	9.5	24.0	--	
323-15PL	6R	9° off [001]			103 (15)	9.3	25.8	--	
(Anticipated life - 1.8 mm (70 mil) rounds from DS Castings: 35 hours at 103 MPa (15 ksi))									
398-3T	14R	Not Determined	1246 (2275)	1.8 mm (70 mil) round	97 (14)	83.3	32.7	48.4	
398-12T	14R					107.3	12.0	17.8	
404-3T	17R					63.6	16.8	46.7	
406-1T	19R					66.9	24.8	39.4	
407-1T	20R					76.4	20.7	38.5	
408-6T	21R					73.4	16.4	49.6	
(Anticipated life - 1.8 mm (70 mil) rounds from DS Castings: 55 hours at 97 MPa (14 ksi))									
*Solution treated as indicated with Argon Quench, plus 982°C (1800°F) for 5 hours, plus 871°C (1600°F) for 20 hours.									
**R = Right-angle crystal selector; H = Helix crystal selector.									

## SECTION V

### 5.0 SC ALLOY DEVELOPMENT

Previous experience with SC Mar-M 200 and the work conducted in this program with SC Mar-M 247 demonstrated that the [001] orientation SC alloys were not significantly stronger than the DS form in stress rupture. Consequently, it was necessary to exploit the alloying freedom provided by the SC alloy macrostructure to obtain a significant improvement in mechanical properties.

For the Mar-M 247 alloy, the obvious modification was to remove all (or part) of the elements (such as B, Zr, Hf, and C) that strengthen grain boundaries in conventionally cast and DS alloys. Since B, Zr, and Hf are also strong melting point depressants, their removal permits the eutectic gamma prime, which does not contribute significantly to strength, to be more fully solutioned and then reprecipitated as fine gamma prime. This approach has also been successfully applied by Boone,<sup>8</sup> Duhl,<sup>9</sup> and Gell<sup>10,11</sup> for other SC nickel-base superalloys.

Based on the work of Jackson,<sup>12</sup> stress-rupture life is a strong function of the volume fraction of fine  $\gamma'$  in the microstructure. Gamma prime in Mar-M 247--even when heat-treated at (or near) the incipient melting temperature--is only partially solutioned; i.e., substantial amounts of eutectic  $\gamma'$  remain. Thus, the melting point limitation of the unmodified Mar-M 247 inhibits realization of the full strengthening potential of the  $\gamma'$  in this alloy.

In addition, cobalt removal or reduction to levels lower than the 10 percent Co present in Mar-M 247 was considered to reduce alloy cost.

Some of the grain boundary strengthening elements such as Hf also enhance oxide scale adhesion on diffusion aluminide coatings.

Consequently, in some instances, a small amount of Hf (or Y, which also enhances oxide scale adhesion) was retained for potential oxidation resistance benefits.

The approach to alloy modification was performed in three steps:

- o An analytical study of eight "paper alloys"
- o A microstructural stability study with equiaxed derivatives
- o Development and characterization of SC derivatives of Mar-M 247.

These aspects of SC alloy development are reviewed in the following paragraphs.

#### 5.1 "Paper Alloy" Study

Based on the above considerations, a preliminary analytical study was performed on eight "paper alloys" derived from the Mar-M 247 chemistry. Alloy chemistries are provided in Table 10.

The analysis consisted of computer calculations of electron vacancy numbers using both  $Nv_{3B}$  and  $Nv_{SS}$  methods. Since both yielded the same results once carbon and boron were removed, only results of the  $Nv_{SS}$  calculations are reported in Table 11. Also included in Table 11 are calculated volume fractions for the phases and alloy density.

This study indicated that all of the candidate SC alloy derivatives had lower calculated electron vacancy numbers than the maximum specification composition of Mar-M 247. Therefore, modifications 3 through 8 were assumed to also be metallurgically stable; that is, free of any topologically close packed (TCP) phases.

ORIGINAL PAGE IS  
OF POOR QUALITY

TABLE 10. COMPOSITIONS (PERCENT WEIGHT) OF MAR-M 247 AND DERIVATIVE SC ALLOYS.

	Compositions of Alloys							
	1	2	3	4	5	6	7	8
Mo	0.50	0.80	0.80	0.70	0.70	0.76	0.72	0.76
W	9.50	10.50	10.50	10.20	10.50	9.98	9.45	9.93
Ta	2.80	3.30	3.30	3.10	3.30	3.14	2.97	3.12
Ti	0.90	1.20	1.20	1.10	1.20	1.14	1.08	1.14
Cr	8.00	8.80	8.80	8.60	8.80	8.36	7.92	8.32
Co	9.00	10.00	-	-	-	5.00	10.00	5.00
Fe	0.15	0.15	0.15	0.15	0.15	0.15	0.15	0.15
Al	5.30	5.70	5.70	5.55	5.70	5.42	5.13	5.39
B	0.010	0.020	-	-	-	-	-	-
Zr	0.030	0.080	-	-	-	-	-	-
C	0.13	0.17	-	-	-	-	-	-
Hf	1.20	1.60	-	-	0.60	-	-	0.60
Mn	0.05	0.05	0.05	0.05	0.05	0.05	0.05	0.05
Si	0.05	0.05	0.05	0.05	0.05	0.05	0.05	0.05
Ni	Bal	Bal	Bal	Bal	Bal	Bal	Bal	Bal

NOTE: No. 1 is minimum of normal specification range.

No. 2 is maximum of normal specification range.

No. 3 is maximum of range with zero B, C, Hf, Zr, and Co.

No. 4 is mid-range chemistry with zero B, C, Hf, Zr, and Co.

No. 5 is alloy No. 3 with 0.6-percent Hf.

No. 6 is alloy No. 3 with 5.0-percent Co.

No. 7 is alloy No. 3 with 10.0-percent Co.

No. 8 is alloy No. 3 with 5.0-percent Co and 0.6-percent Hf.

TABLE 11. COMPUTER ANALYSIS OF MAR-M 247 AND DERIVATIVE COMPOSITIONS LISTED IN TABLE 10.

Modification No.	Carbides (V/O)	Borides (V/O)	$\gamma'$ (V/O)	$\gamma$ (V/O)	$N_{VSS}$	$g/cm^3$ ( $lb/in.^3$ )
1 (min.)	2.90	0.14	54.74	42.45	1.93	8.61 (0.311)
2 (max.)	3.81	0.28	60.57	35.64	2.32	8.64 (0.312)
3	0	0	61.91	38.10	2.13	8.61 (0.311)
4	0	0	59.70	40.30	2.01	8.61 (0.311)
5	0	0	62.16	37.84	2.14	8.64 (0.312)
6	0	0	58.83	41.17	2.08	8.64 (0.312)
7	0	0	55.65	44.35	2.03	8.64 (0.312)
8	0	0	58.77	41.24	2.07	8.67 (0.313)

## 5.2 Microstructural Stability Study

To assess the thermal stability of alloy modifications of Mar-M 247, five chemistries were selected, melted, and cast into equiaxed ingots. The first composition, Alloy 1, is basically Mar-M 247 with hafnium, zirconium, cobalt, and boron eliminated and carbon held at an absolute minimum level. This composition was vacuum melted by Cannon-Muskegon (Muskegon, Michigan) to a very high purity (Table 12). Other alloy compositional variations were produced by remelting portions of the resulting master alloy and adding minor amounts of selected elements during remelting and casting at Jetshapes.

The aim and actual compositions of the five alloy modifications are listed in Table 13. Alloy 2 restores half the normal hafnium in Mar-M 247 to the Alloy 1 composition. Alloy 3 returns half the normal cobalt and hafnium in Mar-M 247 to Alloy 1. Alloy 4 is a molybdenum addition heat, while Alloy 5 is an yttrium modification for environmental resistance.

ORIGINAL PAGE IS  
OF POOR QUALITY

TABLE 12. CHEMICAL COMPOSITION OF MASTER HEAT NO. VF-31  
OF "STRIPPED" MAR-M 247 MELTED BY CANNON-  
MUSKEGON CORPORATION.

Alloy Composition (Weight Percent)		
Element	Aim Chemistry	Heat VF-31
Mo	0.80	0.8
W	10.50	10.2
Ta	3.30	3.4
Ti	1.20	1.1
Cr	8.80	9.0
Co	-	-
Al	5.70	5.5
C	-	0.018
Hf	-	-
Zr	-	-
Oxygen*		4
Nitrogen*		6
Ag*		<1
Bi*		<0.5
Mg*		7
Pb*		<1
Se*		<1
Te*		<0.5
Tl*		<1
Ni		Bal
*Parts per million for gases and trace elements		

The solidus and liquidus temperatures of Mar-M 247 and the five alloy modifications were determined by differential thermal analysis (DTA) through interpretation of the cooling curves. Although the values may not have been exact, they were directly comparable and are presented in Table 14.

To assess alloy sensitivity to sigma and mu phase precipitation, stability tests were conducted on the five alloys using exposures of 843°C (1550°F)/1176 hours and 1093°C (2000°F)/50 hours, respectively. Prior to testing, the alloy samples were given either the solution plus coating cycle plus age or the coating cycle plus age heat treatments. Two solution treatments were

ORIGINAL PAGE IS  
OF POOR QUALITY

TABLE 13. AIM AND ACTUAL COMPOSITIONS OF MODIFIED MAR-M 247 ALLOYS.

Element	Alloy Composition (Weight Percent)									
	Alloy 1		Alloy 2		Alloy 3		Alloy 4		Alloy 5	
	Aim	Actual	Aim	Actual	Aim	Actual	Aim	Actual	Aim	Actual
Mo	0.80	0.8	0.8	0.76	0.8	0.77	2.0	1.70	0.8	0.75
W	10.50	10.2	10.2	10.27	9.4	10.03	10.1	10.21	10.2	10.04
Ta	3.30	3.4	3.4	3.25	3.2	3.24	3.4	3.00	3.4	3.07
Ti	1.20	1.1	1.1	1.15	1.0	1.10	1.1	1.10	1.1	1.11
Cr	8.80	9.0	9.0	9.10	8.5	8.67	8.9	8.77	9.0	8.78
Co	0	--	--	--	5.0	5.13	--	--	--	--
Al	5.70	5.75	5.75	5.48	5.45	5.42	5.65	5.47	5.75	5.52
C	0	0.018	0.018	0.017	0.018	0.014	0.018	0.015	0.018	0.015
Hf	0	--	0.6	0.63	0.6	0.60	--	--	--	--
Zr	0	0	LAP**	<0.01	LAP	<0.01	--	--	--	--
Oxygen*	--	4	--	--	--	--	--	--	--	--
Nitrogen*	--	6	--	--	--	--	--	--	--	--
Ni	Bal	Bal	Bal	Bal	Bal	Bal	Bal	Bal	Bal	Bal
Y	0	--	--	--	--	--	--	--	0.4	0.50

\*PPM

\*\*Low as possible.

NOTE: Actual composition of Alloy 1 furnished by Cannon-Muskegon Corp.;  
all other analyses from National Spectrographic Corp. (Cleveland, Ohio).

TABLE 14. SOLIDUS AND LIQUIDUS TEMPERATURES  
OF MAR-M 247 AND FIVE ALLOY  
MODIFICATIONS.

Alloy	Solidus	Liquidus
Mar-M 247	1325°C (2417°F)	1383°C (2521°F)
Alloy 1	1345°C (2453°F)	1383°C (2521°F)
Alloy 2	1340°C (2444°F)	1410°C (2570°F)
Alloy 3	1355°C (2471°F)	1390°C (2534°F)
Alloy 4	1325°C (2417°F)	1380°C (2516°F)
Alloy 5	1300°C (2372°F)	1390°C (2534°F)

DTA performed at Harrop Laboratories in  
Columbus, Ohio.

evaluated on Alloy No. 1: 1260°C (2300°F)/2 hours and 1288°C (2350°F)/2 hours. The other alloys were all given the 1260°C (2300°F)/2-hour solution treatments. These alloys were tested as equiaxed cast ingots.

Metallographic characterization of the alloys and the heat treatments performed are summarized in the following paragraphs. Significant instabilities were not detected after either the 843° or 1093°C (1550° or 2000°F) exposures. Representative microstructures of as-cast, heat-treated and 843°C (1550°F) exposed alloys are also provided.

#### 5.2.1 Alloy 1

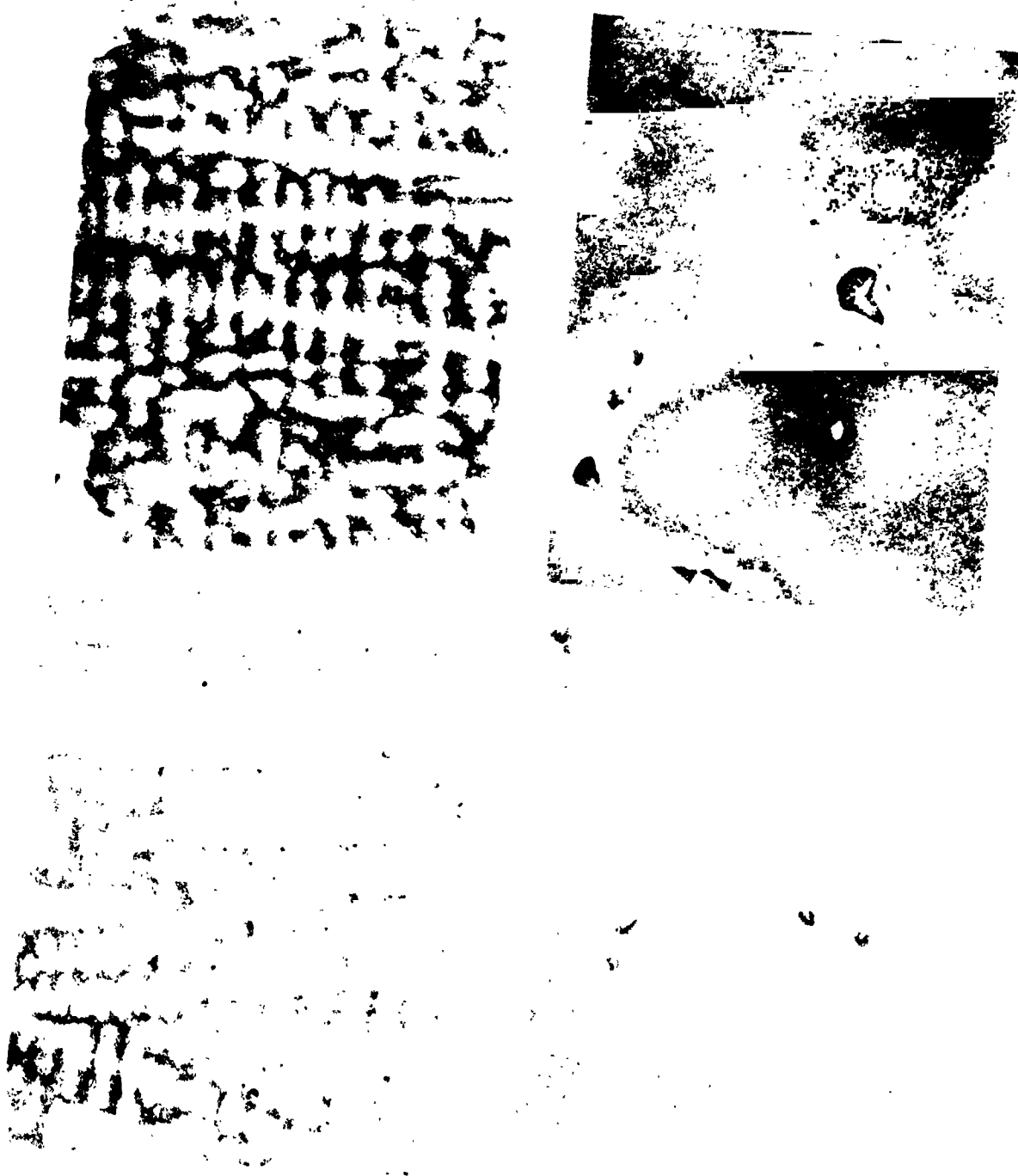
Figure 15 depicts the alloy microstructure in the as-cast condition and after a 1260°C (2300°F)/2 hour heat treatment. Inspection of the microstructure indicates that this temperature was too low to completely solution the gamma prime phase. In contrast, as shown in Figure 16 (top), a 2-hour exposure at 1288°C (2350°F) was effective in solutioning the gamma prime phase. Small needles or platelets, which were subsequently found to be  $\alpha$ -tungsten, were also observed in the solutioned microstructure.

The microstructures at the bottom of Figure 16 show the effects of the 843°C (1550°F)/1176 hour exposure after the following heat-treatments:

- o 982°C (1800°F)/5 hours (simulated coating cycle) + 871°C (1600°F)/20 hours (gamma prime precipitation)
- o 1260°C (2300°F)/2 hours + 982°C (1800°F)/5 hours + 871°C (1600°F)/20 hours
- o 1288°C (2350°F)/2 hours + 982°C (1800°F)/5 hours + 871°C (1600°F)/20 hours



ORIGINAL PAGE IS  
OF POOR QUALITY



(80X)

(400X)

P78650-1

Figure 15. Microstructures of Alloy Modification No. 1.  
Upper Photos As-Cast, Lower Photos After  
1260°C (2300°F) 2 Hour Solution Treatment.

ORIGINAL PAGE IS  
OF POOR QUALITY



Figure 16. Microstructures of Alloy Modification No. 1.

P78650-2

Top: As-Cast + 1288°C (2350°F)/2 Hr  
Solution Treatment (500X).

Bottom: 100X After 843°C (1550°F)/1176 Hr  
Exposure.

Left: 982°C (1800°F)/5 Hours + 871°C 1600°F)/  
20 Hrs Prior to Exposure;

Center: Same as Left but with 1260°C (2300°F)/  
2 Hr Solution Treatment;

Right: Same as Left but with 1288°C (2350°F)/  
2 Hr Solution Treatment.

Some grain boundary changes were observed for the last condition, but the matrix (present only in an SC blade) remained unaffected.

#### 5.2.2 Alloy 2

Figure 17 shows the typical as-cast microstructure and modifications of this microstructure resulting from a 1260°C (2300°F)/2 hour heat treatment, and from a complete heat treatment. The 1260°C (2300°F) temperature again appeared too low for effective solution treatment. No effect of the coating and aging thermal cycles was evident. Typical microstructures after thermal exposure are shown in Figure 18. Some isolated needles or platelets were evident in the 1260°C (2300°F) treated material, which probably formed prior to the 843°C (1550°F)/1176 hour exposure.

#### 5.2.3 Alloy 3

Microstructures are shown in Figure 19 prior to exposure and in Figure 20 after exposure. The hafnium-modified eutectic gamma-prime did not dissolve at 1260°C (2300°F). Some type of needle phase formed around the "swirly" gamma-prime on the nonsolutioned alloy, but the amount formed was not enough to cause concern.

#### 5.2.4 Alloy 4

Structures prior to exposure are shown in Figure 21 and after exposure in Figure 22. This relatively high Mo alloy modification formed more of the needle phase during solution treatment than did the other alloys. The 843°C (1550°F)/1176 hours exposure appeared to have had no effect on the alloy.

ORIGINAL PAGE IS  
OF POOR QUALITY

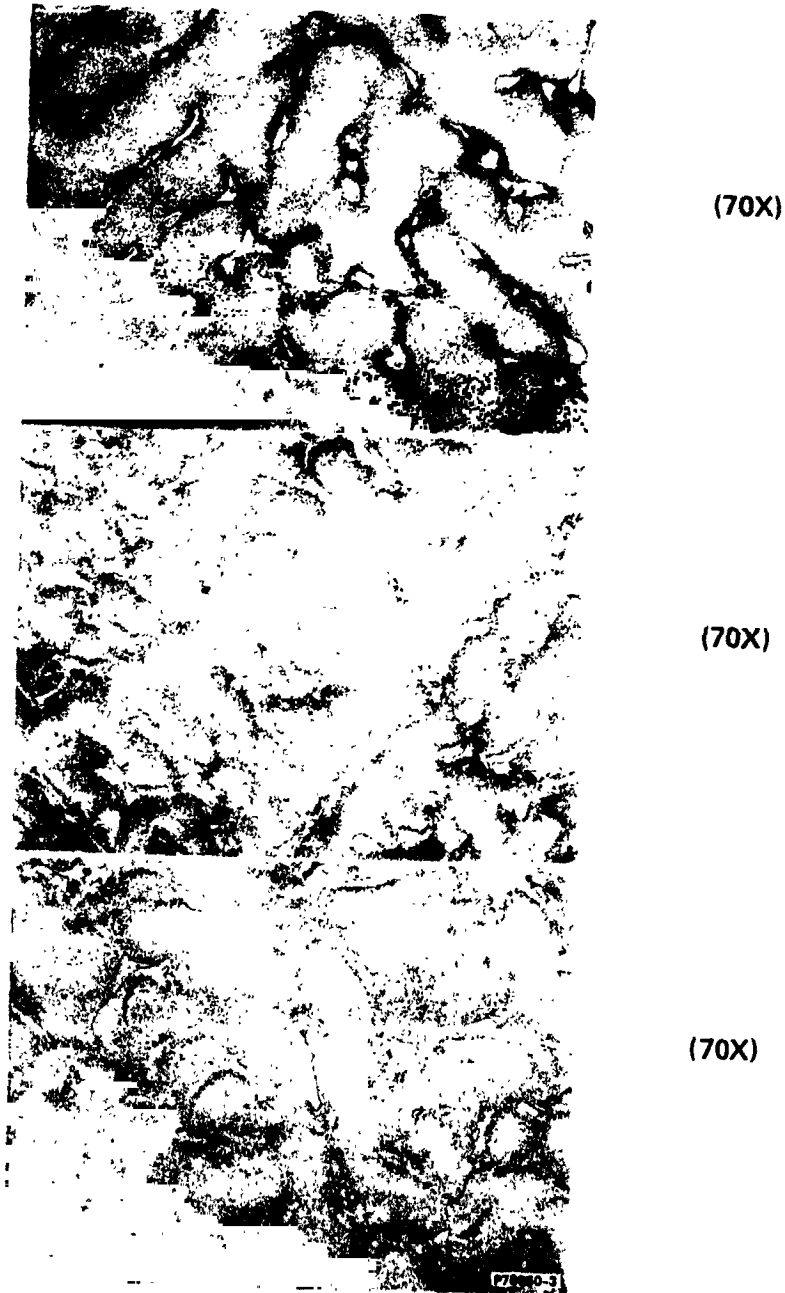


Figure 17. Microstructures of Alloy Modification No. 2.  
Top: As-Cast.  
Center: After  $1260^{\circ}\text{C}$  ( $2300^{\circ}\text{F}$ )/2 Hr Solution  
Treatment.  
Bottom: After  $1260^{\circ}\text{C}$  ( $2300^{\circ}\text{F}$ )/2 Hrs +  $982^{\circ}\text{C}$   
( $1800^{\circ}\text{F}$ )/5 Hrs +  $871^{\circ}\text{C}$  ( $1600^{\circ}\text{F}$ )/  
20 Hours.

ORIGINAL PAGE IS  
OF POOR QUALITY

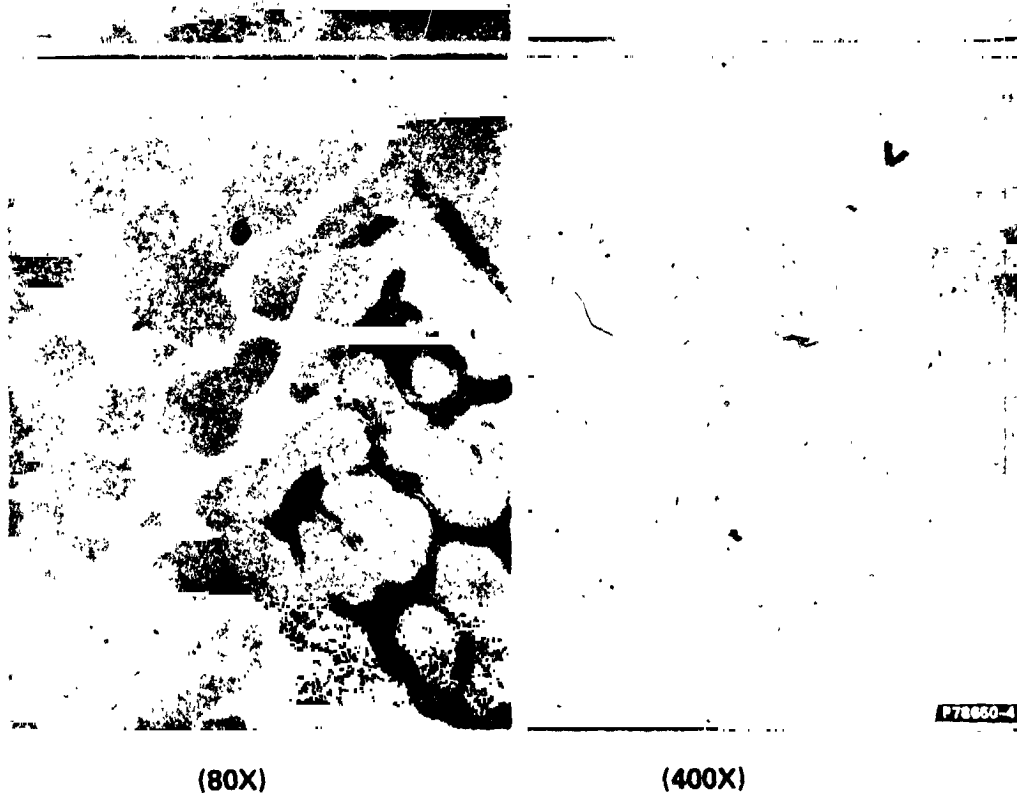


Figure 18. Microstructures of Alloy Modification No. 2 after  
843°C (1550°F)/1176 Hour Exposure.  
Top: Prior Heat Treatment - 1260°C (2300°F)/2 Hrs +  
982°C (1800°F)/5 Hrs + 871°C (1600°F)/20 Hrs.  
Bottom: Prior Heat Treatment - 982°C (1800°F)/5 Hrs  
+ 871°C (1600°F) 20 Hrs.

ORIGINAL PAGE IS  
OF POOR QUALITY



(70X)



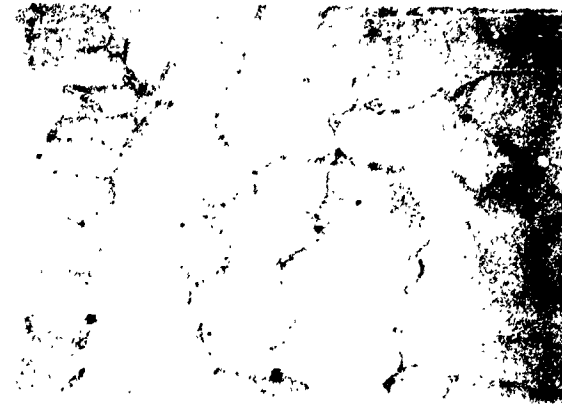
(350X)



(350X)

Figure 19. Microstructures of Alloy Modification No. 3.  
Top: As-Cast.  
Center: After 1260°C (2300°F)/2 Hrs.  
Bottom: After 1260°C (2300°F)/2 Hr + 982°C  
(1800°F)/5 Hrs + 871°C (1600°F)/  
20 Hrs.

ORIGINAL PAGE IS  
OF POOR QUALITY



(75X)



(75X)

(375X)

Figure 20. Microstructures of Alloy Modification No. 3  
after 843°C (1550°F)/1176 Hr. Exposure.  
Top: Prior Heat Treatment - 1260°C (2300°F)/  
2 Hrs + 982°C (1800°F)/5 Hrs + 871°C  
(1600°F)/20 Hrs.  
Center and Bottom: Prior Heat Treatment - 982°C  
(1800°F)/5 Hrs. + 871°C  
(1600°F)/20 Hrs.

ORIGINAL PAGE IS  
OF POOR QUALITY

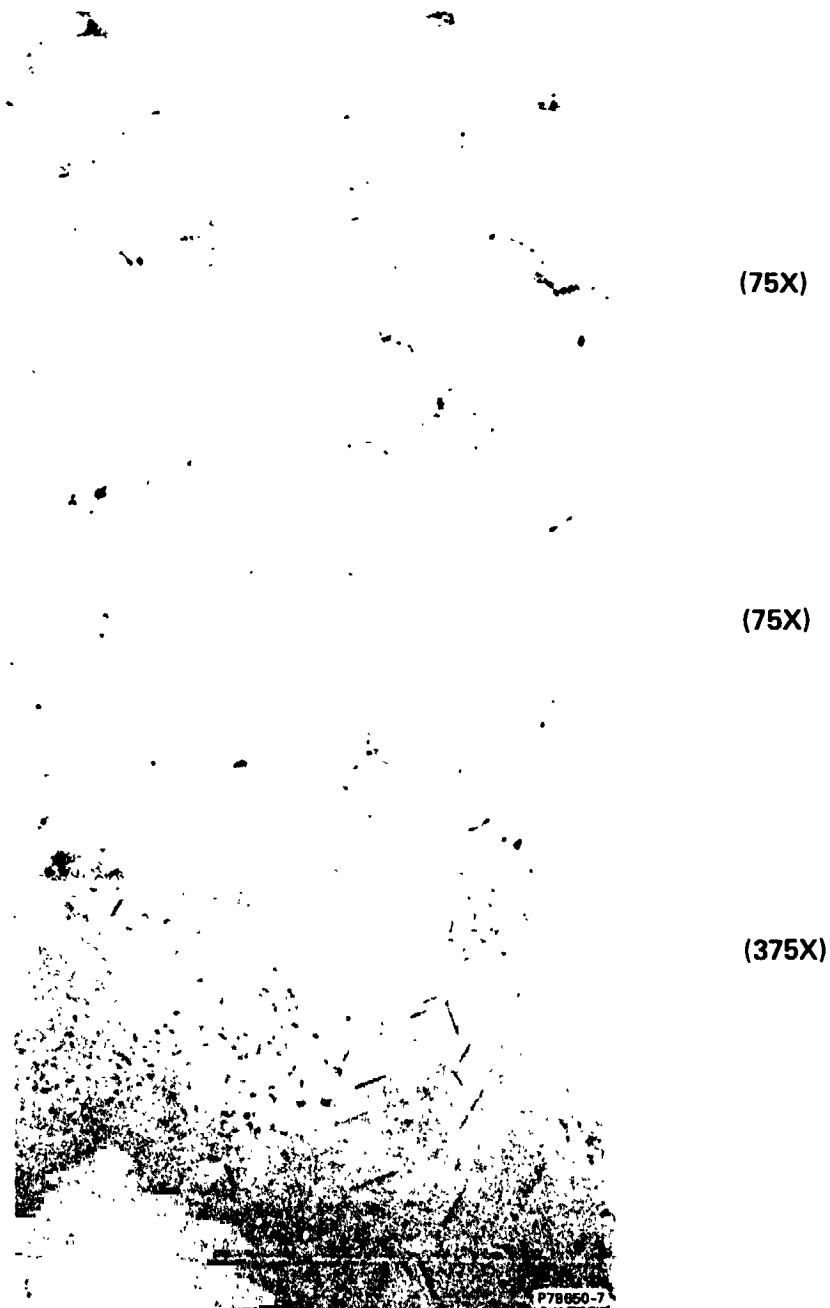


Figure 21. Microstructures of Alloy Modification No. 4.  
Top: As-Cast.  
Center and Bottom: After 1260°C (2300°F)/  
2 Hrs + 982°C (1800°F)/  
5 Hrs + 871°C (1600°F)/  
20 Hrs.



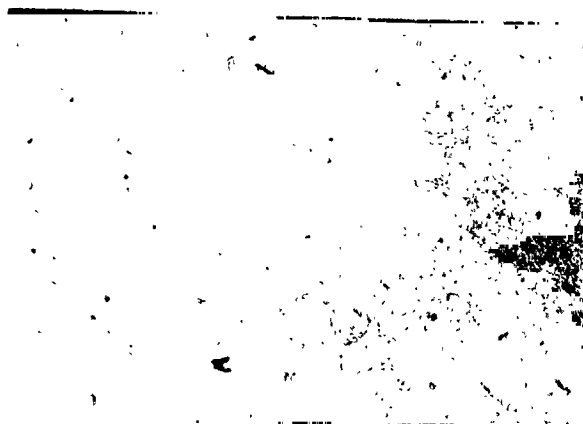
ORIGINAL PHOTOGRAPH  
OF POOR QUALITY



(75X)



(375X)



(375X)

P78650-8

Figure 22. Microstructures of Alloy Modification No. 4  
after 843°C (1550°F)/1176 Hr Exposure.

Top and Center: Prior Heat Treatment  
982°C (1800°F)/5 Hrs  
+ 871°C (1600°F)/20 Hrs.

Bottom: Prior Heat Treatment 1260°C  
(2300°F)/2 Hrs + 982°C (1800°F)/  
5 Hrs + 871°C (1600°F)/20 Hrs.

#### 5.2.5 Alloy 5

This yttrium-bearing alloy formed a peculiar gray second phase that is readily seen in the unetched photos of Figure 23. The overall photos suggested that the yttrium was tied up as a low-melting phase, some of which apparently incipiently melted at 1260°C (2300°F)/2 hour heat treatment. No indications of instability are evident in the photos of Figure 24.

#### 5.3 SC Derivatives of Mar-M 247

Based on the "paper alloy" study and the furnace exposure tests for microstructural stability, it was decided to procure small master alloy heats and evaluate the five alloys in Table 13 in exothermically cast SC form. This evaluation included establishing a heat treatment for each alloy and assessing their metallurgical and mechanical property characteristics. These aspects of SC derivative alloy development from Mar-M 247 are reviewed in the following paragraphs.

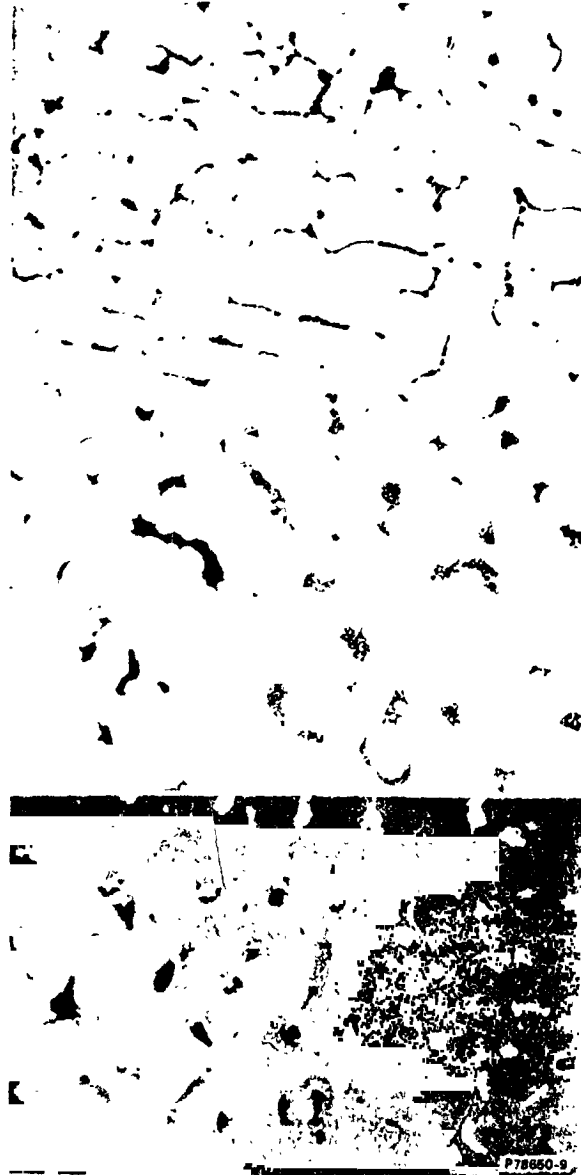
##### 5.3.1 Master Alloys

New master heats were procured from Cannon-Muskegon for this phase of the program. Aim and actual master alloy chemistries are provided in Table 15. Alloy 5 was produced using a late addition of yttrium to the Alloy 1 master heat during subsequent melting at Jetshapes. The procedures to produce the master alloys are reviewed in another publication.<sup>13</sup>

##### 5.3.2 SC Casting Campaigns

As discussed in Section III, the initial molds of the Mar-M 247 derivative SC alloys were contaminated with zirconium during melting in a zirconia crucible. Thus, these SC alloys could not be adequately solution heat-treated and resulting strengths were below DS Mar-M 247.

ORIGINAL PAGE IS  
OF POOR QUALITY



(70X)  
UNETCHED

(70X)  
UNETCHED

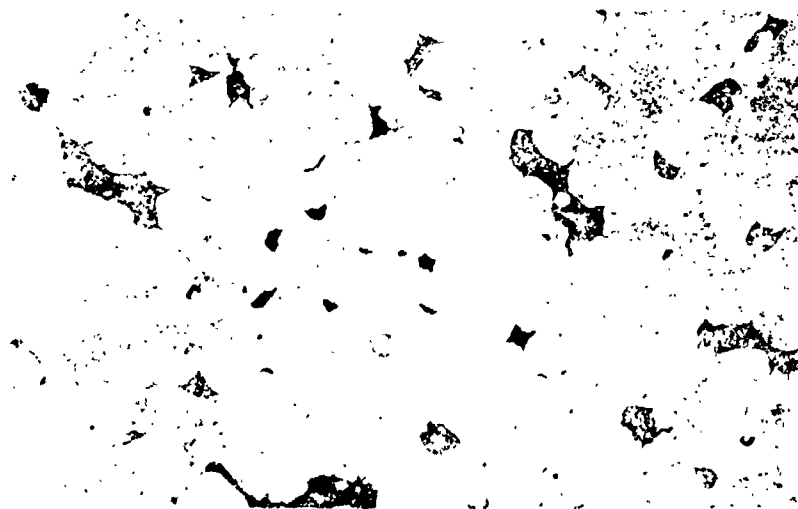
(70X)  
UNETCHED

Figure 23. Microstructures of Alloy Modification No. 5.  
Top: As-Cast.  
Center and Bottom: 1260°C (2300°F)/2 Hr  
Solution Treatment.

ORIGINAL PAGE IS  
OF POOR QUALITY



100X



100X

Figure 24. Microstructures of Alloy Modification No. 5 after 843°C (1550°F)/1176 Hr Exposure.  
Top: Prior Heat Treatment - 982°C (1800°F)/ 5 Hrs + 871°C (1600°F)/20 Hrs.  
Bottom: Prior Heat Treatment - 1260°C (2300°F)/ 2 Hrs + 982°C (1800°F)/5 Hrs + 871°C (1600°F)/20 Hrs.

ORIGINAL PAGE IS  
OF POOR QUALITY

TABLE 15. COMPOSITIONS OF MAR-M 247 ALLOY MODIFICATIONS MELTED  
BY CANNON-MUSKEGON.

Element	Alloy Composition (Weight Percent)								
	Alloy 1			Alloy 2		Alloy 3		Alloy 4	
	Aim	VF-31 Actual	VF-154 Actual	Aim	VF-100 Actual	Aim	VF-99 Actual	Aim	VF-98 Actual
Mo	0.8	0.8	0.8	0.8	0.8	0.8	0.8	2.0	2.1
W	10.5	10.2	10.4	10.2	10.0	9.4	9.2	10.1	9.9
Ta	3.3	3.4	3.4	3.4	3.5	3.2	3.3	3.4	3.5
Ti	1.2	1.1	1.1	1.1	1.0	1.0	0.93	1.1	1.0
Cr	9.0	9.0	9.0	9.0	9.3	8.5	8.2	8.9	9.0
Co	--	--	--	--	--	5.0	5.1	--	--
Al	5.75	5.5	5.8	5.75	5.8	5.45	5.54	5.65	5.74
C	--	0.018	0.0034	0	0.0032	0	0.0018	0	0.0022
Hf	--	--	--	0.6	0.6	0.6	0.6	--	--
Zr	LAP**		--	0.01	LAP	--	LAP	--	--
Oxygen*	--	4	--	--	5	--	6	--	6
Nitrogen*	--	6	--	--	3	--	14	--	4
Ni	Bal	Bal	Bal	Bal	Bal	Bal	Bal	Bal	Bal

\*ppm

\*\*Low as possible

Actual compositions provided by Cannon-Muskegon

This above problem was solved by melting the alloys in a magnesia crucible instead of a zirconia crucible. A second casting campaign was initiated to evaluate SC alloy modifications 1 to 4. (Alloy 5 was dropped from further consideration at this time. Both the zirconium contamination and the yttrium addition were concentrated in the incipient melting zones.) As in the previous casting campaigns, the DS blade configuration from MATE Project 1 was used for the casting evaluation. Single-crystal TFE731 high-pressure turbine blades were cast with Mar-M 247 and modified Alloys 1, 2, 3, and 4. A magnesia crucible was used to melt the alloys at a nominal temperature of 1593°C (2900°F). Ten molds were cast, each containing twelve SC blades. The results of visual examination of the product of these molds are shown in Table 16; 64 percent of the blades, which filled with metal, were single-crystal with the desired [001] grain orientation within 15 degrees of the blade's longitudinal axis. SC Alloys 1 and 3 appeared to have the best castability based on this limited data.

TABLE 16. VISUAL INSPECTION RESULTS FOR SC TFE731 TURBINE  
BLADES OF MAR-M 247 AND MODIFIED SUPERALLOYS.\*

Alloy (Mold No.)	Blades Filled** With Metal	Single-Crystal Airfoil and Root***
Mar-M 247 (467)	8	2
Mar-M 247 (468)	10	7
Alloy 1 (458)	12	8
Alloy 1 (481)	12	10
Alloy 2 (465)	5	2
Alloy 2 (482)	12	6
Alloy 3 (464)	10	7
Alloy 3 (483)	12	9
Alloy 4 (466)	8	6
Alloy 4 (484)	8	5
	<u>97</u>	<u>62</u>

\*Cast with MgO crucible.

\*\*Each mold contained 12 blade cavities.

\*\*\*[001] grain orientation within 15° of blade longitudinal axis.

A comparison of master melt and SC blade chemistries is provided in Table 17. These results indicated that magnesium pickup ranged from 2 to 12 ppm; magnesium additions at this level were considered innocuous. Changing from a zirconia to a magnesia crucible to melt Alloys 1 through 4 reduced the zirconium in the SC blades by a factor of about 40.

### 5.3.3 Heat Treatment Study

The solution heat-treatment ranges were assessed by furnace exposure followed by metallographic examination. Results of this evaluation are summarized in Table 18. As-cast and solutioned microstructures of Alloys 1 through 4 are presented in Figures 25 to 28, respectively. Based on these results, Alloys 1 and 4 were solutioned at 1316°C (2400°F) for 2 hours and 1324°C (2415°F) for 2 hours. The hafnium modified Alloys 2 and 3 exhibited incipient melting at lower temperatures and were solutioned at 1288°C

ORIGINAL PAGE IS  
OF POOR QUALITY

TABLE 17. MASTER MELT AND BLADE CHEMISTRIES OF MAR-M 247 AND MODIFIED MAR-M 247 SINGLE-CRYSTAL ALLOYS MELTED WITH A MAGNESIA CRUCIBLE.

Element	Actual Alloy Composition (Weight Percent)									
	Mar-M 247		Alloy 1		Alloy 2		Alloy 3		Alloy 4	
	Range	Blade	Master Melt	Blade	Master Melt	Blade	Master Melt	Blade	Master Melt	Blade
Mo	0.50-0.80	0.7	0.8	0.8	0.8	0.8	0.8	0.8	2.1	2.1
W	9.50-10.50	9.8	10.4	10.7	10.0	10.0	9.2	9.4	9.9	10.2
Ta	2.80-3.80	3.0	3.4	3.5	3.5	3.6	3.3	3.3	3.5	3.6
Ti	0.90-1.20	1.0	1.1	1.1	1.0	1.0	0.93	0.9	1.0	1.0
Cr	8.00-8.80	8.0	9.0	7.5	9.3	8.8	8.2	.7	9.0	8.6
Co	9.00-11.00	10.1	--	--	--	--	5.1	5.1	--	--
Al	5.30-5.70	5.4	5.8	5.6	5.8	5.7	5.54	5.6	5.74	5.6
C	0.13-0.17	0.13	0.003	0.0012	0.003	0.0019	0.002	0.0016	0.002	0.0019
Hf	1.20-1.60	1.1	--	<0.01	0.6	0.6	0.6	0.6	--	--
Zr	0.03-0.08	0.03	0.01	0.002	0.014	0.017	0.005	0.009	0.001	0.002
B	0.01-0.02	0.016	--	--	--	--	--	--	--	--
Mg	--	0.0002	--	0.0005	--	0.0012	--	0.0006	--	0.0004
Ni	Bal	Bal	Bal	Bal	Bal	Bal	Bal	Bal	Bal	Bal

NOTE: Master melt and blade chemistries were determined by Cannon-Muskegon.

TABLE 18. SOLUTIONING HEAT-TREATMENT CHARACTERISTICS OF MODIFIED MAR-M 247 SC ALLOY TFE731 HP TURBINE BLADES.\*

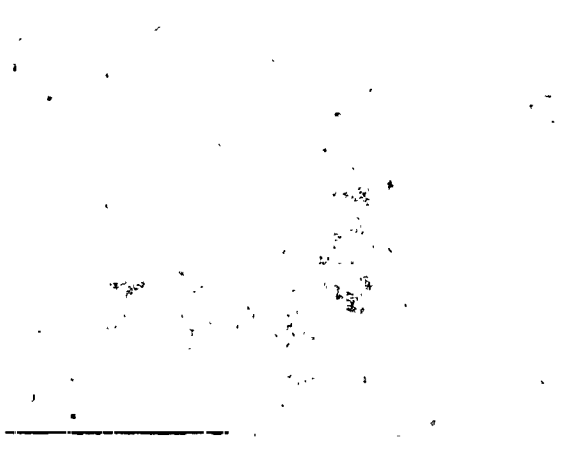
Solution Treatment °C (°F)/Hours	SC Alloy Modification Number			
	1	2	3	4
1288 (2350)/4	Partial solutioning	---	Partial solutioning	---
1302 (2375)/2	Partial solutioning	Partial solutioning, incipient melting	Partial solutioning, incipient melting	~85% solutioning
1316 (2400)/2	~85% solutioning	80% solutioning, incipient melting	85% solutioning, incipient melting	~95% solutioning
1316 (2400)/2 1329 (+2425)/2	>90% solutioning	---	---	Complete solutioning
1343 (2450)/2	Incipient melting	---	---	Incipient melting
1288 (2350)/2 1316 (+2400)/2	---	Incipient melting	Incipient melting	---
1288 (2350)/2 1302 (+2375)/2	---	75% solutioning, incipient melting	85% solutioning incipient melting	---

\*SC alloys melted in megnesia crucible and cast at Jetshapes, Inc.

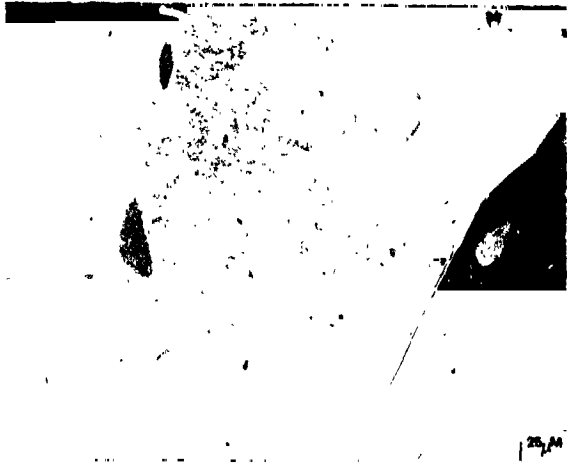
ORIGINAL: 17755  
OF POOR QUALITY



AS CAST



1288°C (2350°F)  
FOR 4 HOURS



1316°C (2400°F)  
FOR 2 HOURS  
AND  
1329°C (2425°F)  
FOR 2 HOURS

P78850-11

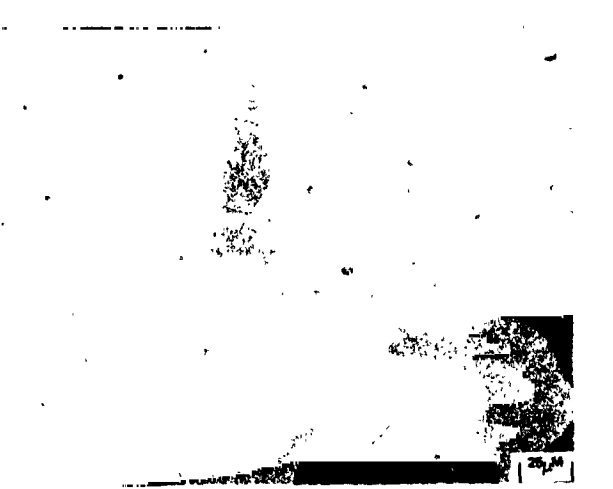
Figure 25. Microstructures of Alloy 1 Turbine Blades in As-Cast and Solution Heat-Treated Conditions.



ORIGINAL PAGE IS  
OF POOR QUALITY



AS CAST



1302°C (2375°F) FOR  
2 HOURS


P78650-12

Figure 26. Microstructures of Alloy 2 Turbine Blades  
in As-Cast and Solution Heat-Treated  
Conditions.


ORIGINAL PAGE IS  
OF POOR QUALITY




AS CAST



1288°C (2350°F) FOR  
4 HOURS



1288°C (2350°F) FOR 2  
HOURS



1302°C (2375°F) FOR 2  
HOURS

25 μm

P78650-13

Figure 27. Microstructures of Alloy 3 Turbine Blades  
in As-Cast and Solution Heat-Treated  
Conditions.

ORIGINAL PAGE IS  
OF POOR QUALITY



AS CAST



1316°C (2400°F) FOR 2 HOURS

1316°C (2400°F) FOR 2 HOURS AND  
1329°C (2425°F) FOR 2 HOURS

P78650-14

Figure 28. Microstructures of Alloy 4 Turbine Blades  
in As-Cast and Solution Heat-Treated  
Conditions.

ORIGINAL PAGE IS  
OF POOR QUALITY

(2350°F) for 2 hours and 1296°C (2365°F) for 4 hours. EDX analysis indicated that the lower incipient melting temperatures of Alloys 2 and 3 were associated with a hafnium rich eutectic; magnesium was not detected in incipient melting zones.

For SC Alloy 1, the solutioning temperature was significantly above the 1288°C (2350°F) used earlier for the equiaxed casting (Figure 12). This result is attributed to the significantly larger dendrite arm spacing of the SC alloy relative to the equiaxed alloy.

Solutioned [1246°C (2275°F) for 2 hours in vacuum] microstructures of SC Mar-M 247 blades, which were cast with the alloy melted in magnesia and zirconia crucibles, are compared in Figure 29. Both microstructures were similar; solutioning of the  $\gamma'$  was incomplete and a small amount of incipient melting was present. SC Mar-M 247 was not adversely affected by the zirconia crucibles.

At the conclusion of the vacuum solution heat treatment, the blades were fan-Argon quenched. Inspection of solution heat-treatment records indicated that approximately 1.7 minutes were required during fan-Argon quenching to reduce the temperature from 1324°C (2415°F) to 816°C (1500°F).

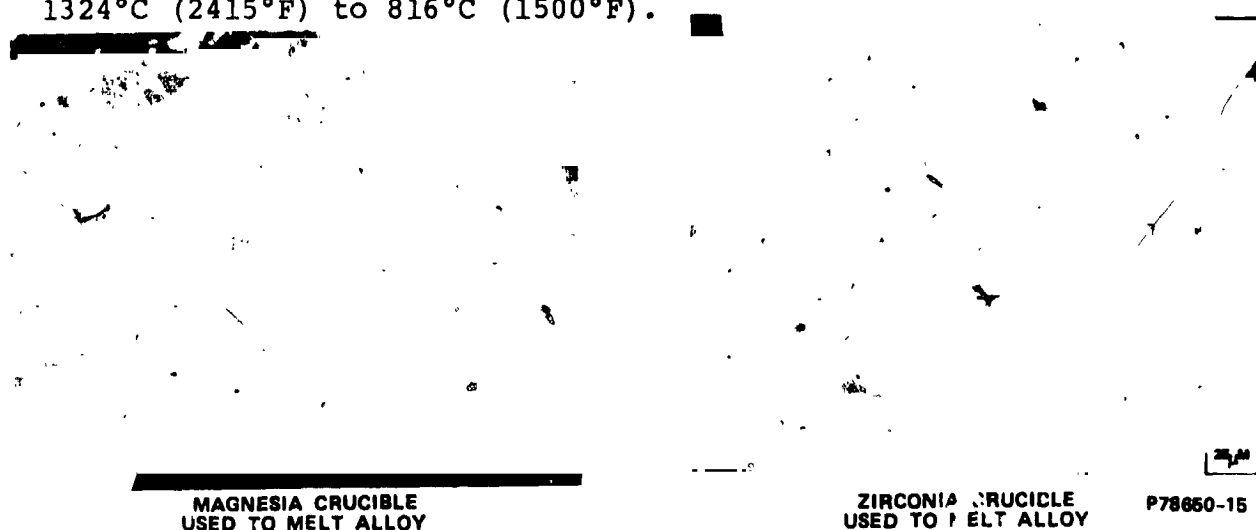


Figure 29. Solutioned - 1246°C (2275°F) for 2 Hrs in Vacuum -  
Microstructures of Mar-M 247 SC Turbine Blades.

Fan-Argon quenching was found to be a critical part of the solution heat treatment when it inadvertently was not activated until a batch of specimens had cooled to 1038°C (1900°F); in this case, 4.4 minutes were required to cool through the 1324° to 816°C (2415° to 1500°F) range. The relatively slow cooling rate from the solutioning temperature resulted in a coarser (lower-strength) gamma-prime precipitate morphology as shown in Figure 30.

#### 5.3.4 Property Characterization

The SC alloy derivatives of Mar-M 247 were screened for tensile and stress-rupture strengths, oxidation resistance, and density in order to facilitate selection of two promising alloys for design data generation and subsequent engine testing. This effort provided data for both properly processed SC alloys and deviate material (SC alloys contaminated with Zr from the crucible and SC components that were improperly heat treated). Subsequent paragraphs review the properties of the properly processed material followed by a discussion of the effects of improper processing on SC alloy properties.

#### 5.3.5 Tensile Tests

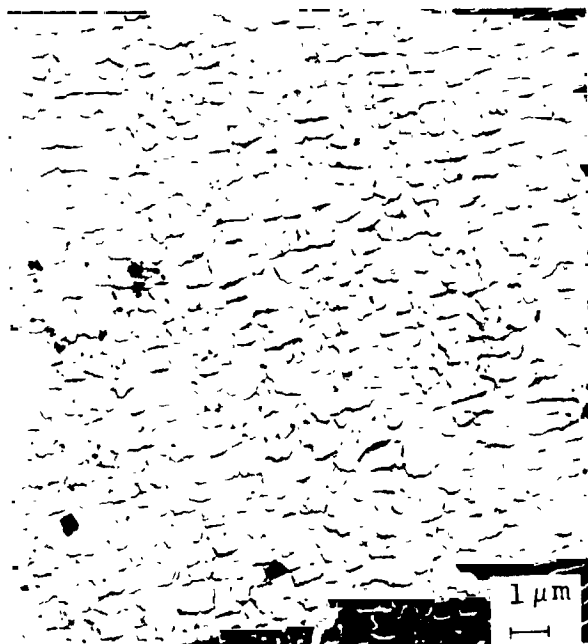
Longitudinal tensile test data was obtained for SC Alloys 1 through 4 at 760°C (1400°F), a temperature typical of blade attachments. As indicated in Table 19, SC Alloys 1, 2, and 4 exhibited average yield and ultimate strengths of 1235 (179) and 1366 MPa (198 ksi), respectively. For reference, average yield and ultimate strength levels for DS Mar-M 247 were 973 (141) and 1235 MPa (179 ksi), respectively. SC Alloy 3 tensile properties were similar to those of DS and SC of Mar-M 247 at 760°C (1400°F).

ORIGINAL PAGE IS  
OF POOR QUALITY



a. PROPER HEAT TREATMENT

1316°C (2400°F) for 2 Hrs +  
1324°C (2415°F) for 2 Hrs with  
Fan-Argon Quench - 1.7 Min to  
816°C (1500°F), with 982°C  
(1800°F) for 5 Hrs + 871°C  
(1600°F) for 20 Hrs.



b. IMPROPER HEAT TREATMENT

1316°C (2400°F) for 2 Hrs +  
1324°C (2415°F) for 2 Hrs with  
Delayed Argon Quench - 4.4 Min.  
to 816°C (1500°F) with 982°C  
(1800°F) for 5 Hrs + 871°C  
(1600°F) for 20 Hrs.

Figure 30. SEM Microstructures of Gamma-Prime Precipitates  
in SC Alloy 1 Showing Effect of Fan-Argon  
Quenching from the Solution Heat Treatment.

ORIGINAL PAGE IS  
OF POOR QUALITY

TABLE 19. 760°C (1400°F) TENSILE TEST RESULTS ON 1.8 MM (0.070 INCH) DIAMETER LONGITUDINAL TEST SPECIMENS MACHINED FROM SINGLE-CRYSTAL TURBINE BLADES OF ALLOYS 1 THROUGH 4.

Specimen No.	Alloy	Orientation	UTS	0.2% Y.S.	EL (%)	RA (%)
			MPa (ksi)	MPa (ksi)		
481-3L	1	Longitudinal	1379 (200)	1289 (187)	3.7	11.8
481-7L	1	Longitudinal	1407 (204)	1338 (194)	6.0	14.2
482-7L	2	Longitudinal	1310 (190)	1234 (179)	4.8	15.3
482-10L	2	Longitudinal	1386 (201)	1269 (184)	8.5	14.0
483-7L	3	Longitudinal	1200 (174)	938 (136)	9.5	14.4
483-12L	3	Longitudinal	1179 (171)	958 (139)	7.7	15.2
484-5L-2	4	Longitudinal	1413 (205)	1165 (169)	3.8	13.3
484-6L-2	4	Longitudinal	1289 (187)	1103 (160)	3.4	9.7

Heat Treatment:

- Alloys 1 and 4 - 1316°C (2400°F) for 2 hours, plus 1324°C (2415°F) for 2 hours, plus 982°C (1800°F) for 5 hours, plus 871°C (1600°F) for 20 hours.
- Alloys 2 and 3 - 1288°C (2350°F) for 2 hours plus 1296°C (2365°F) for 4 hours, plus 982°C (1800°F) for 5 hours, plus 871°C (1600°F) for 20 hours.

NOTE:

Alloys were melted in a magnesia crucible prior to casting.

### 5.3.6 Stress-Rupture Tests

Stress-rupture data were obtained for SC Alloys 1 through 4 and SC Mar-M 247 at 760° (1400°), 982° (1800°), and 1093°C (2000°F); test results are provided in Tables 20 to 22 for the respective temperatures.

Examination of the data indicated that all of the modified SC alloys were significantly stronger than SC Mar-M 247. SC Alloys 1, 2, and 4 exhibited excellent rupture lives under these test conditions, while SC Alloy 3 was only slightly weaker at all temperatures. Based on the Larson-Miller extrapolation, at a 103 MPa (15 ksi) stress level, SC Alloy 1 had 58° and 3°C (105° and 5°F) advantages in temperature capability (for a given rupture life) relative to SC Mar-M 247 and SC Alloy 4, respectively. At the 207 MPa (30

ORIGINAL PAGE IS  
OF POOR QUALITY

TABLE 20. 760°C (1400°F) STRESS-RUPTURE RESULTS ON 1.8 MM (0.070 INCH) DIAMETER SPECIMENS MACHINED FROM SINGLE-CRYSTAL TURBINE BLADES.\*

SPECIMEN NUMBER	ORIENTATION	ALLOY	TEMPERATURE °C (°F)	STRESS MPa (ksi)	RUPTURE LIFE (HOURS)	ELONGATION (%)	R of A (%)
467-3L	LONG.	Mar-M 247	760 (1400)	724 (105)	213.4	6.8	15.2
468-6L	LONG.	Mar-M 247		724 (105)	276.6	7.9	16.8
467-3T	TRANS.	Mar-M 247		724 (105)	338.7	10.0	20.9
468-6T	TRANS.	Mar-M 247		724 (105)	32.7	9.6	16.2
481-5L	LONG.	1		758 (110) + 793 (115)	790.2**	6.9	13.2
481-12L	LONG.	1		758 (110) + 793 (115)	725.2**	7.1	15.4
481-5T	TRANS.	1		758 (110) + 793 (115)	551.8**	10.8	23.2
481-12T	TRANS.	1		758 (110)	308.6	3.8	10.0
465-4L	LONG.	2		758 (110) + 793 (115)	618.5**	6.8	19.8
482-4L	LONG.	2		758 (110) + 793 (115)	622.0**	5.9	14.7
465-4T	TRANS.	2		758 (110)	405.5	5.3	12.5
482-4T	TRANS.	2		758 (110)	393.6	2.9	11.0
483-1L	LONG.	3		758 (110)	317.8	15.4	23.7
483-2L	LONG.	3		758 (110)	291.8	16.9	25.3
484-5L	LONG.	4		758 (110) + 793 (115)	894.2**	8.0	15.3
484-6L	LONG.	4		758 (110) + 793 (115)	773.2**	6.6	15.2

\*Heat treatments:

- Mar-M 247 - 1246°C (2275°F) for 2 hours with Argon Quench, plus 982°C (1800°F) for 5 hours, plus 871°C (1600°F) for 20 hours.
- Alloys 1 and 4 - 1316°C (2400°F) for 2 hours, plus 1324°C (2415°F) for 2 hours with Argon Quench, plus 982°C (1800°F) for 5 hours, plus 871°C (1600°F) for 20 hours.
- Alloys 2 and 3 - 1288°C (2350°F) for 2 hours plus 1296°C (2365°F) for 4 hours with Argon Quench, plus 982°C (1800°F) for 5 hours, plus 871°C (1600°F) for 20 hours.

\*\*Specimens were unloaded from 758 (110) to 793 MPa (115 ksi) after 500 hours.

ksi) stress level, SC Alloy 4 had 18° and 6°C (32° and 11°F) advantages relative to SC Mar-M 247 and SC Alloy 1, respectively. SC Alloy 2 rupture lives were intermediate to those of SC Alloys 1 and 4. At 760°C (1400°F), SC Alloy 4 also exhibited the longest rupture lives.

Transverse [100] stress-rupture data were obtained for SC Alloys 1, 2, and SC Mar-M 247. Generally, the rupture lives of the transverse [100] material were approximately equivalent to the longitudinal [001] material.

Ductilities of all the SC alloys tested were satisfactory for turbine blade applications.



ORIGINAL PAGE IS  
OF POOR QUALITY

TABLE 21. 982°C (1800°F) STRESS-RUPTURE RESULTS ON 1.8 MM (0.070 INCH) DIAMETER SPECIMENS MACHINED FROM SINGLE-CRYSTAL TURBINE BLADES.\*

SPECIMEN NUMBER	ORIENTATION	ALLOY	TEMPERATURE °C (°F)	STRESS MPa (ksi)	RUPTURE LIFE (HOURS)	ELONGATION (%)	R of A (%)
468-5L	LONG.	Mar-M 247	982 (1800)	207 (30)	123.5	23.6	45.7
468-7L	LONG.	Mar-M 247			120.5	27.4	44.5
468-5T	TRANS.	Mar-M 247			115.4	36.4	53.9
468-7T	TRANS.	Mar-M 247			116.4	27.8	46.0
458-3L	LONG.	1			189.3	24.3	42.6
458-4L	LONG.	1			198.1	15.7	41.3
481-3T	TRANS.	1			174.4	15.6	26.3
481-7T	TRANS.	1			189.5	26.0	34.2
482-6L	LONG.	2			216.8	21.1	36.8
482-3L	LONG.	2			217.1	19.2	43.6
482-6T	TRANS.	2			164.9	8.5	26.7
482-3T	TRANS.	2			258.4	8.9	33.3
483-3L	LONG.	3			180.2	22.5	28.9
483-8L	LONG.	3			161.3	10.2	28.3
484-1L	LONG.	4			251.4	23.7	30.4
484-3L	LONG.	4			249.7	24.8	37.2

TABLE 22. 1083°C (2000°F) STRESS-RUPTURE RESULTS ON 1.8 MM (0.070 INCH) DIAMETER SPECIMENS MACHINED FROM SINGLE-CRYSTAL TURBINE BLADES.\*

Specimen Number	Orientation	Alloy	Temperature °C (°F)	Stress MPa (ksi)	Rupture Life (hours)	Elongation (%)	R of A (%)
468-4L	Long.	Mar-M 247	1093 (2000)	103 (15)	72.4	22.4	66.5
468-9L	Long.	Mar-M 247			39.0	27.2	49.9
458-6L	Long.	1			501.8	11.2	34.5
458-11L	Long.	1			453.7	10.8	33.7
482-1L	Long.	2			456.8	13.7	40.5
482-2L	Long.	2			458.4	5	28.2
483-9L	Long.	3			247.8	11.0	20.0
483-10L	Long.	3			199.1	16.9	31.0
484-2L	Long.	4			399.9	11.0	30.7
484-4L	Long.	4			457.2	16.3	27.1

\*Heat treatments:

- Mar-M 247 - 124°C (2275°F) for 2 hours with Argon Quench, plus 982°C (1800°F) for 5 hours, plus 871°C (1600°F) for 20 hours.
- Alloys 1 and 4 - 1316°C (2400°F) for 2 hours, plus 1324°C (2415°F) for 2 hours with Argon Quench, plus 982°C (1800°F) for 5 hours, plus 871°C (1600°F) for 20 hours.
- Alloys 2 and 3 - 1288°C (2350°F) for 2 hours plus 1296°C (2365°F) for 4 hours with Argon Quench, plus 982°C (1800°F) for 5 hours, plus 871°C (1600°F) for 20 hours.

Typical microstructures of SC Alloys 1 to 4 in the pretest condition and after evaluation in 760°, 982°, and 1093°C (1400°, 1800°, and 2000°F) stress-rupture tests are provided in Figures 31 to 38. Inspection of these figures indicated that, with the exception of Alloy 2, only traces (if any) of the eutectic  $\gamma'$  remained. Only minor amounts of incipient melting were observed in the microstructures of SC Alloys 2 and 3.

In addition, the dendritic regions of SC Alloys 1, 2, and 4 exhibited numerous small particulate and acicular phases that energy dispersive X-ray (EDX) analysis indicated to be rich in tungsten. EDX analysis showed that the acicular particles also contained some nickel.

Results from Dr. J. F. Radavich (Micromet Laboratories, W. Lafayette, Indiana) of the microstructural analysis of stress-rupture tested MFB bars of SC Alloys 1 and 4 indicated that the tungsten-rich particulate and acicular phases were  $\alpha$ -tungsten and  $\mu$  phases, respectively. This was consistent with analysis of blade alloy chemistries by Cannon-Muskegon that indicated the carbon contents of the blades were less than 20 ppm. At this low carbon level, the probability of an  $M_6C$  tungsten-carbide formation was extremely low.

Examination of the post-test microstructures of the stress-rupture specimens indicated that secondary creep cracks generally initiated at small pores in the interdendritic regions. [The interdendritic regions were about 20 percent lower in tungsten

ORIGINAL PAGE IS  
OF POOR QUALITY

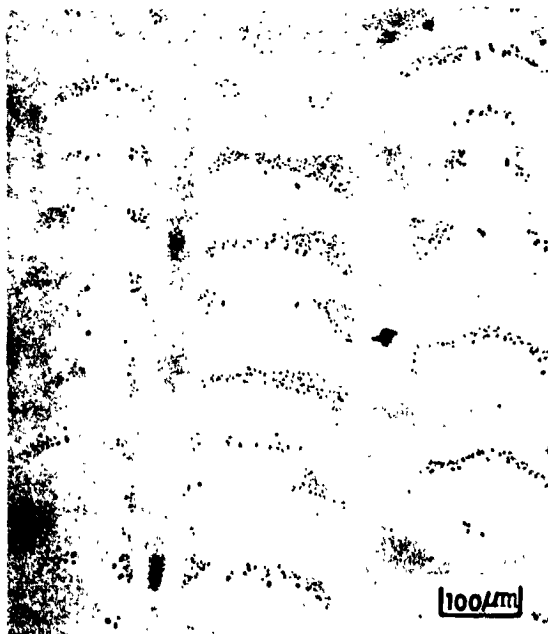


P78644-1

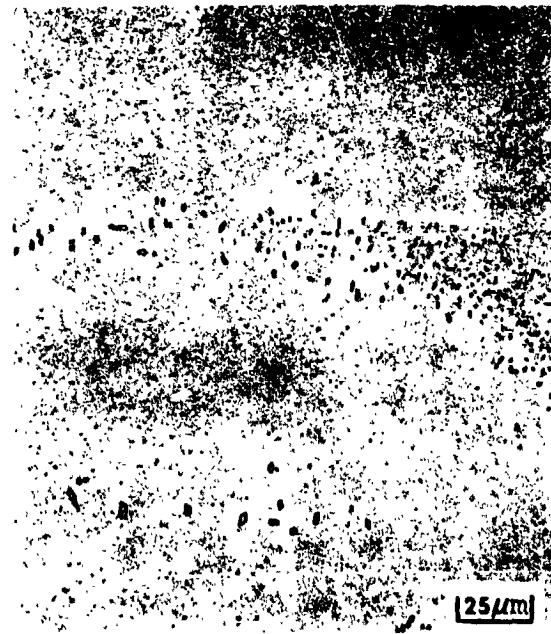


P78644-2

a. PRETEST MICROSTRUCTURE



P78644-3

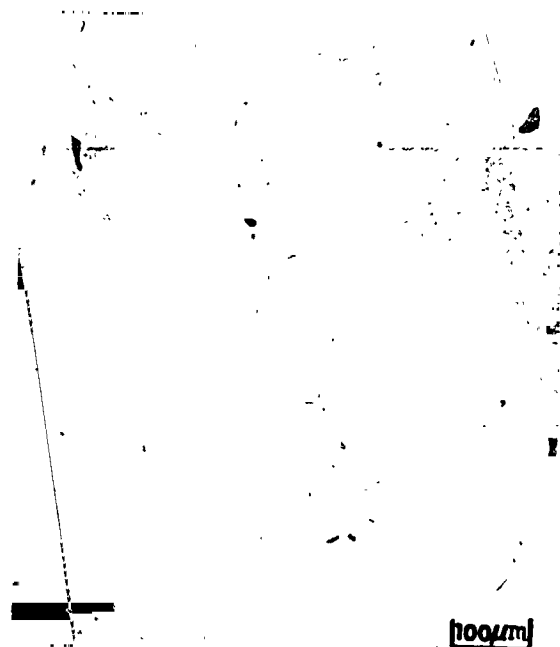


P78644-4

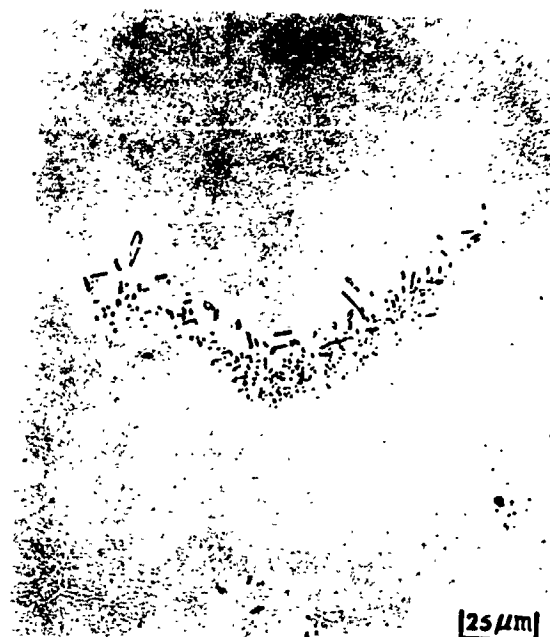
- b. 760°C (1400°F) - 500 HOURS FOR 758 MPa (110 KSI)  
PLUS 290.2 HOURS FOR 793 MPa (115 KSI)

Figure 31. Pretest and Stress-Rupture Tested Microstructures  
of SC Alloy 1, Part 1.

ORIGINAL PAGE IS  
OF POOR QUALITY

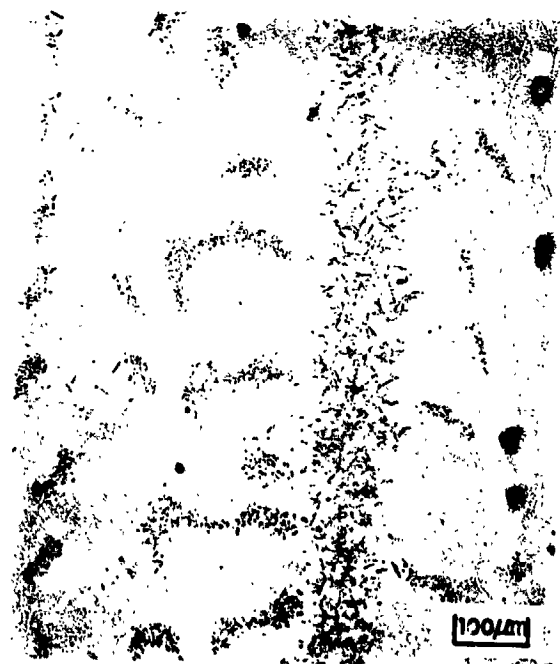


P78643-1



P78643-2

c. 982°C (1800°F) - 189.3 HOURS AT 207 MPa (30 KSI)



P78643-3



P78643-4

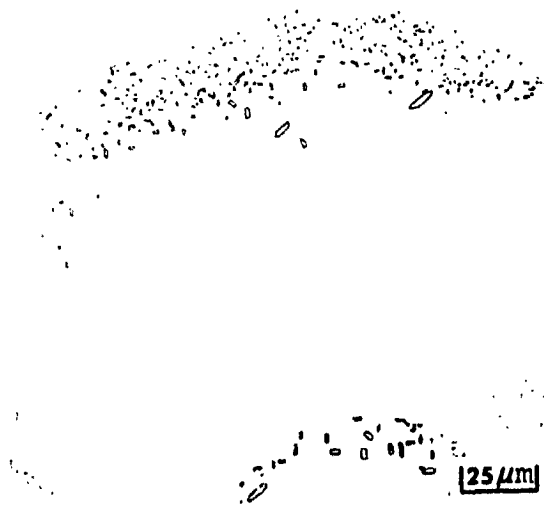
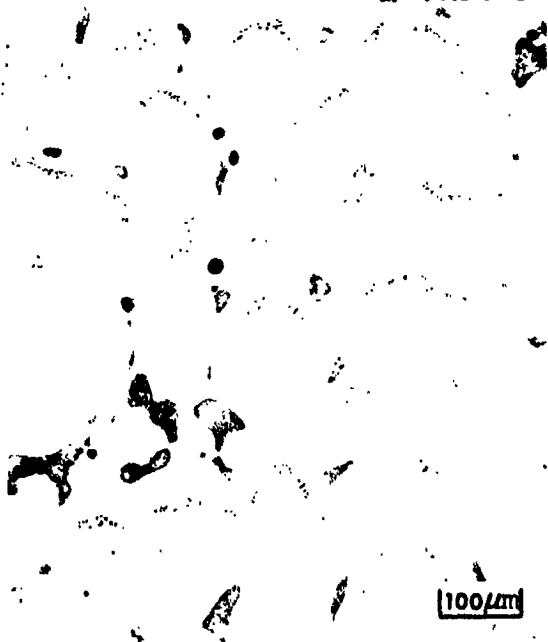
d. 1093°C (2000°F) - 501.8 HOURS AT 103 MPa (15 KSI)

Figure 32. Pretest and Stress-Rupture Tested Microstructures  
of SC Alloy 1, Part 2.

ORIGINAL PAGE 18  
OF POOR QUALITY



**a. PRETEST MICROSTRUCTURE**



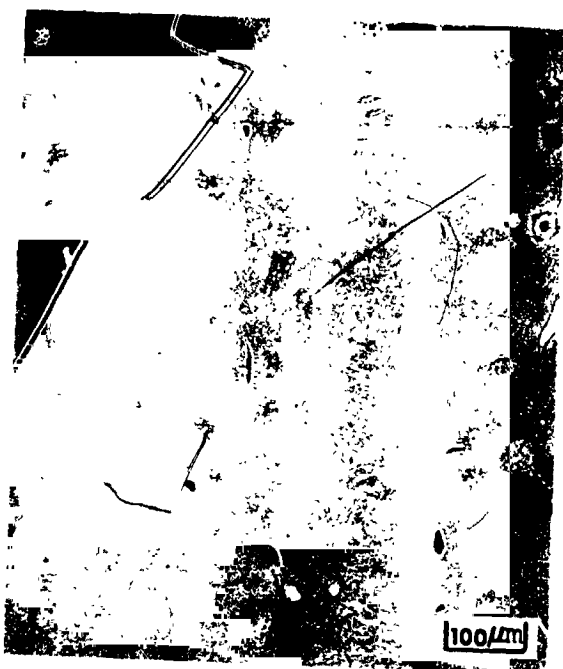
P78642-3

P78642-4

b. 760°C (1400°F) – 500 HOURS FOR 758 MPa (110 KSI) PLUS 122 HOURS FOR  
793 MPa (115 KSI)

Figure 33. Pretest and Stress-Rupture-Tested Microstructures  
of SC Alloy 2, Part 1.

ORIGINAL PAGE IS  
OF POOR QUALITY



P78649-1



P78649-2

c. 982°C (1800°F) - 217 HOURS AT 207 MPa (30 KSI)



P78649-3



P78649-4

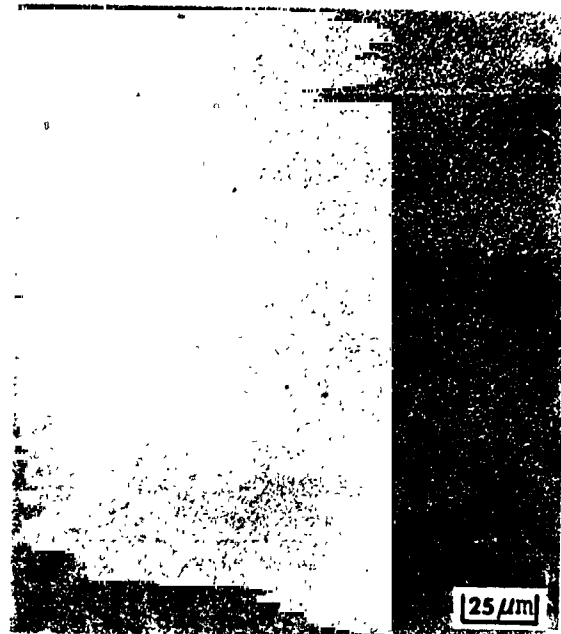
d. 1093°C (2000°F) - 458.4 HOURS AT 103 MPa (15 KSI)

Figure 34. Pretest and Stress-Rupture Tested Microstructures  
of SC Alloy 2, Part 2.

ORIGINAL PAGE IS  
OF POOR QUALITY

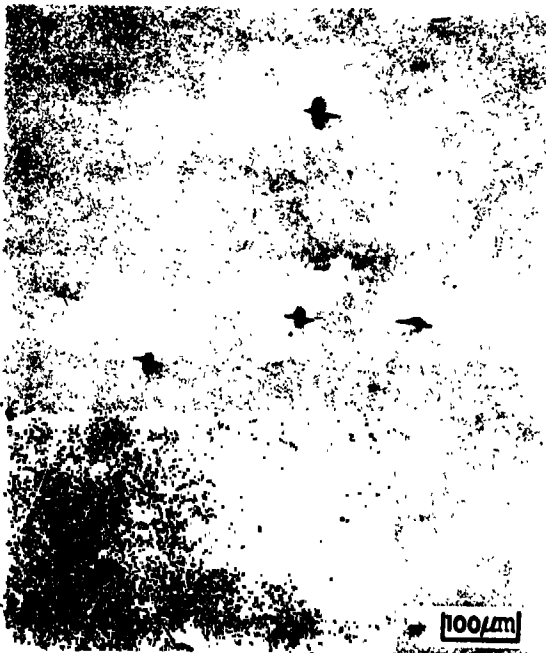


P78645-1



P78645-2

a. PRETEST MICROSTRUCTURE.



P78645-3



P78645-4

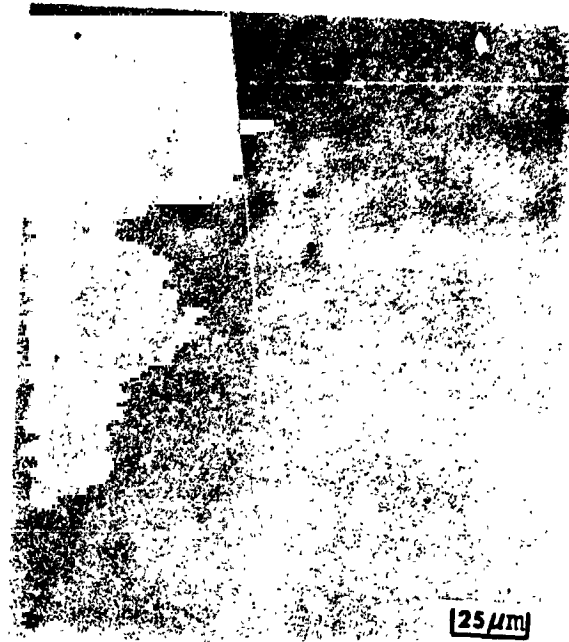
b. 760°C (1400°F) — 317.8 HOURS AT 758 MPa (110 KSI).

Figure 35. Pretest and Stress-Rupture-Tested Microstructures  
of SC Alloy 3, Part 1.

ORIGINAL PAGE IS  
OF POOR QUALITY



P78646-1



P78646-2

c. 982°C (1800°F) – 180.2 HOURS AT 207 MPa (30 KSI)



P78646-3



P78646-4

d. 1093°C (2000°F) – 247.8 HOURS AT 103 MPa (15 KSI)

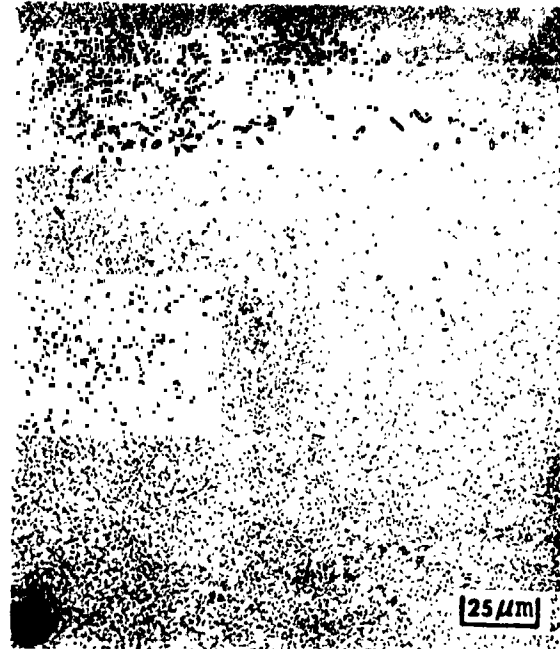
Figure 36. Pretest and Stress-Rupture Tested Microstructures  
of SC Alloy 3, Part 2.



ORIGINAL PAGE IS  
OF POOR QUALITY



P78647-1

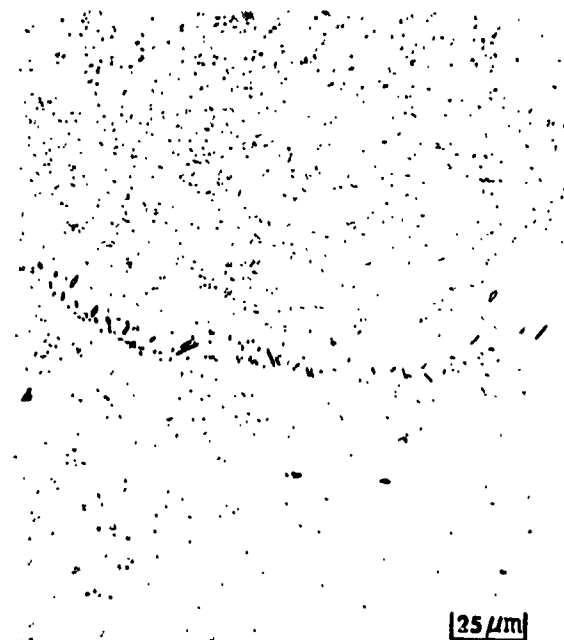


P78647-2

a. PRETEST MICROSTRUCTURE.



P78647-3



P78647-4

b. 760°C (1400°F) – 500 HOURS FOR 758 MPa (110 KSI) PLUS 394.2 HOURS  
FOR 794 MPa (115 KSI).

Figure 37. Pretest and Stress-Rupture Tested Microstructures  
of SC Alloy 4, Part 1.

ORIGINAL PAGE IS  
OF POOR QUALITY



P78648-1

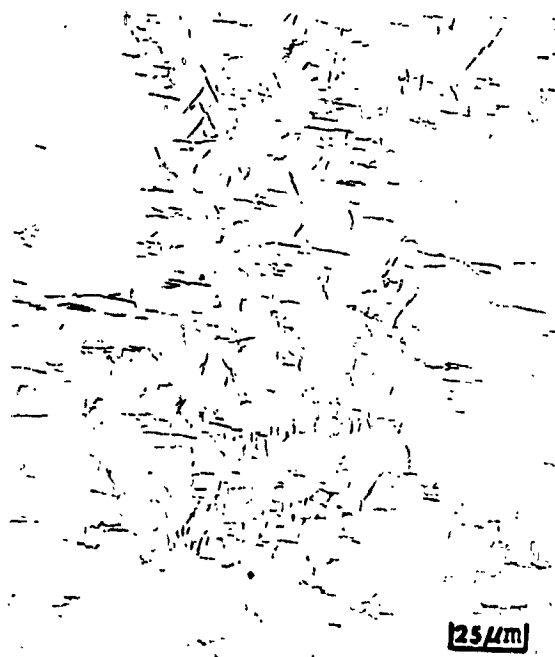


P78648-2

c. 982°C (1800°F) – 251.4 HOURS AT 207 MPa (30 KSI)



P78648-3



P78648-4

d. 1093°C (2000°F) – 457.2 HOURS AT 103 MPa (15 KSI)

Figure 38. Pretest and Stress-Rupture-Tested Microstructures  
of SC Alloy 4, Part 2.

than the dendrite cores and were free of tungsten-rich secondary phases.]

#### 5.3.7 Oxidation Evaluation

Burner-rig cyclic-oxidation tests were conducted at 1093°C (2000°F) for 100 hours. Pre- and post-test measurements of the specimens indicated that SC Mar-M 247 and Alloys 1 through 5 all exhibited metal losses less than or equal to 25  $\mu\text{m}$  (0.001 inch). Metallographic examination indicated that, in addition to the material loss, a  $\gamma'$  depletion zone was present in the alloy adjacent to the surface; the thickness of the alloy depletion zone varied from about 25 to 64  $\mu\text{m}$  (0.001 to 0.0025 inch). This test confirmed that the SC alloys would require protective coatings for use in advanced commercial engines. (Protective coatings are evaluated in the next section).

#### 5.3.8 Density

Densities of SC turbine blades cast from Mar-M 247 and Alloys 1 through 4 as determined by the water immersion method are presented in Table 23. These densities were in excellent agreement with predicted densities from the paper alloy study.

TABLE 23. DENSITIES OF SINGLE-CRYSTAL TFE731  
TURBINE BLADE CASTINGS.

Alloy	Density	
	gm/cc	(lb/in. <sup>3</sup> )
Mar-M 247	8.62	(0.311)
Modified Alloy 1	8.62	(0.311)
Modified Alloy 2	8.62	(0.311)
Modified Alloy 3	8.62	(0.311)
Modified Alloy 4	8.63	(0.312)

### 5.3.9 Improper Processing

ORIGINAL PAGE IS  
OF POOR QUALITY

As noted previously, mechanical property data was obtained in two instances for SC alloys that were improperly processed. The first instance involved zirconium contamination (from a zirconia crucible), while the second was associated with slow cooling from the solutioning temperature. Stress-rupture test results at 1093°C (2000°F) and 103 MPa (15 ksi) are provided in Figure 39. These results illustrate the magnitude of life reduction associated with the improperly processed material.

Test data for zirconium contaminated SC Alloys 1 through 5 are provided in Tables 24 to 28, respectively, which show that not one of the alloys realized its rupture life potential. This result is predominantly attributed to use of a nonoptimum solution heat treatment temperature, 1260°C (2300°F), to avoid substantial incipient melting.

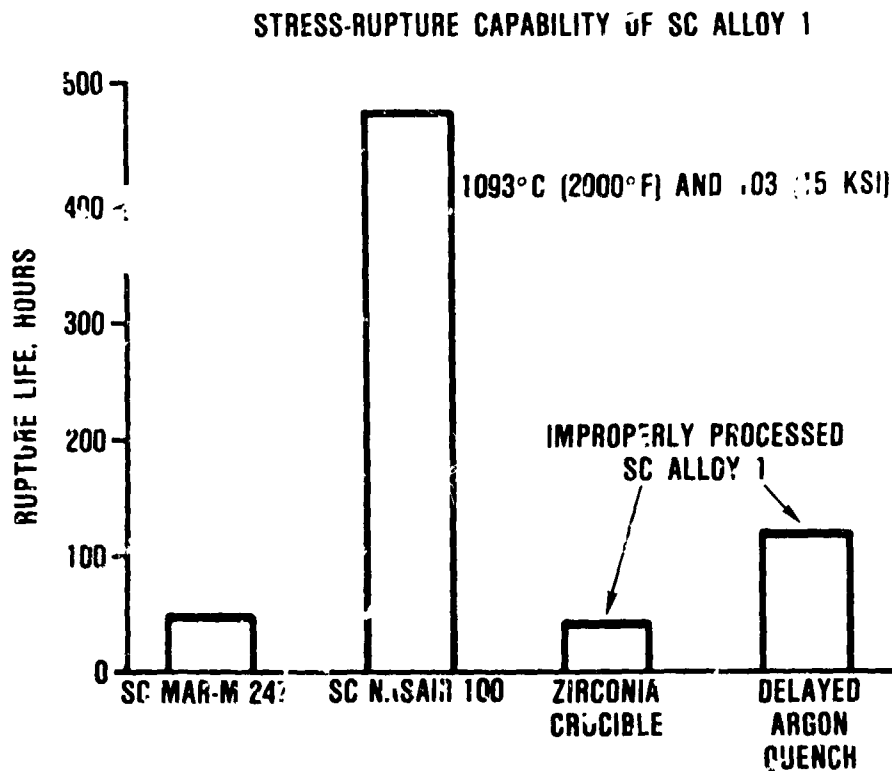


Figure 39. Effect of Improper Processing on Stress-Rupture Capability of SC Alloy 1.

ORIGINAL PAGE IS  
OF POOR QUALITY

TABLE 24. STRESS-RUPTURE TEST RESULTS ON 1.8 MM (0.070 INCH) DIAMETER LONGITUDINAL TEST SPECIMENS MACHINED FROM SINGLE-CRYSTAL TURBINE BLADES OF HEAT-TREATED\* ALLOY 1+Zr.

Specimen Number	Temperature °C (°F)	Stress MPa (ksi)	Rupture Life (Hours)	Elongation (%)	R of A (%)
426-1L	982 (1800)	207 (30)	71.8	13.9	24.8
426-3L	982 (1800)	207 (30)	79.0	22.6	45.6
426-2L	1038 (1900)	131 (19)	121.2	17.3	34.7
426-5L	1038 (1900)	131 (19)	113.8	17.5	39.2
426-9L	1038 (1900)	131 (19)	129.6	22.2	36.1
426-4L	1093 (2000)	103 (15)	41.2	29.5	58.2
426-7L	1093 (2000)	103 (15)	43.4	30.0	49.8
*1260°C (2300°F) for 2 hours with Argon Quench, plus 982°C (1800°F) for 5 hours, plus 871°C (1600°F) for 20 hours.					

TABLE 25. STRESS-RUPTURE TEST RESULTS ON 1.8 MM (0.070 INCH) DIAMETER LONGITUDINAL TEST SPECIMENS MACHINED FROM SINGLE-CRYSTAL TURBINE BLADES OF HEAT-TREATED\* ALLOY 2+Zr.

Specimen Number	Temperature °C (°F)	Stress MPa (ksi)	Rupture Life (Hours)	Elongation (%)	R of A (%)
433-1L	982 (1800)	207 (30)	77.8	44.6	54.1
433-5L	982 (1800)	207 (30)	72.2	28.1	44.8
433-6L	1038 (1900)	131 (19)	109.7	30.5	53.7
433-8L	1038 (1900)	131 (19)	106.1	29.2	52.6
433-2L	1093 (2000)	103 (15)	25.2	32.8	58.8
433-7L	1093 (2000)	103 (15)	38.3	29.7	59.1
*1260°C (2300°F) for 2 hours with Argon Quench, plus 982°C (1800°F) for 5 hours, plus 871°C (1600°F) for 20 hours.					

ORIGINAL PAGE IS  
OF POOR QUALITY

TABLE 26. STRESS-RUPTURE TEST RESULTS ON 1.8 MM (0.070 INCH) DIAMETER LONGITUDINAL TEST SPECIMENS MACHINED FROM SINGLE-CRYSTAL TURBINE BLADES OF HEAT-TREATED\* ALLOY 3+Zr.

Specimen Number	Temperature °C (°F)	Stress MPa (ksi)	Rupture Life (Hours)	Elongation (%)	R of A (%)
428-9L	760 (1400)	724 (105)	132.1	14.9	15.4
447-8L	760 (1400)	724 (105)	141.4	12.8	17.6
447-2L	982 (1800)	207 (30)	69.9	33.2	38.9
447-6L	982 (1800)	207 (30)	81.8	17.2	24.1
428-10L	1038 (1900)	131 (19)	158.3	25.3	38.5
447-4L	1038 (1900)	131 (19)	229.3	30.3	73.5
447-7L	1038 (1900)	131 (19)	100.2	3.5	7.3
447-1L	1093 (2000)	103 (15)	77.3	10.6	39.1
447-3L	1093 (2000)	103 (15)	69.1	23.6	64.7

\*1260°C (2300°F) for 2 hours with Argon Quench, plus 982°C (1800°F) for 5 hours, plus 871°C (1600°F) for 20 hours.

TABLE 27. STRESS-RUPTURE TEST RESULTS ON 1.8 MM (0.070 INCH) DIAMETER LONGITUDINAL TEST SPECIMENS MACHINED FROM SINGLE-CRYSTAL TURBINE BLADES OF HEAT-TREATED\* ALLOY 4+Zr.

Specimen Number	Temperature °C (°F)	Stress MPa (ksi)	Rupture Life (Hours)	Elongation (%)	R of A (%)	Remarks
431-2L	760 (1400)	724 (105)	101.5	10.5	17.6	Casting Porosity
431-9L	760 (1400)	724 (105)	131.3	12.1	27.0	
413-1L	982 (1800)	207 (30)	45.1	3.8	7.3	
431-4L	982 (1800)	207 (30)	80.4	28.8	37.8	
413-2L	1038 (1900)	131 (19)	82.1	14.5	38.5	
413-3L	1038 (1900)	131 (19)	71.9	14.3	30.0	
431-7L	1038 (1900)	131 (19)	92.7	16.5	39.4	
413-5L	1093 (2000)	103 (15)	26.5	11.8	34.1	
413-7L	1093 (2000)	103 (15)	24.5	15.9	41.8	

\*1260°C (2300°F) for 2 hours with Argon Quench, plus 982°C (1800°F) for 5 hours, plus 871°C (1600°F) for 20 hours.

ORIGINAL PAGE IS  
OF POOR QUALITY

TABLE 28. STRESS-RUPTURE TEST RESULTS ON 1.8 MM (0.070 INCH) DIAMETER LONGITUDINAL TEST SPECIMENS MACHINED FROM SINGLE-CRYSTAL TURBINE BLADES OF HEAT-TREATED ALLOY 5+Zr.

Specimen Number	Temperature °C (°F)	Stress MPa (ksi)	Rupture Life (Hours)	Elongation (%)	R of A (%)
432-6L	760 (1400)	724 (105)	156.3	14.0	17.2
432-9L	760 (1400)	724 (105)	99.6	6.8	22.9
414-1L	982 (1800)	207 (30)	50.8	15.0	32.3
414-3L	982 (1800)	207 (30)	54.7	14.4	20.1
414-4L	1038 (1900)	131 (19)	78.3	12.5	31.7
414-6L	1038 (1900)	131 (19)	102.2	11.9	22.9
432-5L	1038 (1900)	131 (19)	107.2	22.1	41.2
414-8L	1093 (2000)	103 (15)	39.0	9.5	27.8
414-10L	1093 (2000)	103 (15)	32.7	10.5	24.9

\*1260°C (2300°F) for 2 hours with Argon Quench, plus 982°C (1800°F) for 5 hours, plus 871°C (1600°F) for 20 hours.

Effects of slow cooling from the solutioning temperature were reductions in tensile strength and rupture life as illustrated for SC Alloy 1 in Tables 29 and 30, respectively. As discussed previously, these reductions were associated with a significantly coarser gamma-prime size (see Figure 30).

#### 5.3.10 SC Alloy Selection

Based on stress-rupture and tensile data, casting yields, alloy composition, and microstructural stability, SC Alloys 1 and 3 were selected for design property characterization and component fabrication for engine evaluation.

SC Alloy 1, subsequently renamed SC NASAIR 100, was selected on the basis of its high stress-rupture and tensile properties, plus the best yield in the casting trials. Although the mu phase

ORIGINAL PAGE 13  
OF POOR QUALITY

TABLE 29. TENSILE TEST RESULTS ON 1.8 MM (0.070 INCH) DIAMETER TEST SPECIMENS MACHINED FROM SC ALLOY 1 TURBINE BLADES THAT WERE IMPROPERLY HEAT TREATED.\*

Specimen Number	Master Heat	Orientation	Temperature C° (°F)	UTS MPa (ksi)	0.2% Y.S. MPa (ksi)	Elongation (%)	R of A (%)
427-2L-2	VF-154	Longitudinal	RT	876 (127)	827 (120)	12.8	18.3
508-2L-2	VF-154	Longitudinal	RT	924 (134)	827 (120)	17.4	23.0
427-7L-2	VF-154	Longitudinal	760 (1400)	1131 (164)	1076 (156)	10.1	15.3
509-1L-2	VF-154	Longitudinal	760 (1400)	1220 (177)	1179 (171)	8.6	15.7
427-1L-2	VF-154	Longitudinal	871 (1600)	1034 (150)	910 (132)	14.7	18.7
508-1L-2	VF-154	Longitudinal	871 (1600)	1020 (148)	910 (132)	15.2	21.8
427-5L-2	VF-154	Longitudinal	982 (1800)	648 (94)	517 (75)	25.5	31.4
509-7L-2	VF-154	Longitudinal	982 (1800)	731 (106)	621 (90)	15.3	20.8
427-3L-2	VF-154	Longitudinal	1093 (2000)	434 (63)	352 (51)	31.7	49.7
509-5L-2	VF-154	Longitudinal	1093 (2000)	407 (59)	338 (49)	36.0	49.4
*Heat treatment consisted of 1316°C (2400°F) for 2 hours, plus 1324°C (2415°F) for 2 hours with Argon Quench, plus 982°C (1800°F) for 5 hours, plus 871°C (1600°F) for 20 hours. Fan cooling was not activated until blades had cooled to 1038°C (1900°F) resulting in lower strength than previously measured.							

was of concern based on previous experience in other alloy systems with sigma, the mu level present in NASAIR 100 was a small volume fraction and did not have any significant effect on the properties evaluated.

SC Alloy 3 was selected on the basis of microstructural stability--e.g., freedom from the mu phase and good castability. The stress-rupture capability of SC Alloy 3 was also a significant improvement relative to that of DS Mar-M 247, but was less than SC NASAIR 100.



ORIGINAL PAGE IS  
OF POOR QUALITY

TABLE 30. STRESS-RUPTURE RESULTS ON 1.8 MM (0.070 INCH)  
DIAMETER SPECIMENS MACHINED FROM SC ALLOY 1  
TURBINE BLADES THAT WERE IMPROPERLY HEAT  
TREATED.\*

Specimen Number	Orientation	Temp. °C (°F)	Stress MPa (ksi)	Life (Hours)	Rupture Elongation (%)	R of A (%)
427-7L-1	Longitudinal	760 (1400)	827 (120)	40.3	8.4	38.3
427-7T	Transverse	760 (1400)	827 (120)	20.4	8.9	26.0
508-1L-1	Longitudinal	871 (1600)	400 (58)	217.3	16.7	31.5
508-1T	Transverse	871 (1600)	517 (75)	40.7	12.3	28.2
427-5L-1	Longitudinal	982 (1800)	172 (25)	1085.0	11.9	25.6
509-7L-1	Longitudinal	1038 (1900)	131 (19)	192.1	12.8	38.5
427-3L-1	Longitudinal	1093 (2000)	103 (15)	121.2	16.2	33.0
509-5L-1	Longitudinal	1093 (2000)	90 (13)	202.5	12.6	33.7
*Heat treatment consisted of 1316°C (2400°F) for 2 hours, plus 1324°C (2415°F) for 2 hours with Argon Quench, plus 982°C (1800°F) for 5 hours, plus 871°C (1600°F) for 20 hours. Fan cooling was not activated until blades had cooled to 1038°C (1900°F) resulting in lower strength than previously measured.						

## SECTION VI

### 6.0 ALLOY PROPERTY CHARACTERIZATION

Two SC alloys, NASAIR 100 (formerly Alloy 1) and Alloy 3, were characterized for mechanical, environmental, and physical properties to validate the final design of the turbine blade. This was accomplished by casting additional turbine blades and test bars at Jetshapes, followed by comprehensive testing of castings and test specimens by Garrett and independent laboratories.

#### 6.1 Test Material Production

##### 6.1.1 Master Alloys

Seven hundred and twenty-five kilograms (1600 pounds) of NASAIR 100 and 297 kilograms (655 pounds) of Alloy 3 were procured from Cannon-Muskegon to be used for design data generation and component manufacture (Section VIII). These alloys were provided in the form of small 120 to 150 kg (265 to 331 lb) master heats. Comparisons of master melt and alloy specifications are provided in Tables 31 and 32 for NASAIR 100 and Alloy 3, respectively. Inspection of these chemistries indicates that all of the heats were acceptable. In addition, a portion of NASAIR 100 (Alloy 1) heat VF-154 remained from the alloy development task and was used to cast three molds; consequently, this heat chemistry is also included in Table 31.

##### 6.1.2 Blade and Specimen Castings

SC TFE731 blades, bars, and rectangular slab castings were produced--using the casting technology described in Section III--to provide test material for the SC alloy property evaluations.

ORIGINAL PAGE IS  
OF POOR QUALITY

TABLE 31. NASAIR 100 MASTER MELT CHEMISTRIES (WEIGHT PERCENT).

Element	Specification Range %	Heat							
		VF-154	VF-219	VF-220	VF-232	VF-235	VF-236	VF-237	VF-437
Mo	0.8-1.2	0.8	1.0	1.0	1.0	0.9	1.0	1.0	1.0
W	10.0-11.0	10.4	10.2	10.3	10.4	10.5	10.4	10.4	10.5
Ta	3.1-3.5	3.4	3.3	3.4	3.3	3.3	3.3	3.3	3.3
Ti	1.0-1.4	1.1	1.0	1.0	1.0	1.1	1.1	1.1	1.14
Cr	8.5-9.5	9.0	9.1	8.8	8.8	8.7	8.8	8.9	9.0
Co	0.5 max	--	<0.1	<0.1	<0.1	<0.1	<0.15	<0.1	<0.1
Al	5.6-5.9	5.8	5.7	5.6	5.7	5.6	5.8	5.7	5.7
Zr	0.03 max	0.01	<0.01	<0.01	<0.01	<0.01	<0.01	<0.01	<0.006
B	0.002 max	--	<0.002	<0.002	-	-	-	-	0.0018
C	0.006 max	0.0034	<0.0025	<0.003	<0.003	<0.005	<0.006	-	<0.0002
Ni	Balance	Balance	Balance	Balance	Balance	Balance	Balance	Balance	Balance

NOTE: Cannon-Muskegon Certification Chemical Analysis

TABLE 32. ALLOY 3 MASTER MELT CHEMISTRIES (WEIGHT PERCENT).

Element	Alloy 3 Specification	VF-291	Heat VF-292	VF-442
Mo	0.65-0.95	0.8	0.8	0.8
W	9.0-10.0	9.5	9.5	9.5
Ta	3.1-3.5	3.3	3.3	3.3
Ti	0.9-1.2	1.0	1.0	1.0
Cr	8.0-9.0	8.6	8.6	8.6
Co	4.5-5.5	5.0	5.0	5.0
Al	5.5-5.8	5.8	5.8	5.6
Hf	0.2-0.3	0.25	0.25	0.24
C	0.006 Max	<0.003	<0.003	0.0026
B	0.002 Max	NA	NA	0.002
Zr	0.03 Max	<0.01	<0.01	<0.01
Ni	Balance	Balance	Balance	Balance

NA : Not analyzed.

Results from this casting campaign are reviewed in Tables 33 through 35 for SC NASAIR 100 and SC Alloy 3 TFE731 blades, bars, and burner-rig specimens, respectively. These tables indicate that of the blades, bars, and burner-rig specimens that were filled with metal, yields of material suitable for testing were 49, 63, and 61 percent, respectively.

Compositional analyses of SC NASAIR 100 and SC Alloy 3 blades cast during the campaign are provided in Tables 36 and 37. All of the blades analyzed were either within or very close to the specification limits. The minor deviations indicated are not considered significant.

TABLE 33. VISUAL INSPECTION RESULTS FOR SC TFE731 BLADES OF NASAIR 100 AND ALLOY 3.

Alloy	Mold No.	Blades Filled with Metal	Single-Crystal Airfoil and Root*
NASAIR 100	427	10	0
	457	2	1
	458	12	8
	508	3	1
	509	10	3
	511	12	3
	512	10	4
	513	10	4
	591	12	7
	647	12	2
	648	12	9
Alloy 3	675	11	4
	688	12	9
	691	10	2
*[001] grain orientation within 15° of the blade axis.			

ORIGINAL PAGE IS  
OF POOR QUALITY

TABLE 34. VISUAL INSPECTION RESULTS FOR SC BAR CASTINGS.

Alloy	Mold No.	Bars Filled with Metal	SC Bars Acceptable for Fatigue Testing*
NASAIR 100	521	14	2
	544	12	12
	547	6	3
	552	12	8
	553	12	7
	567	12	10
	568	12	10
	569	12	11
	570	12	10
	653	12	4
Alloy 3	582	12	7
	666	12	5
	687	7	5
	689	7	7
	695	12	6
	709	12	10

\*[001] grain orientation within 15° of the bar axis.

TABLE 35. VISUAL EXAMINATION OF BURNER-RIG SPECIMEN CASTINGS.

Alloy	Mold No.	Specimens Filled with Metal	Single-Crystal Specimens
NASAIR 100	548	10	5
NASAIR 100	549	12	8
Alloy 3	655	12	7
Alloy 3	673	12	8

ORIGINAL PAGE  
OF POOR QUALITY

During the casting campaign, test material was selected by etching the blades and bars and visually examining them for [001] orientation within 15 degrees of the bar or blade axis. A limited number of confirmatory tests for orientation were conducted using the Laué method at Technology of Materials in Santa Barbara, California. Laué inspection results, provided in Table 38, confirmed the orientations determined by visual examination in all cases.

TABLE 36. CHEMISTRIES OF SC NASAIR 100 TFE731 TURBINE BLADES.

Mold No.	Blade No.	Heat No.	COMPOSITION (WEIGHT PERCENT)										
			Mo	W	Ta	Ti	Cr	Co	Al	Zr	B	C	Ni
427	427-8	VF-154	0.81	10.6	3.51	1.06	8.95	0.1	5.6	<0.01	<0.002	0.004	Bal
508	508-3	VF-154	0.81	10.4	3.51	1.06	9.02	0.1	5.8	<0.01	<0.002	0.003	Bal
509	509-8	VF-154	0.89	10.5	3.44	1.04	9.24	0.1	5.7	<0.01	<0.002	0.006	Bal
511	511-1	VF-220	0.99	10.5	3.25	0.96	9.87	0.1	5.5	<0.01	<0.002	0.005	Bal
513	513-10	VF-220	0.97	10.4	3.30	0.98	9.97	0.1	5.6	<0.01	<0.002	0.005	Bal
591	591-30	VF-235	0.80	10.2	3.36	1.02	9.68	0.1	5.7	<0.03	<0.002	0.004	Bal
647	647-10	VF-235	0.94	10.6	3.50	1.05	9.21	0.1	5.6	<0.01	<0.002	0.006	Bal
648	648-11	VF-235	0.82	10.5	3.52	1.00	9.50	0.1	5.6	<0.01	0.002	0.003	Bal
	Specification Range	Min.	0.8	10.0	3.1	1.0	8.5	0.5	5.6	0.03	0.002	0.006	Bal
		Max.	1.2	11.0	3.5	1.4	9.5	Max.	5.9	Max.	Max.	Max.	Bal

Analysis performed by the Garrett Turbine Engine Company.

TABLE 37. CHEMISTRIES OF SC ALLOY 3 TURBINE BLADES.

Mold No.	Blade No.	Heat No.	COMPOSITION (WEIGHT PERCENT)											
			Mo	W	Ta	Ti	Cr	Co	Al	Hf	Zr	B	C	Ni
675	675-11	VF-292	0.78	9.5	3.25	0.96	8.20	5.2	5.5	0.27	<0.01	<0.002	0.006	Bal
688	688-10	VF-292	0.76	9.4	3.20	0.90	8.90	5.2	5.6	0.30	<0.01	<0.002	0.006	Bal
691	691-7	VF-292	0.76	9.6	3.30	0.90	8.90	5.1	5.5	0.30	<0.01	<0.002	0.004	Bal
	Speci- fication Range	Min	0.65	9.0	3.1	0.9	8.0	4.5	5.5	0.2	0.03	0.002	0.006	Bal
		Max	0.95	10.0	3.5	1.2	9.0	5.5	5.8	0.3	Max	Max	Max	

Analysis performed by The Garrett Turbine Engine Company.

ORIGINAL PAGE IS  
OF POOR QUALITY

Alloy	Visual Orientation of Blade*	Laue Orientation Blade* MFB Specimen**
SC NASAIR 100	$\leq 15^\circ$ of [001]	$12^\circ$ of [001]
SC NASAIR 100	$\leq 15^\circ$ of [001]	$14^\circ$ of [001]
SC NASAIR 100	$\leq 15^\circ$ of [001]	$3.2^\circ$ of [001]
SC NASAIR 100	$> 15^\circ$ of [001]	$31^\circ$ of [001]
SC NASAIR 100	$> 15^\circ$ of [001]	$34^\circ$ of [001]
SC NASAIR 100	$\leq 15^\circ$ of [001]	$1.5^\circ$ of [001]
SC NASAIR 100	$\leq 15^\circ$ of [001]	$8^\circ$ of [001]
SC Alloy 3	$\leq 15^\circ$ of [001]	$15.5^\circ$ of [001]
SC Alloy 3	$\leq 15^\circ$ of [001]	$4^\circ$ of [001]
SC Alloy 3	$\leq 15^\circ$ of [001]	$8^\circ$ of [001]
*Orientation from the blade stacking axis.		
**Orientation from the specimen axis.		

To assess the potential significance of mu phase precipitation, fully heat-treated SC NASAIR 100 and SC Alloy 3 blades and bars were exposed at  $982^\circ\text{C}$  ( $1800^\circ\text{F}$ ) for 1000 hours.

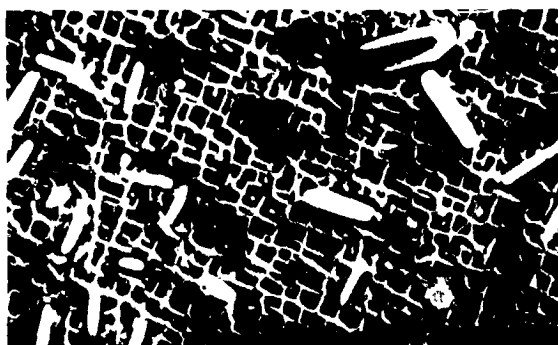
Metallographic and scanning electron microscope (SEM) examination (Figure 40) to assess the effect of exposure on NASAIR 100 and Alloy 3 microstructural stability indicated that the major effect of 1000-hours exposure on both alloys was gamma-prime coarsening, with NASAIR 100 also exhibiting some acicular phase (mu) in the dendritic areas. Alloy 3 exhibited no evidence of topologically close-packed phases.

Extraction and identification of secondary phases was performed by Dr. J. F. Radavich of Micromet Laboratories in West Lafayette, Indiana. Results of this evaluation, provided in Table 39, and indicate that the following secondary phases were observed in addition to the gamma and gamma-prime majority phases:

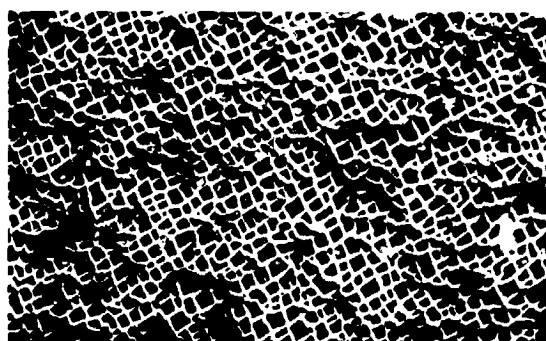
ORIGINAL PAGE IS  
OF POOR QUALITY

SC NASAIR 100

SC ALLOY 3



$\gamma$ ,  $\gamma'$ ,  $\alpha$  - W

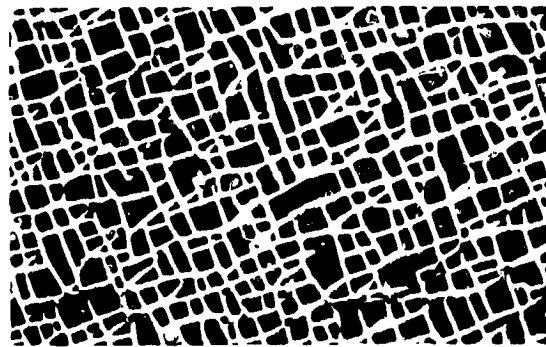


$\gamma$ ,  $\gamma'$

FULLY PROCESSED



Mu PRECIPITATION  
 $\gamma'$  COARSENING



$\gamma'$  COARSENING

P72137-9

5000X MAG

FULLY PROCESSED + 982 C (1800 F)/1000 HOURS

Figure 40. Furnace Exposure Effects on SC Alloy  
Microstructure.



TABLE 39. RESULTS OF SECONDARY PHASE EXTRACTION AND CHARACTERIZATION OF SC NASAIR 100 AND SC ALLOY 3 TURBINE BLADE CASTINGS.

Alloy	Condition	Relative Amount of Phases			
		MC	TiN	$\alpha$ W	mu
SC NASAIR 100	HT*	Weak	Weak	Strong	--
SC NASAIR 100	HT* +982°C (1800°F)/ 1000 hrs.	Weak	Weak	Strong	Strong
SC Alloy 3	HT**	Weak	Weak	--	--
SC Alloy 3	HT** +982°C (1800°F)/ 1000 hrs.	Weak	Weak	Weak	--
<p>HT* - Heat treatment consisted of 1316°C (2400°F) for 2 hours, plus 1324°C (2415°F) for 2 hours with rapid Argon Quench, plus 982°C (1800°F) for 5 hours, plus 871°C (1600°F) for 20 hours.</p> <p>HT** - Heat treatment consisted of 1288°C (2350°F) for 2 hours, plus 1296°C (2365°F) for 4 hours with rapid Argon Quench, plus 982°F (1800°F) for 5 hours, plus 871°C (1600°F) for 20 hours.</p>					

- o SC NASAIR 100 -  $\alpha$ W was the principal secondary phase that was detected in the fully processed microstructure; trace amounts of MC carbide and TiN phases were also detected. After the 1000-hour exposure at 982°C (1800°F), the mu phase was also identified as a principal secondary phase.
- o SC Alloy 3 - In the fully processed condition, only trace amounts of the MC carbide and TiN phases were detected. After the 1000-hour exposure at 982°C (1800°F), trace amounts of  $\alpha$ W were also identified. No mu phase was observed.

Following casting and inspections, blades and bars were heat treated, machined into test specimens, and tested. Results are provided in the following paragraphs.

## 6.2 Mechanical Properties

SC NASAIR 100 was characterized for tensile, creep-rupture, high-cycle fatigue (HCF), and low-cycle-fatigue (LCF) strengths. Similar data were obtained for SC Alloy 3, but in reduced quantities. These evaluations are reviewed in this section.

### 6.2.1 Tensile Properties

#### SC NASAIR 100

Tensile data for SC NASAIR 100 were obtained by Joliet Metallurgical Laboratories (Joliet, Illinois) over the range of 21° to 1093°C (70 to 2000°F), using 1.8 mm (0.070 inch) diameter minibars that were machined from TFE731 turbine blades (Figure 13). Blades tested in this evaluation were produced from four master heats. Test data for uncoated specimens are provided in Table 40 and average properties are shown graphically in Figure 41. Inspection of these data indicates that strength is maximum and ductility is minimum at 760°C (1400°F). The test results also indicated comparable tensile strengths for longitudinal and transverse specimens, provided orientations are within 15 degrees of [001] and within 15 degrees of [100], respectively. For transverse specimens with axes exceeding 15 degrees of the [100], strengths were generally lower.

Variability of tensile strength was also maximum at 760°C (1400°F) as shown in Figure 42. The amount of scatter observed is very similar to that found in SC Mar-M 247 (Figure 14). Based on

ORIGINAL PAGE IS  
OF POOR QUALITY

TABLE 40. TENSILE TEST RESULTS FOR 1.8 MM (0.070 INCH) DIAMETER TEST SPECIMENS MACHINED FROM SC NASAIR 100 TURBINE BLADES.

Specimen Number	Master Heat	Grain Orientation	Orientation			Temperature °C (°F)	UTS MPa (ksi)	0.2% Y.S. MPa (ksi)	Elongation (%)	R of A (%)
			Within 15 Degrees of [001]	Within 15 Degrees of [100]	>15 Degrees of [100]					
511-9L-2	VF-220	Longitudinal	X			21 (70)	972 (141)	945 (137)	13.0	17.9
511-12L-2	VF-220	Longitudinal	X			21 (70)	1027 (149)	972 (141)	13.2	19.0
648-1L-2	VF-235	Longitudinal	X			21 (70)	1027 (149)	986 (143)	16.0	23.9
648-3L-2	VF-235	Longitudinal	X			21 (70)	1106 (172)	1034 (150)	9.8	11.8
591-11L-2	VF-235	Longitudinal	X			21 (70)	1007 (146)	986 (143)	16.1	22.1
648-3T-2	VF-235	Transverse		X		21 (70)	986 (143)	958 (139)	19.5	28.2
511-7T-2	VF-220	Transverse			X	21 (70)	958 (139)	917 (133)	15.3	11.1
513-6T-2	VF-220	Transverse			X	21 (70)	903 (131)	869 (126)	19.1	22.4
646-2L-2	VF-235	Longitudinal	X			649 (1200)	1138 (165)	965 (140)	8.6	9.7
648-4L-2	VF-235	Longitudinal	X			649 (1200)	1110 (161)	958 (139)	11.6	12.5
591-15L-2	VF-235	Longitudinal	X			649 (1200)	1234 (179)	1034 (150)	5.8	6.9
648-4T-2	VF-235	Transverse		X		649 (1200)	1076 (156)	965 (140)	5.4	8.3
648-6T-2	VF-235	Transverse		X		649 (1200)	1089 (158)	938 (136)	10.0	11.8
648-7T-2	VF-235	Transverse		X		649 (1200)	1062 (154)	945 (137)	8.7	19.8
481-3L	VF-154	Longitudinal	X			760 (1400)	1379 (200)	1289 (187)	3.7	11.8
481-7L	VF-154	Longitudinal	X			760 (1400)	1407 (204)	1338 (194)	6.0	14.2
481-11L-1	VF-154	Longitudinal	X			760 (1400)	1358 (197)	1276 (185)	3.6	9.9
513-8L-1	VF-220	Longitudinal	X			760 (1400)	1303 (189)	1096 (159)	7.3	9.0
513-8L-2	VF-220	Longitudinal	X			760 (1400)	1262 (183)	1089 (158)	2.9	5.5
648-5L-2	VF-235	Longitudinal	X			760 (1400)	1255 (182)	1124 (163)	2.5	2.7
648-6L-2	VF-235	Longitudinal	X			760 (1400)	1420 (206)	1338 (194)	4.4	5.4
591-9L-2	VF-235	Longitudinal	X			760 (1400)	1358 (197)	1303 (189)	7.1	10.4
753-1L-1	VF-237	Longitudinal	X			760 (1400)	1379 (200)	1269 (184)	6.0	12.7
765-1L-1	VF-237	Longitudinal	X			760 (1400)	1319 (200)	1234 (179)	6.7	14.9
774-1L-1	VF-237	Longitudinal	X			760 (1400)	1351 (196)	1220 (177)	1.7	4.1
513-8T-1	VF-220	Transverse		X		760 (1400)	1262 (183)	1117 (162)	5.7	7.8
513-8T-2	VF-220	Transverse		X		760 (1400)	1255 (182)	1138 (165)	6.0	10.4
511-12T-2	VF-220	Transverse			X	760 (1400)	1110 (161)	896 (130)	11.8	13.8
481-1L-2	VF-154	Longitudinal	X			871 (1600)	1124 (163)	925 (134)	7.5	15.3
457-1L-2	VF-154	Longitudinal	X			871 (1600)	1124 (163)	986 (143)	13.3	17.4
511-11L-2	VF-220	Longitudinal	X			871 (1600)	1117 (162)	965 (140)	11.2	14.6
513-7L-2	VF-220	Longitudinal	X			871 (1600)	1151 (167)	1000 (145)	11.3	12.0
591-19L-1	VF-235	Longitudinal			X	871 (1600)	972 (141)	883 (128)	11.9	18.7
591-19L-2	VF-235	Longitudinal			X	871 (1600)	986 (143)	903 (131)	8.5	17.4
511-11T-2	VF-220	Transverse			X	871 (1600)	952 (138)	821 (119)	15.4	17.0
511-7T-2	VF-220	Transverse		X		871 (1600)	1083 (157)	1000 (145)	4.9	9.9
513-9T-2	VF-220	Transverse			X	871 (1600)	1014 (147)	929 (136)	13.7	17.9
481-2L-2	VF-154	Longitudinal	X			982 (1800)	862 (125)	648 (94)	17.4	18.3
511-10L-2	VF-220	Longitudinal	X			982 (1800)	821 (119)	717 (104)	17.9	25.1
513-9L-2	VF-220	Longitudinal	X			982 (1800)	827 (120)	738 (107)	17.3	25.3
648-7L-2	VF-235	Longitudinal	X			982 (1800)	841 (122)	731 (106)	23.5	36.5
591-21L-2	VF-235	Longitudinal	X			982 (1800)	827 (120)	696 (101)	26.8	28.6
591-22L-2	VF-235	Longitudinal	X			982 (1800)	862 (125)	724 (105)	22.5	31.9
481-2L-1	VF-154	Longitudinal	X			1093 (2000)	483 (70)	386 (56)	20.5	39.3
458-9L-2	VF-154	Longitudinal	X			1093 (2000)	510 (74)	400 (58)	14.1	50.1
511-7L-2	VF-220	Longitudinal	X			1093 (2000)	469 (68)	379 (55)	36.1	49.3
513-6L-2	VF-220	Longitudinal	X			1093 (2000)	469 (68)	365 (53)	26.8	39.0
648-8L-2	VF-235	Longitudinal	X			1093 (2000)	462 (67)	386 (56)	26.5	52.2
591-23L-2	VF-235	Longitudinal	X			1093 (2000)	483 (70)	338 (49)	29.4	59.0
511-9T-2	VF-220	Transverse			X	1093 (2000)	448 (65)	345 (50)	21.1	25.3
511-10T-2	VF-220	Transverse			X	1093 (2000)	441 (64)	338 (49)	23.8	29.4
591-9T-2	VF-235	Transverse		X		1093 (2000)	455 (66)	310 (45)	27.0	49.4

Heat Treatment consisted of 1316°C (2400°F) for 2 hours, plus 1324°C (2415°F) for 2 hours with Rapid Argon Quench, plus 982°C (1800°F) for 5 hours plus 871°C (1600°F) for 40 hours.

ORIGINAL PAGE IS  
OF POOR QUALITY

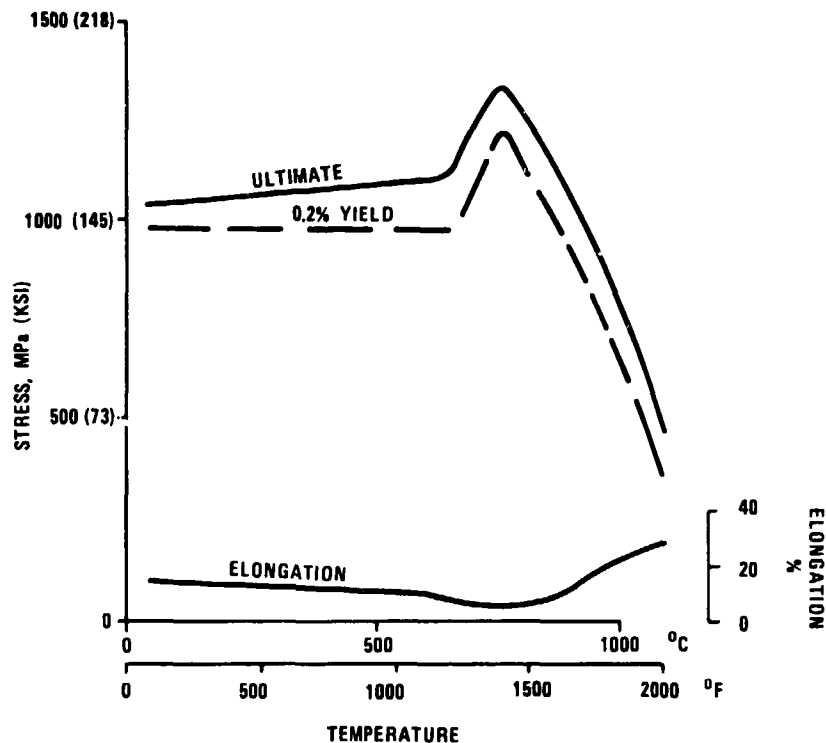


Figure 41. Average Tensile Properties of SC NASAIR 100 with Specimen Axis within  $15^\circ$  of  $\langle 001 \rangle$ .

the results for SC MAR-M 247, about half of the 250 MPa (36 ksi) width of the scatterband is attributable to permitting specimen orientation to vary within 15 degrees of the  $\langle 001 \rangle$ .

Tensile tests were also performed on diffusion aluminide (RT-21) coated 1.8 mm (0.070 inch) diameter minibar specimens. The test specimens were machined from solution heat-treated SC NASAIR 100 turbine blade castings, and then RT-21 coated by Chromalloy American Corporation, Orangeburg, New York, to a coating thickness of  $43\mu\text{m}$  (1.7 mils) followed by an  $871^\circ\text{C}$  ( $1600^\circ\text{F}$ ), 20 hours post-coat heat treatment. Tensile test results from room temperature to  $1093^\circ\text{C}$  ( $2000^\circ\text{F}$ ) for longitudinal and transverse orientations are provided in Table 41. The effects of coating on tensile properties were reduced ductility up to  $760^\circ\text{C}$  ( $1400^\circ\text{F}$ ) and

ORIGINAL PAGE IS  
OF POOR QUALITY

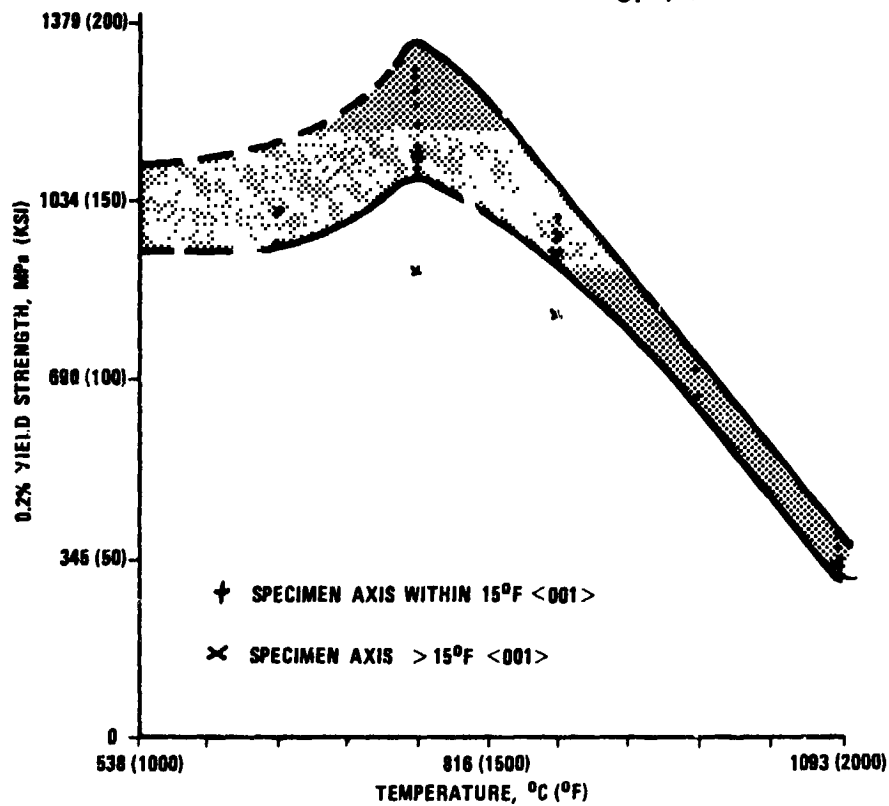


Figure 42. Yield Stress Data for SC NASAIR 100.

TABLE 41. TENSILE TEST RESULTS FOR DIFFUSION-ALUMINIDE (RT-21) COATED 1.8 MM (0.070 INCH) DIAMETER TEST SPECIMENS MACHINED FROM SC NASAIR 100 TURBINE BLADES.

Specimen Number	Master Heat	Grain Orientation	Orientation			Temperature °C (°F)	UTS MPa (ksi)	0.2% Y.S. MPa (ksi)	Elongation (%)	R of A (%)
			Within 15 Degrees of [001]	Within 15 Degrees of [100]	>15 Degrees of [100]					
511-8L-2	VF-220	Longitudinal	x			21 (70)	1172 (170)	1000 (145)	6.9	6.2
513-5L-2	VF-220	Longitudinal	x			21 (70)	1117 (162)	1000 (145)	9.6	8.3
511-4T-1	VF-220	Transverse			x	21 (70)	896 (130)	883 (128)	9.1	20.9
513-1T-1	VF-220	Transverse			x	21 (70)	910 (132)	889 (129)	13.9	17.9
511-6L-2	VF-220	Longitudinal	x			649 (1200)	1165 (169)	1007 (146)	4.4	8.5
513-4L-2	VF-220	Longitudinal	x			649 (1200)	1124 (163)	1014 (147)	5.3	7.6
511-5T-1	VF-220	Transverse		x		649 (1200)	1138 (165)	1014 (147)	2.5	2.8
513-3T-1	VF-220	Transverse		x		649 (1200)	1055 (153)	958 (139)	2.2	4.9
511-5L-2	VF-220	Longitudinal	x			649 (1400)	1338 (194)	1220 (177)	0.5	0.7
513-3L-2	VF-220	Longitudinal	x			649 (1400)	1310 (190)	1179 (171)	3.8	4.7
511-8T-1	VF-220	Transverse		x		649 (1400)	1282 (186)	1248 (181)	2.2	7.3
513-5T-1	VF-220	Transverse			x	649 (1400)	1260 (174)	1124 (163)	3.5	4.7
511-4L-2	VF-220	Longitudinal	x			871 (1600)	1103 (160)	979 (142)	14.7	18.5
513-2L-2	VF-220	Longitudinal	x			871 (1600)	1117 (162)	979 (142)	15.1	15.7
511-3L-2	VF-220	Longitudinal	x			1093 (2000)	441 (64)	331 (48)	31.1	48.6
513-1L-2	VF-220	Longitudinal	x			1093 (2000)	414 (60)	303 (44)	31.9	44.2
511-3T-1	VF-220	Transverse			x	1093 (2000)	427 (62)	310 (45)	23.9	34.9
513-2T-1	VF-220	Transverse		x		1093 (2000)	434 (63)	331 (48)	6.7	14.8

Heat treatment consisted of 1316°C (2400°F) for 2 hours, plus 1324°C (2415°F) for 2 hours with Rapid Argon Quench, plus RT-21 coated, plus 871°C (1600°F) for 20 hours.

ORIGINAL PAGE IS  
OF POOR QUALITY

increased yield strength at room temperature. These differences are not considered significant since the blade root will not be coated.

Tensile test results for SC NASAIR 100 in the fully processed + 982°C (1800°F)/1000-hours exposure condition are provided in Table 42. Inspection of this data indicates that, in general, the exposure reduced the tensile strength of NASAIR 100 while slightly increasing ductility. At 871° (1600°) and 982°C (1800°F), average yield and ultimate strengths were reduced by about 15 percent.

At room temperature, the 982°C (1800°F)/1000 hours exposure resulted in strength reductions in the order of 30 percent, while increasing ductility by about 60 percent. This loss in strength, however, was not considered significant in the turbine blade since

TABLE 42. SC NASAIR 100 TENSILE TEST RESULTS AFTER EXPOSURE AT 982°C (1800°F) FOR 1000 HOURS.\*

Specimen Number	Master Heat	Orientation**	Temperature C° (°F)	UTS MPa (ksi)	0.2% Y.S. MPa (ksi)	Elongation (%)	R of A (%)
647-9L-2	VF-233	Longitudinal	21 (70)	758 (110)	676 (98)	21.0	28.1
647-3L-2	VF-233	Longitudinal	21 (70)	765 (111)	600 (87)	26.7	28.1
591-36T-1	VF-235	Transverse	21 (70)	848 (123)	662 (96)	30.6	31.2
591-36T-2	VF-235	Transverse	21 (70)	834 (121)	655 (95)	31.5	31.2
591-36L-2	VF-235	Longitudinal	871 (1600)	952 (138)	793 (115)	12.9	17.2
648-9L-2	VF-235	Longitudinal	871 (1600)	1000 (145)	855 (124)	27.0	26.5
647-12L-1	VF-233	Longitudinal	982 (1800)	703 (102)	614 (89)	25.0	26.1
591-35L-2	VF-235	Longitudinal	982 (1800)	724 (105)	634 (92)	18.5	27.8

\*Tensile tests were conducted using 1.8 mm (0.070 inch) diameter test specimens machined from SC turbine blades that have been heat treated and then exposed to 982°C (1800°F) for 1000 hours. Prior to the 982°C (1800°F) exposure, heat treatment consisted of 1316°C (2400°F) for 2 hours, plus 1324°C (2415°F) for 2 hours with rapid Argon Quench, plus 982°C (1800°F) for 5 hours, plus 871°C (1600°F) for 20 hours.

\*\*Longitudinal and transverse orientations are within 15° of [001] and 15° of [100], respectively.

ORIGINAL PAGE 19  
OF POOR QUALITY

the cooler portions of the turbine blade (i.e., firtree attachment) will never reach temperatures approaching 982°C (1800°F).

SC Alloy 3

Comparative tensile data for SC Alloy 3 MFB minibar specimens were obtained for the same conditions evaluated for SC NASAIR 100. Tensile data for uncoated SC Alloy 3 specimens are provided in Table 43, and average tensile properties for SC Alloy 3 and SC NASAIR 100 are compared in Table 44. Inspection of these data indicates that SC Alloy 3 is weaker in the 760° to 982°C (1400° to 1800°F) temperature range relative to SC NASAIR 100. Also, SC Alloy 3 does not exhibit the pronounced maximum strength at 760°C (1400°F) that was observed with SC NASAIR 100. Scatter in the strength data appeared to be comparable to that previously observed for SC MAR-M 247 and SC NASAIR 100. Ductility values for SC Alloy 3 were slightly increased at intermediate temperatures relative to SC NASAIR 100.

TABLE 43. TENSILE TEST RESULTS ON 1.8 MM (0.070 INCH) DIAMETER TEST SPECIMENS MACHINED FROM SC ALLOY 3 TURBINE BLADES.

Specimen Number	Master Heat	Grain Orientation	Orientation			Temperature °C (°F)	UTS MPa (ksi)	0.2% Y.S. MPa (ksi)	Elongation (%)	R of A (%)
			Within 1° Degrees of (001)	Within 15 Degrees of (100)	15 Degrees of (100)					
688-1L-2	VF-291	Longitudinal	X			21 (70)	1117 (162)	1000 (145)	7.6*	16.6
675-6L-2	VF-291	Longitudinal	X			21 (70)	938 (136)	938 (136)	21.3	24.1
483-7L	VF-99	Longitudinal	X			760 (1400)	1200 (174)	938 (136)	9.5	14.4
483-12L	VF-99	Longitudinal	X			760 (1400)	1179 (171)	958 (139)	7.7	15.2
688-2L-2	VF-291	Longitudinal	X			760 (1400)	938 (136)	883 (128)	14.4	16.6
675-3L-2	VF-291	Longitudinal	X			760 (1400)	1220 (177)	1000 (145)	2.6	5.3
688-2T-2	VF-291	Transverse		X		760 (1400)	1220 (177)	1000 (145)	3.5	5.3
675-1T-2	VF-291	Transverse		X		760 (1400)	1014 (147)	896 (130)	7.4	12.5
787-1L-1	VF-292	Longitudinal	X			760 (1400)	1055 (153)	889 (128)	5.3	8.9
791-1L-1	VF-292	Longitudinal	X			760 (1400)	1365 (198)	1089 (158)	6.3	14.0
793-1L-1	VF-442	Longitudinal	X			760 (1400)	1338 (194)	1234 (178)	4.5	9.5
688-3L-2	VF-291	Longitudinal	X			871 (1600)	1117 (162)	862 (125)	10.8	17.2
675-4L-2	VF-291	Longitudinal	X			871 (1600)	1103 (160)	807 (117)	14.7	24.5
688-4L-2	VF-291	Longitudinal	X			982 (1800)	772 (112)	621 (90)	38.1	48.3
675-5L-2	VF-291	Longitudinal	X			982 (1800)	745 (108)	627 (91)	30.3	50.0
675-1L-2	VF-291	Longitudinal	X			1093 (2000)	414 (60)	283 (41)	30.7	50.0
675-6L-1	VF-291	Longitudinal	X			1093 (2000)	427 (62)	310 (45)	33.9	50.3
675-5T-2	VF-291	Transverse		X		1093 (2000)	421 (61)	269 (39)	31.3	53.8
675-6T-2	VF-291	Transverse		X		1093 (2000)	441 (64)	352 (51)	19.2	40.6

Heat treatment consisted of 1288°C (2350°F) for 2 hours, plus 1296°C (2365°F) for 4 hours with Rapid Argon Quench, plus 982°C (1800°F) for 5 hours, plus 871°C (1600°F) for 20 hours.

\*Failed in gauge mark.

ORIGINAL PAGE IS  
OF POOR QUALITY

TABLE 44. AVERAGE TENSILE PROPERTIES OF  $\langle 00 \rangle \pm 15^\circ$  ORIENTATION SC ALLOYS.

Alloy	Orientation Temperature		SC Alloys Ultimate Strength		0.2% Yield Strength		Elongation, %	R of A, %
	$^\circ\text{C}$	$^\circ\text{F}$	MPa	(ksi)	MPa	(ksi)		
NASAIR 100	21	(70)	1034	(150)	979	(142)	14.6	20.5
	649	(1200)	1117	(162)	965	(140)	8.4	11.5
	760	(1400)	1338	(194)	1220	(177)	4.9	9.1
	871	(1600)	1117	(162)	972	(141)	9.6	13.8
	982	(1800)	841	(122)	710	(103)	20.9	27.6
	1093	(2000)	476	(69)	365	(53)	28.6	48.3
ALLOY 3	21	(70)	1027	(149)	965	(140)	14.5	20.4
	760	(1400)	1172	(170)	986	(143)	6.8	11.4
	871	(1600)	1110	(161)	834	(121)	12.7	20.8
	982	(1800)	758	(110)	627	(91)	34.2	49.1
	1093	(2000)	427	(62)	372	(54)	28.8	48.7

A limited amount of tensile tests were performed on diffusion aluminide (RT-21) coated minibar specimens, and test data is provided in Table 45. As was the case for coated SC NASAIR 100, ductility was reduced for coated SC Alloy 3 at 21° and 760°C (70° and 1400°F). Coated SC Alloy 3 was slightly stronger at 760°C (1400°F) and weaker at 1093°C (2000°F) than the uncoated specimens.

Tensile test results for SC Alloy 3 specimens in the fully processed plus 982°C (1800°F)/1000-hour exposure condition are provided in Table 46. Inspection of these data indicates that the exposure reduced strength and increased ductility at room temperature. At 871° and 982°C (1600° and 1800°F), ultimate strengths were reduced, but yield strengths remained about constant or increased slightly.



ORIGINAL PAGE 13  
OF POOR QUALITY

TABLE 45. TENSILE TEST RESULTS ON DIFFUSION-ALUMINIDE (RT-21) COATED 1.8 MM (0.070 INCH) DIAMETER TEST SPECIMENS MACHINED FROM SC ALLOY 3 BLADES.

Specimen Number	Master Heat	Orientation	Temperature C° (°F)	UTS MPa (ksi)	0.2% Y.S. MPa (ksi)	Elongation (%)	R of A (%)
675-7L-1	VF-291	Longitudinal	21 (70)	1041 (151)	952 (138)	6.3	9.0
688-8L-1	VF-291	Longitudinal	21 (70)	972 (141)	938 (136)	12.5	15.9
675-2L-2	VF-291	Longitudinal	760 (1400)	1158 (168)	945 (137)	3.4	5.8
688-5L-2	VF-291	Longitudinal	760 (1400)	1220 (177)	952 (138)	4.2	8.8
675-7L-2	VF-291	Longitudinal	1093 (2000)	393 (57)	228 (33)	29.4	58.9
688-6L-2	VF-291	Longitudinal	1093 (2000)	379 (55)	241 (35)	35.5	55.3
Heat treatment consisted of 1288°C (2350°F) for 2 hours, plus 1296°C (2365°F) for 4 hours with rapid Argon Quench, plus RT-21 coating, plus 871°C (1600°F) for 20 hours.							
*Specimen orientations are all within 15 degrees of [001] direction.							

### 6.2.2 Creep-Rupture

#### SC NASAIR 100

Stress-rupture and creep data were obtained for longitudinal and transverse SC NASAIR 100 MFB minibar specimens (Figure 13) with stress axes within 15° of the [001] or [100] directions. Uncoated creep-rupture data obtained in the program are presented in Table 47. Analysis of the data indicated that there was no significant difference for longitudinal and transverse specimens as long as the specimen orientation was within 15° of an  $\langle 001 \rangle$  direction.

ORIGINAL PAGE IS  
OF POOR QUALITY

TABLE 46. SC ALLOY 3 TENSILE TEST RESULTS AFTER EXPOSURE AT  
982°C (1800°F) FOR 1000 HOURS.\*

Specimen Number	Master Heat	Orientation**	Temperature C° (°F)	UTS MPa (ksi)	0.2% Y.S. MPa (ksi)	Elongation (%)	R of A (%)
688-7L-2	VF-291	Longitudinal	21 (70)	731 (106)	724 (105)	55.3	39.8
688-9L-2	VF-291	Longitudinal	21 (70)	827 (120)	738 (107)	25.0	28.1
675-8T-1	VF-291	Transverse	21 (70)	1007 (146)	855 (124)	17.5	20.5
675-8T-2	VF-291	Transverse	21 (70)	917 (133)	841 (122)	16.6	20.9
688-9L-2	VF-291	Longitudinal	871 (1600)	979 (142)	883 (128)	13.5	15.9
688-10L-2	VF-291	Longitudinal	871 (1600)	979 (142)	862 (125)	19.5	23.3
688-10L-1	VF-291	Longitudinal	982 (1800)	676 (98)	607 (88)	15.1	23.1
675-8L-2	VF-291	Longitudinal	982 (1800)	717 (104)	641 (93)	11.7	15.5

\*Tensile tests were conducted using 1.8 mm (0.070 inch) diameter test specimens machined from SC turbine blades that have been heat treated and then exposed to 982°C (1800°F) for 1000 hours. Prior to the 982°C (1800°F) exposure, heat treatment consisted of 1288°C (2350°F) for 2 hours, plus 1296°C (2365°F) for 4 hours with rapid Argon Quench, plus 982°C (1800°F) for 5 hours, plus 871°C (1600°F) for 20 hours.

\*\*Longitudinal and transverse orientations are within 15° of [001] and 15° of [100], respectively.

Stress versus Larson-Miller parameter relationships for times to one- and two-percent creep strain and rupture life are provided in Figures 43, 44, and 45, respectively. Inspection of these figures indicates a relatively large amount of scatter in one-percent-creep data. This extent of scatter is partially attributable to mounting the extensometry on the grips (due to the small size of the MFB minibars).

Isothermal stress versus rupture life data for SC NASAIR 100 and SC Alloy 3 are provided in Figure 46. These data indicate that the rupture life curves at 871°, 982°, and 1093°C (1600°, 1800°, and 2000°F) have the same slopes for both alloys. Consequently, the SC NASAIR 100 alloy stress-rupture capability was essentially unaffected by the precipitation of the mu phase.

ORIGINAL PAGE IS  
OF POOR QUALITY

TABLE 47. CREEP-RUPTURE RESULTS ON 1.8 MM (0.070 INCH) DIAMETER SPECIMENS  
MACHINED FROM SC NASAIR 100 TURBINE BLADES.

Specimen Number	Master Heat	Orientation*	Temperature °C (°F)	Stress MPa (ksi)	Rupture Life (hours)	Elongation (%)	R of A (%)	Time to 1.0 Percent (hours)	Time to 2.0 Percent (hours)
648-4L-1	VF-235	Longitudinal	760 (1400)	862 (125)	192.4	12.6	18.1	20	55
591-11L-1	VF-235	Longitudinal		827 (120)	439.7	15.9	19.1	64	159
648-3T-1	VF-235	Transverse		862 (123)	160.6	9.5	11.8	19	56
648-4T-1	VF-235	Transverse		827 (120)	214.3	11.2	15.3	11	41
591-9T-1	VF-235	Transverse		793 (115)	354.6	10.3	14.2	32	116
511-12L-1	VF-220	Longitudinal		793 (115)	488.9	12.3	14.4	72.0	184.5
481-5L	VF-154	Longitudinal		758+793 (110+115**)	790.2	6.9	13.2	--	--
481-12L	VF-154	Longitudinal		758+793 (110+115**)	725.2	7.1	15.4	--	--
481-5T	VF-154	Transverse		758+793 (110+115**)	551.8	10.8	23.2	--	--
481-12T	VF-154	Transverse		758 (110)	308.6	3.8	10.0	--	--
511-7T-1	VF-220	Transverse	871 (1600)	483 (70)	105.8	11.8	23.0	22.0	49.0
509-4L-1	VF-154	Longitudinal		483 (70)	144.4	18.1	24.7	27	55
648-1T-1	VF-235	Transverse		393 (57)	330.9	12.9	17.9	104	183
648-3L-1	VF-235	Longitudinal		379 (55)	586.6	24.5	32.1	146	242
511-11L-1	VF-220	Longitudinal		379 (55)	456.0	20.2	27.5	81.7	178.5
648-7T-1	VF-235	Transverse		359 (52)	355.0	18.4	23.4	50	156
591-11T-1	VF-235	Transverse		345 (50)	477.0	24.9	27.3	188	348
513-7T-1	VF-220	Transverse		345 (50)	519.0	18.1	25.3	74.0	211.5
648-8L-1	VF-235	Longitudinal		345 (50)	644.0	22.5	34.3	167	305
591-15L-1	VF-235	Longitudinal		331 (48)	1008.3	20.9	27.3	234	421
591-22T-1	VF-235	Transverse		324 (47)	650.3	16.0	17.3	144	343
591-22L-1	VF-235	Longitudinal		310 (45)	1382.1	26.9	31.9	210	490
511-10T-1	VF-220	Transverse	982 (1800)	241 (35)	81.2	15.1	22.2	1.7	5.8
648-2L-1	VF-235	Longitudinal		241 (35)	125.8	25.9	36.7	--	22
756-1L-1	VF-237	Longitudinal		241 (35)	69.7	12.1	28.2	--	--
766-1L-1	VF-237	Longitudinal		241 (35)	86.2	13.2	31.7	--	--
782-1L-1	VF-237	Longitudinal		241 (35)	68.4	19.0	29.6	--	--
458-3L	VF-154	Longitudinal		207 (30)	189.3	24.2	42.6	--	--
458-4L	VF-154	Longitudinal		207 (30)	198.1	15.7	41.3	--	--
481-3T	VF-154	Transverse		207 (30)	174.4	15.6	26.3	--	--
481-7T	VF-154	Transverse		207 (30)	189.5	26.0	34.2	--	--
511-12T-1	VF-220	Transverse		207 (30)	209.5	18.8	23.5	9.2	31.1
648-2T-1	VF-235	Transverse		193 (28)	262.7	22.6	29.6	--	50
509-4L-2	VF-154	Longitudinal		179 (26)	763.8	28.3	31.9	27	239
513-9L-1	VF-220	Longitudinal		186 (27)	482.2	13.4	20.4	22.5	186.0
511-10L-1	VF-220	Longitudinal		172 (25)	616.5	20.7	27.9	30.5	363.5
513-9T-1	VF-220	Transverse		172 (25)	627.9	11.1	15.3	69.5	497.3
591-15T-1	VF-235	Transverse		159 (23)	886.3	7.0	14.6	86	719
427-4L-2	VF-154	Longitudinal		159 (23)	1404.1	12.8	20.7	30	225
457-1L-1	VF-154	Longitudinal		152 (22)	1143.9	19.6	31.8	40	729
511-9L-1	VF-220	Longitudinal	1038 (1900)	131 (19)	451.0	7.2	15.5	12.0	331.5
513-7L-1	VF-220	Longitudinal	1066 (1950)	131 (19)	249.1	10.7	25.3	124.3	233.6
511-9T-1	VF-220	Transverse	1093 (2000)	131 (19)	69.2	5.3	10.1	9.2	56.7
509-6L-1	VF-154	Longitudinal		131 (19)	90.7	12.5	21.7	--	33
509-6L-2	VF-154	Longitudinal		110 (16)	363.4	18.2	28.0	--	--
458-6L	VF-154	Longitudinal		103 (15)	501.8	11.2	34.5	--	--
459-11L	VF-154	Longitudinal		103 (15)	453.7	10.8	33.7	--	--
511-11T-1	VF-220	Transverse		103 (15)	223.4	5.3	8.1	17.3	214.7
511-7L-1	VF-220	Longitudinal		103 (15)	273.1	8.4	30.0	19.5	260.1
513-6L-1	VF-220	Longitudinal		90 (13)	386.6	11.2	22.8	11.2	319.3
513-6T-1	VF-220	Transverse		90 (13)	335.8	7.9	12.3	--	--
648-6T-1	VF-235	Transverse		83 (12)	610.5	4.2	8.3	102	480
591-21L-1	VF-235	Longitudinal		76 (11)	1234.5	9.4	25.6	681	1057
427-4L-1	VF-154	Longitudinal		69 (10)	2055.2	14.6	17.9	--	--
591-23T-1	VF-235	Transverse		69 (10)	1787.9	9.7	17.2	--	474
458-9L-1	VF-154	Longitudinal		62 (9)	3866.0	10.7	13.9	500	1129

Heat treatment consisted of 1316°C (2400°F) for 2 hours, plus 1324°C (2415°F) for 2 hours with rapid Argon Quench, plus 982°C (1800°F) for 5 hours, plus 871°C (1600°F) for 20 hours.

\*Specimen orientations were within 15 degrees of <001>.

\*\*Specimens were unloaded to 793 MPa (115 ksi) after 500 hours.

ORIGINAL PAGE IS  
OF POOR QUALITY

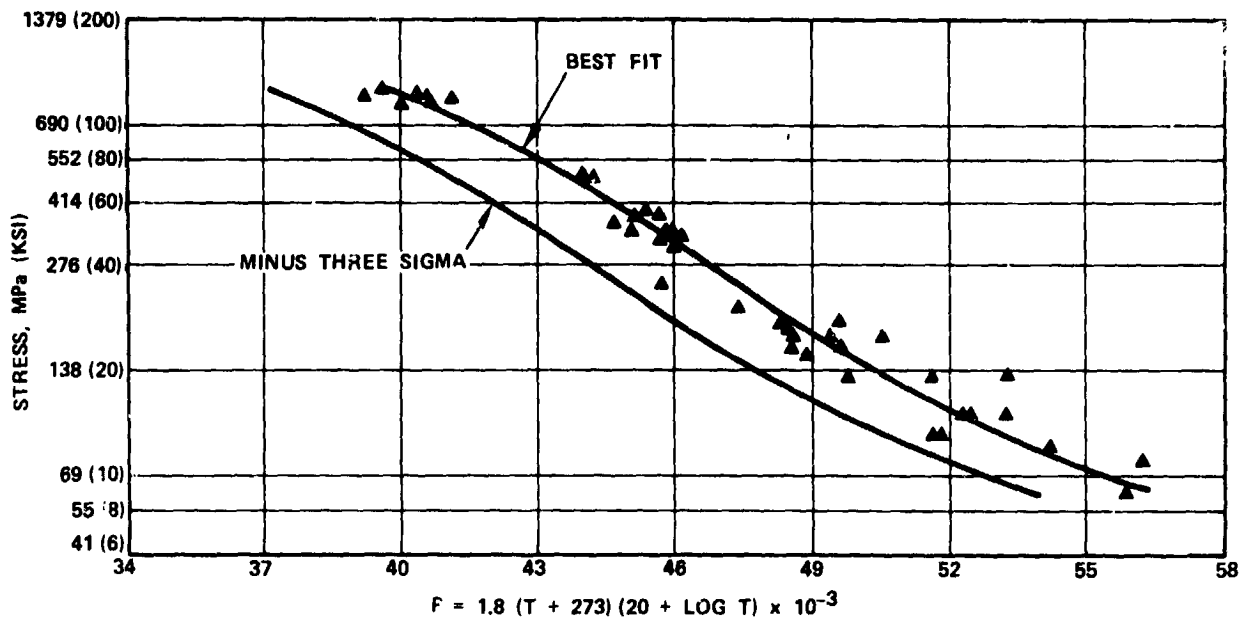


Figure 43. 1.0-Percent Creep of SC NASAIR 100, 1.8 mm (0.070 Inch) Round Specimens.

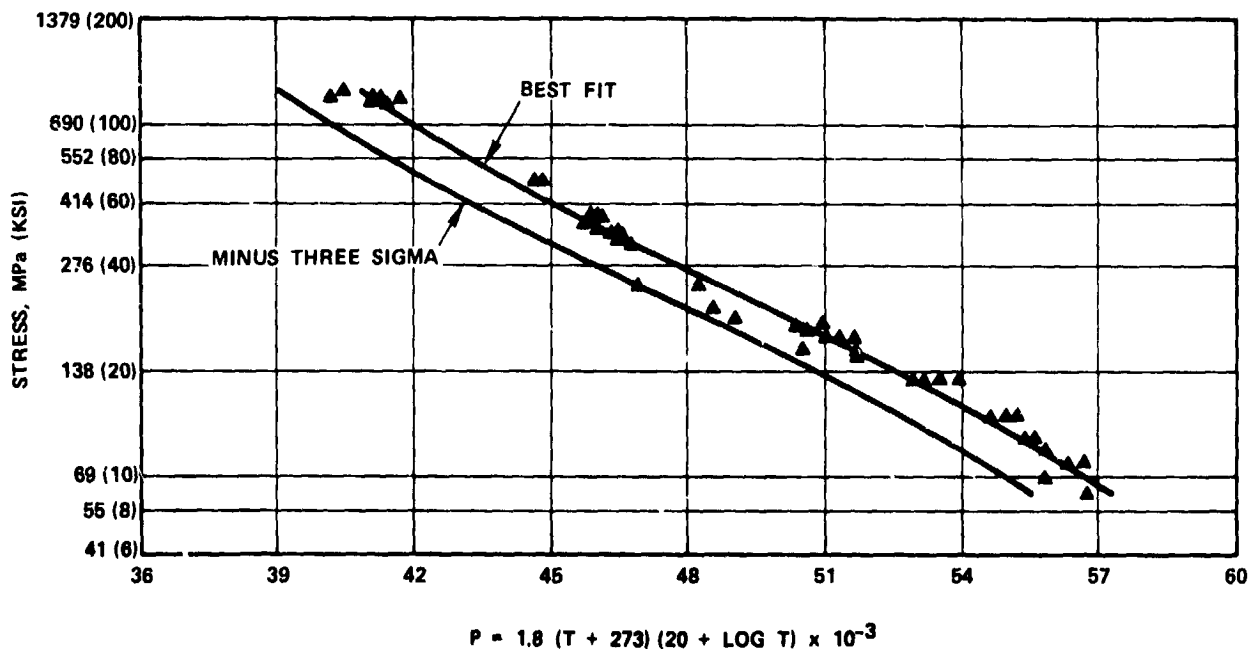


Figure 44. 2.0-Percent Creep of SC NASAIR 100, 1.8 mm (0.070 Inch) Round Specimens.

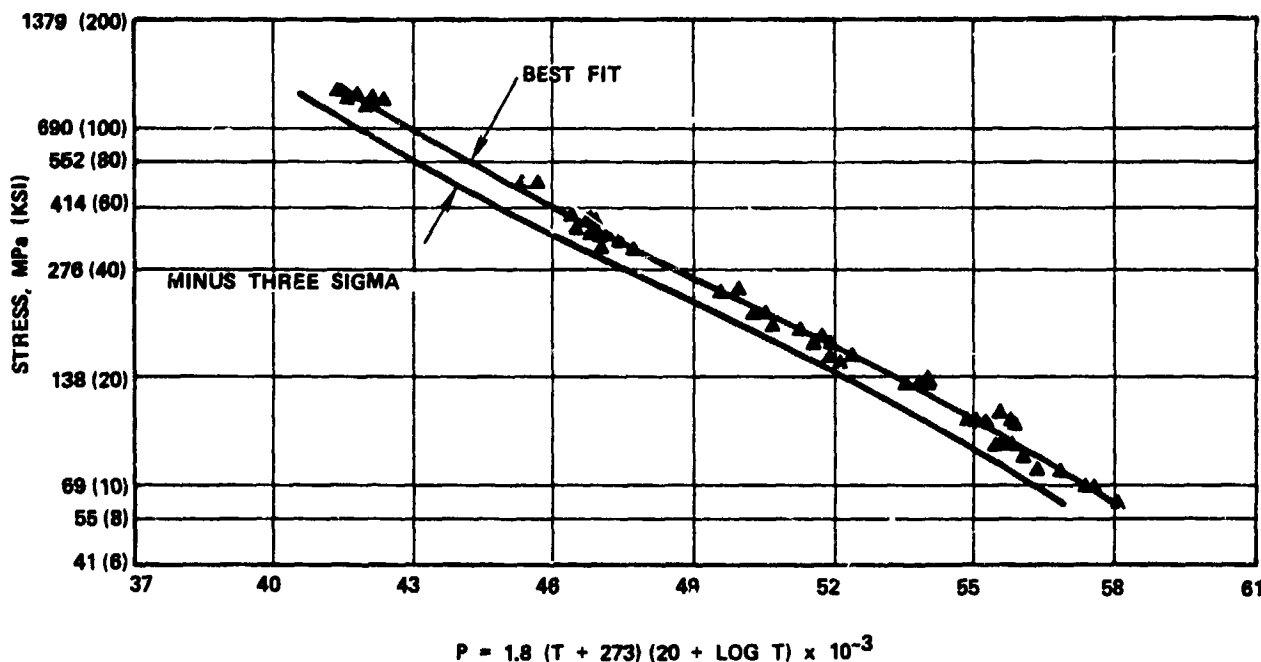


Figure 45. Stress-Rupture of SC NASAIR 100, 1.8 mm (0.070 Inch) Round Specimens.

Microstructural examination of SC NASAIR 100 specimens evaluated at 982° and 1093°C (1800° and 2000°F) with rupture lives less than 100 hours and the longest rupture lives at 760°, 871°, 982°, and 1093°C (1400°, 1600°, 1800°, and 2000°F) are provided in Figures 47 and 48 respectively.

Microstructural examination of the SC NASAIR 100 microstructures after creep-rupture testing indicated the following:

- o At 760°C (1400°F) and 814 MPa (118 ksi), the microstructure remained stable during the 563.8-hour test. This result is consistent with alloy development results, which indicated that the microstructure remained stable after a 790-hour exposure at 760°C (1400°F) [500 hours/759 MPa (110 ksi) + 290 hours/794 MPa (115 ksi)].

ORIGINAL PAGE IS  
OF POOR QUALITY

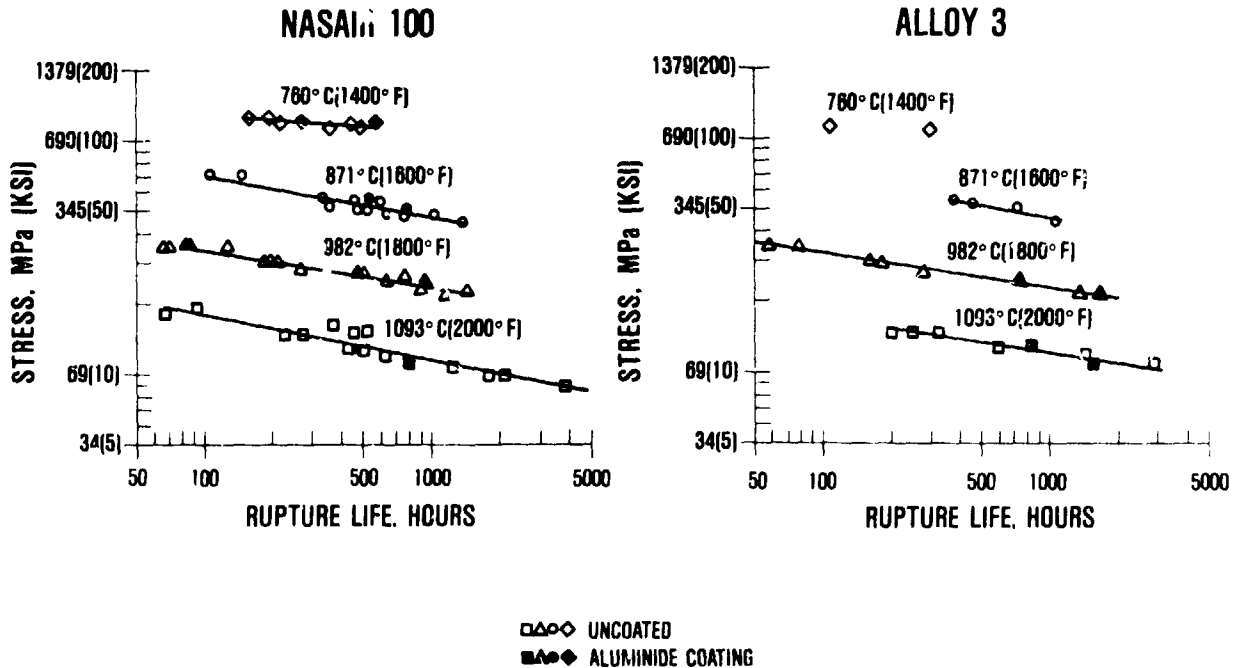


Figure 46. Stress-Rupture Life of SC Alloys.

- o Mu phase precipitation was observed in short-life specimens (less than 100 hours) tested at 871°, 982° and 1093°C (1600°, 1800°, and 2000°F). This result indicates that the mu phase was present in the long-life specimens for greater than 93 percent of the rupture life and did not appreciably affect it.
- o Propensity for mu phase precipitation was greater at 982°C (1800°F) and 1093°C (2000°F) than at 871°C (1600°F).
- o All SC NASAIR 100 and SC Alloy 3 creep-rupture-tested MrB specimens that were metallographically examined during this task revealed that secondary creep cracks were commonly associated with microporosity.

ORIGINAL PAGE IS  
OF POOR QUALITY



982°C (1800°F)/241 MPa (35 KSI)/86.2 HOURS



P77247-1

1093°C (2000°F)/131 MPa (19 KSI)/69.2 HOURS

Figure 47. Short-Life Microstructures of Creep-Rupture-Tested SC NASAIR 100 MFB Specimens. 400X Magnification.

ORIGINAL PAGE IS  
OF POOR QUALITY

(100X)

(400X)

760°C (1400°F)/814 MPa (118 KSI)/563.8 HOURS

(100X)

P77247-4

(400X)

871°C (1600°F)/310 MPa (45 KSI)/1382.1 HOURS

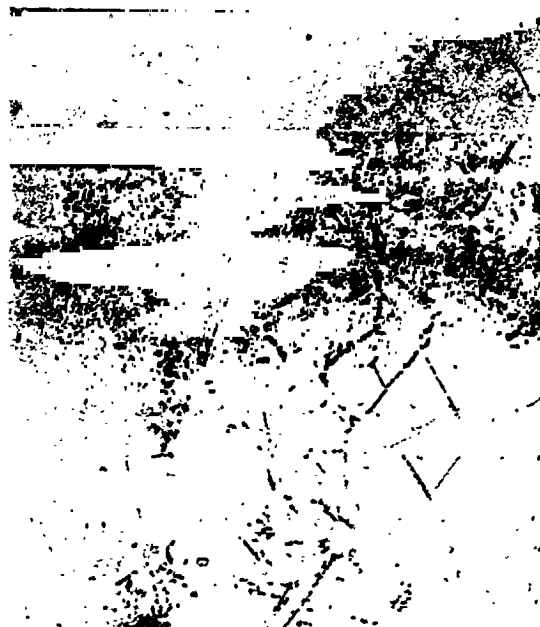
Figure 48, Part 1. Long-Life Microstructures of Long-Time  
Creep-Rupture-Tested SC NASAIR 100 MFB  
Specimens.



ORIGINAL PAGE IS  
OF POOR QUALITY



(100X)



(400X)

982°C (1800°F)/159 MPa (23 KSI)/1404.1 HOURS



(100X)



P77247-6  
(400X)

1083°C (2000°F)/62 MPa (9 KSI)/3866.0 HOURS

Figure 48, Part 2. Long-Life Microstructures of Long-Time Creep-Rupture-Tested SC NASAIR 100 MFB Specimens.

ORIGINAL PAGE IS  
OF POOR QUALITY

For some superalloy systems, application of protective oxidation resistant coatings can severely degrade the creep-rupture life.<sup>14</sup> Consequently, creep-rupture tests were performed with diffusion-aluminide (RT-21) coated SC NASAIR 100 specimens in order to evaluate potential coating effects. Results obtained in this evaluation are provided in Table 48. Two specimen stress levels are shown in Table 48, one that includes the coating (specimen stress) and a calculated stress that uses an area consisting of the base material minus the coating (substrate stress); the substrate stress assumes that the coating does not support any significant load. Orientation of all coated test specimens is longitudinal and within 15 degrees of [001].

Computer analysis of the coated creep (substrate stress data) versus uncoated data revealed no statistical difference in the time to 0.5-, 1.0-, and 2.0-percent strain or rupture life indicating no degradation of SC NASAIR 100 creep properties from application of the diffusion aluminide RT-21 coating. The coated data are also compared with the uncoated data in isothermal stress versus rupture life curves (Figure 46) to illustrate the above conclusion.

TABLE 48. CREEP-RUPTURE TEST RESULTS ON DIFFUSION-ALUMINIDE (RT-21) COATED 1.8MM (0.070 INCH) DIAMETER TEST SPECIMENS MACHINED FROM SC NASAIR 100 BLADES.

Specimen Number	Master Heat	Orientation*	Temperature °C (°F)	Specimen Stress MPa (ksi)	Substrate Stress MPa (ksi)	Rupture Life (Hours)	Elongation (%)	R of A (%)	Time to 0.5 Percent (Hours)	Time to 1.0 Percent (Hours)	Time to 2.0 Percent (Hours)
513-5L-1	VP-220	Longitudinal	760 (1400)	779 (113)	841 (122)	276.6	8.3	13.3	13.5	50.1	122.8
511-8L-1	VP-220	Longitudinal	760 (1400)	752 (109)	814 (118)	563.8	8.5	15.9	32.2	124.8	260.0
511-6L-1	VP-220	Longitudinal	871 (1600)	359 (52)	386 (56)	533.9	16.8	19.0	28.1	113.2	223.0
513-4L-1	VP-220	Longitudinal	871 (1600)	317 (46)	345 (50)	770.2	16.1	23.3	68.5	213.0	370.7
511-5L-1	VP-220	Longitudinal	982 (1800)	172 (25)	186 (27)	478.6	16.1	23.5	21.5	82.8	335.9
513-3L-1	VP-220	Longitudinal	982 (1800)	152 (22)	172 (25)	925.3	16.6	22.7	25.0	217.6	693.6
511-4L-1	VP-220	Longitudinal	1038 (1900)	124 (18)	138 (20)	759.3	13.9	21.4	0.3	---	---
513-2L-1	VP-220	Longitudinal	1078 (1900)	97 (14)	103 (15)	1614.4	12.3	20.2	7.8	351.1	1354.4
511-3L-1	VP-220	Longitudinal	1093 (2000)	83 (12)	90 (13)	46.3	13.0	23.7	1.6	9.1	380.0
513-1L-1	VP-220	Longitudinal	1093 (2000)	69 (10)	76 (11)	789.0	10.1	19.2	28.2	---	749.7

Heat treatment consisted of 1316°C (2400°F) for 2 hours, plus 1324°C (2415°F) for 2 hours with rapid Argon Quench, plus RT-21 coated, plus 871°C (1600°F) for 20 hours.

\*Specimen orientations are all within 15 degrees of [001] direction.

ORIGINAL PAGE IS  
OF POOR QUALITY

Creep-rupture tests were also performed to assess the effects of a 982°C(1800°F)/1000 hour exposure on the rupture life. As previously indicated in Figure 40, this exposure coarsens the gamma prime phase and permits the mu phase to precipitate in NASAIR 100. Stress-rupture results for exposed SC NASAIR 100 are compared with similar unexposed data and with data for exposed and unexposed SC Alloy 3 in Table 49 and Figure 49.

Examination of these data reveals the following:

- o SC NASAIR 100 and SC Alloy 3 data obtained after the 982°C (1800°F)/1000-hour exposure was contained (with two exceptions--one high and one low) within the typical and minus three sigma lines for fully processed NASAIR 100.
- o After the 982°C (1800°F)/1000-hours exposure, typical values for both SC NASAIR 100 and SC Alloy 3 appear to be approximately one-half a Larson-Miller parameter lower than fully processed SC NASAIR 100.

TABLE 49. RUPTURE LIFE COMPARISON OF SC NASAIR 100 AND ALLOY 3 BEFORE AND AFTER EXPOSURE AT 982°C (1800°F) FOR 1000 HOURS.

Alloy	Test Temperature °C (°F)	Stress MPa (Ksi)	Rupture Life (Hours)	
			Fully Heat Treated	After Exposure at 982°C (1800°F) for 1000 Hours*
NASAIR 100	982 (1800)	241 (35)	125.8, 81.2	100.6
Alloy 3		241 (35)	---	76.8
NASAIR 100		207 (30)	189.3, 174.4	95.1
NASAIR 100			198.1, 189.5	196.8
NASAIR 100			209.5	---
Alloy 3		186 (27)	180.2	160.3
Alloy 3			161.3	191.7
NASAIR 100			482.2	268.0
Alloy 3		186 (27)	278.2	208.4
NASAIR 100		172 (25)	616.5, 627.9	200.8
Alloy 3		172 (25)	---	484.8

\*Fully heat treated prior to exposure.

ORIGINAL PAGE IS  
OF POOR QUALITY

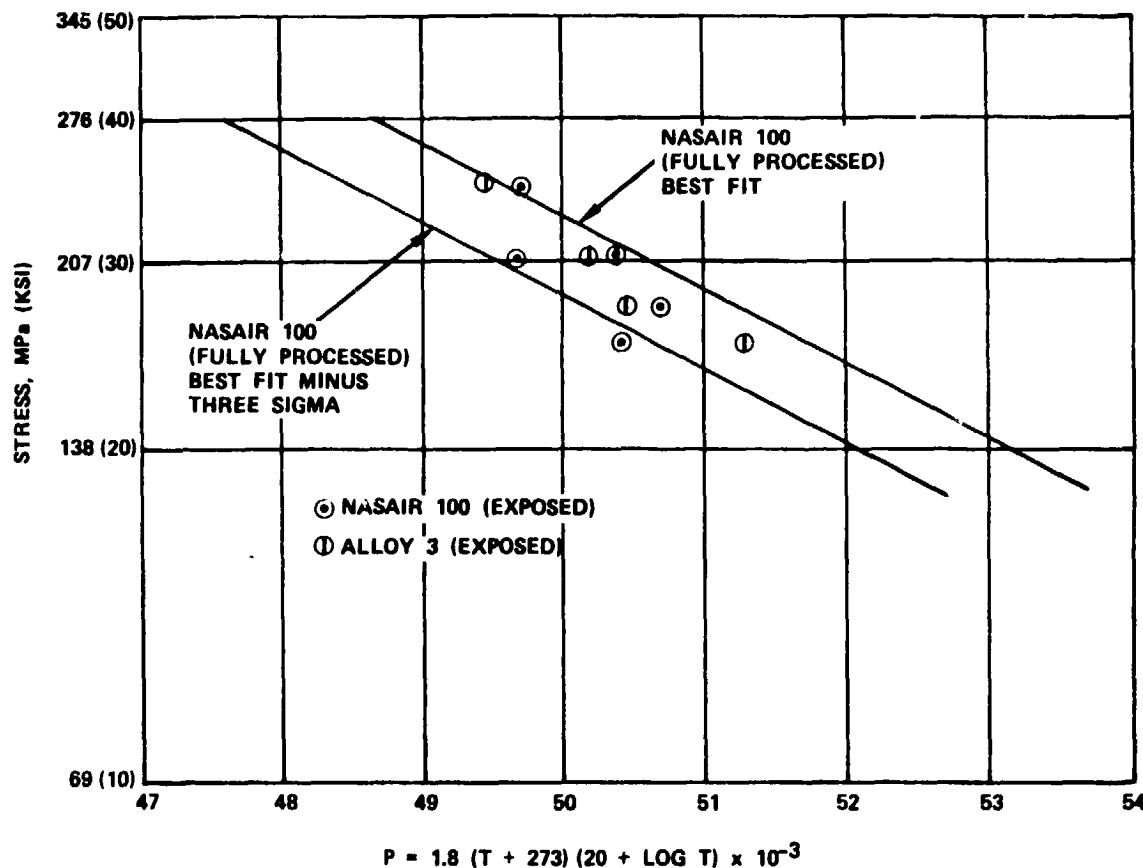


Figure 49. Exposed - 982°C (1800°F)/1000 Hours - SC NASAIR 100 and SC Alloy 3 Rupture Data Compared to SC NASAIR 100 Larson-Miller Stress-Rupture Curve (Fully Processed).

These reductions are thought to be predominantly associated with gamma prime coarsening. To support this conclusion, life reductions were comparable to those observed when the SC NASAIR 100 microstructure was degraded by gamma prime coarsening as a result of improper (slow) cooling from the solutioning temperature (compare Table 30 with Table 49).

### SC Alloy 3

Comparative creep-rupture data for SC Alloy 3 MFB minibar specimens were obtained for the same conditions evaluated for SC NASAIR 100. Uncoated and coated creep-rupture data obtained in the program are provided in Tables 50 and 51, respectively. As with SC NASAIR 100, analysis of the data indicated that there was no significant difference for longitudinal and transverse specimens as long as the specimen orientation was within 15 degrees of an  $\langle 001 \rangle$  direction.

Stress versus Larson-Miller parameter relationships for times to one- and two-percent creep strain and rupture life are provided in Figures 50, 51, and 52, respectively. Coated and uncoated data are provided in these figures and demonstrate (on a substrate stress basis) that the RT-21 diffusion aluminide coating did not affect the creep properties.

Isothermal stress versus rupture life data for SC Alloy 3 (and SC NASAIR 100) are provided in Figure 46. Examination of the data in this figure and the data provided in Tables 47 and 50 indicate that SC Alloy 3 is slightly weaker than SC NASAIR 100 over the 138 to 793 MPa (20 to 115 ksi) stress/760° to 982°C (1400° to 1800°F) temperature ranges, which are of primary importance to turbine blade design.

Post-test microstructural examination of SC Alloy 3 specimens revealed no evidence of TCP phase formation after 1685.5 hours at 982°C/152 MPa (1800°F/22 ksi) and 2835.5 hours at 1093°C/76 MPa (2000°F/11 ksi), indicating elevated temperature phase stability. Microstructures of longest rupture life specimens at 760°, 871°, 982°, and 1093°C (1400°, 1600°, 1800°, and 2000°F) are provided in Figure 53.

ORIGINAL PAGE IS  
OF POOR QUALITY

TABLE 50. CREEP-RUPTURE RESULTS ON 1.8 MM (0.070 INCH) DIAMETER SPECIMENS MACHINED FROM SC ALLOY 3 TURBINE BLADES.

Specimen Number	Master Heat	Orientation*	Temperature °C (°F)	Stress MPa (ksi)	Rupture Life (hours)	Elongation (%)	R of A (%)	Time to 1.0 Percent (hours)	Time to 2.0 Percent (hours)
688-1L-1	VF-291	Longitudinal	760 (1400)	793 (115)	106.5	15.1	19.5	3	10
675-1L-1	VF-291	Longitudinal	760 (1400)	758 (110)	294.3	14.8	20.6	6	19
483-1L	VF-99	Longitudinal	760 (1400)	758 (110)	317.8	15.4	23.7	--	--
483-2L	VF-99	Longitudinal	760 (1400)	758 (110)	291.8	16.9	25.3	--	--
688-2L-1	VF-291	Longitudinal	871 (1600)	379 (55)	378.8	11.2	14.6	14	126
688-1T-1	VF-291	Transverse	871 (1600)	365 (53)	459.2	11.2	20.4	151	248
688-2T-1	VF-291	Transverse	871 (1600)	345 (50)	712.5	19.1	23.7	125	323
675-3L-1	VF-291	Longitudinal	871 (1600)	310 (45)	1052.9	15.4	27.8	193	425
792-1L-1	VF-292	Longitudinal	982 (1800)	241 (35)	58.6	21.7	29.8	--	--
794-1L-1	VF-443	Longitudinal	982 (1800)	241 (35)	78.4	20.3	27.3	--	--
483-3L	VF-99	Longitudinal	982 (1800)	207 (30)	180.2	22.5	28.9	--	--
483-8L	VF-99	Longitudinal	982 (1800)	207 (30)	161.3	10.2	28.3	--	--
675-4L-1	VF-291	Longitudinal	982 (1800)	186 (27)	278.2	17.4	29.8	30	125
688-3L-1	VF-291	Longitudinal	982 (1800)	152 (22)	1335.4	12.8	19.1	80	564
483-9L	VF-99	Longitudinal	1093 (2000)	163 (15)	247.8	11.0	20.0	--	--
483-10L	VF-99	Longitudinal	1093 (2000)	103 (15)	199.1	16.9	31.0	--	--
675-5T-1	VF-291	Transverse	1093 (2000)	103 (15)	320.0	5.3	12.1	--	48
675-5L-1	VF-291	Longitudinal	1093 (2000)	90 (13)	581.9	7.5	13.1	--	354
675-6T-1	VF-291	Transverse	1093 (2000)	83 (12)	1431.1	5.0	6.9	--	716
688-4L-1	VF-291	Longitudinal	1093 (2000)	76 (11)	2835.5	9.4	11.7	530	1090

\*Specimen orientations were within 15 degrees of <001>.

Heat treatment consisted of 1288°C (2350°F) for 2 hours, plus 1291°C (2365°F) for 4 hours with rapid Argon Quench, plus 982°C (1800°F) for 5 hours, plus 871°C (1600°F) for 20 hours.

TABLE 51. CREEP-RUPTURE RESULTS ON DIFFUSION-ALUMINIDE (RT-21) COATED 1.8 MM (0.070 INCH) DIAMETER TEST SPECIMENS MACHINED FROM SC ALLOY 3 TURBINE BLADES.

Specimen Number	Master Heat	Orientation	Temperature °C (°F)	Specimen Stress MPa (ksi)	Substrate Stress MPa (ksi)	Rupture Life (hours)	Elongation (%)	R of A (%)	Time to 1.0 Percent (hours)	Time to 2.0 Percent (hours)
675-2L-1	VF-291	Longitudinal	982 (1800)	152 (22)	172 (25)	736.7	11.6	20.0	23	102
688-5L-1	VF-291	Longitudinal	982 (1800)	138 (20)	152 (22)	1685.5	11.3	21.6	210	1240
688-6L-1	VF-291	Longitudinal	1093 (2000)	83 (12)	90 (13)	807.4	3.8	11.2	--	--
688-2L-1	VF-291	Longitudinal	1093 (2000)	69 (10)	76 (11)	1532.6	7.4	12.1	190	700

Heat treatment consisted of 1288°C (2350°F) for 2 hours, plus 1296°C (2365°F) for 4 hours with rapid Argon Quench, plus RT-21 coating, plus 871°C (1600°F) for 20 hours.

ORIGINAL PAGE IS  
OF POOR QUALITY

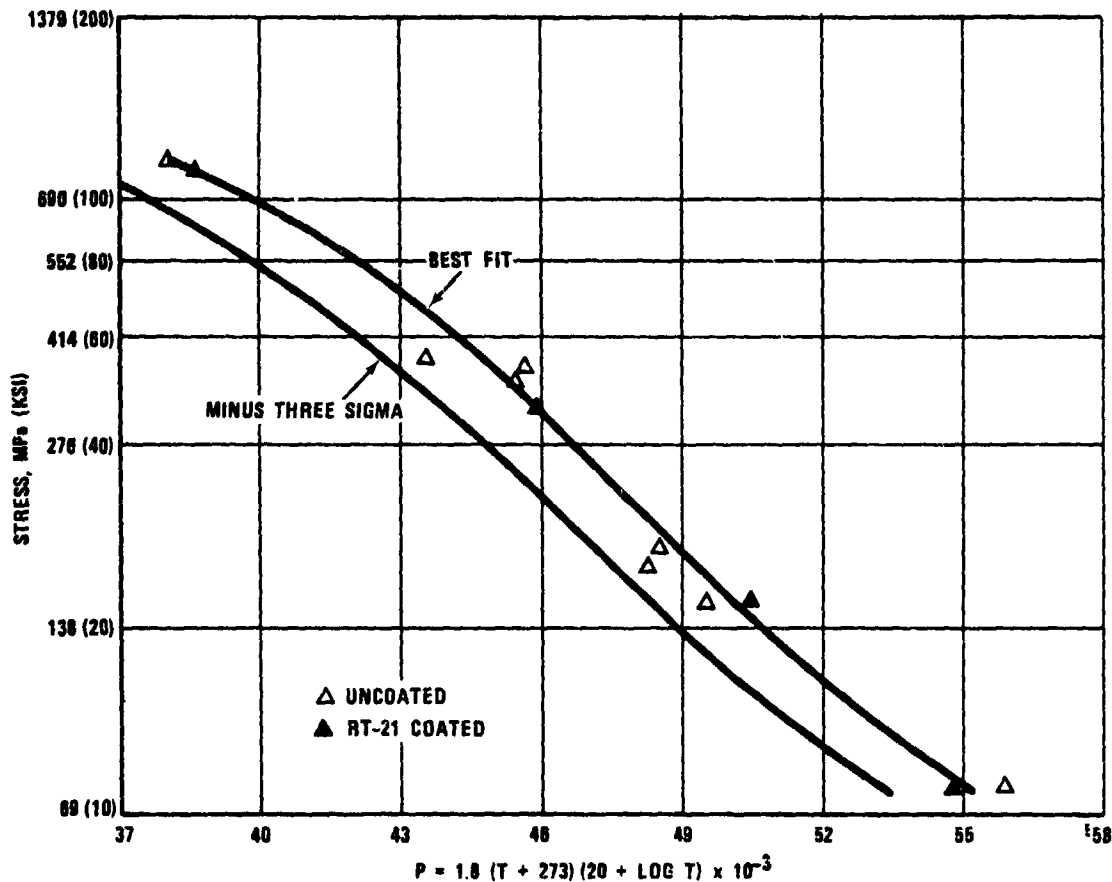


Figure 50. 1.0-Percent Creep of SC Alloy 3, 1.8 mm (0.070 Inch) Round Specimens.

### 6.2.3 Low-Cycle Fatigue

Axial strain controlled low-cycle-fatigue (LCF) tests were performed at Mar-Test, Inc. of Cincinnati, Ohio. These tests were performed using 6.35 mm (0.25 inch) gauge diameter specimens (Figure 54) machined from cast slabs (SC NASAIR 100) or bars (SC Alloy 3). Data were obtained at 760°C (1400°F) at a 0.33 Hertz (20 cpm) frequency and an A ratio ( $\frac{\text{Alternating Stress Amplitude}}{\text{Mean Stress}}$ ) of infinity. Test results are reviewed in the following paragraphs.

ORIGINAL PAGE IS  
OF POOR QUALITY

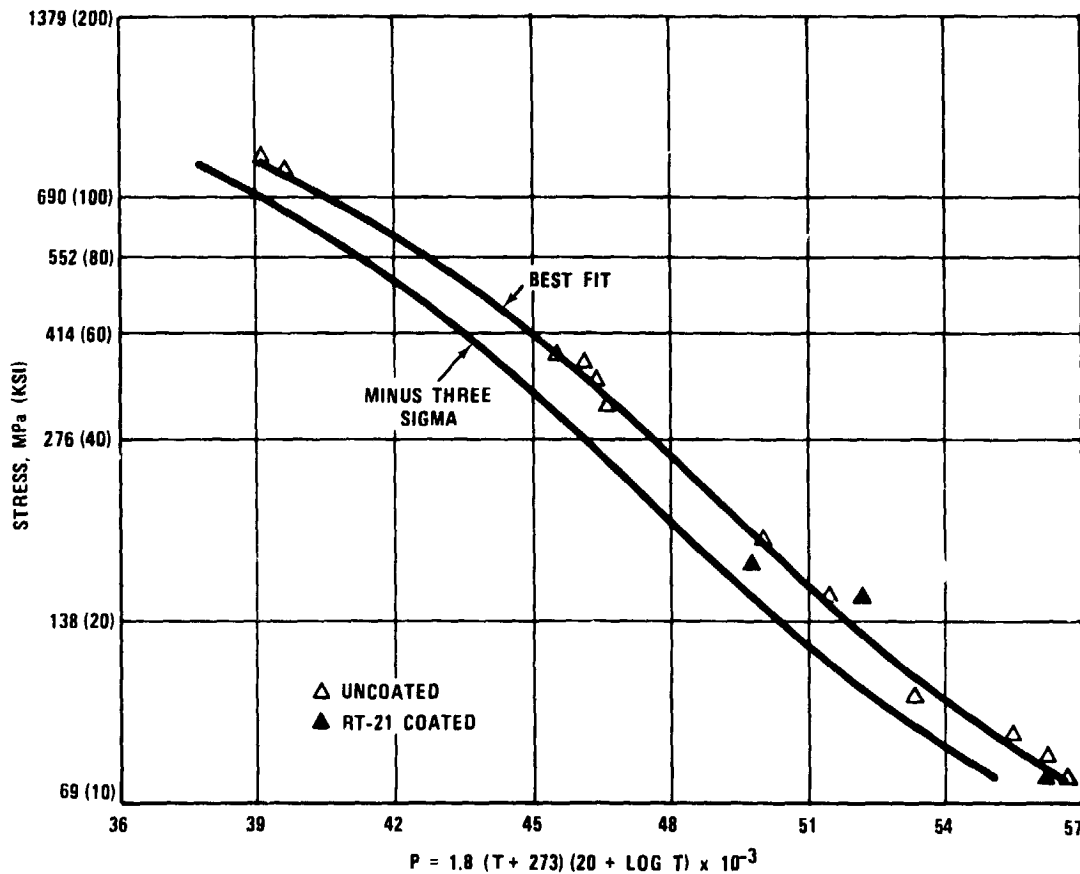


Figure 51. 2.0-Percent Creep of SC Alloy 3, 1.8 mm (0.070 Inch) Round Specimens.

#### SC NASAIR 100

LCF tests of SC NASAIR 100 were conducted at total strain ranges between 1.2 and 2.5 percent. Test data are provided in Table 52. Computer generated best-fit and minus-three-sigma strain range versus cycles to fatigue curves are provided in Figure 55 for longitudinally oriented specimens. The average LCF curve indicated that a total percent strain range of 1.45 percent would yield an LCF life of 10,000 cycles for longitudinally (within 15° of [001]) oriented SC NASAIR 100.



ORIGINAL PAGE 19  
OF POOR QUALITY

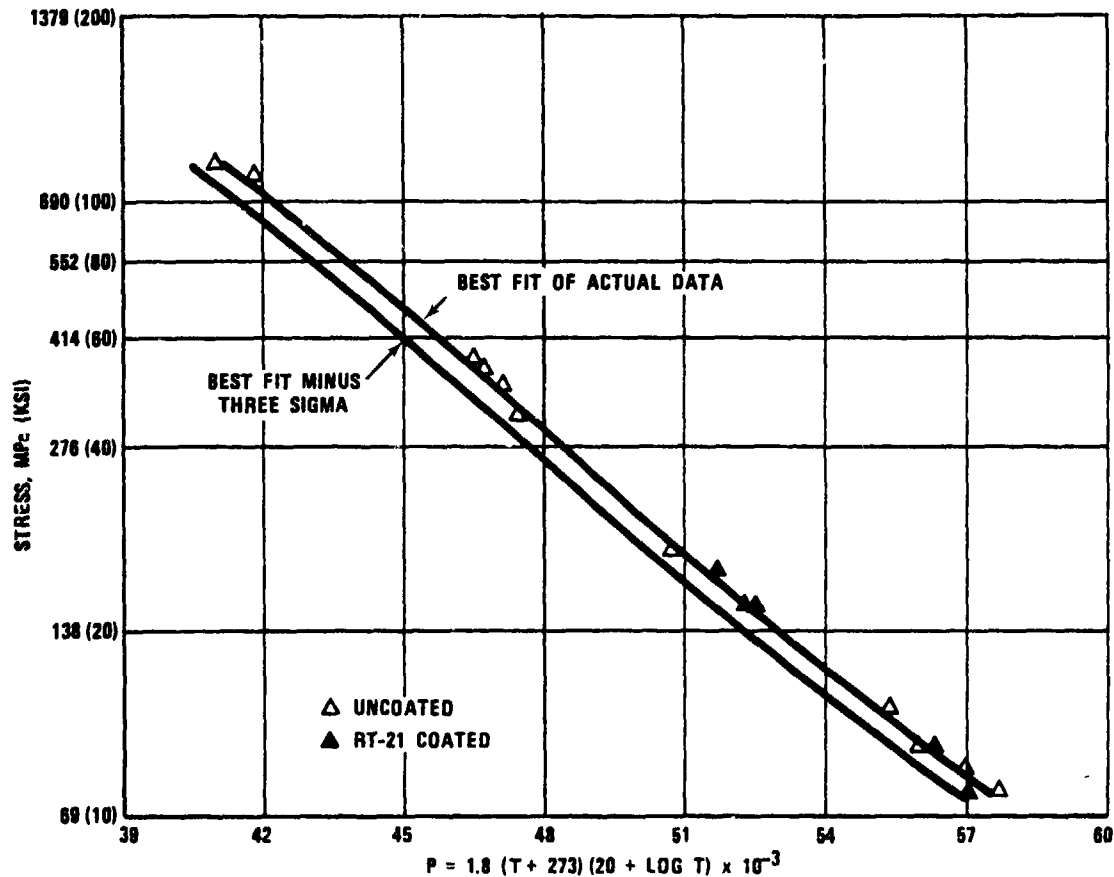


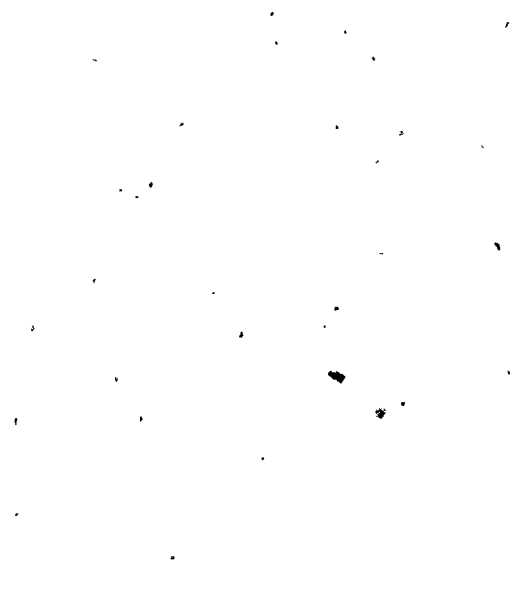
Figure 52. Stress-Rupture of SC Alloy 3, 1.8 mm (0.070 Inch) Round Specimens.

Macroexamination at 40x and SEM examination at higher magnifications were performed on the fracture surfaces of the LCF tested specimens. In all instances, cracking in these specimens initiated at microporosity (Figure 56). Cracks typically propagated initially in Stage II, approximately perpendicular to the applied stress in the (001) plane, and then switched to Stage I and propagated on a crystallographic plane. The duration of the initial Stage II mode of crack propagation seemed to be greater for longer life specimens that were tested at lower stresses.


ORIGINAL PAGE IS  
OF POOR QUALITY



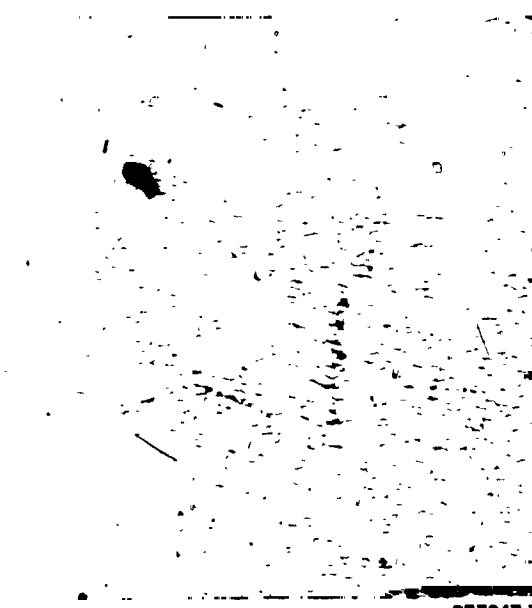
760°C (1400°F)/758 MPa (110 KSI)  
294.3 HOURS



871°C (1600°F)/310 MPa (45 KSI)  
1052.9 HOURS



982°C (1800°F)/152 MPa (22 KSI)  
1685.5 HOURS



1093°C (2000°F)/76 MPa (11 KSI)  
2835.5 HOURS

Figure 53. Long-Life Microstructures of Long-Time Creep-Rupture-Tested SC Alloy 3 MFB Specimens (400X Magnification).

ORIGINAL PAGE IS  
OF POOR QUALITY

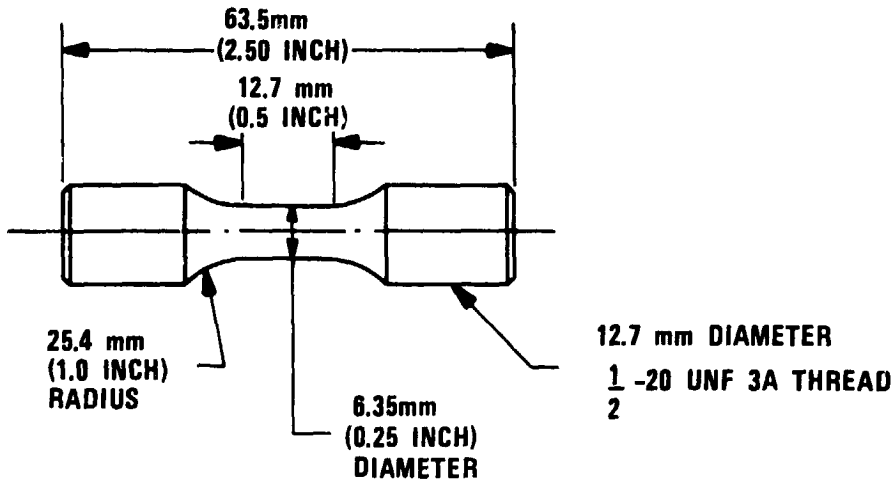


Figure 54. LCF Test Specimen.

TABLE 52. LOW-CYCLE-FATIGUE TEST RESULTS - AXIAL-AXIAL STRAIN-CONTROLLED TESTS,  
6.35 MM (0.25 INCH) DIAMETER TEST SPECIMENS  
MACHINED FROM NASAIR 100 SLAB CASTINGS.

Specimen Number	Orientation*	A Ratio	Temperature °C (°F)	Total Strain Range (%)	Elastic Modulus 10 <sup>6</sup> GPa (10 <sup>6</sup> psi)	N <sub>f</sub> (Cycles)	Remarks
11	Longitudinal	∞	760 (1400)	2.50	84.1 (12.2)	427	
1	Longitudinal	∞		2.40	78.6 (11.4)	750	
12	Longitudinal	∞		2.20	82.1 (11.9)	2,005	
3	Longitudinal	∞		2.00	80.7 (11.7)	2,677	
8	Longitudinal	∞		1.80	84.1 (12.2)	2,133	
5	Longitudinal	∞		1.70	83.4 (12.1)	4,283	
7	Longitudinal	∞		1.60	83.4 (12.1)	5,460	
2	Longitudinal	∞		1.50	82.1 (11.9)	15,845	
6	Longitudinal	∞		1.40	80.0 (11.6)	14,540	
10	Longitudinal	∞		1.30	85.5 (12.4)	15,060	
9	Longitudinal	∞		1.20	77.9 (11.3)	29,600+	Test terminated
16	Transverse	∞		1.50	80.7 (11.7)	1,818	Shrinkage porosity
Heat treatment consisted of 1316°C (2400°F) for 2 hours, plus 1324°C (2415°F) for 2 hours with Rapid Argon Quench, plus 982°C (1800°F) for 5 hours, plus 871°C (1600°F) for 20 hours.							
A ratio = $\frac{\text{alternating stress amplitude}}{\text{mean stress}}$ , Frequency = 0.33 Hertz.							
Longitudinal within 15 degrees of [001] and Transverse within 15 degrees of [100]							

ORIGINAL PAGE 1  
OF POOR QUALITY

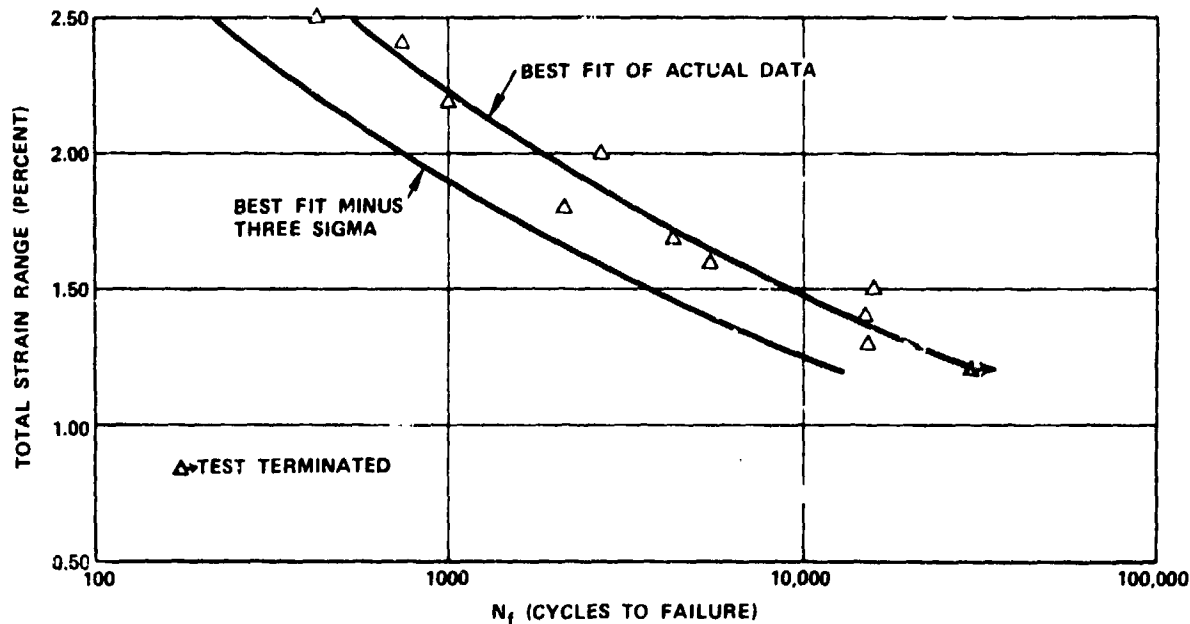


Figure 55. Strain-Controlled 760°C (1400°F) LCF Test Results for Longitudinal 6.35 mm (0.25 Inch) Diameter Test Specimens Machined from SC NASAIR 100 Slab Castings.

The single transversely oriented NASAIR 100 specimen that was LCF tested at 1.50 total percent strain range failed in 1,818 cycles, which was significantly lower than the longitudinally oriented specimen tested at the same strain range. SEM examination of the transversely oriented specimen fracture surfaces revealed substantial (unacceptable) shrinkage porosity, which explained the lower life.

### SC Alloy 3

LCF data for SC Alloy 3 were acquired at total strain ranges between 1.2 and 1.8 percent, test data are provided in Table 53.

ORIGINAL PAGE IS  
OF POOR QUALITY

760°C (1400°F)/1.30-PERCENT RANGE/A = ∞/0.33 Hz

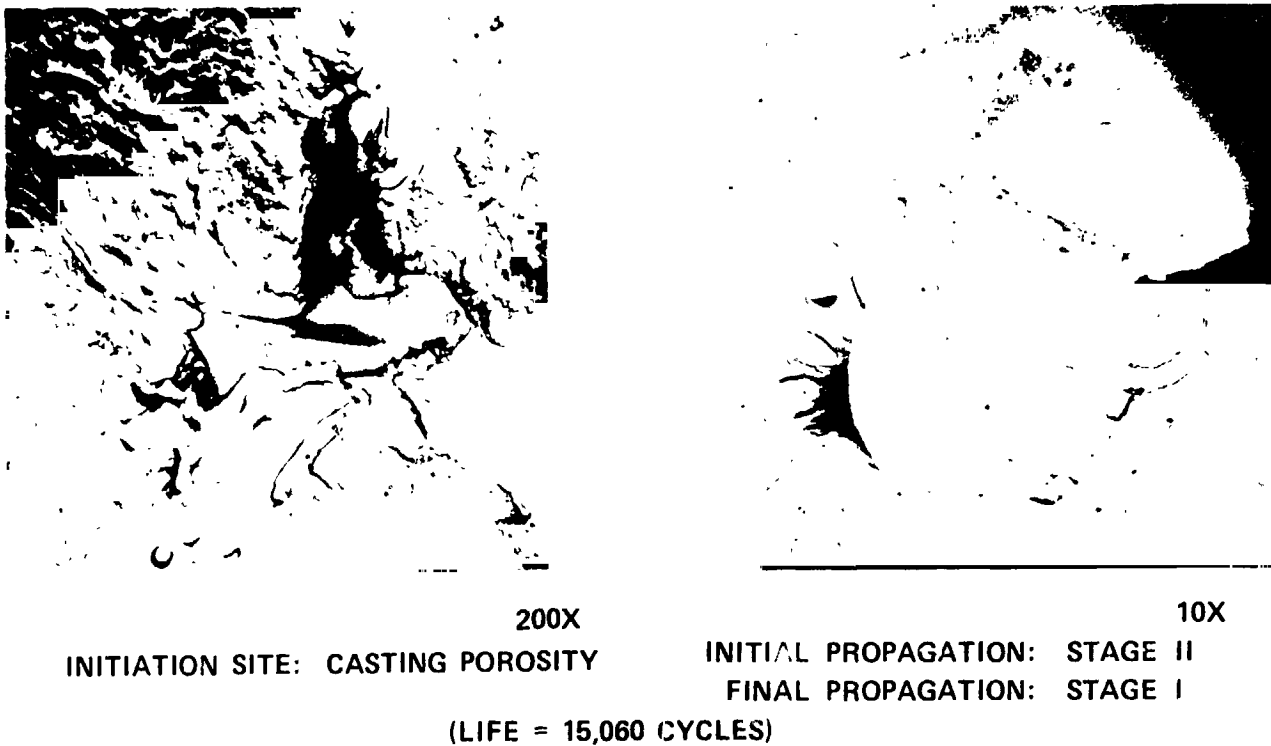


Figure 56. LCF Fracture of SC NASAIR 100.

A comparison of the SC Alloy 3 data with that for SC NASAIR 100 is provided in Figure 57 on a strain range basis. This comparison indicates that SC Alloy 3 has a lower cyclic strain range capability than SC NASAIR 100.

The elastic modulus of SC Alloy 3 was about 20 percent greater than that for SC NASAIR 100. Consequently, on a stress range basis, SC Alloy 3 and SC NASAIR 100 are essentially equivalent (as shown in Figure 58).

ORIGINAL PAGE IS  
OF POOR QUALITY

TABLE 53. LOW-CYCLE-FATIGUE TEST RESULTS - AXIAL-AXIAL STRAIN-CONTROLLED TESTS,  
- 6.35 MM (0.25 INCH) DIAMETER TEST SPECIMENS MACHINED FROM SC ALLOY 3  
SEPARATELY CAST BARS.

Specimen Number	Orientation*	A Ratio	Temperature °C (°F)	Total Strain Range (Percent)	Elastic Modulus 10 <sup>6</sup> GPa (10 <sup>6</sup> psi)		N <sub>f</sub> (Cycles)
687-5	Longitudinal	∞	760 (1400)	1.8	--	--	--**
687-6	Longitudinal	∞		1.8	97.9	(14.2)	756
687-4	Longitudinal	∞		1.6	101.4	(14.7)	1,510
692-1	Longitudinal	∞		1.4	97.9	(14.2)	6,071
687-7	Longitudinal	∞		1.3	96.5	(14.0)	9,668
687-3	Longitudinal	∞		1.2	100.0	(14.5)	14,545

Heat treatment consisted of 1288°C (2350°F) for 2 hours, plus 1296°C (2365°F) for 4 hours with Rapid Argon Quench, plus 982°C (1800°F) for 5 hours, plus 871°C (1600°F) for 20 hours.

A ratio =  $\frac{\text{alternating stress amplitude}}{\text{mean stress}}$  Frequency - 0.33 Hz

\*Within 15° of [001]

\*\*Equipment malfunction

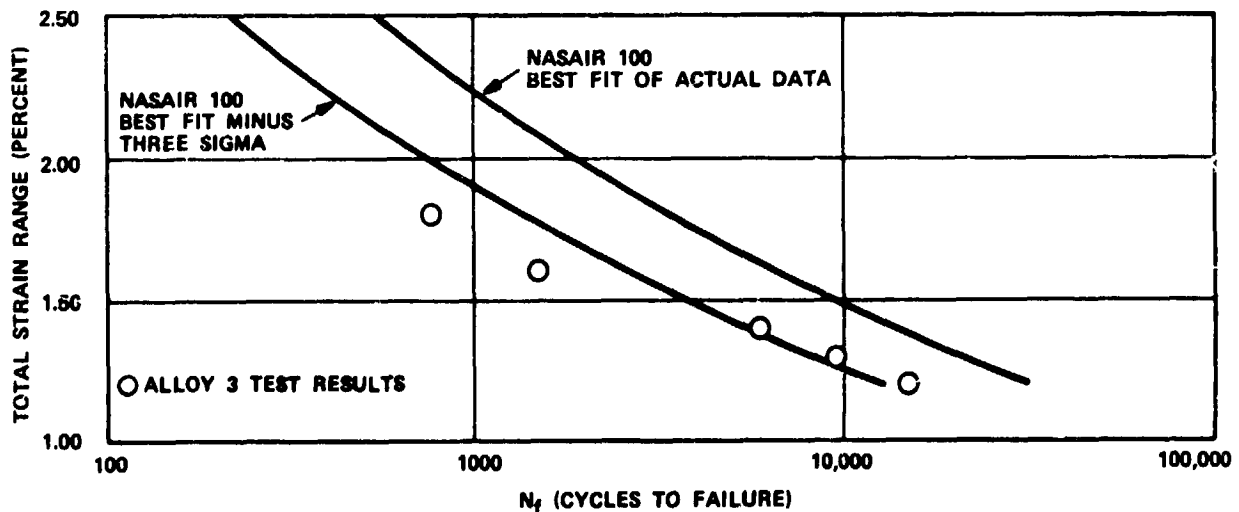


Figure 57. SC Alloy 3 Strain-Controlled LCF Test Results  
Compared to SC NASAIR 100 LCF Curve at 760°C  
(1400°F).

$760^{\circ}\text{C}(1400^{\circ}\text{F})/\text{A} = \infty/0.33 \text{ HERTZ}$

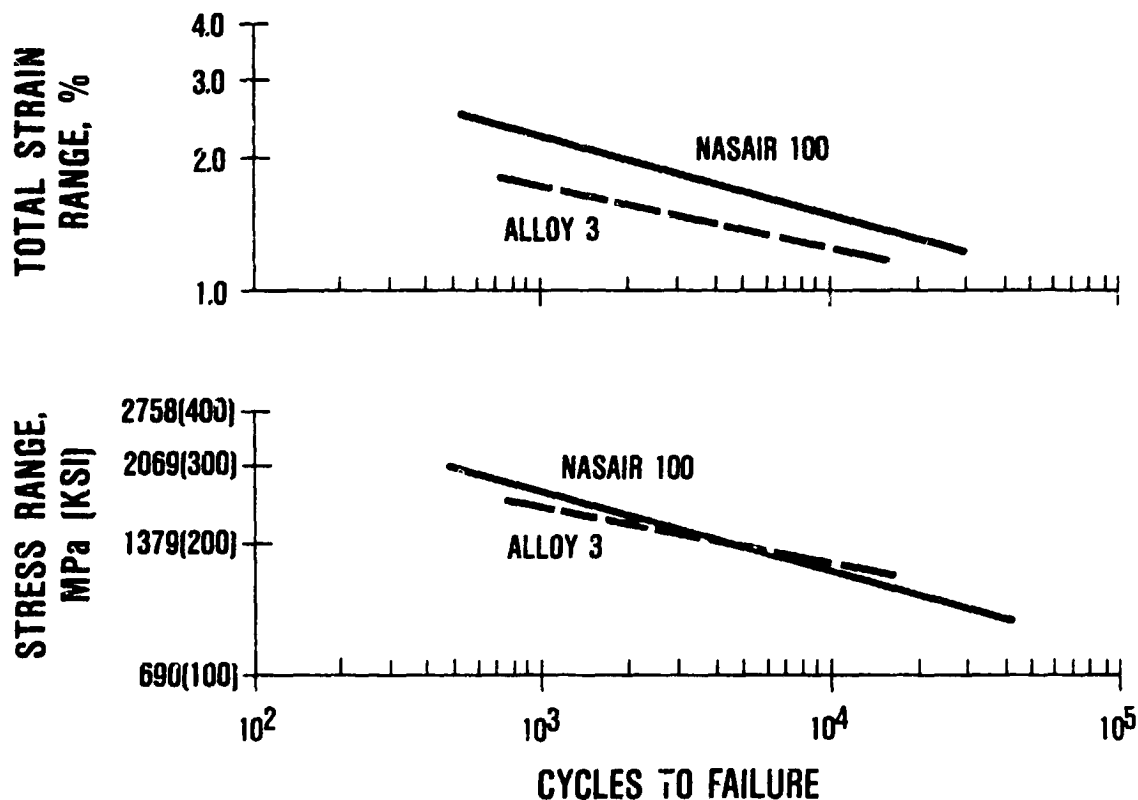


Figure 58. Low-Cycle Fatigue of SC Alloy.

In subsequent LCF tests performed under a Garrett R&D program, the modulus of SC NASAIR 100 was found to be equivalent to that of SC Alloy 3. Reasons for the relatively low modulus for SC NASAIR 100 (Table 52) were not determined.

Examination (40X) of fracture surfaces on the SC Alloy 3 specimens LCF tested at  $760^{\circ}\text{C}$  ( $1400^{\circ}\text{F}$ ) revealed subsurface Stage II initiation and Stage I crack propagation. SEM examination of the fracture surfaces revealed that the initiation sites are associated with microporosity. The fracture mode on the SC Alloy 3 specimens was similar to those observed on SC NASAIR 100 specimens.

ORIGINAL PAGE IS  
OF POOR QUALITY

#### 6.2.4 High-Cycle Fatigue

Axial HCF tests were performed under load control by Metcut Research Associates in Cincinnati, Ohio. These tests were performed with both smooth ( $K_t = 1.0$ ) and notched ( $K_t = 3.0$ ) 6.35 mm (0.25 inch) gauge diameter specimens (shown in Figures 59 and 60, respectively). Data were obtained at A ratios of infinity and 0.95, 871° and 982°C (1600° and 1800°F), at a frequency of 60 Hertz (3600 cpm). The HCF data were obtained with specimens in the uncoated, RT-21 diffusion aluminide coated, and exposed [982°C (1800°F)/1000 hours] conditions. Test results for SC NASAIR 100 and SC Alloy 3 are reviewed in the following paragraphs.

##### A Ratio Effects

The effect of stress ratio,  $A$  = Alternating stress amplitude/mean stress, on HCF life was evaluated with smooth specimens at 871°C (1600°F). Test data are provided in Tables 54 and 55 for SC NASAIR 100 and SC Alloy 3, respectively.

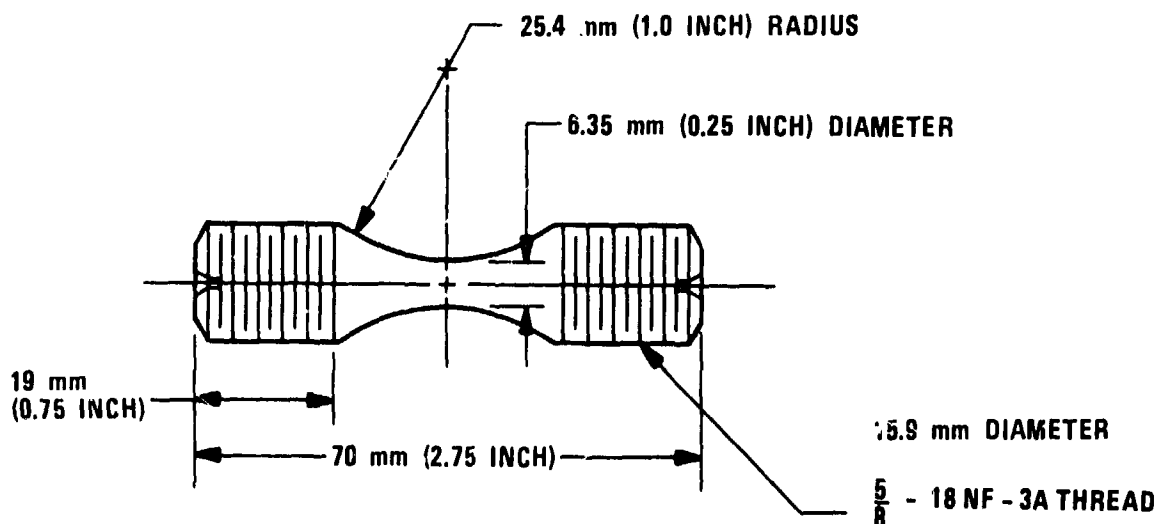


Figure 59. Smooth HCF Test Specimen.



ORIGINAL PAGE IS  
OF POOR QUALITY

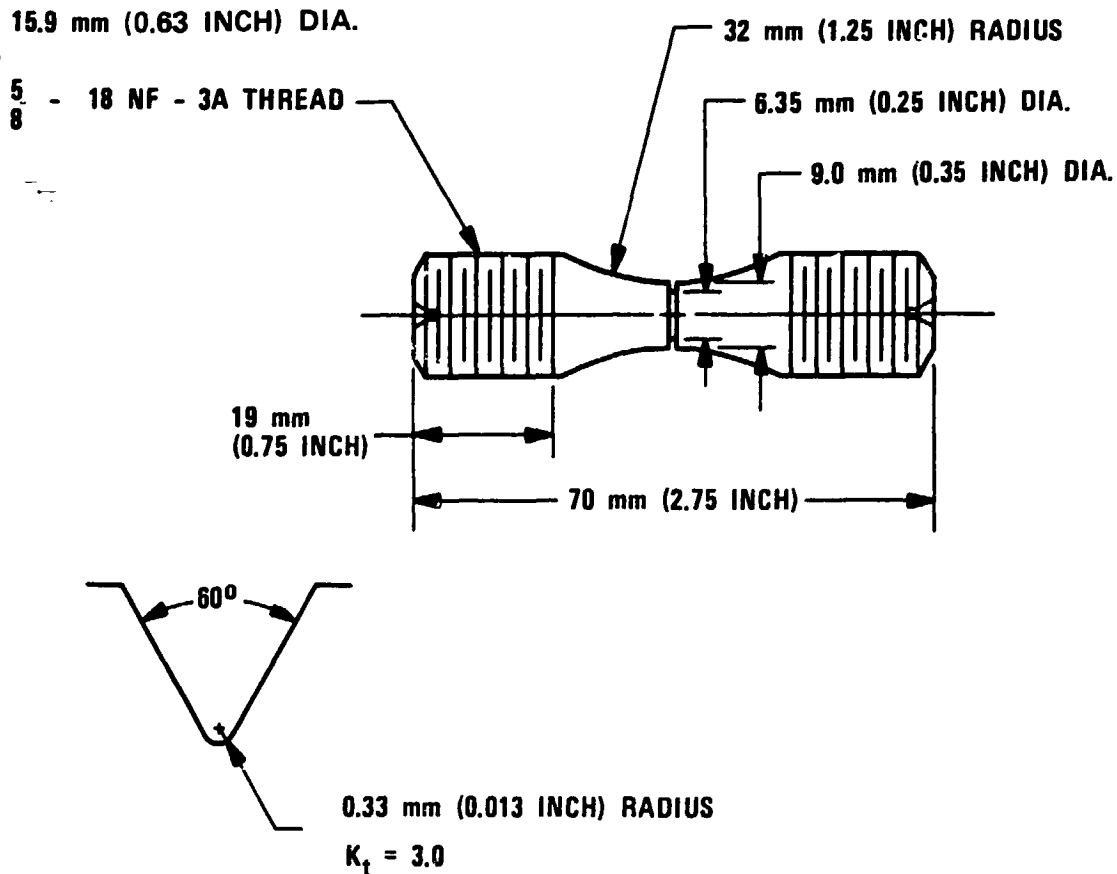


Figure 60. Notched HCF Test Specimen.

Test data are also compared graphically in Figure 61 with similar data for DS MAR-M 247 generated previously during Garrett's NASA-MATE Project 1.<sup>1</sup> Inspection of this data indicates that the  $10^7$  cycle runout strengths of SC NASAIR 100 and SC Alloy 3 exceed that of DS MAR-M 247, with SC NASAIR 100 having the highest strength. As expected, pulsating tension conditions ( $A = 0.95$ ) resulted in higher maximum stress and lower alternating stress amplitude at  $10^7$  cycle runout for each alloy relative to the cycle with equal tension and compression ( $A = \text{infinity}$ ).

Examination of the fracture surfaces of these specimens revealed that cracks typically initiated at subsurface microporosity. Cracks typically propagated initially in Stage II,

TABLE 54. EFFECT OF A RATIO ON HIGH-CYCLE-FATIGUE LIFE OF SMOOTH 6.35 MM (0.25 INCH) DIAMETER UNCOATED SC NASAIR 100 SPECIMENS.

Specimen Number	Master Heat	Configuration	A Ratio	Temperature °C (°F)	Stress MPa (ksi)		Cycles to Failure	Remarks
					Maximum	Alternating Amplitude		
544-2	VF-220	Smooth	∞	871 (1600)	552 (80)	552 (80)	44,000	Adaptor broke - reloaded and tested
570-40	VF-235	Smooth	∞		517 (75)	517 (75)	24,000	
544-8	VF-220	Smooth	∞		483 (70)	483 (70)	400,000	
569-27	VF-235	Smooth	∞		448 (65)	448 (65)	86,000	Runout - test terminated
521-13	VF-220	Smooth	∞		414 (60)	414 (60)	298,000	
553-3	VF-220	Smooth	∞		414 (60)	414 (60)	2,825,000	
547-4	VF-220	Smooth	∞		379 (55)	379 (55)	984,000	Runout - test terminated
567-7	VF-235	Smooth	∞		379 (55)	379 (55)	1,553,000	
569-24	VF-235	Smooth	∞		365 (53)	365 (53)	10,000,000+	
552-1	VF-220	Smooth	∞		345 (50)	345 (50)	10,000,000+	Runout - test terminated
568-13	VF-235	Smooth	∞		345 (50)	345 (50)	10,000,000+	
567-8	VF-235	Smooth	0.95		689 (100)	338 (49)	244,000	
547-16	VF-220	Smooth	0.95		621 (90)	303 (44)	353,000	Runout - test terminated
570-38	VF-235	Smooth	0.95		621 (90)	303 (44)	2,124,000	
553-6	VF-220	Smooth	0.95		552 (80)	269 (39)	2,223,000	
554-1	VF-220	Smooth	0.95		552 (80)	269 (39)	9,247,000	Runout - test terminated
552-2	VF-220	Smooth	0.95		517 (75)	255 (37)	1,175,000	
544-4	VF-220	Smooth	0.95		517 (75)	255 (37)	8,406,000	
568-14	VF-235	Smooth	0.95		483 (70)	234 (34)	8,711,000	Runout - test terminated
569-28	VF-235	Smooth	0.95		483 (70)	234 (34)	10,000,000+	
568-17	VF-235	Smooth	0.95		448 (65)	221 (32)	10,000,000+	
569-25	VF-235	Smooth	0.95		448 (65)	221 (32)	10,000,000+	Runout - test terminated

Heat treatment consisted of 1316°C (2400°F) for 2 hours, plus 1324°C (2415°F) for 2 hours with rapid Argon Quench, plus 982°C (1800°F) for 5 hours, plus 871°C (1600°F) for 20 hours.

A Ratio =  $\frac{\text{alternating stress amplitude}}{\text{mean stress}}$

Frequency = 60 Hertz

ORIGINAL PAGE IS  
OF POOR QUALITY

ORIGINAL PAGE IS  
OF POOR QUALITY

TABLE 55. EFFECT OF A RATIO ON HIGH-CYCLE-FATIGUE LIFE OF SMOOTH 6.35 MM (0.25 INCH) DIAMETER UNCOATED SC ALLOY 3 SPECIMENS.

Specimen Number	Master Heat	Configuration	A Ratio	Temperature °C (°F)	Stress MPa (ksi)		Cycles to Failure	Remarks
					Maximum	Alternating Amplitude		
689-4	VF-291	Smooth	∞	871 (1600)	448 (65)	448 (65)	80,000	
709-1	VF-291	Smooth	∞		414 (60)	414 (60)	360,000	
582-1	VF-291	Smooth	∞		379 (55)	379 (55)	7,000	Unacceptable porosity
709-7	VF-291	Smooth	∞		345 (50)	345 (50)	1,561,000	
695-2	VF-291	Smooth	∞		310 (45)	310 (45)	10,000,000+	Runout - test terminated
582-1	VF-291	Smooth	∞		310 (45)	310 (45)	10,000,000+	Runout - test terminated
709-5	VF-291	Smooth	0.95		483 (70)	234 (34)	415,000	Porosity
689-6	VF-291	Smooth	0.95		448 (65)	221 (32)	5,398,000	
709-9	VF-291	Smooth	0.95		414 (60)	200 (29)	7,950,000	
666-7	VF-291	Smooth	0.95		414 (60)	200 (29)	10,000,000+	Runout - test terminated
695-6	VF-291	Smooth	0.95		379 (55)	186 (27)	10,000,000+	Runout - test terminated
582-4	VF-291	Smooth	0.95		379 (55)	186 (27)	10,000,000+	Runout - test terminated

Heat treatment consisted of 1288°C (2350°F) for 2 hours, plus 1296°C (2365°F) for 4 hours with rapid Argon Quench, plus 982°C (1800°F) for 5 hours, plus 871°C (1600°F) for 20 hours.

A Ratio =  $\frac{\text{alternating stress amplitude}}{\text{mean stress}}$

Frequency = 60 Hertz

approximately perpendicular to the applied stress in the (001) plane and then switched to Stage I and propagated on a crystallographic plane. This trend is indicated in Figure 62 for an SC NASAIR 100 specimen that failed at 6,477,000 cycles. Close examination of the casting pore associated with initiation also indicated that a small amount of crystallographic cracking was associated with initiation, but this condition was not typical.

In both HCF and LCF tests, cracks commonly propagated in Stage II and then switched to Stage I. This trend contrasted with fatigue test results for equiaxed and columnar grain DS superalloys where the reverse trend was normally observed.

ORIGINAL PAGE IS  
OF POOR QUALITY

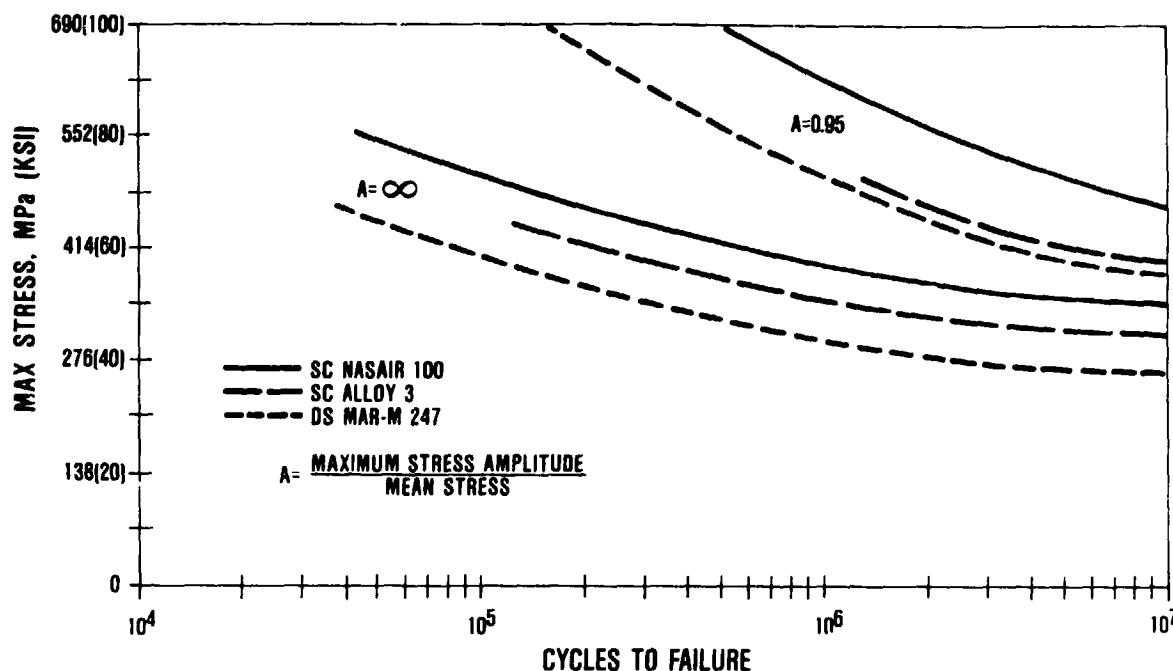


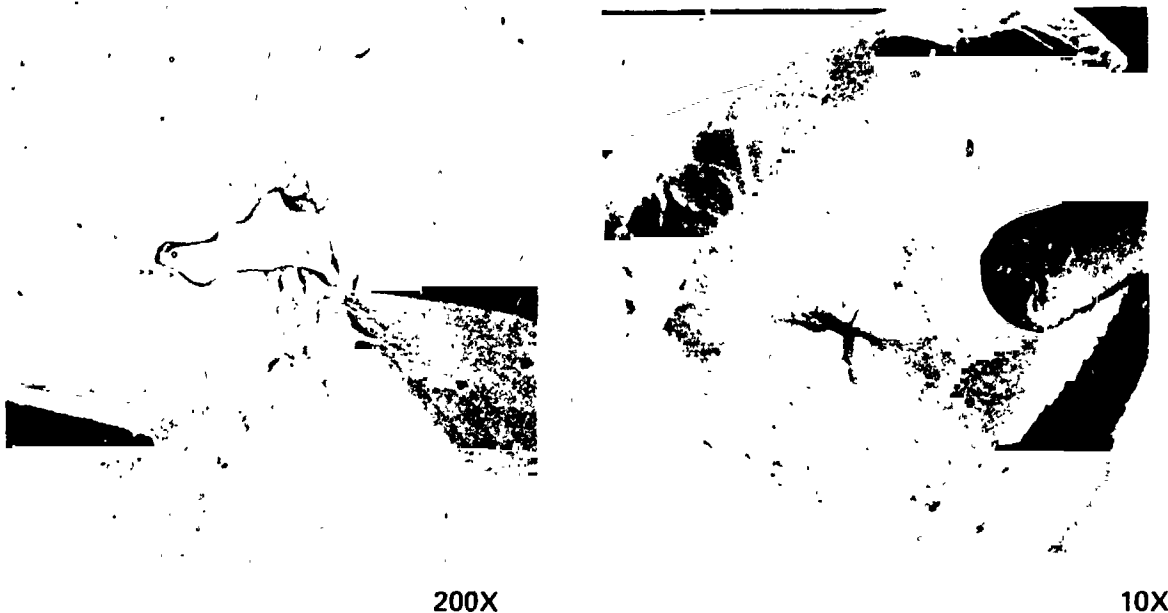
Figure 61. Effect of A Ratio on HCF Capability at 871°C (1600°F).

Leverant and Gell,<sup>15,16</sup> in studies of fatigue crack propagation in DS and SC MAR-M 200, determined that Stage I cracks propagated in a stable fatigue mode on {111} planes and tended to propagate preferentially, but not exclusively, in the <110> directions. These investigations also showed that crack initiation and propagation on the {111} slip planes of SC MAR-M 200 were favored by lower temperatures and higher frequencies, while crack propagation in Stage II, perpendicular to the applied stress, was favored by higher temperatures and lower frequencies.<sup>17</sup>

The extent of Stage I and Stage II cracking in SC NASAIR 100 and SC Alloy 3 is partially inconsistent with those conclusions for SC MAR-M 200. Stage II cracking can be a significant portion of the fracture surface in both low temperature LCF tests and intermediate temperature HCF tests.

ORIGINAL PAGE IS  
OF POOR QUALITY

871°C (1600°F)/552 MPa (80 KSI)/A = 0.95/60 Hz



INITIATION SITE: CASTING POROSITY

INITIAL PROPAGATION: STAGE II

FINAL PROPAGATION: STAGE I

LIFE = 6,477,000 CYCLES

Figure 62. HCF Fracture of SC NASAIR 100.

Reasons for the occurrence of Stage II cracking prior to Stage I cracking are also unclear at this time. Purushothaman and Tien<sup>18</sup> examined slow fatigue crack propagation in [001] oriented SC MAR-M 200 and verified that Stage II cracks were propagating by slip on multiple (111) planes. On the other hand, Sadananda and Shahinian<sup>19</sup> have recently presented evidence that fatigue cracks can propagate in Udimet 700 in the (001) plane in a cyclic pseudo-cleavage mode.

#### Notched Tests

Notched HCF tests were performed at 871°C (1600°F) with an A ratio of 0.95 (pulsating tension) and a frequency of 60 Hertz (3600

ORIGINAL PAGE 19  
OF POOR QUALITY

cpm). As indicated in Figure 60, the 6.35 mm (0.25 inch) gauge diameter was enveloped with a notch with a stress concentration factor,  $K_t$ , equal to three.

Results of these tests are provided in Table 56 and indicate that both SC NASAIR 100 and SC Alloy 3 have equivalent  $10^7$  cycle run-out lives at a maximum stress of 345 MPa (50 ksi) or an alternating stress amplitude of 168 MPa (24.3 ksi).

### Temperature

HCF tests were conducted at both 871° and 982°C (1600° and 1800°F) to establish the effect of temperature on HCF stress capability. Data obtained for SC NASAIR 100 and SC Alloy 3 at 982°C (1800°F) and an A ratio of infinity are provided in Table 57. A

TABLE 56. NOTCHED ( $K_t = 3.0$ ) HIGH-CYCLE-FATIGUE LIFE OF UNCOATED 6.35 MM (0.25 INCH) DIAMETER SC ALLOY SPECIMENS.

Specimen Number	Master Heat	Alloy	A Ratio	Temperature °C (°F)	Stress MPa (ksi)		Cycles to Failure	Remarks
					Maximum	Alternating Amplitude		
544-3	VF-220	SC NASAIR 100*	0.95	871 (1600)	483 (70)	234 (34)	20,000	
570-37	VF-235		0.95		448 (65)	221 (32)	116,000	
544-5	VF-220		0.95		448 (65)	221 (32)	255,000	
521-21	VF-220		0.95		414 (60)	200 (29)	57,000	
569-26	VF-235		0.95		414 (60)	200 (29)	1,017,000	
569-29	VF-235		0.95		379 (55)	186 (27)	---	Machine malfunction
568-18	VF-235		0.95		379 (55)	186 (27)	94,000	
570-41	VF-235		0.95		379 (55)	186 (27)	833,000	Porosity
567-9	VF-235		0.95		379 (55)	186 (27)	1,176,000	
567-12	VF-235		0.95		345 (50)	165 (24)	10,000,000+	Runout - test terminated
568-15	VF-235		0.95		345 (50)	165 (24)	10,000,000+	Runout - test terminated
689-5	VF-291	SC Alloy 3**	0.95		448 (65)	221 (32)	204,000	
709-8	VF-291		0.95		414 (60)	200 (29)	315,000	
689-7	VF-291		0.95		379 (55)	186 (27)	588,000	
582-6	VF-291		0.95		379 (55)	186 (27)	1,368,000	
709-10	VF-291		0.95		345 (50)	165 (24)	10,000,000+	Runout - test terminated
582-8	VF-291		0.95		345 (50)	165 (24)	10,000,000+	Runout - test terminated

\*Heat treatment consisted of 1316°C (2400°F) for 2 hours, plus 1324°C (2415°F) for 2 hours with rapid Argon Quench, plus 982°C (1800°F) for 5 hours, plus 871°C (1600°F) for 20 hours.

\*\*Heat treatment consisted of 1288°C (2350°F) for 2 hours, plus 1296°C (2365°F) for 4 hours with rapid Argon Quench, plus 982°C (1800°F) for 5 hours, plus 871°C (1600°F) for 20 hours.

A Ratio =  $\frac{\text{alternating stress amplitude}}{\text{mean stress}}$

Frequency = 60 Hertz

ORIGINAL PAGE IS  
OF POOR QUALITY

TABLE 57. HIGH-CYCLE-FATIGUE RESULTS FOR UNCOATED SC ALLOY 6.35 MM (0.25 INCH) DIAMETER SPECIMENS TESTED AT 982°C (1800°F).

Specimen Number	Master Heat	Alloy	Surface Condition	Configuration	A Ratio	Temperature °C (°F)	Stress MPa (ksi)		Cycles to Failure	Remarks
							Maximum	Alternating Amplitudes		
552-5	VP-220	SC NASAIR 100*	Uncoated	Smooth	-	982 (1800)	345 (50)	345 (50)	967,000	
567-10	VP-235		Uncoated	Smooth	-		310 (45)	310 (45)	4,830,000	
568-19	VP-235		Uncoated	Smooth	-		276 (40)	276 (40)	491,000	
569-30	VP-235		Uncoated	Smooth	-		276 (40)	276 (40)	7,703,000	
570-39	VP-225		Uncoated	Smooth	-		241 (35)	241 (35)	10,000,000+	Runout - test terminated
549-9	VP-220		Uncoated	Smooth	-		207 (30)	207 (30)	10,000,000+	Runout - test terminated
646-1	VP-291	SC Alloy 3**	Uncoated	Smooth	-		276 (40)	276 (40)	470,000	
709-2	VP-291		Uncoated	Smooth	-		241 (35)	241 (35)	3,363,000	
695-5	VP-291		Uncoated	Smooth	-		207 (30)	207 (30)	10,000,000+	Runout - test terminated

\*Heat treatment for SC NASAIR 100 consisted of 1316°C (2400°F) for 2 hours plus 1324°C (2415°F) for 2 hours with rapid Argon Quench, plus 982°C (1800°F) for 5 hours, plus 871°C (1600°F) for 20 hours.

\*\*Heat treatment for SC Alloy 3 consisted of 1288°C (2350°F) for 2 hours plus 1296°C (2365°F) for 4 hours with Rapid Argon Quench, plus 982°C (1800°F) for 5 hours, plus 871°C (1600°F) for 20 hours.

A Ratio =  $\frac{\text{Alternating Stress Amplitude}}{\text{Mean Stress}}$ , Frequency = 0.33 Hertz

comparison with similar data obtained at 871°C (1600°C) can be made using Tables 54, 55, and 57. This comparison indicates that the higher test temperature resulted in approximately a 30-percent reduction in HCF run-out stress capability for both alloys at the higher temperature.

### Coatings

Protective coatings are essential to the long-time surface stability of superalloys in a turbine environment. However, under some conditions of cyclic strain amplitude and coating thickness, cracks initiating in the coating can propagate into the superalloy. Thin coatings generally show the least tendency to penetrate into the superalloy.<sup>14,20</sup>

To quantify any coating effects on the HCF capabilities of the SC alloys, smooth 6.35 mm (0.25 inch) gauge diameter HCF specimens were diffusion aluminide (RT-21) coated to a thickness of 25 to 50  $\mu\text{m}$  (0.001 to 0.002 inch) by Chromalloy American Corporation in Orangeburg, New York.

After coating, HCF tests were conducted at 871° and 982°C (1600 and 1800°F) and A ratios of 0.95 and infinity. Test data for SC NASAIR 100 and SC Alloy 3 are provided in Tables 58 and 59, respectively. In addition, a comparison with coated and uncoated data for SC NASAIR 100, SC Alloy 3, and DS MAR-M 247 is provided in Figure 63 for an A ratio equal to infinity.

Inspection of these data indicates that the coating effects on the  $10^7$  cycle life capability of the alloy were not significant at the coating thickness evaluated.

Examination of the  $10^7$  cycle run-out specimens, however, indicated in all instances that the coating had initiated numerous cracks in both alloys. Photomicrographs of diffusion aluminide coated SC NASAIR 100 after  $10^7$  cycles of testing at 871° and 982°C (1600° and 1800°F) are provided in Figures 64 and 65 to illustrate the extent of coating cracking at runout. At both temperatures, coating-initiated cracks were observed to propagate a short distance into the alloy. HCF conditions that would not initiate coating cracks were not determined.

#### Long-Time Exposure

A limited number of HCF tests were conducted at 982°C (1800°F) with SC NASAIR 100 and SC Alloy 3 specimens that were machined from fully processed bars that had a subsequent 982°C (1800°F)/1000-hour furnace exposure. As noted previously, this exposure coarsens the gamma prime phase in both alloys and results in precipitation of the mu phase in NASAIR 100.

Results of tests for the SC alloys in the exposed condition are provided in Table 60. Figure 66 is a comparison between exposed and typical unexposed data. Inspection of these data indicates that the furnace exposure had no effect on the HCF strength of either alloy.



ORIGINAL PAGE IS  
OF POOR QUALITY

TABLE 58. HIGH-CYCLE-FATIGUE CAPABILITY OF DIFFUSION ALUMINIDE (RT-21) COATED 6.35 MM (0.25 INCH) DIAMETER SC NASAIR 100 SPECIMENS.

Specimen Number	Master Heat	Configuration	A Ratio	Temperature °C (°F)	Stress MPa (ksi)		Cycles to Failure	Remarks
					Maximum	Alternating Amplitude		
570-43	VF-235	Smooth	0.95	871 (1600)	689 (100)	338 (49)	41,000	
569-36	VF-235	Smooth	0.95		689 (100)	338 (49)	201,000	
544-14	VF-220	Smooth	0.95		621 (90)	303 (44)	546,000	
567-3	VF-235	Smooth	0.95		621 (90)	303 (44)	1,180,000	
544-25	VF-220	Smooth	0.95		586 (85)	283 (41)	2,894,000	
552-13	VF-220	Smooth	0.95		552 (80)	269 (39)	6,477,000	
553-23	VF-220	Smooth	0.95		552 (80)	269 (39)	8,455,000	
552-24	VF-220	Smooth	0.95		483 (70)	234 (34)	2,900,000	
568-21	VF-235	Smooth	0.95		483 (70)	234 (34)	4,070,000	
568-23	VF-235	Smooth	0.95		483 (70)	234 (34)	10,000,000+	Runout - test terminated
553-8	VF-220	Smooth	0.95		448 (65)	221 (32)	10,000,000+	Runout - test terminated
569-32	VF-235	Smooth	0.95		448 (65)	221 (32)	10,000,000+	Runout - test terminated
544-11	VF-220	Smooth	"		552 (80)	552 (80)	36,000	
570-45	VF-235	Smooth	"		517 (75)	517 (75)	36,000	
544-22	VF-220	Smooth	"		483 (70)	483 (70)	48,000	
569-31	VF-235	Smooth	"		483 (70)	483 (70)	118,000	
568-20	VF-235	Smooth	"		414 (60)	414 (60)	250,000	
552-11	VF-220	Smooth	"		414 (60)	414 (60)	494,000	
567-6	VF-235	Smooth	"		379 (55)	379 (55)	3,512,000	
553-28	VF-220	Smooth	"		379 (55)	379 (55)	5,428,000	
570-42	VF-235	Smooth	"		365 (53)	365 (53)	682,000	Porosity
552-18	VF-220	Smooth	"		345 (50)	345 (50)	15,000	Extensive casting porosity
553-22	VF-220	Smooth	"		345 (50)	345 (50)	10,000,000+	Runout - test terminated
567-1	VF-235	Smooth	"		345 (50)	345 (50)	10,000,000+	Runout - test terminated
544-16	VF-220	Smooth	"	982 (1800)	345 (50)	345 (50)	27,000	
553-27	VF-220	Smooth	"		310 (45)	310 (45)	7,660,000	
569-33	VF-235	Smooth	"		276 (40)	276 (40)	7,583,000	
567-5	VF-235	Smooth	"		276 (40)	276 (40)	8,166,000	
552-17	VF-220	Smooth	"		276 (40)	276 (40)	10,000,000+	Runout - test terminated
568-22	VF-235	Smooth	"		241 (35)	241 (35)	10,000,000+	Runout - test terminated

Heat treatment consisted of 1316°C (2400°F) for 2 hours, plus 1324°C (2415°F) for 2 hours with rapid Argon Quench, plus RT-21 coated, plus 871°C (1600°F) for 20 hours.

A Ratio =  $\frac{\text{alternating stress amplitude}}{\text{mean stress}}$

Frequency = 60 Hertz

ORIGINAL PAGE IS  
OF POOR QUALITY

TABLE 59. HIGH-CYCLE-FATIGUE CAPABILITY OF DIFFUSION-ALUMINIDE (RT-21) COATED  
6.35 MM (0.25 INCH) DIAMETER SC ALLOY 3 SILEMENS.

Specimen Number	Master Heat	Configuration	A Ratio	Temperature °C (°F)	Stress MPa (ksi)		Cycles to Failure	Remarks
					Maximum	Alternating Amplitude		
695-4	VF-291	Smooth	0.95	871 (1600)	414 (60)	200 (29)	34,000	Unacceptable porosity
709-6	VF-291	Smooth	0.95		414 (60)	200 (29)	4,821,000	
582-5	VF-291	Smooth	0.95		379 (55)	186 (27)	10,000,000+	Runout - test terminated
582-2	VF-291	Smooth	"	982 (1800)	310 (45)	310 (45)	1,387,000	
695-1	VF-291	Smooth	"		310 (45)	310 (45)	3,492,000	
709-3	VF-291	Smooth	"		276 (40)	276 (40)	10,000,000+	Runout - test terminated
709-4	VF-291	Smooth	"	982 (1800)	310 (45)	310 (45)	96,000	
695-3	VF-291	Smooth	"		276 (40)	276 (40)	2,175,000	
582-3	VF-291	Smooth	"		241 (35)	241 (35)	10,000,000+	Runout - test terminated

Heat treatment consisted of 1288°C (2350°F) for 2 hours plus 1296°C (2365°F) for 4 hours with Argon Quench, plus RT-21 coating, plus 871°C (1600°F) for 20 hours.

A Ratio =  $\frac{\text{Alternating Stress Amplitude}}{\text{Mean Stress}}$

Frequency = 60 Hertz

A = ∞/60 HERTZ

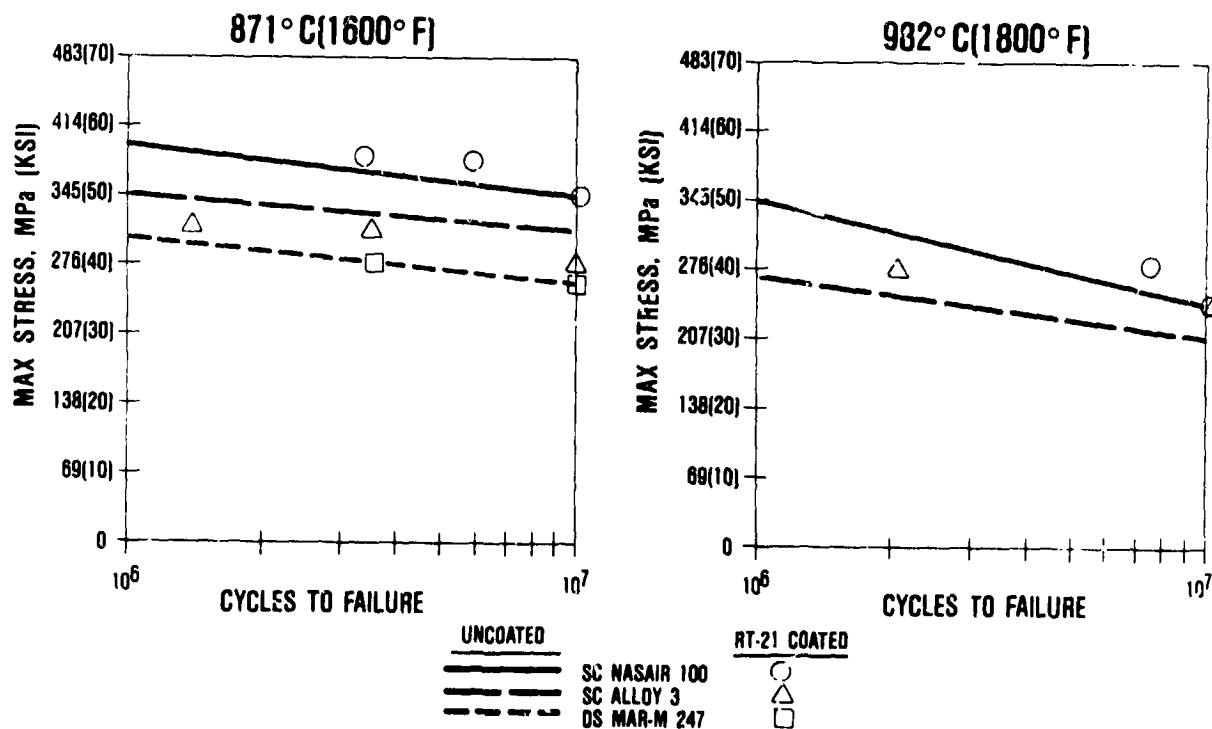


Figure 63. Diffusion-Aluminide (RT-21) Coating Effects on HCF Properties.

ORIGINAL PAGE IS  
OF POOR QUALITY.

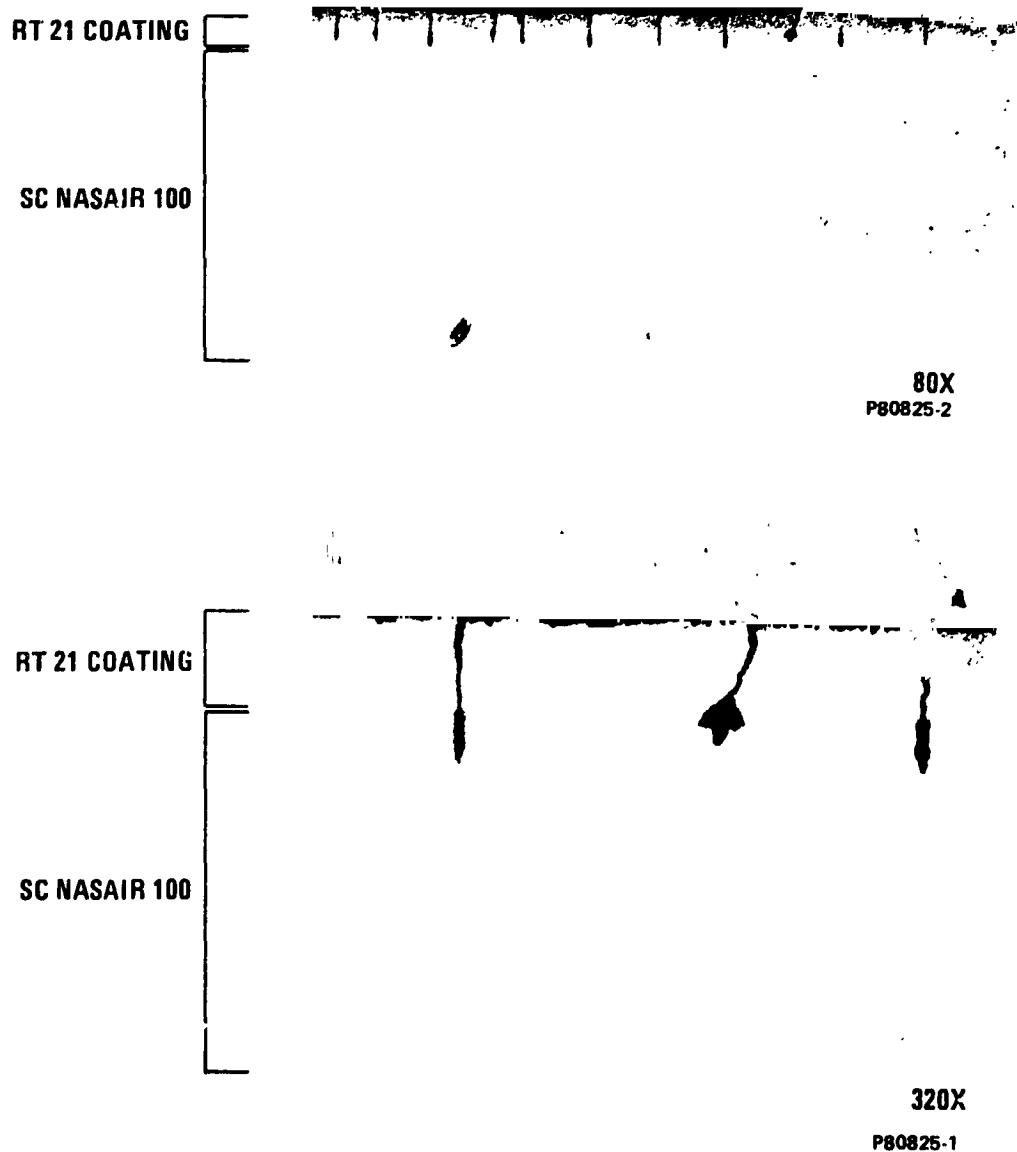


Figure 64. HCF Cracks in RT-21 Diffusion-Aluminide-Coated SC NASAIR 100 Specimens After  $10^7$  Cycles at  $871^{\circ}\text{C}$  ( $1600^{\circ}\text{F}$ ) and a Maximum Stress of 345 MPa (50 ksi). (A ratio equal to  $\infty$ ).

ORIGINAL PAGE IS  
OF POOR QUALITY

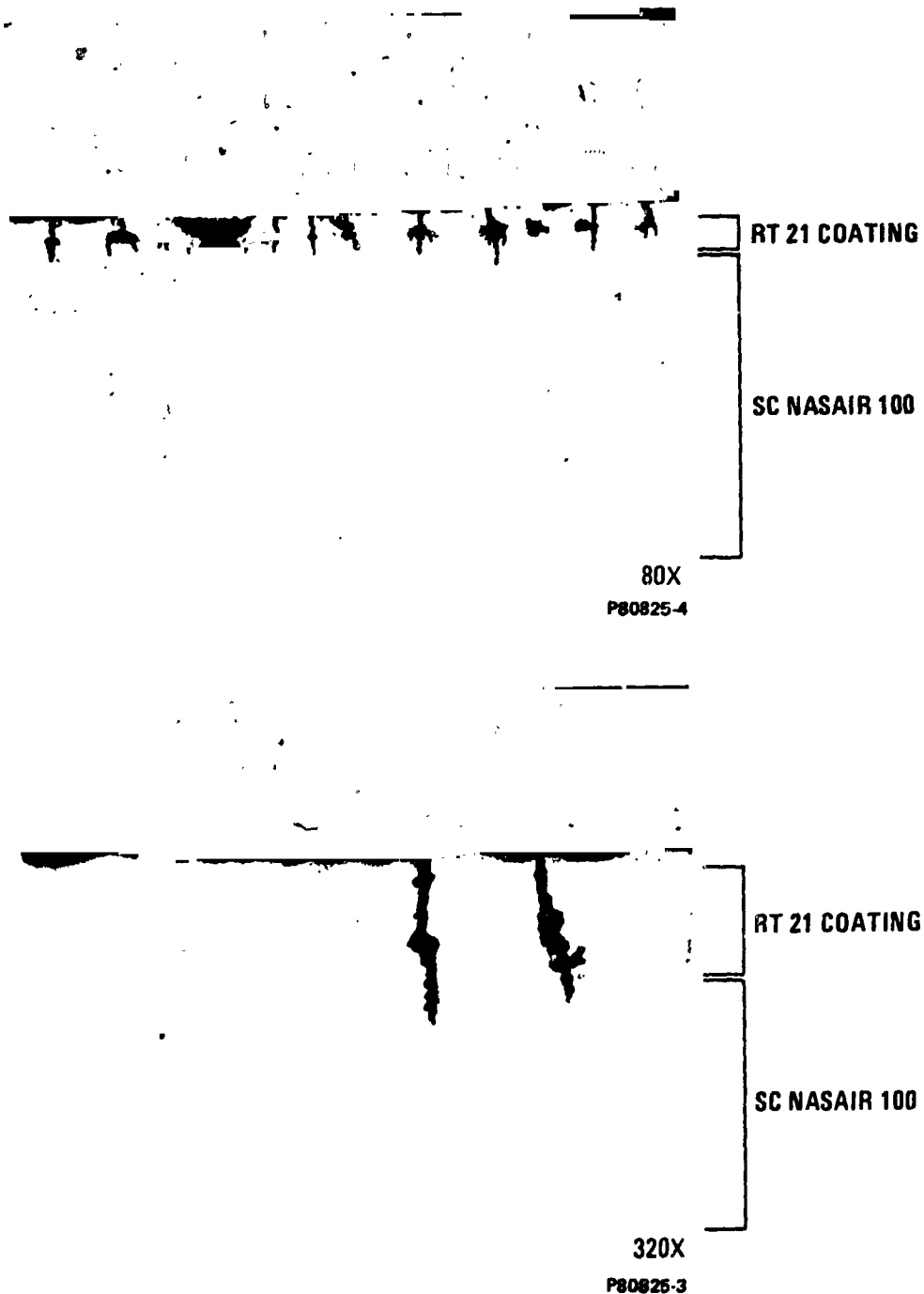


Figure 65. HCF Cracks in RT-21 Diffusion-Aluminide-Coated SC NASAIR 100 Specimens After  $10^7$  Cycles at  $982^{\circ}\text{C}$  ( $1800^{\circ}\text{F}$ ) and a Maximum Stress of 241 MPa (35 ksi).  $A = \infty$ .

ORIGINAL PAGE 19  
OF POOR QUALITY

TABLE 60. HIGH-CYCLE-FATIGUE RESULTS FOR AXIAL-AXIAL TEST OF UNCOATED 6.35 MM (0.25 INCH) DIAMETER SPECIMENS MACHINED FROM EXPOSED\* SC NASAIR 100 AND SC ALLOY 3 SEPARATELY CAST TEST BARS.

Specimen Number	Master Heat	Alloy	Configuration	A Ratio	Temperature °C (°F)	Stress MPa (ksi)		Cycles to Failure	Remarks
						Maximum	Alternating Amplitude		
653-1	VF-236	SC NASAIR 100	Smooth	—	982 (1800)	310 (45)	310 (45)	2,205,000	Runout-test terminated
653-2	VF-236	SC NASAIR 100	Smooth	—		276 (40)	276 (40)	6,912,000	
653-3	VF-236	SC NASAIR 100	Smooth	—		241 (35)	241 (35)	10,000,000+	
666-1	VF-291	SC Alloy 3	Smooth	—		276 (40)	276 (40)	3,124,000	Runout-test terminated
666-2	VF-291	SC Alloy 3	Smooth	—		241 (35)	241 (35)	6,614,000	
666-3	VF-291	SC Alloy 3	Smooth	—		207 (30)	207 (30)	10,000,000+	

\*Prior to exposure at 982°C (1800°F) for 1000 hours:

SC NASAIR 100 heat treatment consisted of 1316°C (2400°F) for 2 hours, plus 1324°C (2415°F) for 2 hours with rapid Argon Quench, plus 982°C (1800°F) for 5 hours, plus 871°C (1600°F) for 20 hours.

SC Alloy 3 heat treatment consisted of 1288°C (2350°F) for 2 hours, plus 1296°C (2365°F) for 4 hours with rapid Argon Quench, plus 982°C (1800°F) for 5 hours, plus 871°C (1600°F) for 20 hours.

A Ratio =  $\frac{\text{alternating stress amplitude}}{\text{mean stress}}$  Frequency = 60 Hertz

### 6.3 Environmental Tests

Successful operation of SC turbine blades is dependent on maintaining airfoil surface integrity under conditions of high temperature oxidation and intermediate temperature hot corrosion (salt film accelerated oxidation). Consequently, burner rig testing was conducted to assess the environmental resistance of uncoated and RT-21 diffusion aluminide coated SC NASAIR 100 and SC Alloy 3 specimens (Figure 67). Coatings were applied to an approximate thickness of 50  $\mu\text{m}$  (2 mils) by Chromalloy American Corporation in Orangeburg, New York.

Hot-corrosion testing was performed on duplicate specimens of uncoated and RT-21 coated SC NASAIR 100 and SC Alloy 3 at 927°C (1700°F) for 307 hours. Burner rig test parameters included the following:

- o Cycle - 60 minutes hot + 3 minutes forced air cool
- o Fuel - Jet A

ORIGINAL PAGE IS  
OF POOR QUALITY

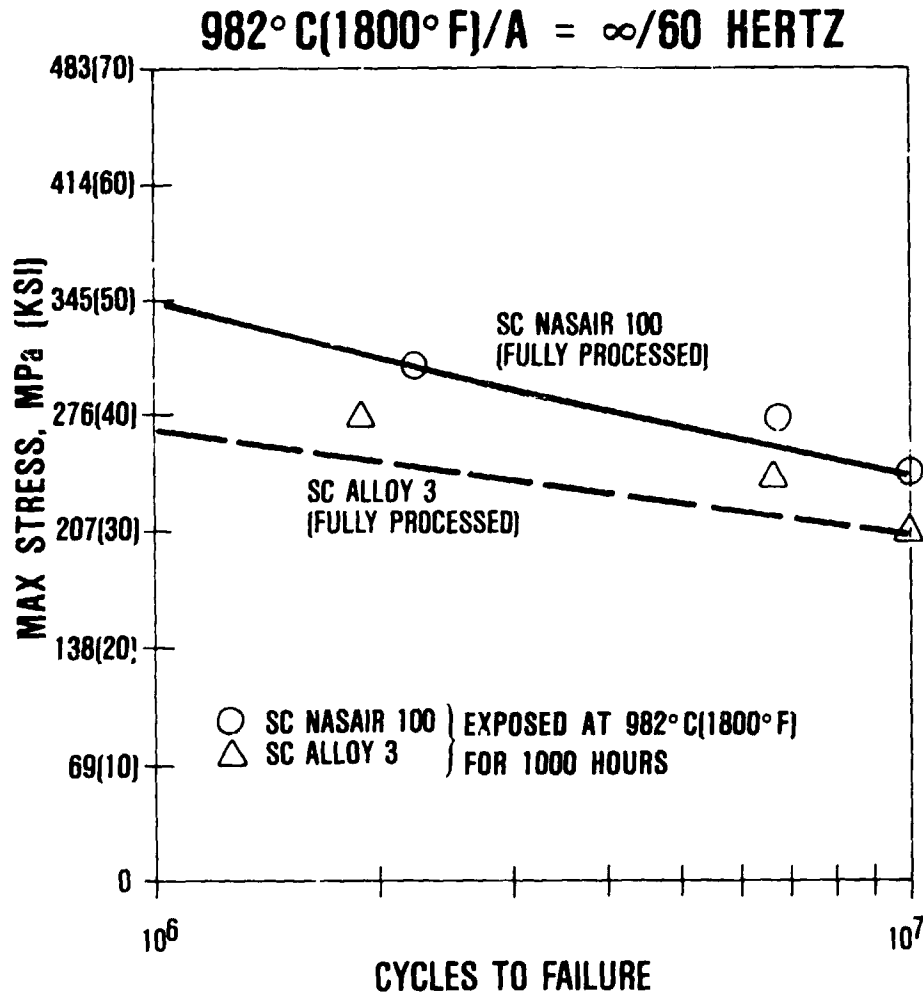


Figure 66. Effect of Long-Term Exposure on HCF Strength.

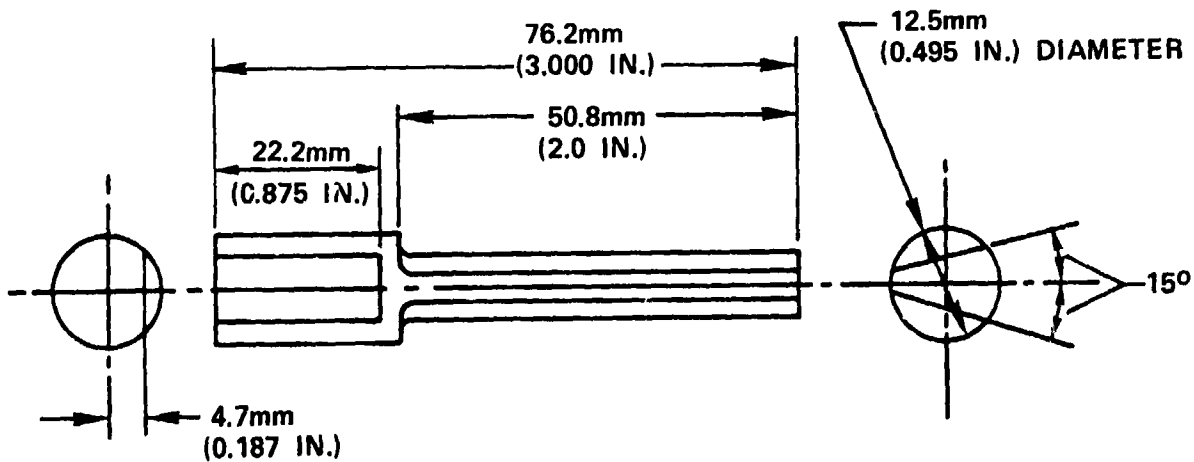


Figure 67. Burner Rig Specimen

ORIGINAL PAGE IS  
OF POOR QUALITY.

- o 5 ppm synthetic sea salt (ASTM D1141-52)
- o Specimen rotation - 1500 rpm

A description of the burner rig is provided in Reference 1.

The appearance of the RT-21 coated SC alloy specimens after hot-corrosion testing at 927°C (1700°F) for 203 and 307 hours is shown in Figure 68. The RT-21 coated SC Alloy 3 specimens exhibit some oxide scale spallation without base-metal corrosion. The RT-21 coated SC NASAIR 100 specimens exhibited coating failure and base-metal corrosion.

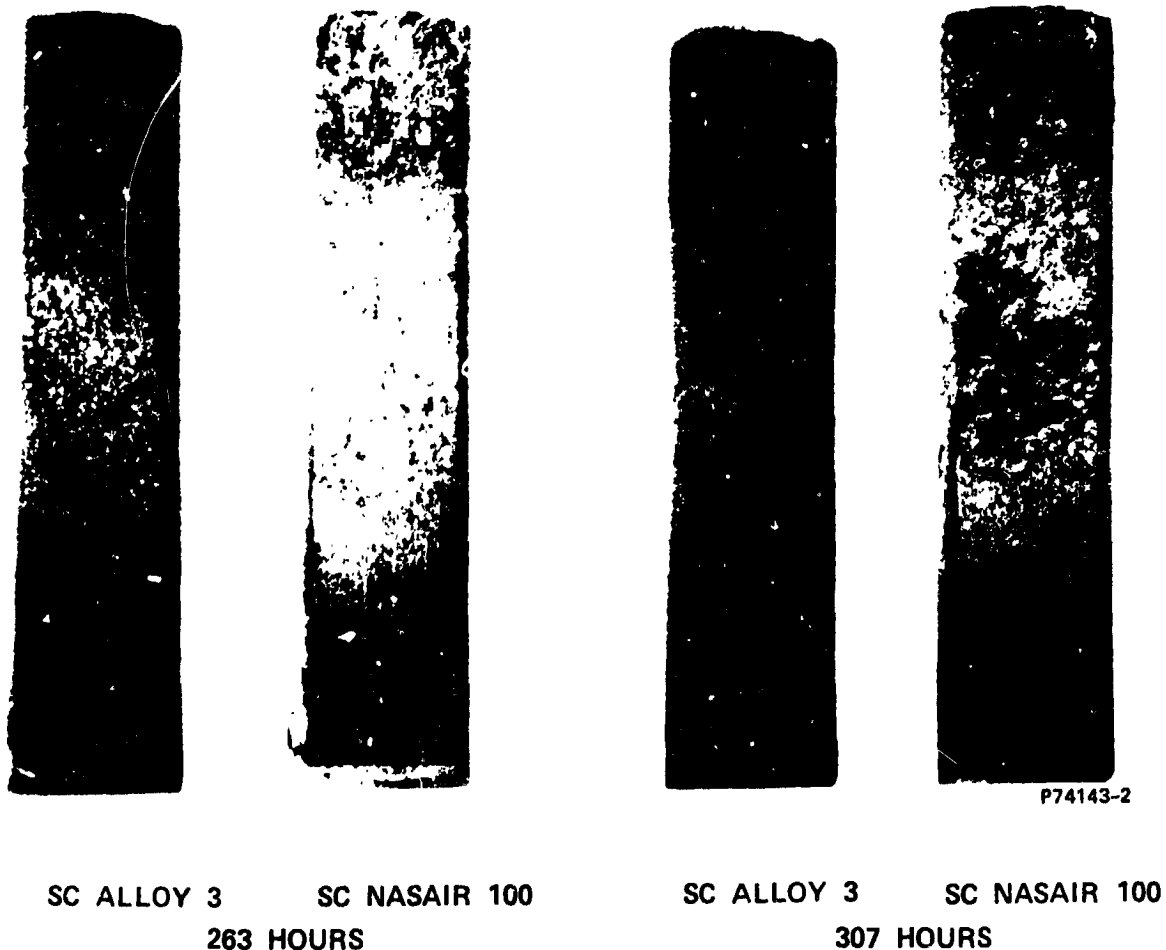


Figure 68. Appearance of RT-21 Diffusion-Aluminide-Coated Specimens after Indicated Hours of Hot-Corrosion Testing at 927°C (1700°F) with 5 ppm Sea Salt. (Magnification: 2X)

ORIGINAL PAGE IS  
OF POOR QUALITY

Weight change data for hot-corrosion tested uncoated and RT-21 coated SC NASAIR 100 and SC Alloy 3 specimens are provided in Table 61. For comparison, the DS Mar-M 247 (uncoated and RT-21 coated) 927°C (1700°F) hot-corrosion test results generated in Project 1 of the MATE Program are also included in Table 61. Based on weight change and visual examination data, the test results indicated the following:

- o Uncoated SC NASAIR 100 and SC Alloy 3 exhibited corrosion similar to uncoated DS Mar-M 247.
- o RT-21 coated SC NASAIR 100 exhibited less corrosion resistance than RT-21 coated SC Alloy 3 or RT-21 coated DS Mar-M 247. Coating failure of RT-21 coated SC NASAIR 100 specimens occurred after 203 hours.

TABLE 61. 927°C (1700°F) HOT-CORROSION TEST RESULTS.

Alloy	Weight change* (in grams) at indicated test time (hours)								Remarks
	25	50	76	101	153	203	256	307	Done
NASAIR 100 (Uncoated)	-0.07	-0.28	-0.87	-1.47	-2.00	-3.41	-4.57	-6.09	Gross corrosion
NASAIR 100 (RT-21 Coated)	+0.01	+0.01	+0.01	0	-0.01	-0.02	-0.04	-0.25	Coating failure after 203 hours
Alloy 3 (Uncoated)	-0.02	-0.07	-0.45	-1.04	-1.61	-2.73	-4.01	-6.75	Gross corrosion
Alloy 3 (RT-21 Coated)	+0.01	+0.01	+0.01	+0.01	+0.01	+0.01	+0.01	+0.01	No coating degradation
	20	40	80	100	160	210	260	310	
DS Mar-M 247 (Uncoated)	-0.06	-0.13	-0.56	-1.09	-2.06	-5.14	-6.63	-9.83	Gross corrosion
DS Mar-M 247 (RT-21 Coated)	0	0	0	0	0	+0.01	0	+0.01	Slight coating degradation

\*Weight change is an average of 2 test specimens



- o RT-21 coated SC Alloy 3 exhibited corrosion resistance as good as, or slightly better than, RT-21 coated DS Mar-M 247. No visual evidence of coating failure was observed on Alloy 3 specimens after 307 hours, whereas the DS Mar-M 247 specimens exhibited slight coating degradation after 310 hours of testing.

Burner rig oxidation testing was conducted on duplicate specimens of uncoated and RT-21 coated SC NASAIR 100 and SC Alloy 3 at 1093°C (2000°F) for 509 hours with the following test parameters:

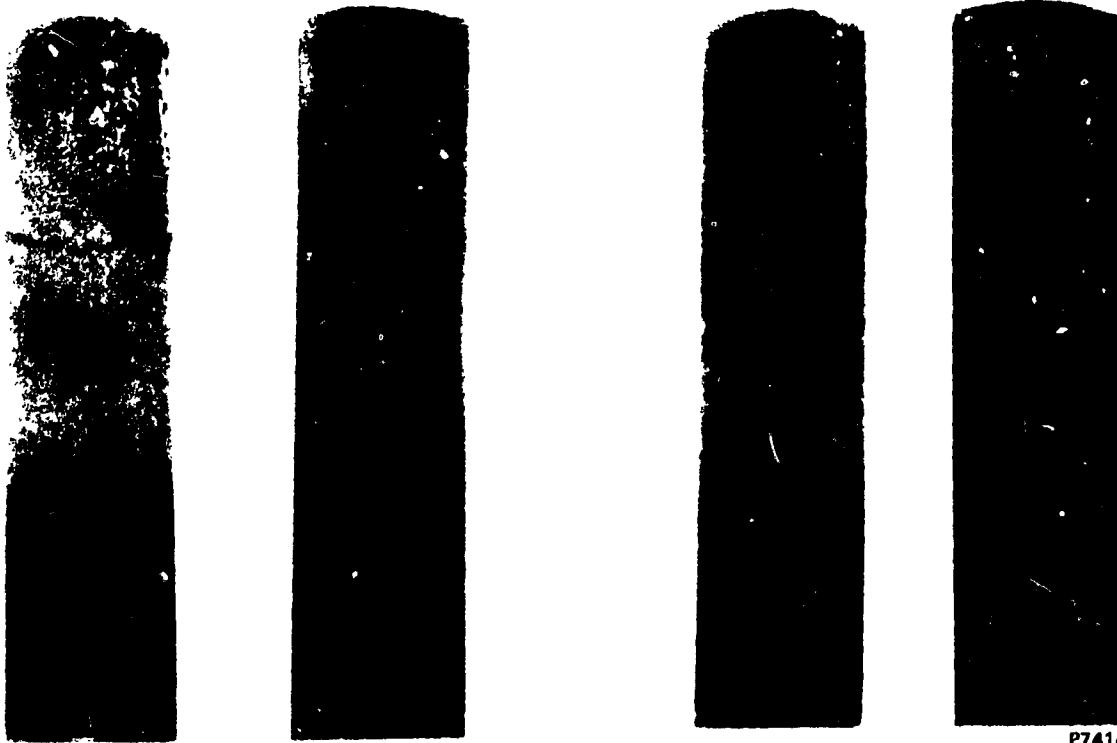
- o Cycle - 60 minutes hot + 3 minutes forced air cool
- o Fuel - Jet A
- o Specimen rotation - 1500 rpm.

The post-test visual appearance of the RT-21 coated SC Alloy specimens is shown in Figure 69 and weight change data for both uncoated and coated specimens are provided in Table 62.

Examination of these data indicates that uncoated SC NASAIR 100 appeared to have slightly better oxidation resistance when compared to uncoated SC Alloy 3. Weight losses for these SC alloys in this 1093°C (2000°F) test were significantly greater (by a factor of 20 to 30) than those observed for uncoated DS Mar-M 247 specimens evaluated for 510 hours at 1038°C (1900°F) in Garrett's NASA-MATE Project 1.<sup>1</sup>

RT-21 coated SC NASAIR 100 and SC Alloy 3 appeared to exhibit comparable oxidation resistance based on weight change data. Visual inspection of the specimens indicated that the RT-21 coated SC Alloy 3 specimens appeared to be degrading by a pitting process, while the RT-21 coated SC NASAIR 100 was degrading by oxide scale spalling (Figure 69).

ORIGINAL PAGE IS  
OF POOR QUALITY



P74143-7

SC ALLOY 3

SC NASAIR 100

SC ALLOY 3

SC NASAIR 100

Figure 69. Appearance of Duplicate RT-21 Coated SC NASAIR 100 and SC Alloy 3 Specimens after Oxidation Testing at 1093°C (2000°F) for 509 Hours. (Magnification: 2X)

TABLE 62. 1093°C (2000°F) OXIDATION TEST RESULTS.

Alloy	Weight Change* (in grams) at indicated test time (in hours)								
	25	50	75	100	151	211	311	413	509
NASAIR 100 (Uncoated)	-0.02	-0.02	-0.03	-0.04	-0.05	-0.08	-0.12	-0.16	-0.22
NASAIR 100 (RT-21 Coated)	0	0	0	-0.01	-0.01	-0.02	-0.04	-0.06	-0.10
Alloy 3 (Uncoated)	-0.02	-0.04	-0.06	-0.07	-0.10	-0.14	-0.21	-0.26	-0.34
Alloy 3 (RT-21 Coated)	+0.01	+0.01	0	-0.01	-0.01	-0.03	-0.05	-0.06	-0.08

\*Weight change is an average of 2 test specimens

Again, weight losses for RT-21 coated SC alloys were significantly greater (a factor of 8 to 10) after 509 hours of testing at 1093°C (2000°F) relative to RT-21 tested for the same time at 1038°C (1900°F). This result is attributable to both the higher test temperature and elimination of all or most of the hafnium from the SC alloys.

#### 6.4 Physical Properties

##### 6.4.1 Thermal Expansion

Thermal expansion measurements were performed by Southern Research Institute in Birmingham, Alabama. Test data were obtained for triplicate specimens (Figure 70) of SC NASAIR 100 material using the quartz dilatometric technique. Measurements were taken

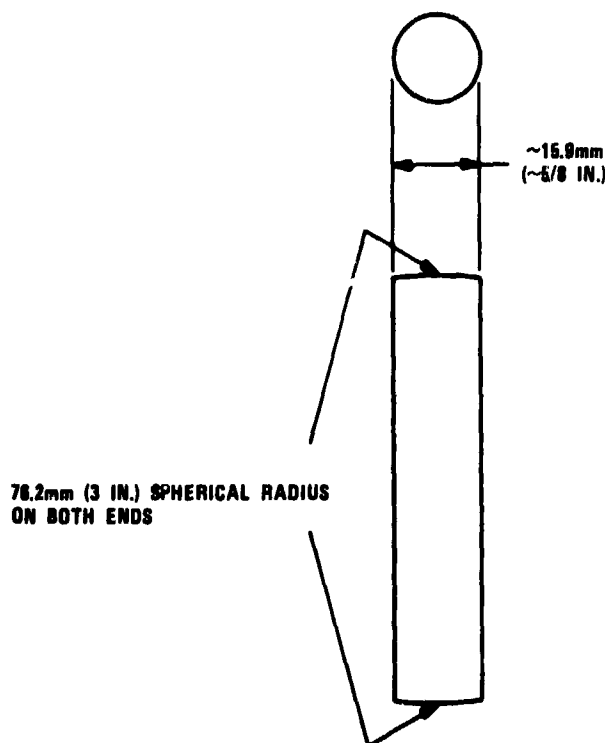


Figure 70. Thermal Expansion Specimen.

ORIGINAL PAGE IS  
OF POOR QUALITY

every 56°C (100°F) from room temperature to 1093°C (2000°F). The thermal expansion for SC NASAIR 100 is presented in Figure 71. As expected, thermal expansion data for SC NASAIR 100 is virtually identical to that for DS Mar-M 247.<sup>1</sup>

#### 6.4.2 Thermal Conductivity

Thermal conductivity measurements were performed by Southern Research Institute. Conductivity data were obtained for triplicate specimens (Figure 72) of SC NASAIR 100 using the comparative rod apparatus technique. The thermal conductivity measurements were taken over the range of 93° to 1093°C (200° to 2000°F) and are provided in Figure 73. Comparison of the SC NASAIR 100 conductivity data to the DS Mar-M 247 conductivity data<sup>1</sup> revealed no significant difference in thermal conductivity between the two alloys.

#### 6.4.3 Elastic Modulus

Dynamic modulus of elasticity data for SC NASAIR 100 specimens were measured by Southern Research Institute (Birmingham, Alabama).

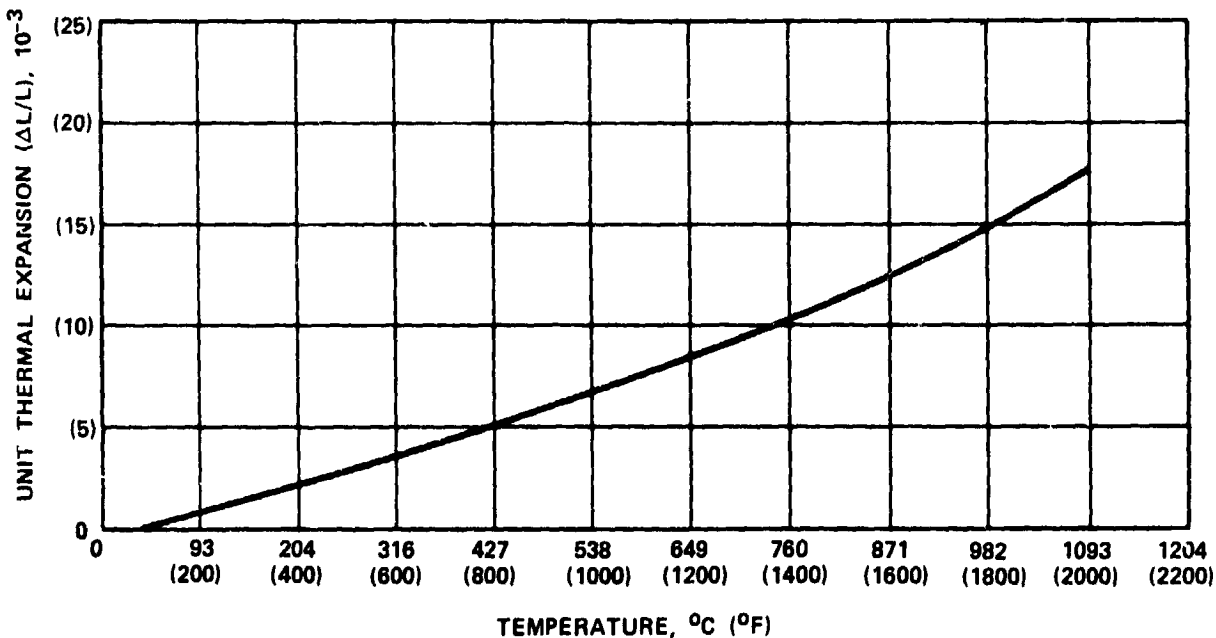


Figure 71. Thermal Expansion of SC NASAIR 100.

ORIGINAL PAGE IS  
OF POOR QUALITY

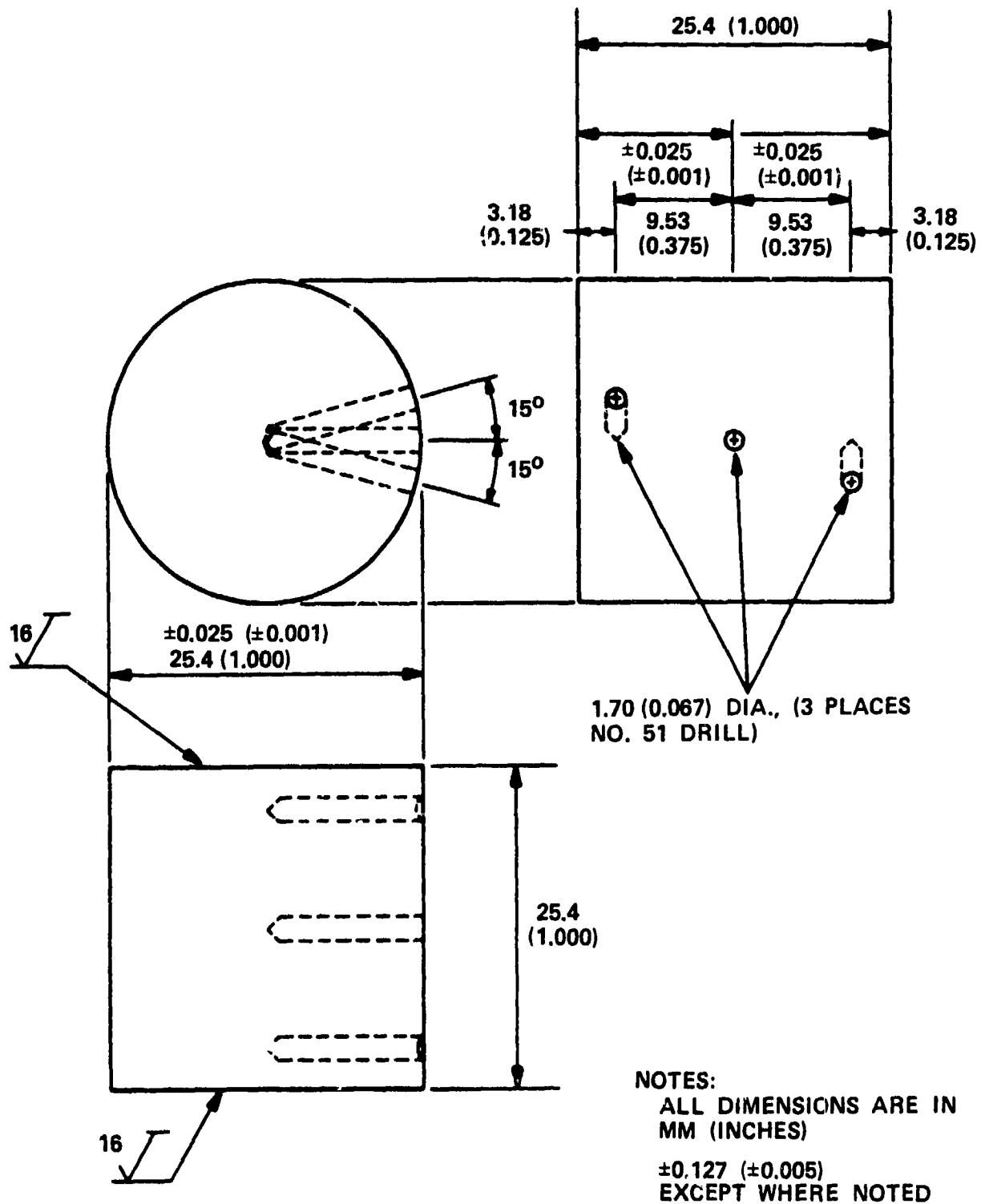


Figure 72. Thermal Conductivity Specimen.

ORIGINAL PAGE IS  
OF POOR QUALITY

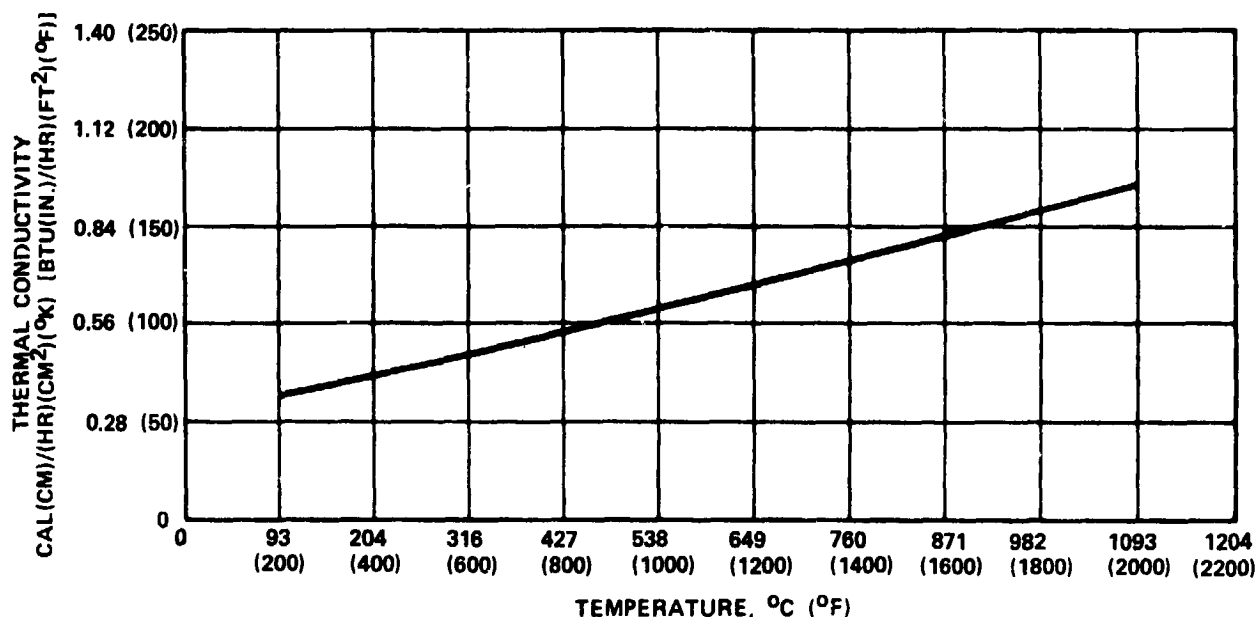


Figure 73. Thermal Conductivity of SC NASAIR 100.

Test specimens were machined from bar [001] and slab [111] castings. The test specimen configuration for these tests was a rectangular plate 10 cm long, 1.3 cm wide and 0.13 cm thick (4 by 0.5 by 0.05 inches). Tests were conducted at room temperature and at 93°C (200°F) temperature increments from 538°C (1000°F) to 982°C (1800°F). Each specimen was measured three times.

The modulus results for fully processed SC NASAIR 100 specimens oriented in the [001] + 2 degree and the [111] + 5 degree directions (determined by the X-ray Laue technique) are provided in Table 63 and Figure 74. Examination of the results indicates the following:

- o [001] specimen. The room temperature modulus measured on SC NASAIR 100 was 114.5 GPa ( $16.6 \times 10^6$  psi), which was slightly lower than anticipated and compares with the published value of 125.6 GPa ( $18.2 \times 10^6$  psi) for pure nickel in the [001] direction.

ORIGINAL PAGE IS  
OF POOR QUALITY

TABLE 63. DYNAMIC MODULUS OF ELASTICITY OF SC NASAIR 100.

	MODULUS OF ELASTICITY, GPa ( $E \times 10^6$ PSI)					
Specimen Orientation	TEMPERATURE, °C (°F)					
	24 (75)	538 (1000)	649 (1200)	760 (1400)	871 (1600)	982 (1800)
[001] + 2°	114.5 (16.6)	108.3 (15.7)	102.8 (14.9)	98.7 (14.3)	90.4 (13.1)	83.5 (12.1)
[111] + 5°	280.8 (40.7)	260.1 (37.7)	251.8 (36.5)	240.1 (34.8)	231.1 (33.5)	215.3 (31.2)
NOTES:						
a. Values are an average of three readings.						
b. Specimen configuration: 10 cm long, 1.3 cm wide, 0.13 cm thick (4.0 by 0.5 x 0.050-inch).						

- o [111] specimen. The room temperature modulus measured on SC NASAIR 100 was 280.8 GPa ( $40.7 \times 10^6$  psi), which is slightly lower than the published modulus value of 293.9 GPa ( $42.6 \times 10^6$  psi) for pure nickel in the [111] direction.
- o A comparison of the data indicates that the elastic modulus of the [111] specimen was about 2.5 times greater than that of the [001] specimen over the temperature range examined.

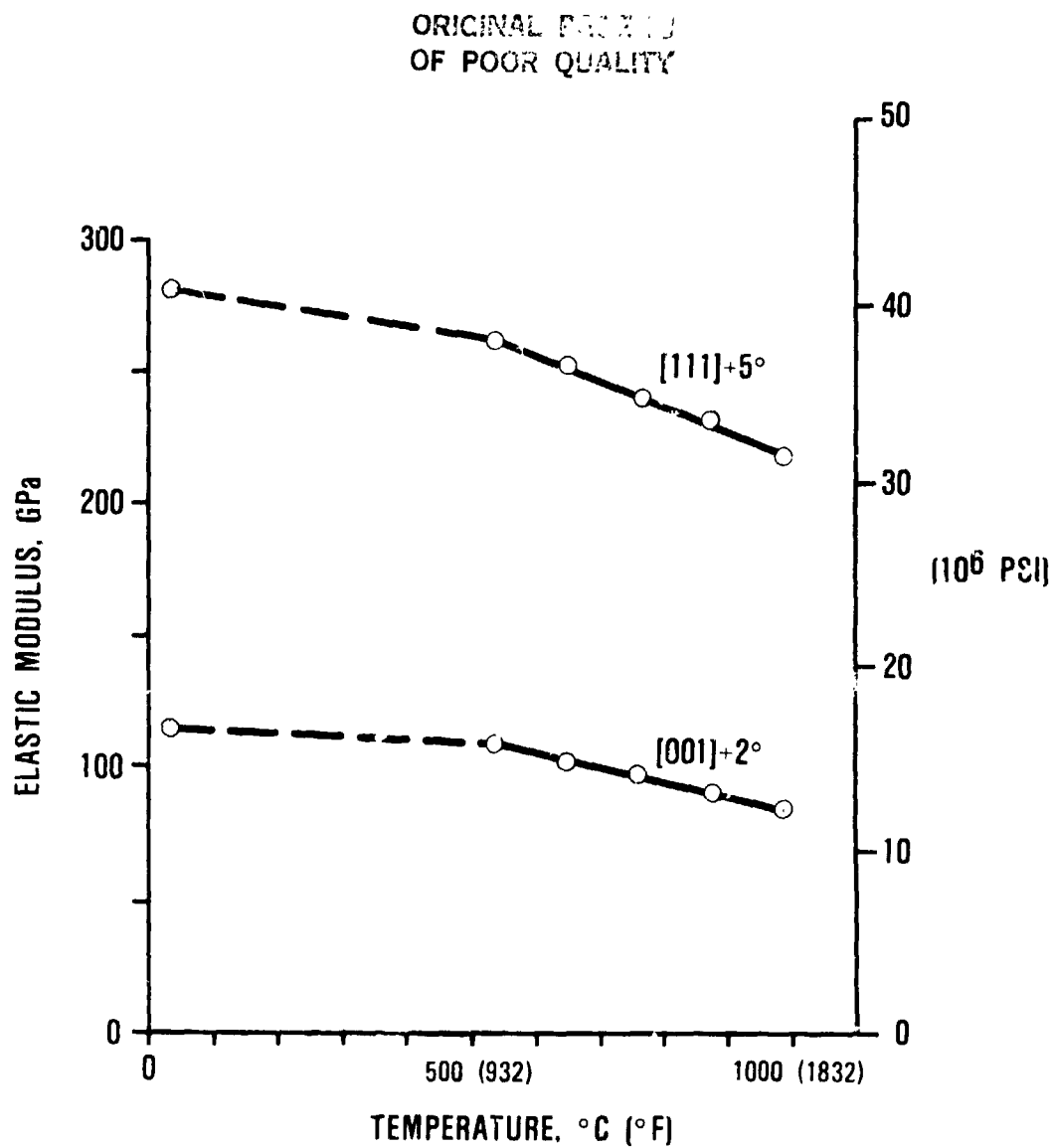


Figure 74. Elastic Modulus of SC NASAIR 100 in [001] and [111] Directions.



## SECTION VII

### 7.0 BLADE DESIGN

#### 7.1 Scope

This task included the design activity required for the development of an uncooled, single-crystal (SC) high-pressure turbine blade for the TFE731 turbofan engine, using the alloys characterized in the previous section. Two blade designs were established in this effort--the preliminary (initial) design and the final design.

The preliminary design (PD) was established early in the program to provide a blade casting design suitable for use in the development of the exothermic SC casting process and associated material evaluations. This design was based on the final design of the DS blade from MATE Project 1.

Actual material properties and other data obtained from preliminary design blades cast in SC NASAIR 100 and SC Alloy 3 were used in establishing the final blade design. The geometry of this final design made it necessary to modify the turbine disk, nozzle, and several other turbine components of the TFE731 engine to permit effective integration of the blade into the engine assembly. The redesign of these turbine components was also completed in this task.

#### 7.2 Preliminary Blade Design

The preliminary blade design (PD) was established primarily to provide a realistic blade configuration to be used in all the SC process and alloy development work scheduled in the first part of this project. This PD blade is the same configuration as the final blade design established for the MATE DS blade in Project 1, and, in fact, used the same wax tooling.

### 7.3 Final Blade Design

#### 7.3.1 Mechanical Design

Single crystal material is characterized by anisotropic material properties. The variance in the modulus of elasticity is especially dramatic, varying from a low of 18 along one of the principal cubic axes (001, 010, 100) to a high of 43 along the cube diagonal (111). This variation in properties will affect both the stresses within the part and the vibratory response of the structure.

To accommodate these SC anisotropic material properties, appropriate Garrett computer analysis programs were modified to include property variations in the input. These program changes allowed both static and dynamic blade response (centrifugal and thermal stress plus vibratory modes and frequencies) to be evaluated.

To study the effect of anisotropic properties analytically, sample check analyses were run at various crystal orientations, using the preliminary design blade configuration.

The finite-element model used for these studies, is shown in Figure 75, and the frequencies calculated with this model are tabulated in Table 6/. The calculated mode shapes for the blades at several natural frequencies and various crystallographic orientations are shown in Figures 76, 77, and 78. The corresponding calculated stress distributions in the turbine blade at various crystallographic orientations are shown in Figures 79, 80, 81, and 82. All stress and vibration studies for this preliminary design phase were calculated at room temperature.

A comparison of these analytical results to the measured frequency response of various PD blades cast with a variety of crystallographic orientations is shown in Figure 83. As can be seen, a significant amount of scatter, attributed to blade-to-blade variations and limitations of GTEC holography capability at that

ORIGINAL PAGE IS  
OF POOR QUALITY

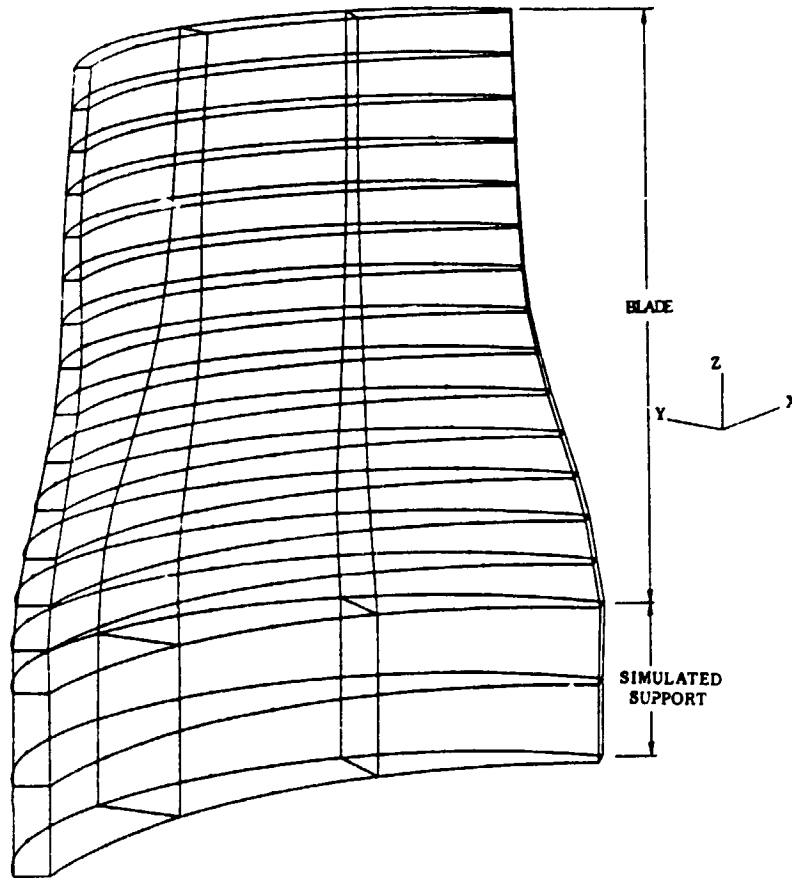
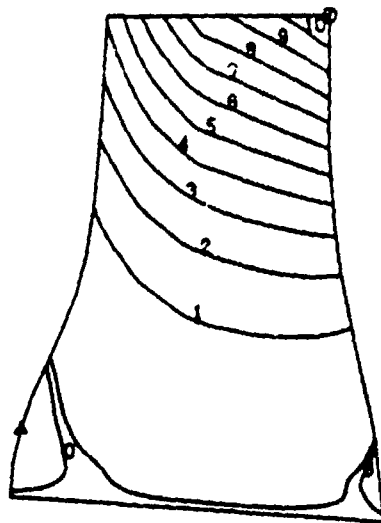


Figure 75. Finite-Element Model (DS TFE731 HPT Blade Used for SC Material Studies).

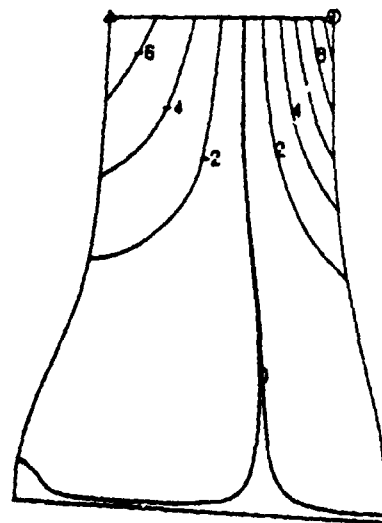
TABLE 64. EFFECT OF CRYSTAL ORIENTATION ON RESONANT FREQUENCIES (SC TFE731 HIGH-PRESSURE TURBINE BLADE).

Material Orientation (Degrees)		Natural Frequencies (Hz)				
Primary <sup>(1)</sup>	Secondary <sup>(2)</sup>					
Isotropic		5504	9876	16463	21017	26471
0	0	5325	10436	15980	20864	26338
15	0	5175	10396	16227	20457	26144
30	0	5173	9653	16321	19838	25366
0	-15	5319	10461	15944	20844	26379
0	-30	5317	10476	15930	20883	26350
(1) Angle between [001] material direction and blade Z-axis (stacking axis)						
(2) Angle between [100] material direction and blade X-axis (rotation axis)						

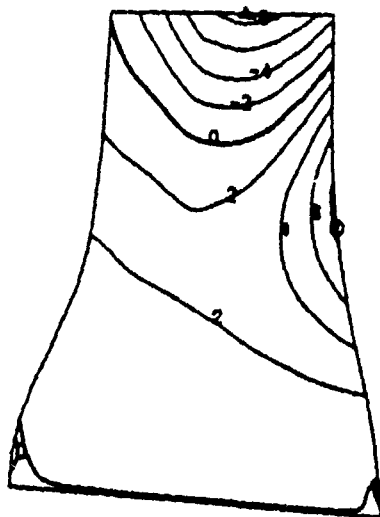
ORIGINAL PAGE 18  
OF POOR QUALITY



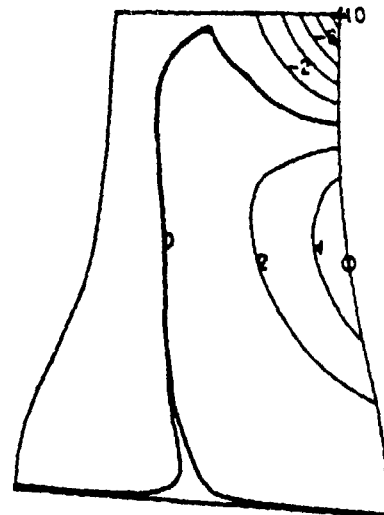
MODE 1 FREQ(HZ)=5325



MODE 2 FREQ(HZ)=10436



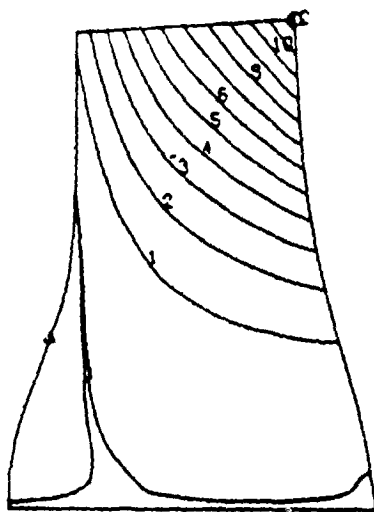
MODE 3 FREQ(HZ)=15980



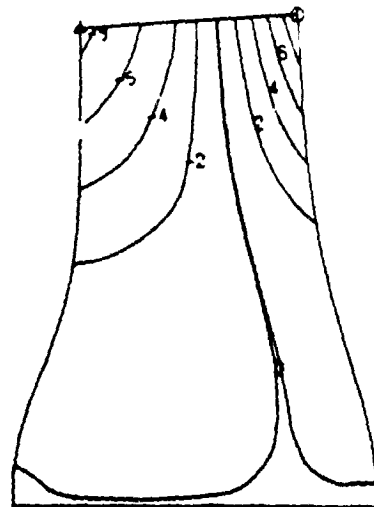
MODE 4 FREQ(HZ)=20864

Figure 76. Mode Shapes for Material and Global Axes  
Aligned, RPM = 0, Room Temperature.

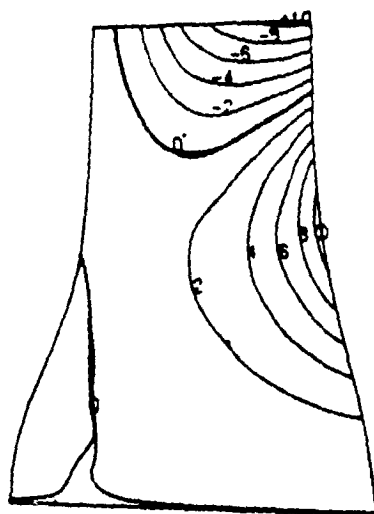
ORIGINAL PAGE 19  
OF POOR QUALITY



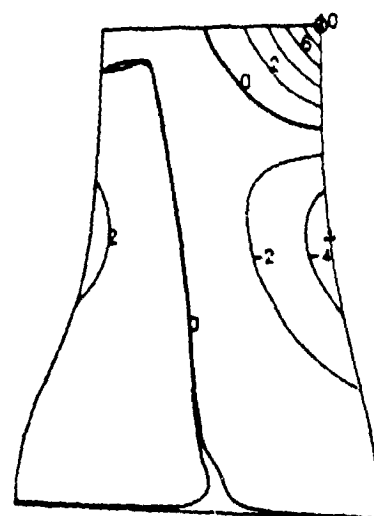
MODE 1 FREQ(HZ)=5173



MODE 2 FREQ(HZ)=9653



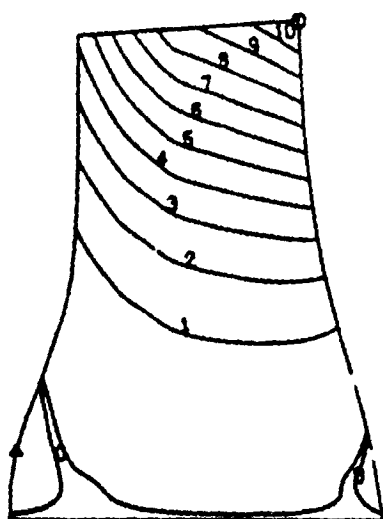
MODE 3 FREQ(HZ)=16321



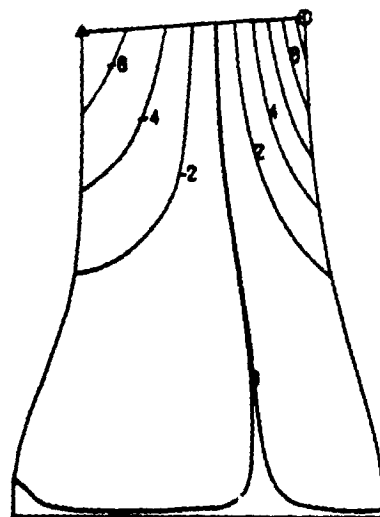
MODE 4 FREQ(HZ)=19838

Figure 77. Mode Shapes for 30-Degree Primary Orientation,  
RPM = 0, Room Temperature.

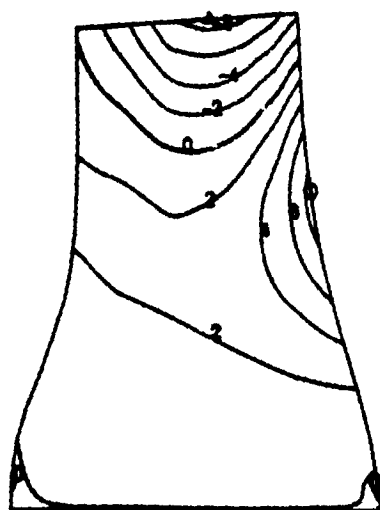
ORIGINAL PAGE 19  
OF POOR QUALITY



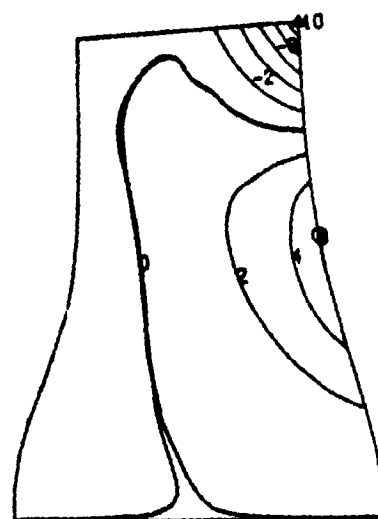
MODE 1 FREQ(HZ)=5317



MODE 2 FREQ(HZ)=10476



MODE 3 FREQ(HZ)=15930



MODE 4 FREQ(HZ)=20883

Figure 78. Mode Shapes for -30-Degree Secondary Orientation,  
RPM = 0, Room Temperature.

ORIGINAL PAGE IS  
OF POOR QUALITY

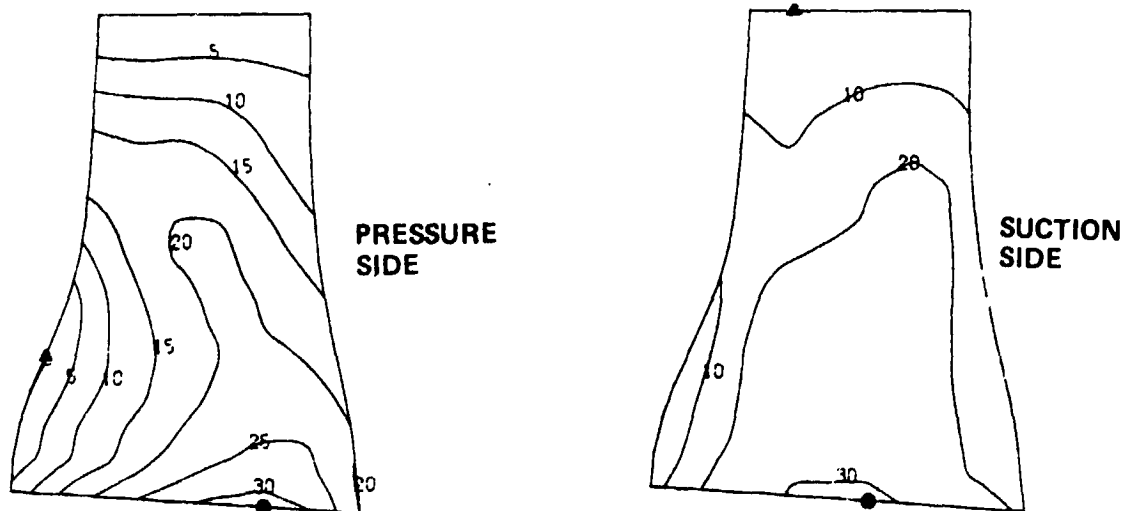


Figure 79. Stress Distribution for Isotropic Material  
RPM = 30,000, Room Temperature, ● = Maxi-  
mum Stress, ▲ = Minimum Stress (ksi).

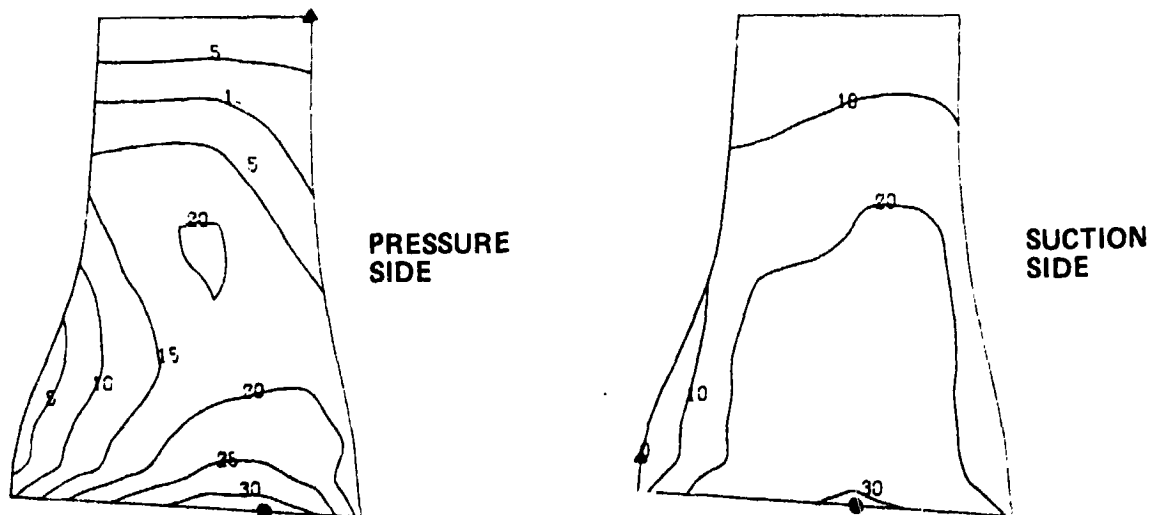


Figure 80. Stress Distribution for Material and Global Axes  
Aligned, RPM = 30,000, Room Temperature, ● = Maxi-  
mum Stress, ▲ = Minimum Stress (ksi).

ORIGINAL PAGE IS  
OF POOR QUALITY

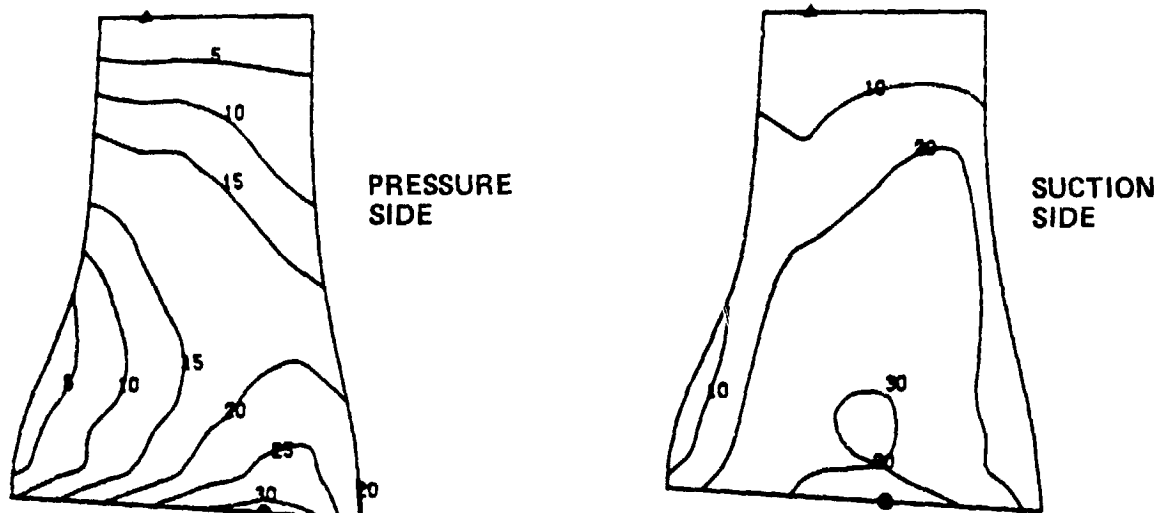


Figure 81. Stress Distribution for 30-Degree Primary Orientation, RPM = 30,000, Room Temperature, ● Maximum Stress, ▲ Minimum Stress (ksi).

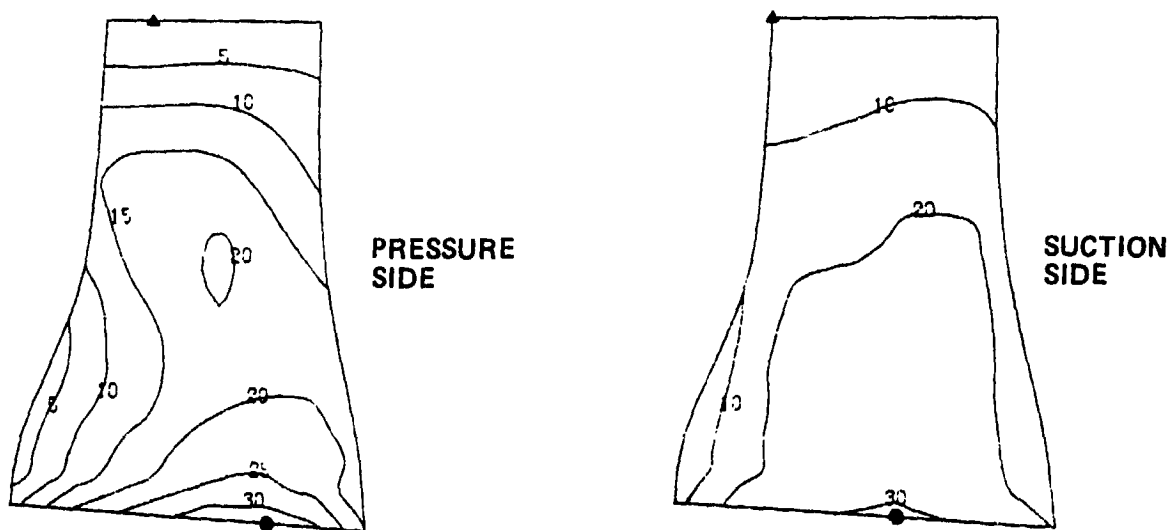
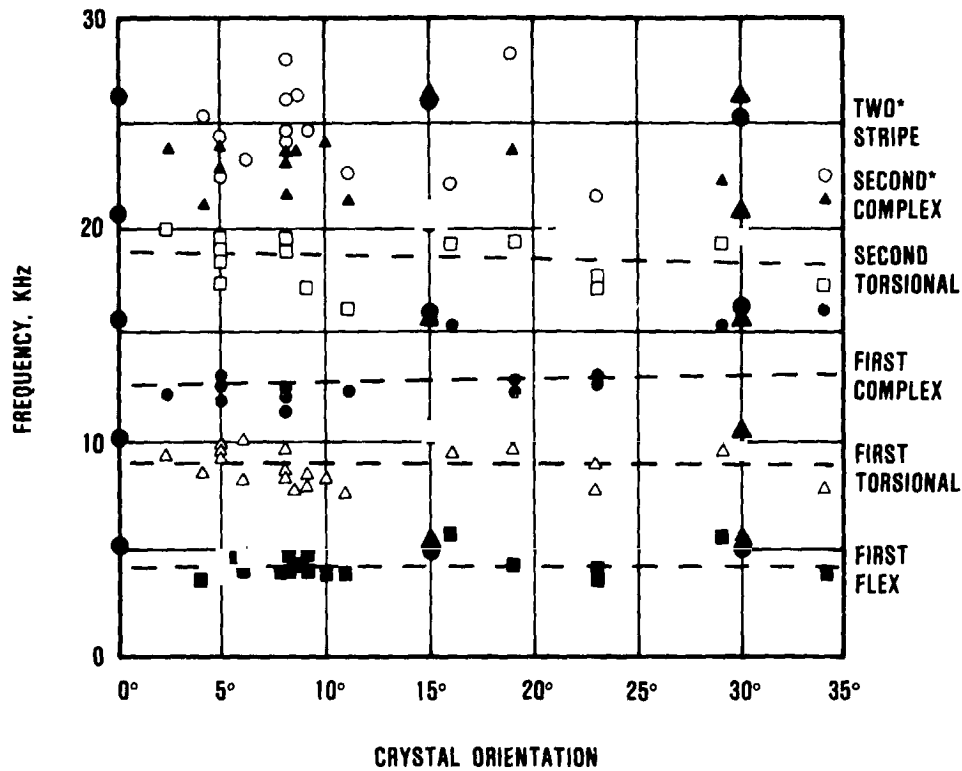


Figure 82. Stress Distribution for 30-Degree Secondary Orientation, RPM = 30,000, Room Temperature, ● Maximum Stress, ▲ Minimum Stress (ksi).



ORIGINAL PAGE IS  
OF POOR QUALITY



LEGEND

- CALCULATED FREQUENCIES, PRIMARY ORIENTATION
- ▲ CALCULATED FREQUENCIES, SECONDARY ORIENTATION
- FIRST FLEX, MEASURED FREQUENCY
- △ FIRST TORSIONAL, MEASURED FREQUENCY
- FIRST COMPLEX, MEASURED FREQUENCY
- SECOND TORSIONAL, MEASURED FREQUENCY
- ▲ SECOND COMPLEX, MEASURED FREQUENCY
- TWO STRIPE, MEASURED FREQUENCY

\*EXCESSIVE SCATTER PROHIBITS MAKING AN ACCURATE ESTIMATE  
OF A BEST FIT CURVE

Figure 83. Comparison of Holography Data and Analytical Predictions of the Crystal Orientation Effect on Vibrational Response.

ORIGINAL PAGE IS  
OF POOR QUALITY

time, exists in the measured holography data. This occurs in the higher order modes, such as the second complex and two stripe. Even with this scatter, there appears to be no significant relationship between crystal orientation and blade frequency for the range of orientations examined. Details of the measured frequency response of these blades are presented in the Table in Appendix A. It should be noted that these results may be influenced by blade size and configuration; and, therefore, this response may not be typical of all single crystal blades.

Stress and vibration analyses of the SC turbine blades at actual engine conditions were initiated using the model shown in Figure 84. The blade configuration for the initial analysis is the same as the PD blade. Using the finite-element program previously modified to include anisotropic SC material properties, the radial and equivalent blade stresses were calculated as shown in Figures 85 and 86. (Equivalent stresses are the conventional method of relating triaxial component stresses to uniaxial material strength.)

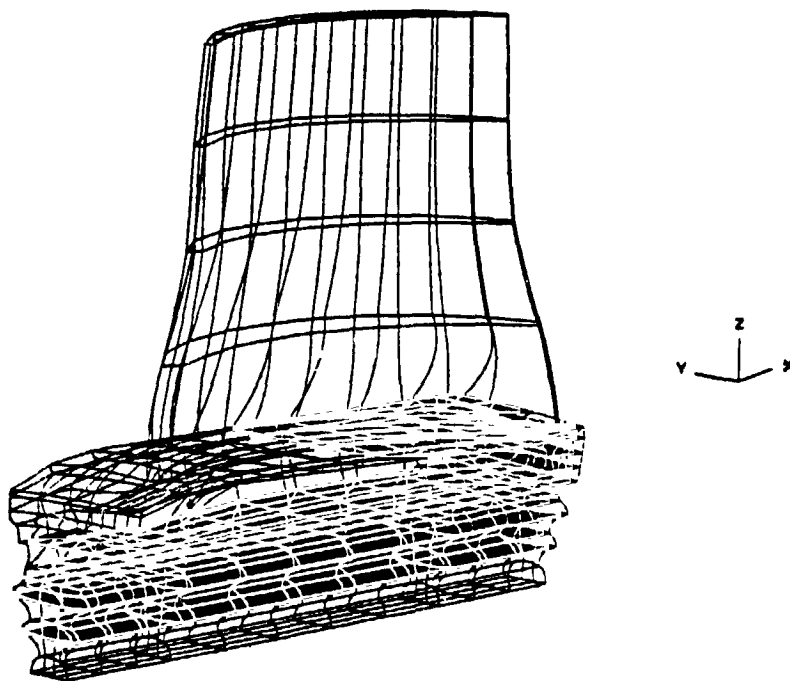


Figure 84. Single-Crystal Blade Model.

ORIGINAL PAGE IS  
OF POOR QUALITY

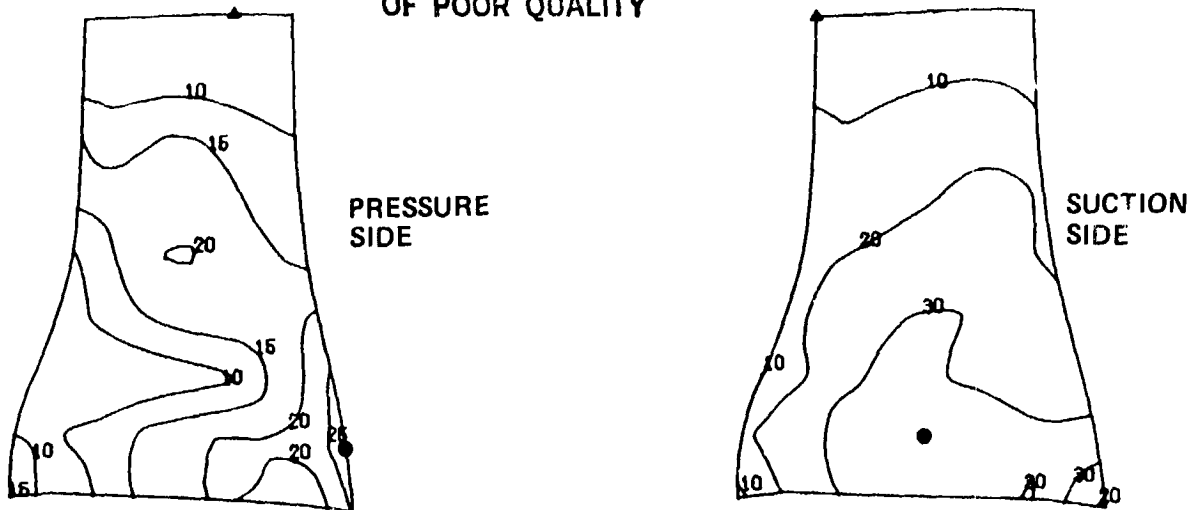


Figure 85. Calculated radial Stresses for the Single-Crystal Blade, RPM = Maximum Takeoff, ● = Maximum, ▲ = Minimum (ksi).

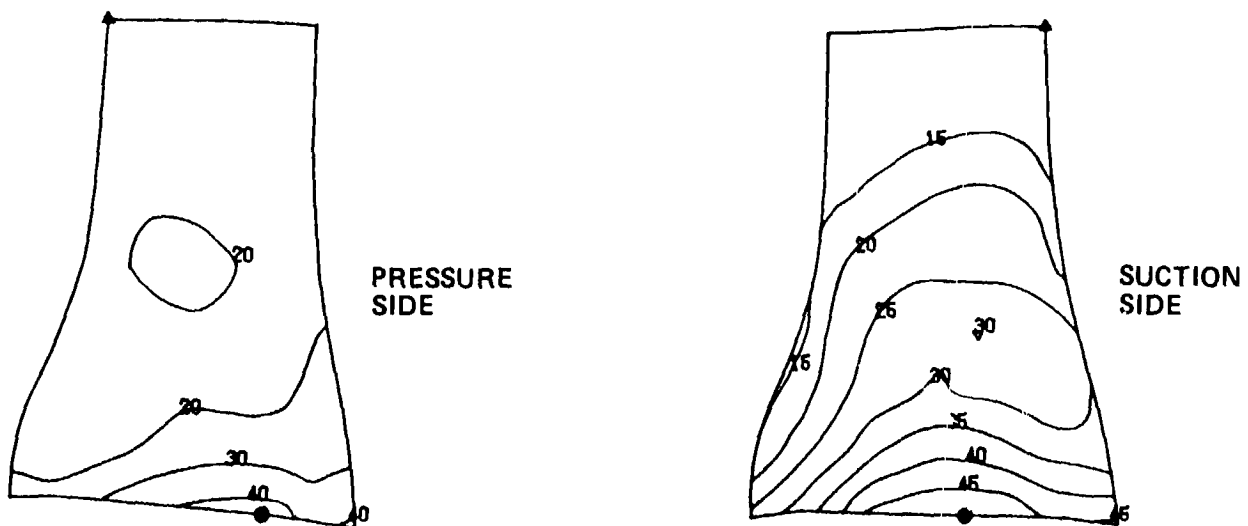


Figure 86. Calculated Equivalent Stresses for the Single-Crystal Blade, RPM = Maximum Takeoff  
● = Maximum, ▲ = Minimum (ksi).

### 7.3.1.1 Blade Life Analysis

Based on the results of this analysis, it was determined that the PD blade configuration was potentially acceptable for the final design. To verify this assessment, a detailed design blade life analysis was initiated. This life was based on the planned MATE 200-hour test mission, which includes the four 50-hour cycles shown in Figures 87, 88, 89, and 90. The normalized engine speeds and scaled temperatures for each operating point are shown in the Table below.

Condition	$N_2$	$T_4$
Takeoff	$N_{TO}$	$T_4$ Max
Max Continuous	0.990 $N_{TO}$	0.975 $T_4$ Max
1	0.987 $N_{TO}$	0.975 $T_4$ Max
2	0.985 $N_{TO}$	0.975 $T_4$ Max
3	0.985 $N_{TO}$	0.975 $T_4$ Max
4	0.985 $N_{TO}$	0.975 $T_4$ Max
5	0.985 $N_{TO}$	0.975 $T_4$ Max
6	0.985 $N_{TO}$	0.975 $T_4$ Max
7	0.985 $N_{TO}$	0.975 $T_4$ Max
8	0.985 $N_{TO}$	0.975 $T_4$ Max
9	0.985 $N_{TO}$	0.975 $T_4$ Max
10	0.985 $N_{TO}$	0.975 $T_4$ Max
11	0.985 $N_{TO}$	0.975 $T_4$ Max
12	0.985 $N_{TO}$	0.975 $T_4$ Max
13	0.985 $N_{TO}$	0.975 $T_4$ Max
Idle	0.608 $N_{TO}$	0.299 $T_4$ Max

ORIGINAL PAGE IS  
OF POOR QUALITY

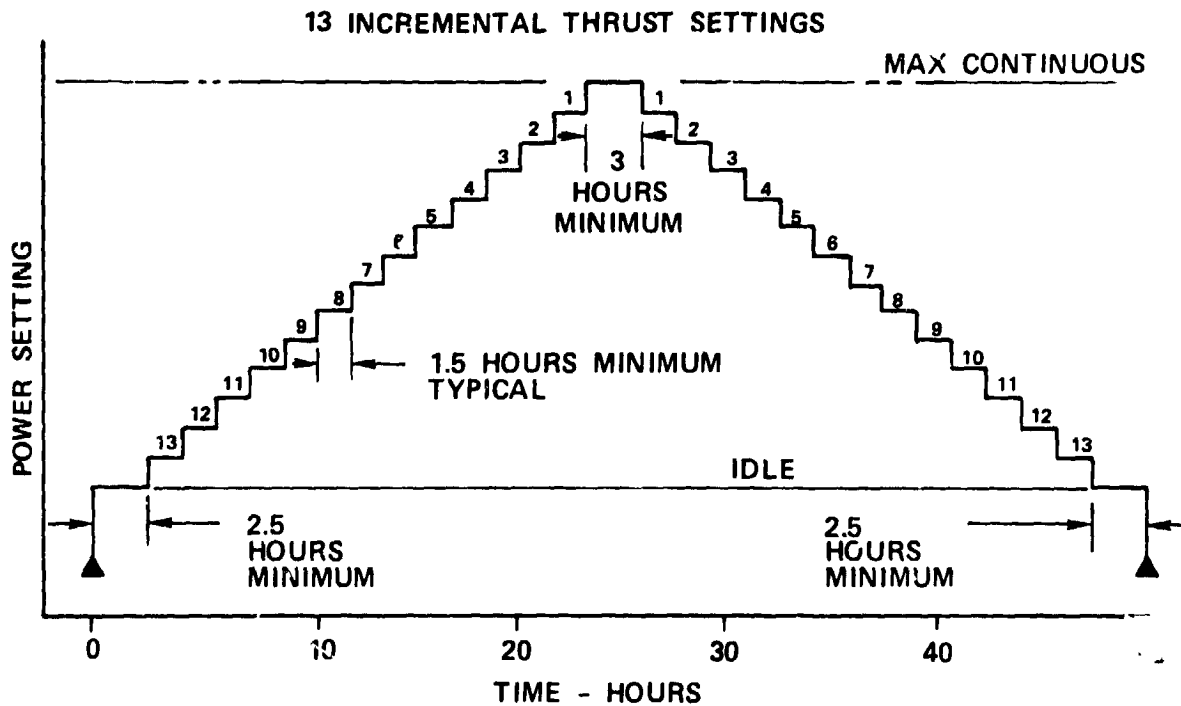


Figure 87. High-Cycle-Fatigue Cycle A.

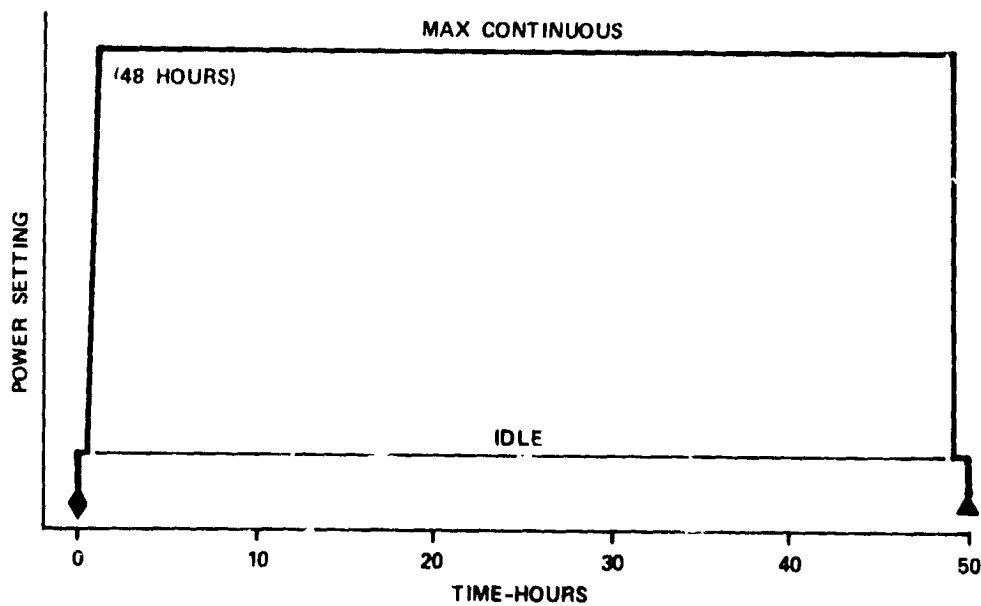


Figure 88. Stress-Rupture Cycle J.

ORIGINAL PAGE IS  
OF POOR QUALITY

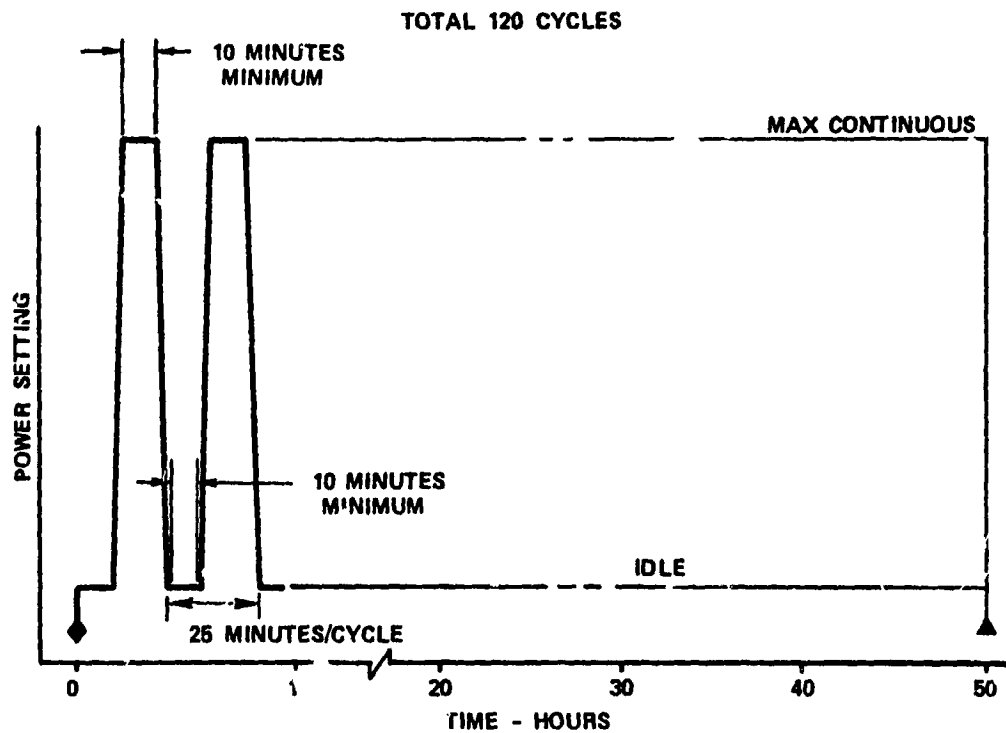


Figure 89. Low-Cycle-Fatigue Cycle C.

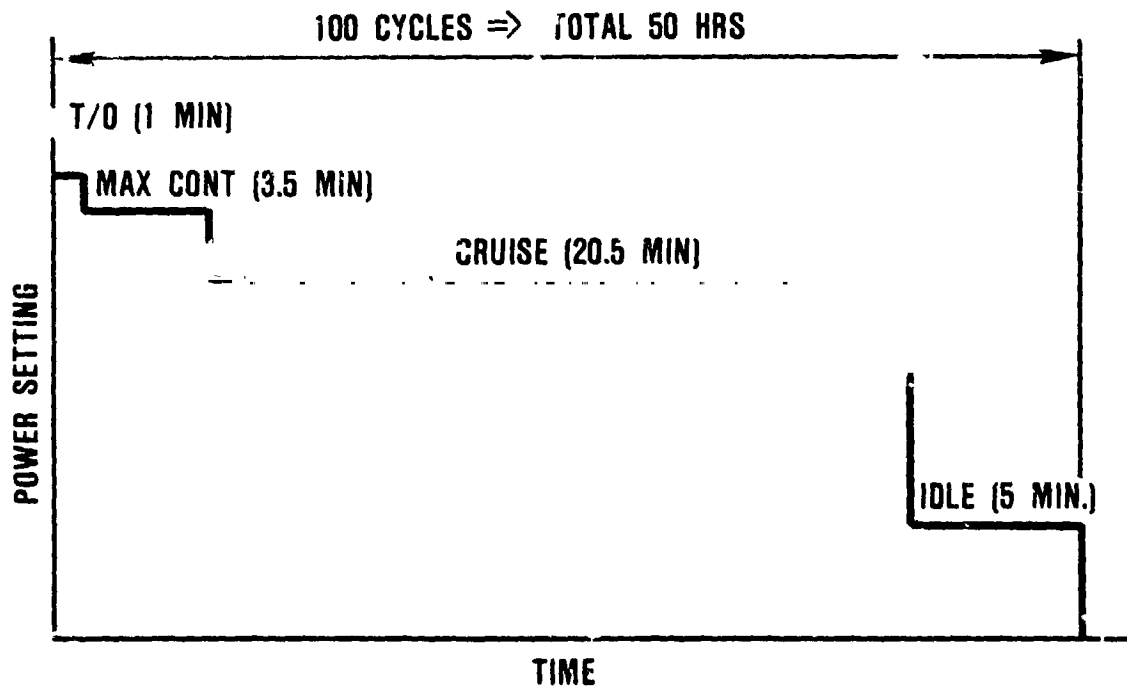


Figure 90. Mission Mix Cycle D.

ORIGINAL PAGE 13  
OF POOR QUALITY

Using these temperatures and corresponding stresses, the stress-rupture damage at each cycle of the mission can be evaluated for the critical elements of the blade and rim. The results of this damage analysis are shown in Table 65. This table shows the stress-rupture damage at the critical life section of the airfoil, approximately 30-percent span (Figure 91), for each mission cycle. Damage analysis of the SC blade indicated that the maximum stress-rupture damage point on the blade was at the "high c" point on the critical section (Figure 92). At this point, approximately 25 percent of the stress-rupture life of the blade was consumed during one 200-hour test cycle. Thus, the calculated blade life is 800 hours of mission life or 4 of the 200-hour test cycles at 1096°C (2005°F)  $T_4$ . The calculated damage due to low-cycle fatigue was found to be negligible even when the fatigue life was based on DS Mar-M 247 material properties.

TABLE 65. STRESS-RUPTURE DAMAGE FRACTION.

Cycle	Airfoil		Blade Firtree			Disk Firtree		
	High "C" Point	Trailing Edge	Lobe 1	Lobe 2	Lobe 3	Lobe 1	Lobe 2	Lobe 3
A	0.028	0.026	<0.001	<0.001	<0.001	0.016	0.029	0.019
B	0.111	0.111	<0.001	<0.001	<0.001	0.065	0.112	0.074
C	0.048	0.044	<0.001	<0.001	<0.001	0.029	0.049	0.033
D	0.060	0.056	<0.001	<0.001	<0.001	0.034	0.059	0.039
Total	0.247	0.237	<0.001	<0.001	<0.001	0.144	0.249	0.165

Comparison of the predicted life of the SC turbine blade to the predicted life of both cooled equiaxed and uncooled DS turbine blades shows that the SC blades offer a considerable advantage over these more conventional materials for advanced high temperature operation. The normalized stress-rupture (S-R) life of the SC

ORIGINAL PAGE 13  
OF POOR QUALITY

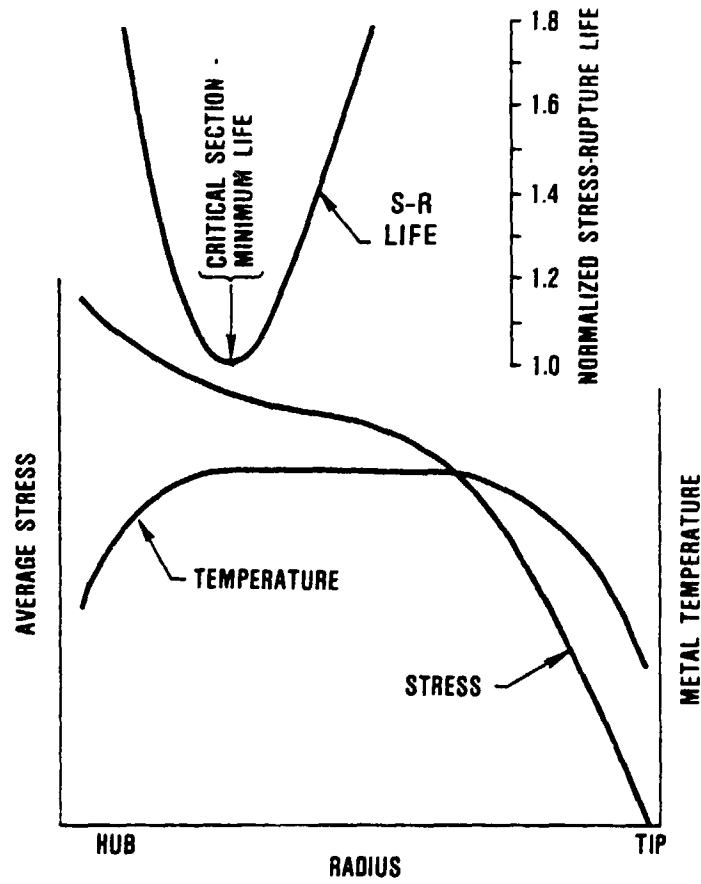


Figure 91. Blade Critical Section Location (Minimum Stress-Rupture Life).

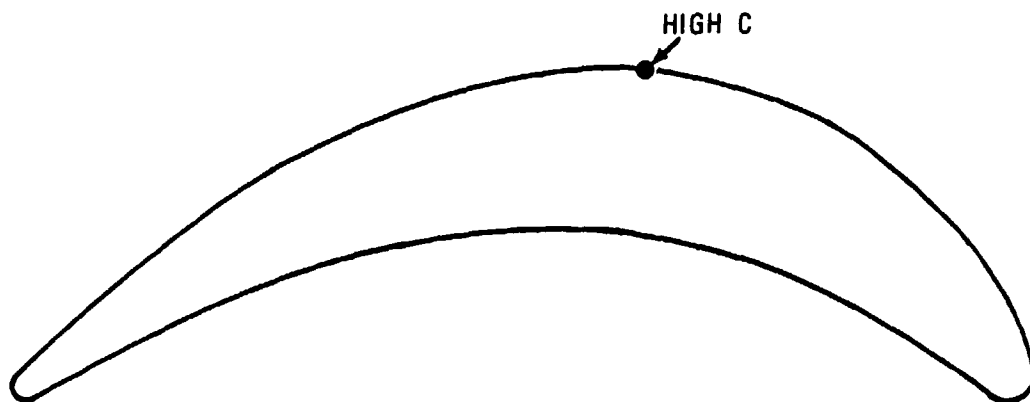


Figure 92. Maximum Stress-Rupture Damage Point.



ORIGINAL PAGE IS  
OF POOR QUALITY

NASAIR 100 turbine blade is compared to other turbine blades in Table 66. As shown, the stress-rupture life of the SC blade was more than twice that of any other blade analyzed at the elevated operating conditions. (Cooling air was held constant for the cooled-blade analysis.)

TABLE 66. COMPARISON OF NORMALIZED STRESS-RUPTURE  
LIVES AT  $T_4 = 1096^\circ\text{C}$  ( $2005^\circ\text{F}$ ) AND  
 $N = N_{TO}$  RPM.

Blade Material	Blade Configuration	Normalized S-R Life
SC NASAIR 100	Solid	1.00
DS Mar-M 247	Solid	0.36
IN-100	Solid	0.09
IN-100	Cooled	0.39

7.3.1.2 Blade Vibration Analysis

The vibratory response of the final blade design configuration at engine operating conditions was calculated using the modified computer programs. Blade vibratory response is influenced by two factors: rotational speed and blade temperature. As rotational speed increases, the blade is stiffened by the centrifugal force field that tends to straighten the blade and increase the resonant frequencies. Conversely, as operating temperatures are increased, the stiffness of the blade and the resonant frequencies are decreased, due to the reduction in material modulus at higher temperatures.

Figures 93 through 96 show the influence of rotational speed on blade stiffness at room temperature. The magnitude of this effect varies with mode shape, with first flex (Figure 93) showing the greatest effect.

ORIGINAL PAGE IS  
OF POOR QUALITY

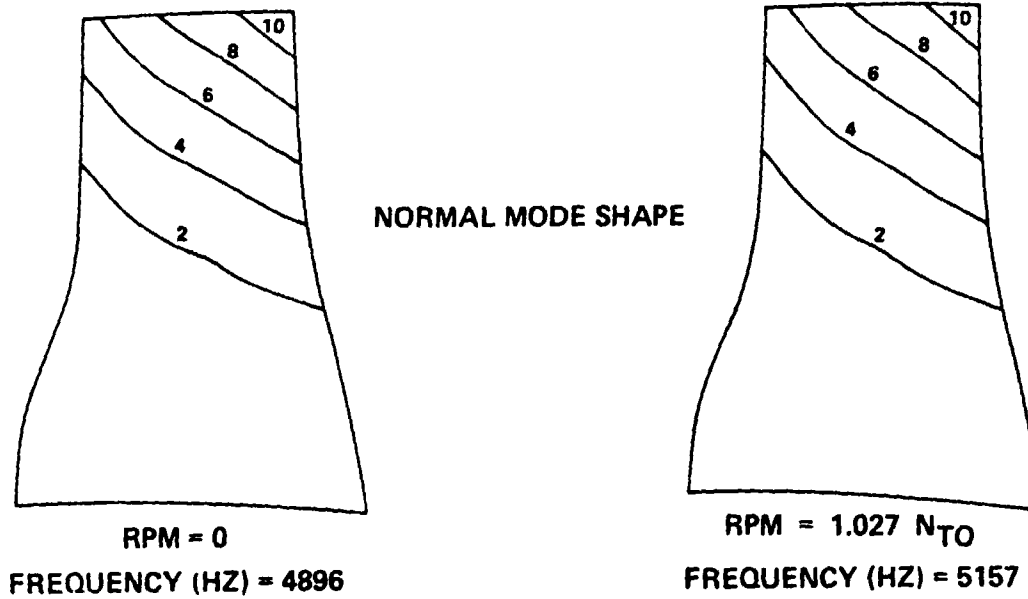


Figure 93. Single-Crystal Blade Vibration Analysis.  
First Flex at Ambient Temperature.

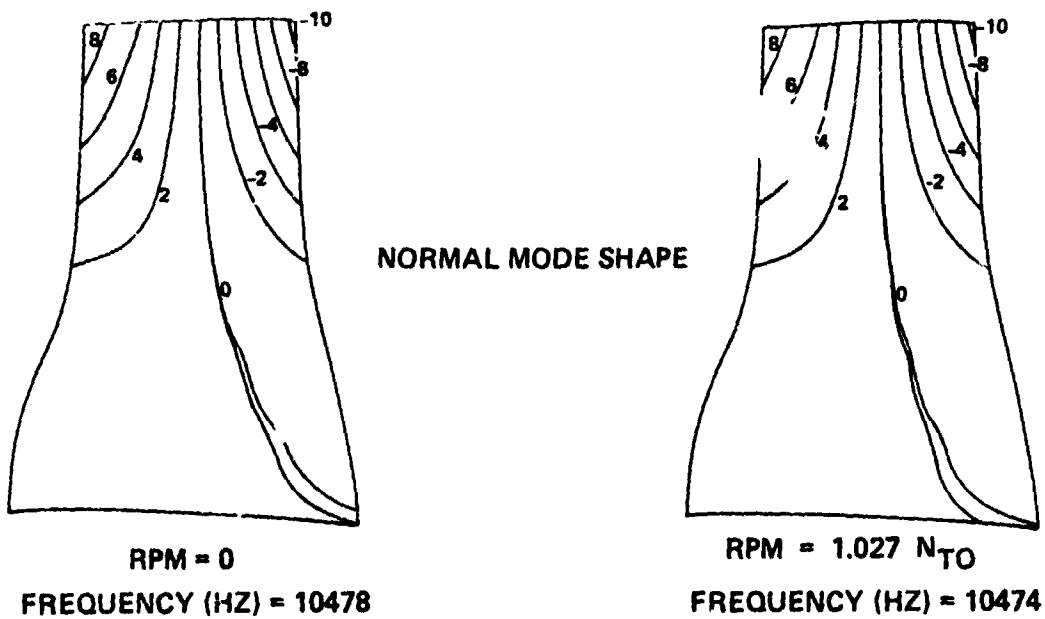


Figure 94. Single-Crystal Blade Vibration Analysis.  
First Torsional at Ambient Temperature.

ORIGINAL PAGE IS  
OF POOR QUALITY

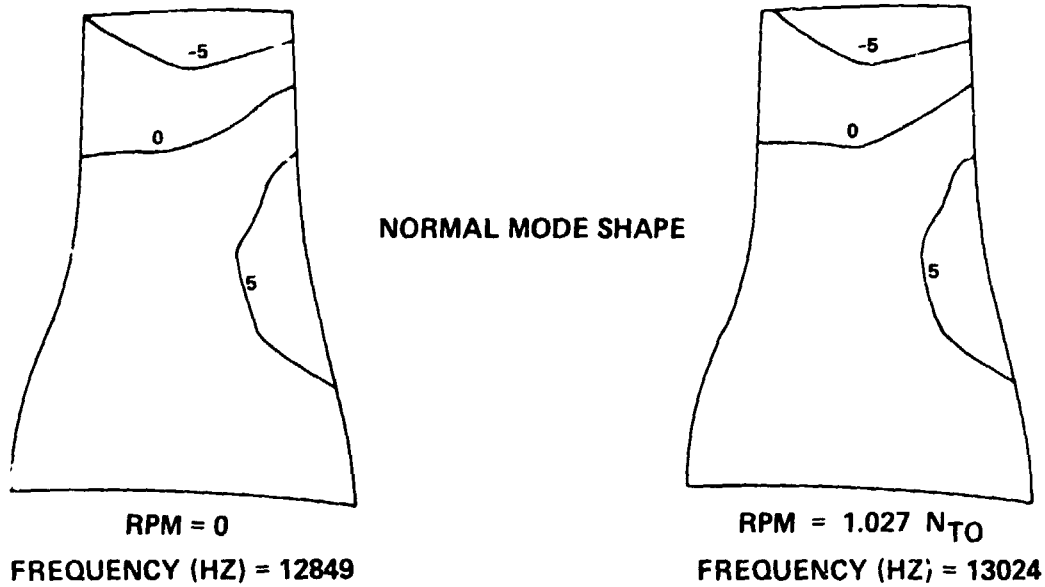


Figure 95. Single-Crystal Blade Vibration Analysis.  
Two Stripe at Ambient Temperature.

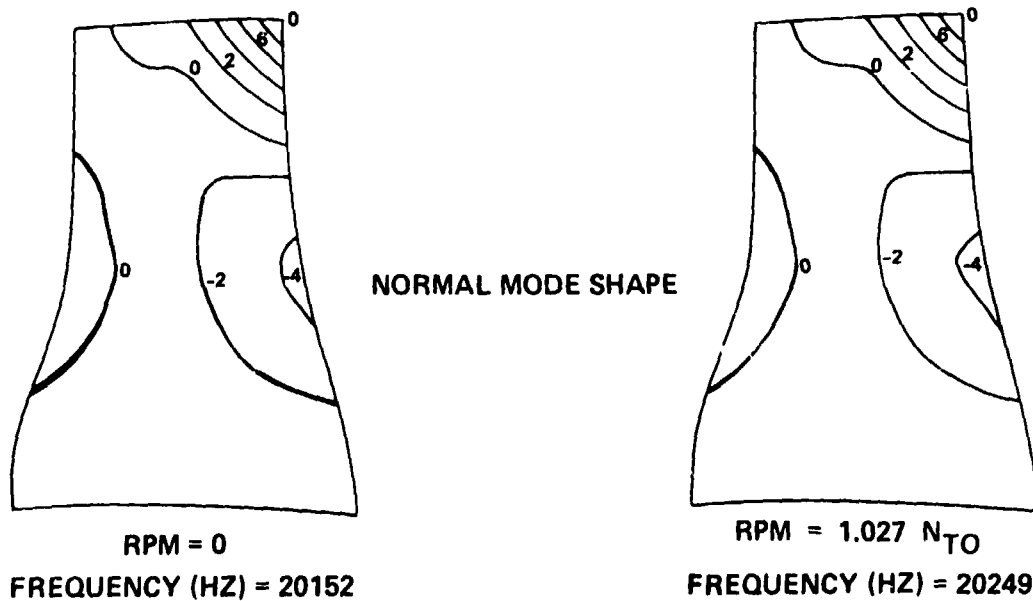


Figure 96. Single-Crystal Blade Vibration Analysis.  
First Complex at Ambient Temperature.

### 7.3.2 Aerodynamic Design

The aerodynamics design of both the SC turbine blade and companion vane are unchanged from the DS blade configuration designed in MATE Project 1. For aerodynamic details of these components such as vector diagrams, aerodynamic loading, flow parameters, etc., see NASA Report CR-159464 (Volume I).

### 7.3.3 Design Modifications

A design modification of the blade tip was investigated to improve the aerodynamic efficiency of the uncooled turbine blades. This design incorporates a small tip winglet on both pressure and suction sides to reduce the aerodynamic losses due to flow across the blade tip. To avoid aerodynamic interference, these tip winglets were added on top of the current DS blade design, thus making the SC blade slightly longer. This required a change to the ID of the shrouds to maintain the current rotor-to-stator clearance and thus avoid a blade tip rub. Stress analysis of the modified blade indicates that the blade load is increased less than 2 percent with the addition of these winglets, and the stress at the tip section is only 27.6 MPa (4.0 ksi). These small changes in centrifugal stress will not appreciably change the mission life.

Design studies were also initiated to reduce the cooling air flow in the rim area of the HP turbine. As a result of these studies, an aft flow discourager was added to the blade with the tooth extending radially inward. This design increases the load on the disk approximately 5 percent and introduces small additional moments to the firtree. These additional forces have a negligible impact on firtree life. A boundary layer dam (platform seal) was also inserted between each blade to reduce platform leakage. This sheet metal seal increases the blade load slightly more than 1 percent and has no significant effect on either blade or disk life.

Figure 97 shows several views of the final design configuration of the SC blade that incorporates all the added performance features. Two drawings of this blade were issued: Part Number 3076078 for SC Alloy NASAIR 100 and Part Number 3076086 for SC Alloy 3. Only the material and heat treatments are different on these drawings. The cast and machined configurations are unchanged.

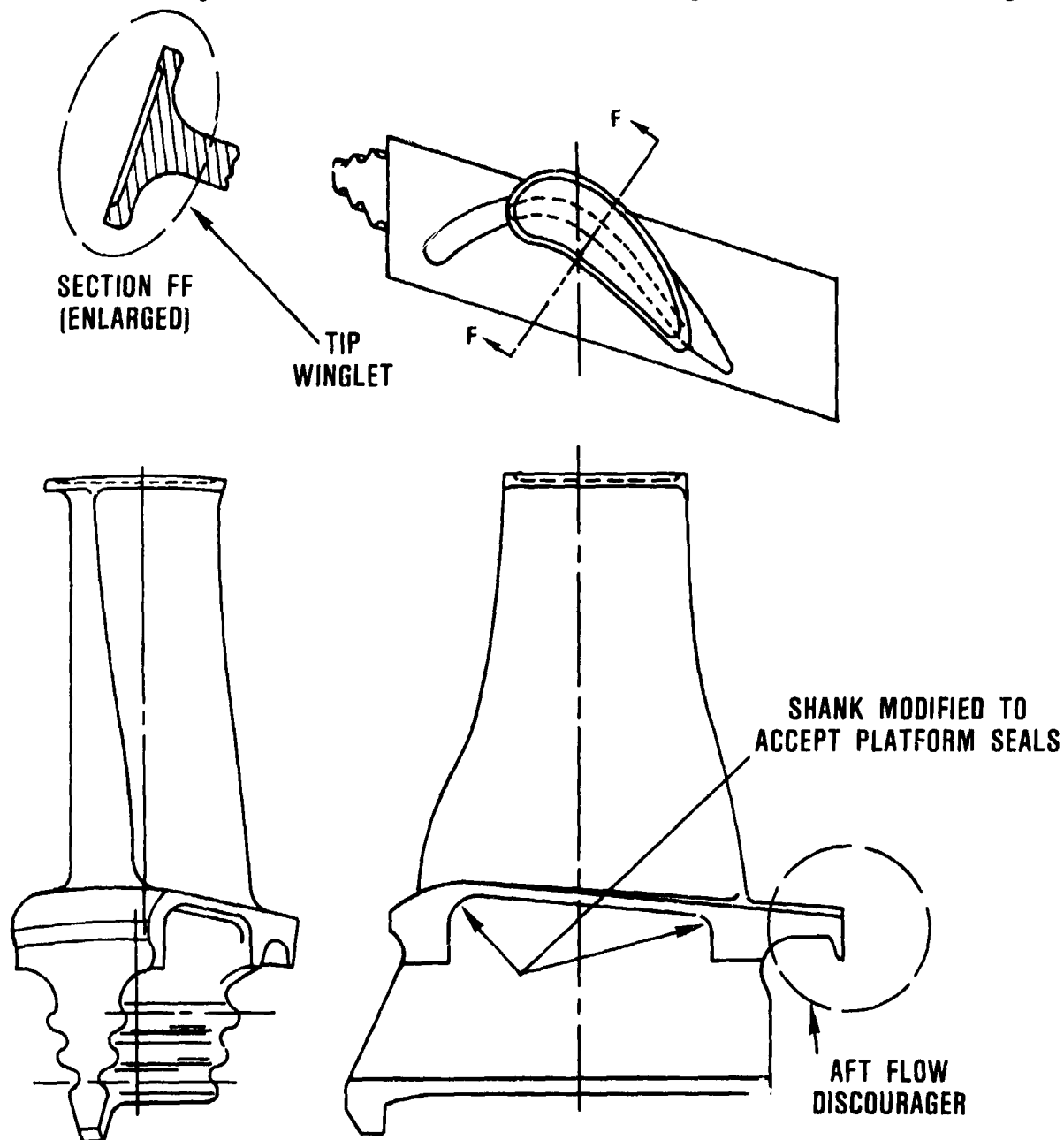


Figure 97. MATE SC Blade - Final Machined Configuration.

## SECTION VIII

### 8.0 COMPONENT MANUFACTURE

The objective of this phase of the program was to manufacture and qualify at least two complete sets of SC turbine blades of the new design for subsequent component and engine tests. This task included modification of the wax pattern tooling, casting and inspection of components, and machining of blade attachments and tips. At the conclusion of the casting campaign, an economic analysis for SC blades in production quantities was completed.

#### 8.1 Tooling

Wax pattern tooling for the new MATE SC turbine blade was produced by modifying the existing tooling from the Project 1 DS turbine blade. This approach saved both time and money, since the basic airfoil shape was not changed. The modified wax pattern for the new MATE TFE731 HPT blade and the blade arrangement in the mold for the casting campaign are shown in Figure 98.

#### 8.2 Casting Campaign

Turbine blades required for component and engine tests were produced using the technology described in Section 3.0. The NASAIR 100 material specification and acceptance standards for SC NASAIR 100 are provided in Appendixes B and C, respectively.

Jetshape's overall yields for the casting campaign are provided in Table 67. As shown, process yields were below expectations. The results of these inspections reflect the problems that must be overcome before the exothermic process is acceptable as a production process for single-crystal blade and vane castings. Most of these problems can be corrected by automating the various facets of the casting operation including mold handling, mold cleaning, exo-

ORIGINAL PAGE IS  
OF POOR QUALITY



Figure 98. Wax Pattern (Lower) and Assembly (Upper) for  
Modified SC TFE731 HP Turbine Blade.

ORIGINAL PAGE IS  
OF POOR QUALITY

TABLE 67. VENDOR INSPECTION SUMMARY FOR SC TFE731 BLADES.

Material	Total Blade Cavities	Rough <sup>1</sup> Visual Accept	Single Grain <sup>2</sup> / Visual Accept	FPI Accept	X-Ray Accept	Laue Accept	Overall Yield
Full Program Results							
NASAIR 100	384	331	177	131	80	60	16%
ALLOY 3	288	263	176	134	99	74	26%
Final Six Molds Cast							
ALLOY 3	72	71	52	48	32	29	40%
1. Incomplete fill, hot tear, mold runout, cracking, grains 2. Vendor evaluation of SC grain and overall visual acceptance							

thermic packing, preheat and exothermic burn, transfer to the casting furnace, and final casting.

The processing at Jetshapes was done by production people, using existing conventional casting equipment with minimal specialized handling equipment. Although they succeeded in surmounting some of the problems of the environment, the yields reflect several ongoing problems in casting these alloys. Improvements in processing are reflected in the improved yields shown in Table 67. These were realized as production of the engine test parts progressed, particularly in single-grain development and in overcoming initial blade losses due to casting runouts.

The FPI and X-ray rejects were predominantly due to inclusions. FPI also revealed a problem with platform shrinkage on the leading- and trailing-edge ends, indicating a need for feeders at those locations. The greatest source of the inclusions came from a lack of mold cavity isolation during exothermic filling, handling



in and out of mold firing, placement and movement in the vacuum casting unit and, finally, crucible breakdown and refractory spalling due to the high casting temperatures required for crystal development.

Considerable progress was made in producing single-crystal castings, but work must be continued on the exothermic process to reduce the pickup of ceramic particles and dross in the casting process. Proper handling equipment, furnace shielding, and a greater degree of mechanization for the production process will eliminate many of these problems.

Comparison of the two alloys used in this task appears to indicate that SC Alloy 3 has a slight advantage in yield of SC blades produced, while NASAIR 100 had somewhat less of a problem with excessive shrinkage. Since most of the NASAIR 100 parts were cast at the beginning of the campaign, the processing experience gained during this task was more beneficial to the Alloy 3 SC blades.

The exothermic pack process is a viable production process for SC castings and could be made better with more process/foundry development work. Its major advantage is the capability to produce SC castings using only slightly modified existing equipment. Its development into a competitive SC casting process for production is an attainable goal with major additional equipment, such as a manipulator for mold handling, multiple chills and cooling sections, and mechanical handling.

### 8.3 Casting Inspection and Testing

Examination of Laue X-ray diffraction data indicated that most of the blades were well within the orientation requirement that the [001] direction must be within 15 degrees of the stacking axis. For the initial group of 102 blades examined, 95 percent of blades were within 10 degrees of the [001] as shown in Figure 99.

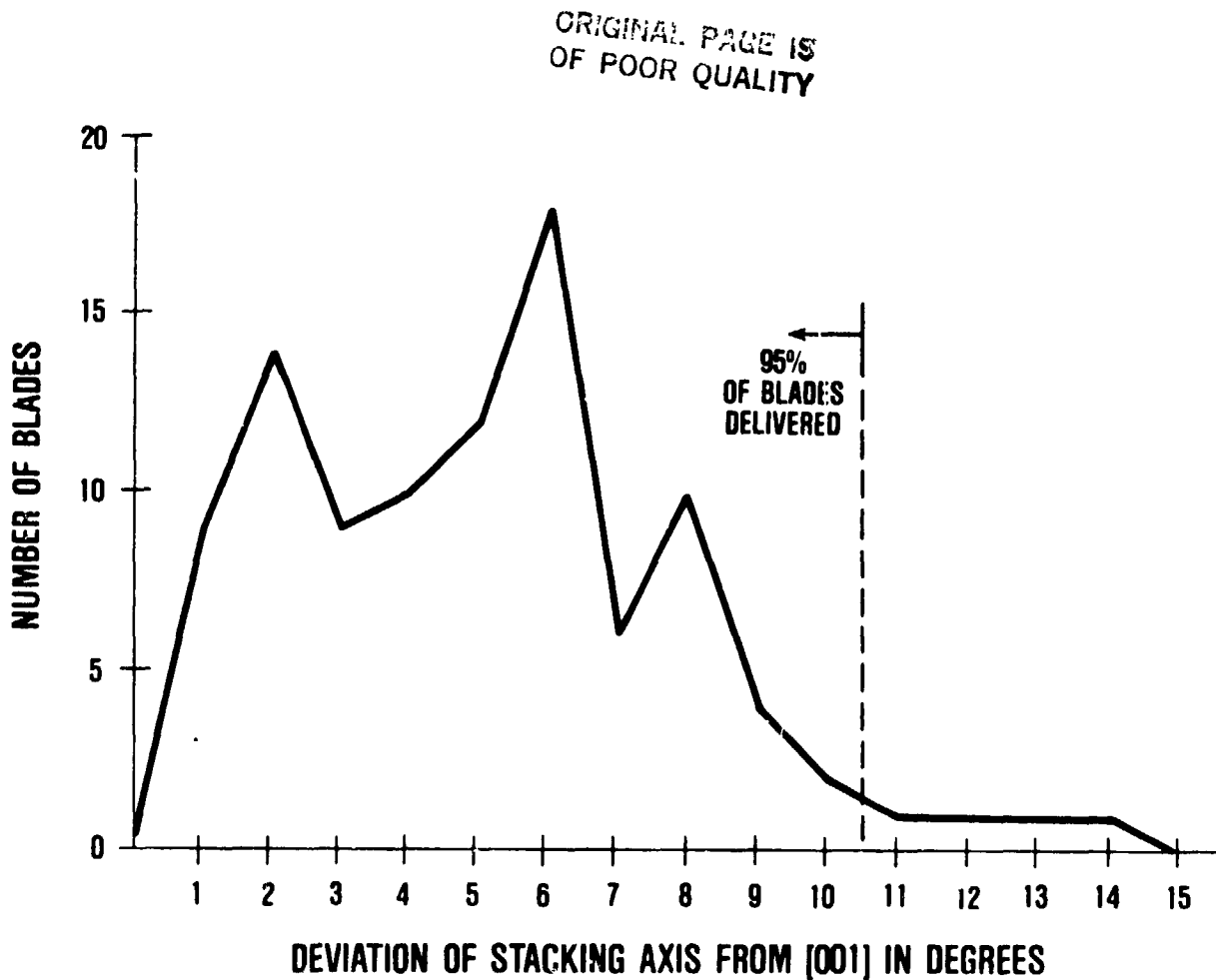


Figure 99. SC Blade Orientation (Laue) Results.

Mechanical property tests--760°C (1400°F) tensile and 982°C (1800°F) stress rupture--from final design SC blade castings of both NASAIR 100 and Alloy 3 exceeded specification minimums. These data were included in Tables 40, 43, 47, and 50.

#### 8.4 Blade Machining

After the blade castings were received at Garrett, they were inspected using visual, radiographic, and FPI methods and shipped to Walbar for final machining. The final machined blade configuration is shown in Figure 100. One hundred and thirty-four blades

ORIGINAL PAGE IS  
OF POOR QUALITY

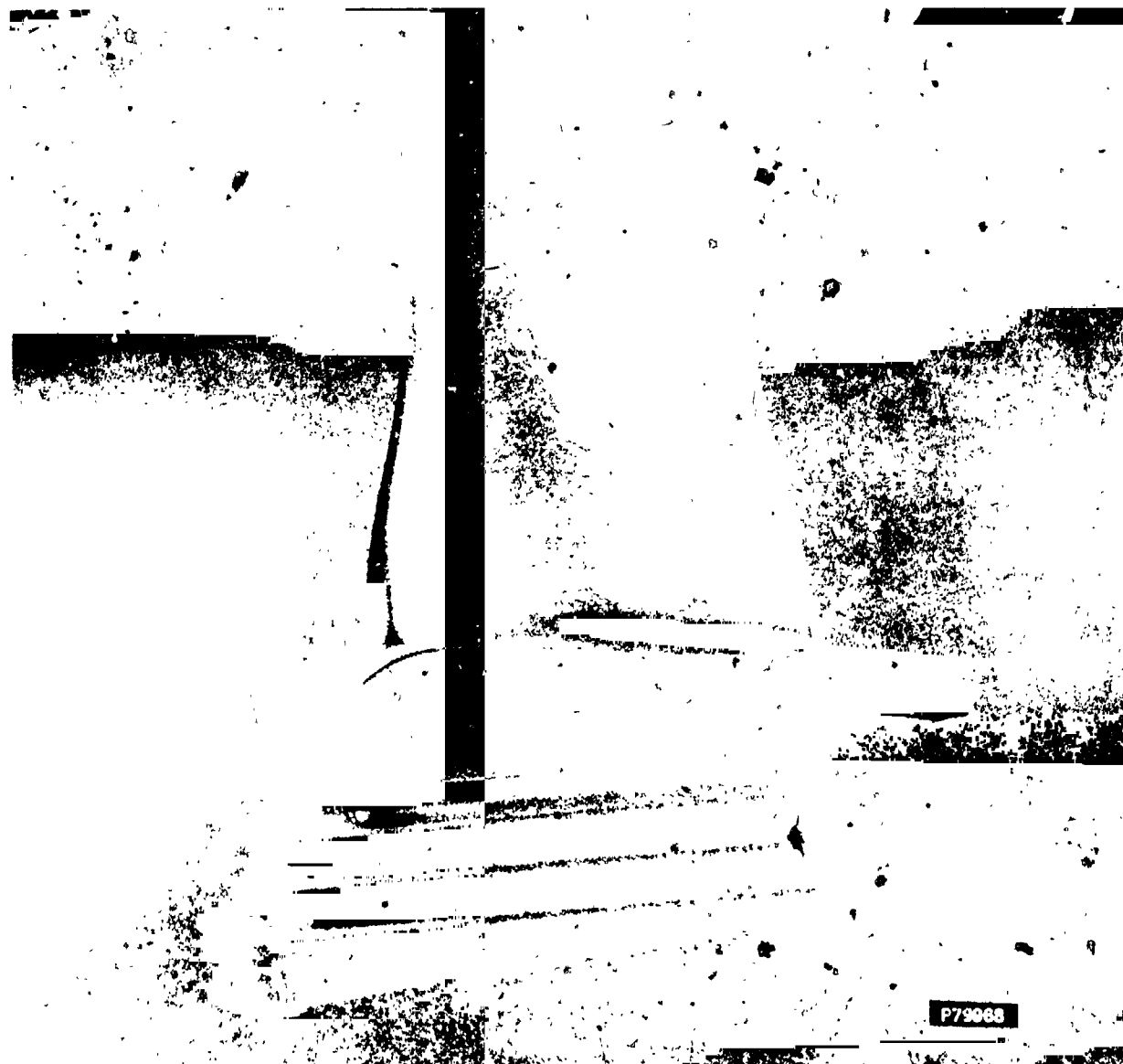


Figure 100. Fully Machined MATE Single-Crystal Turbine Blade.

were machined: 74 NASAIR 100 blades and 60 Alloy 3 blades. None of these blades were coated. Two blades were dimensionally discrepant and subsequently scrapped. FPI of the machined blades again revealed the platform porosity previously noted on the blade casting, but no other significant discrepancies were found.

## SECTION IX

### 9.0 COMPONENT TESTING

Due to the anisotropic material properties of single-crystals, there was concern as to the capability of present analytical computer programs to properly predict all vibratory modes. To avoid problems during engine testing, a two-phase component test program was included to correlate present analytical techniques with test data and to confirm the SC blade design.

#### 9.1 Holographic Testing

The first phase was holography testing of eight SC NASAIR 100 blades and four SC Alloy 3 blades. The blades were clamped at the root in a firtree type fixture that simulated turbine disk and seal plate loads. The clamped blades were excited to low levels of motion by a small crystal driver, while laser equipment produced holographic interferograms to determine the natural frequencies and mode shapes.

Resonant frequencies between 0 and 30 kHz were determined, and mode shapes were recorded both by still photographs and a real time video recorder.

Results of the holography testing indicated that the addition of the tip winglet lowered the natural frequencies of the blade compared to the Project 1 DS blade, but did not significantly alter the resonant mode shapes. A comparison of the first three natural frequencies of the DS Project 1 blade and the SC Project 3 blade is shown in Figure 101. A frequency diagram, shown in Figure 102, was generated using the holography data corrected for material temperature and centrifugal stiffening.

ORIGINAL PAGE IS  
OF POOR QUALITY

MODEL TFE731  
DS HPT BLADE



3400 Hz

FIRST  
FLEXURAL

MATE  
SC HPT BLADE



3198 Hz N100  
3212 Hz A3



8700 Hz

FIRST  
TORSIONAL



7077 Hz N100  
7046 Hz A3



11,200 Hz

TORSIONAL  
COMPLEX



9197 Hz N100  
9407 Hz A3

Figure 101. Comparison of Holography Results  
between DS and SC Turbine Blades.

ORIGINAL PAGE IS  
OF POOR QUALITY

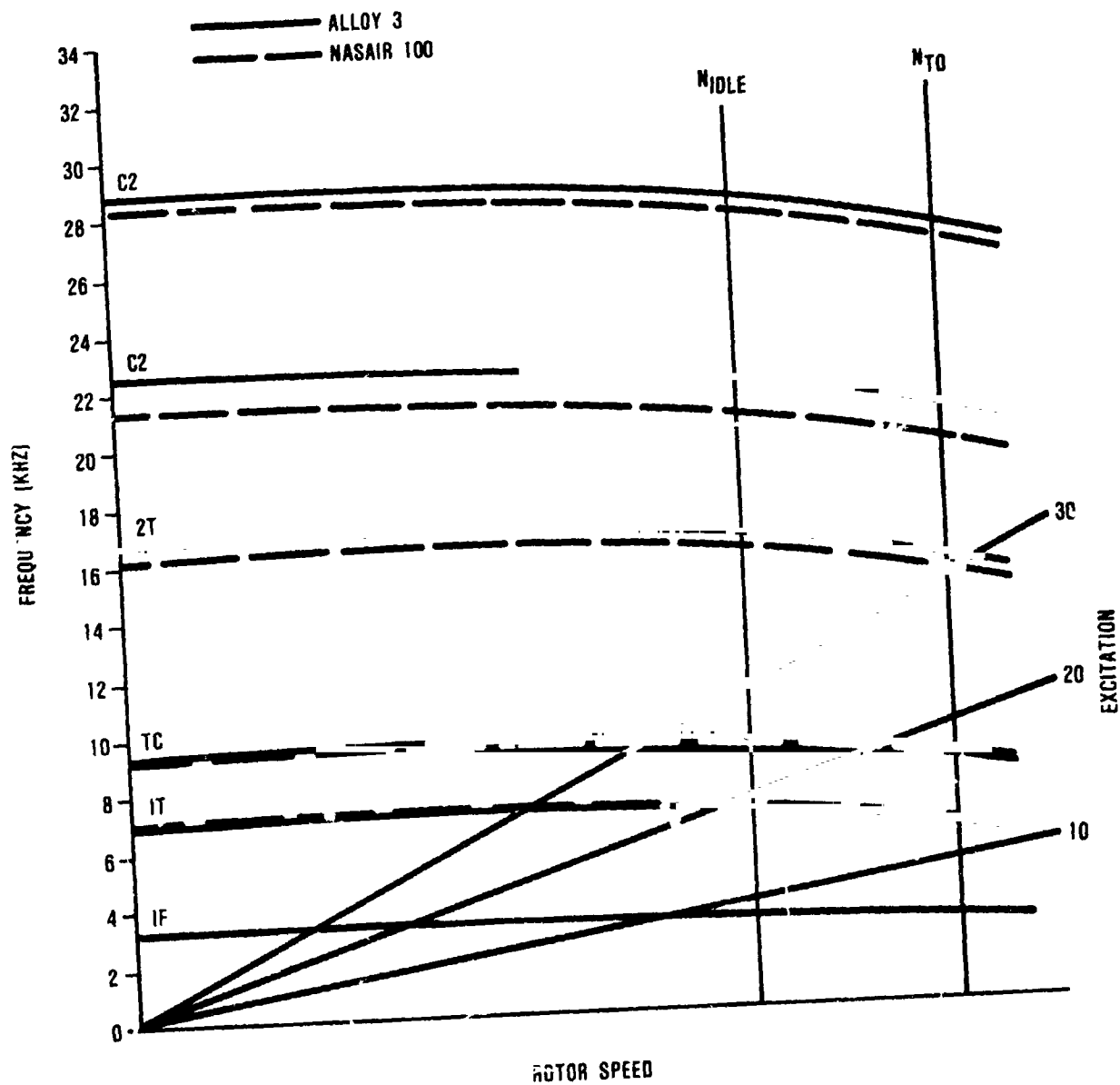


Figure 102. MATE Project 3 Single-Crystal HP Turbine Blade Holography Data and Operating Point Frequency Prediction.

ORIGINAL PAGE IS  
OF POOR QUALITY

Stress-coat testing had been planned to determine the optimum strain-gauge locations, but due to similarities between the resonant mode shapes of the Project 1 DS blade and the Project 3 SC blade, stress-coat testing was not required. Strain-gauge locations were similar to those used in Project 1 component testing.

## 9.2 Firtree Testing

The introduction of single-crystal castings with anisotropic properties makes life prediction of the firtree attachment area very difficult. A comparative subcomponent firtree test of various materials, therefore, appeared to be the fastest and most straightforward method of evaluating the strength of single-crystal castings in the firtree area.

A double-ended male firtree test specimen and corresponding firtree specimen holder (shown in Figure 103) were designed with the

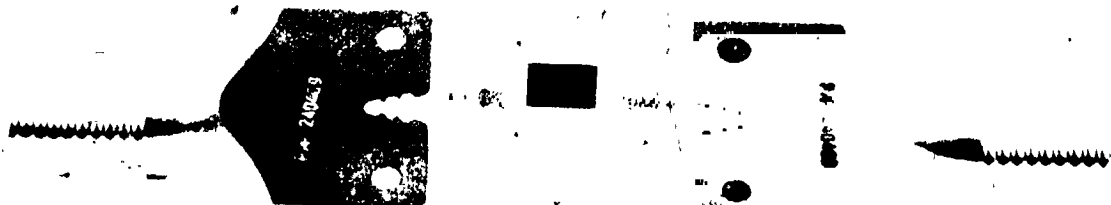


Figure 103. Firtree Specimen and Holder for Project 3 Turbine Blade.

same firtree configuration used for the Project 1 turbine blade. Firtree specimens were machined from cast single-crystal NASAIR 100 bars and from DS Mar-M 247, EQ MAR-M 247, and Waspaloy bars for direct comparison of tensile, low-cycle-fatigue, and stress-rupture capabilities.

Testing was done in air at atmospheric pressure at a temperature of 760°C (1400°F). Results of the low-cycle-fatigue and tensile testing are shown in Figures 104 and 105.

Stress-rupture testing of the SC NASAIR 100 material was attempted at a stress level of 758 MPa (110 ksi) for an expected life of 500 hours. Unfortunately, a failure occurred in the Astroloy firtree specimen holder in less than 100 hours. Examination of the failed holder and the SC specimen indicated that the test load at 760°C (1400°F) was beyond the capabilities of the Astroloy firtree holders. These results were reviewed with the NASA Program Manager, and the remaining stress-rupture testing was canceled.

An examination of the data collected during this testing indicated that the SC firtrees were at least as strong as firtrees made from the more conventional EQ and DS materials currently used in Garrett production HP turbine blades. Therefore, it was concluded that the Project 1 firtree configuration was more than adequate for the MATE Project 3 blade design.

### 9.3 Rig Testing

The second phase of the component testing task determined the vibratory response of the SC blades in an actual engine environment using Garrett's high-pressure rotor rig (HRR). The HRR allows strain-gauge testing of the high-pressure rotating group while operating at actual engine conditions, i.e., 100-percent speed, maximum continuous turbine inlet temperature.



ORIGINAL PAGE IS  
OF POOR QUALITY

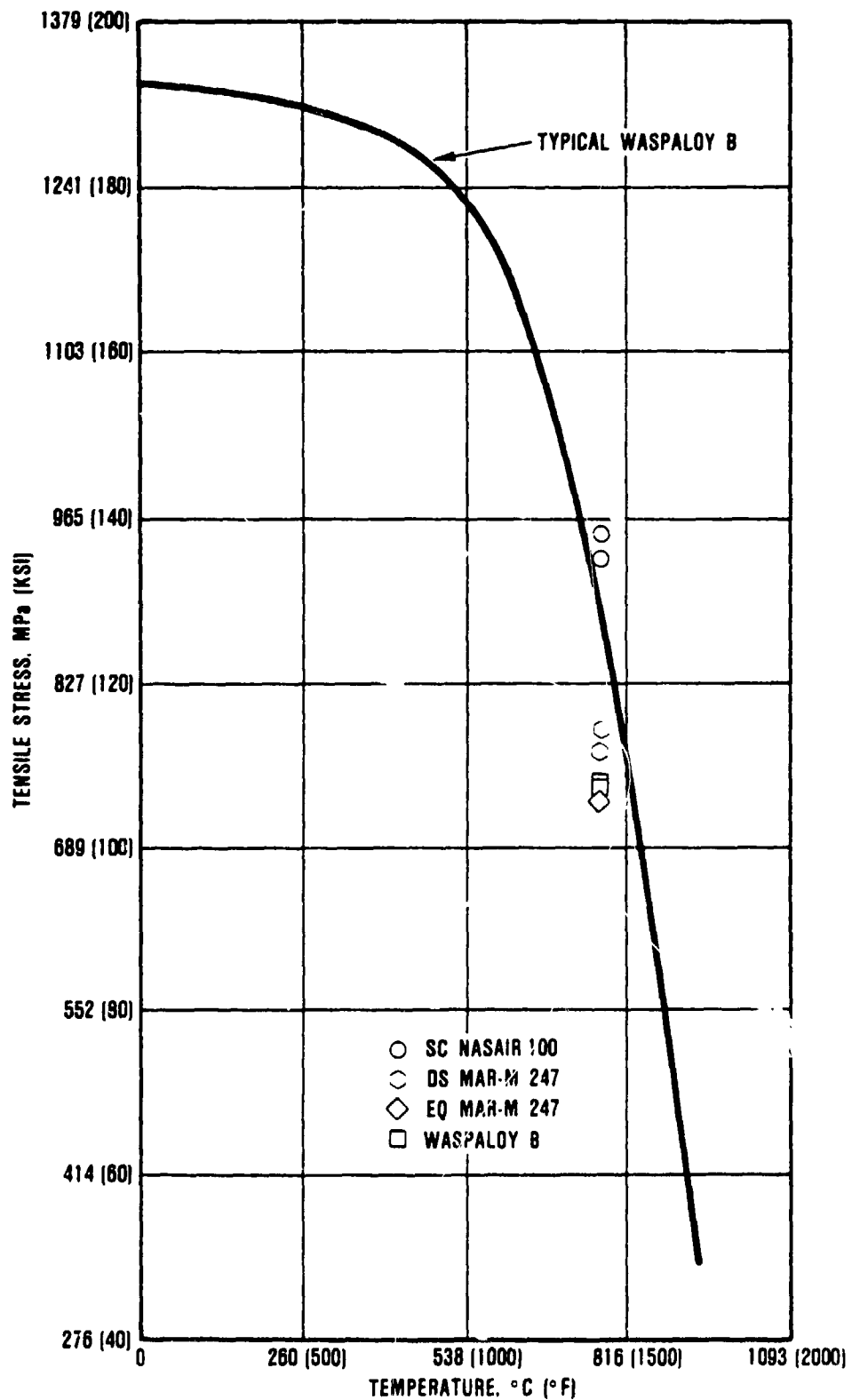


Figure 104. Firtree Tensile Test Results.

ORIGINAL PAGE IS  
OF POOR QUALITY

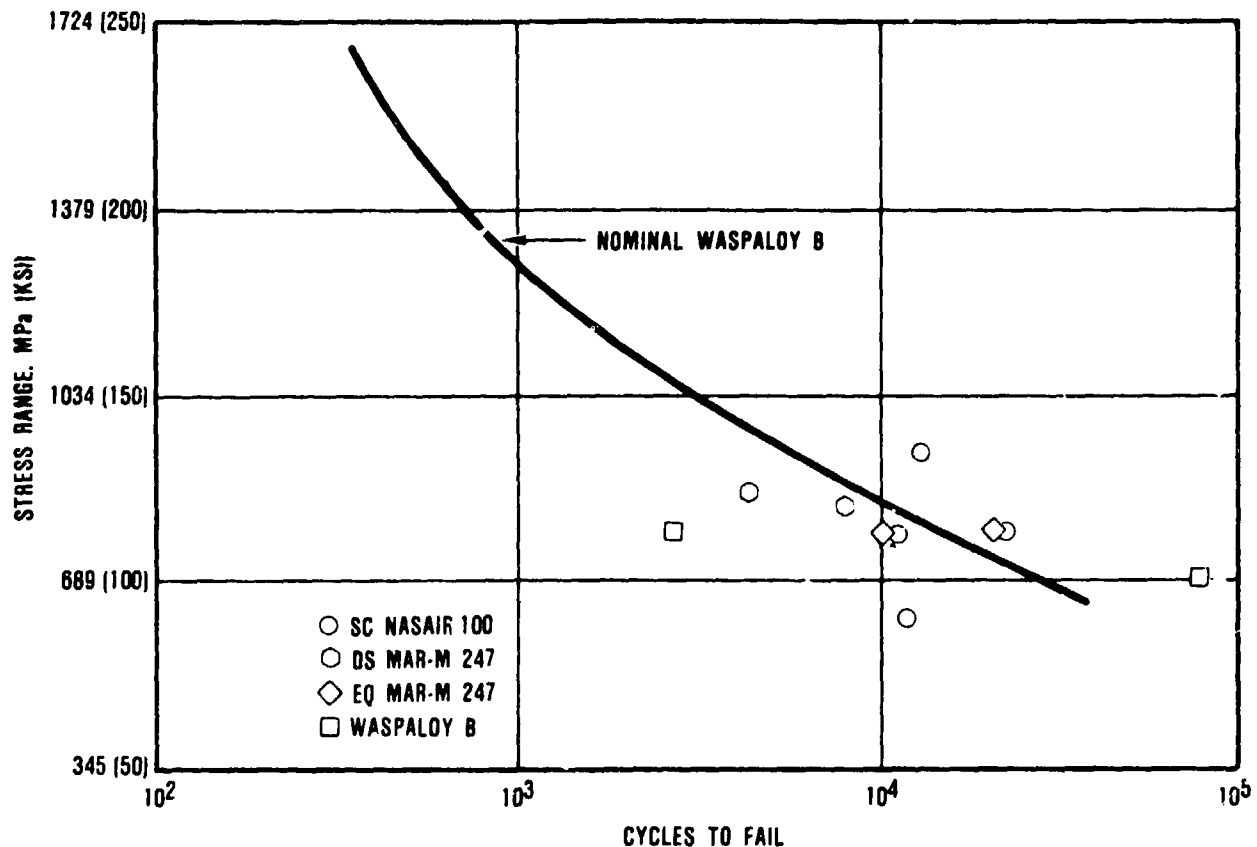
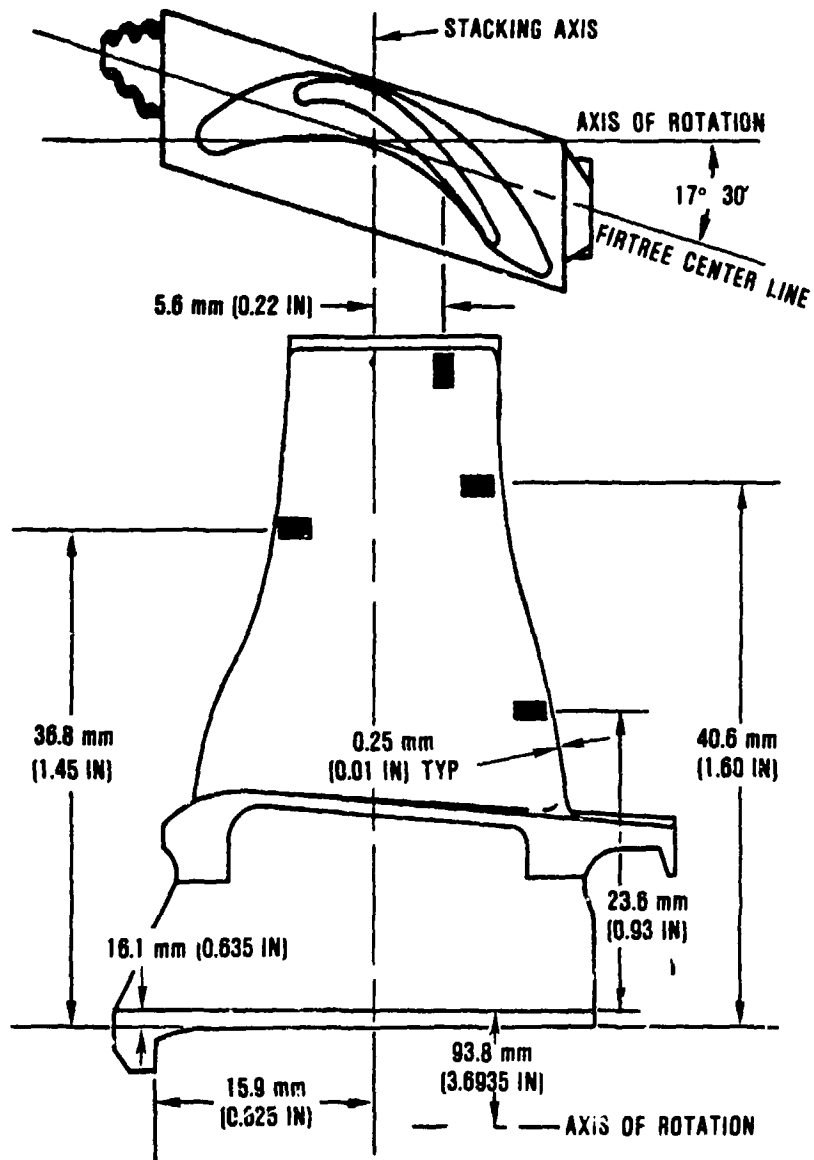


Figure 105. Firtree LCF Test Results at 760°C (1400°F) and R = 0.1.

Twelve SC blades were instrumented with dynamic strain gauges and placed in the rotor assembly. Figures 106, 107, and 108 show, respectively, the strain-gauge locations, the instrumented blades, and the completed rotor assembly containing the instrumented blades.

HRR testing consisted of two slow accelerations and decelerations from idle to maximum takeoff to idle, recording strain-gauge output continually. During testing, a moderate resonance with a peak-to-peak strain level of 1000  $\mu$ inch/inch was noted at 21,300 rpm. No other significant responses were seen. The rig test was completed without incidence and the parts removed for routine post-test inspection.

ORIGINAL PAGE IS  
OF POOR QUALITY



BLADE NO.	IDENT NO.	DISC. LOC.	POSITION
A59	SD 6402	12	LE
A44	SD 8402	44	LE
A26	SD 6402	28	LE
A20	SD 6402	60	LE
N 4	SD 9872	4	TIP
A37	SD 9872	24	TIP
A57	SD 7576	8	CENTER
N24	SD 7576	40	CENTER
A35	SD 7598	48	TE
A41	SD 7598	21	TE
A12	SD 2598	52	TE
N17	SD 2598	32	TE

Figure 106. Strain-Gauge Location, Single-Crystal HP Turbine Blade.

ORIGINAL PAGE IS  
OF POOR QUALITY

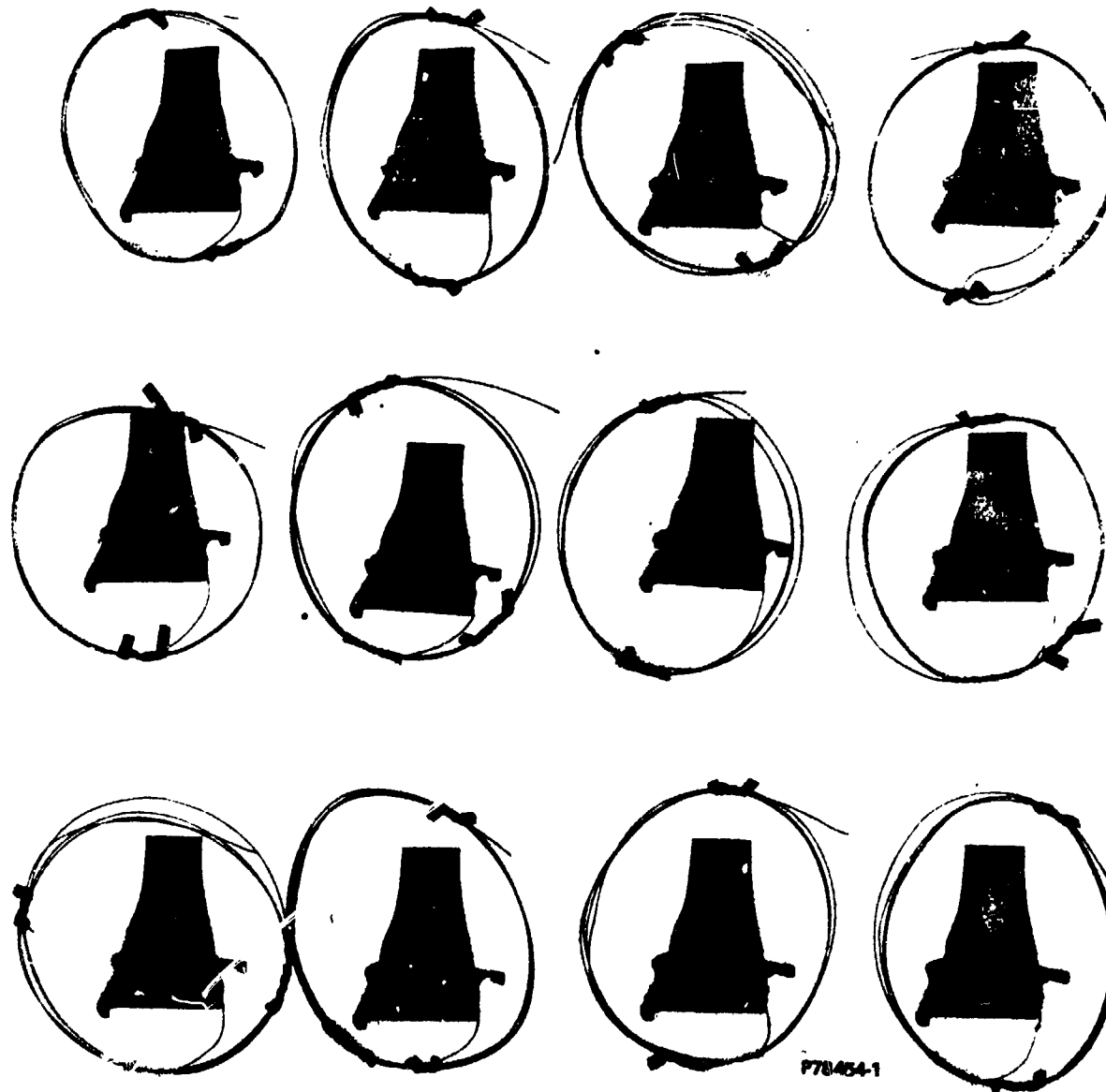


Figure 107. Instrumented SC Turbine Blades.

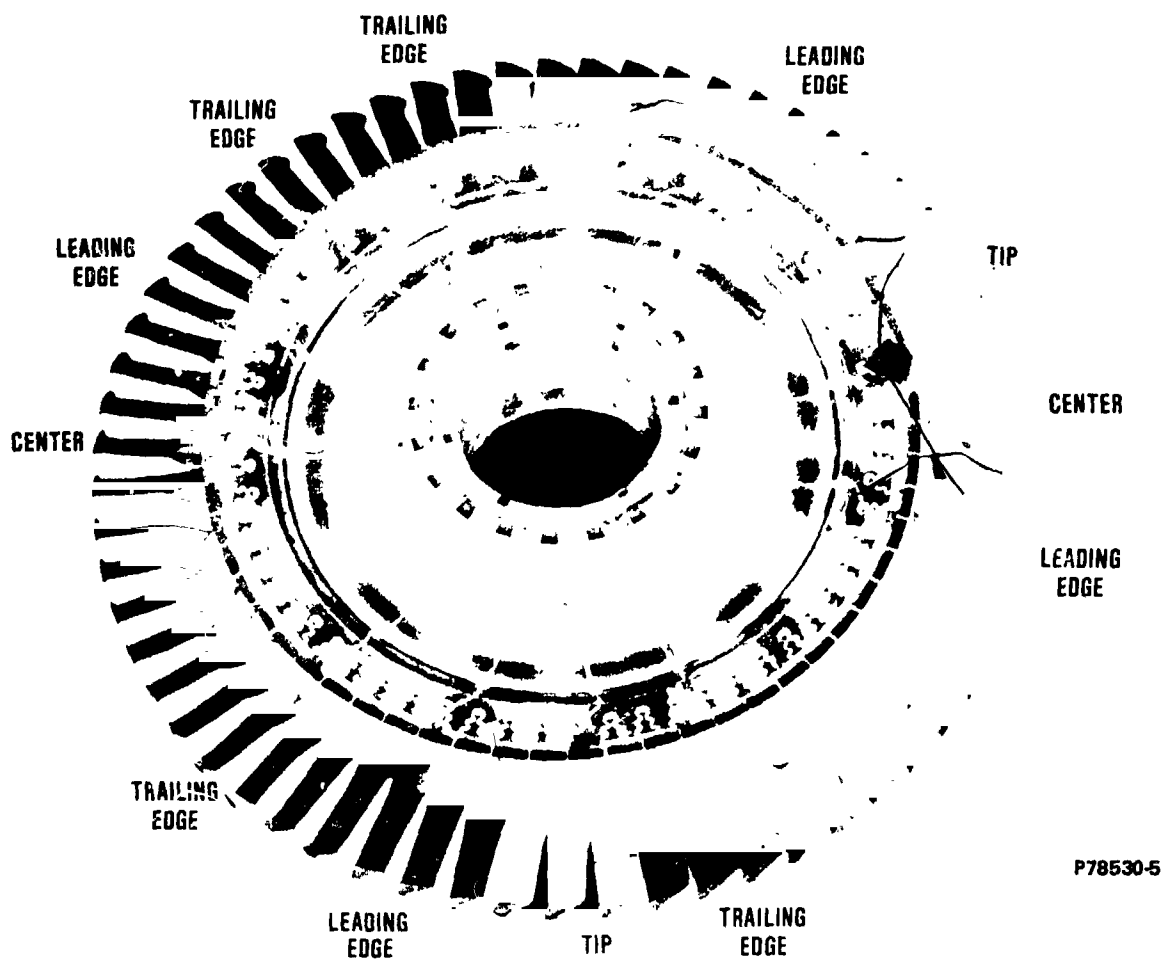


Figure 108. MATE Project 3 Rotor Assembly Showing  
Locations of Instrumented Blades.

#### 9.4 Post-Test Inspection

This inspection of the single-crystal blades unexpectedly revealed four SC Alloy 3 blades with leading-edge cracks at approximately the three-quarter span. No problems or abnormal conditions were found on any NASAIR 100 blades or any of the seals and shroud segments. These four cracked blades were submitted for a complete material analysis.

Results of the analysis indicated that the cracks all occurred at the boundary between a recrystallized secondary grain and the primary grain. These recrystallized secondary grains were all approximately the same shape and size and were at the same location on each of the cracked blades. Figure 109 shows a recrystallized grain on one of the cracked blades (S/N A41) after macroetching. Twinning was also found on the suction side surface. No signs of fatigue were found on the fracture surfaces of any of the four SC Alloy 3 blades.

Further examination of these blades indicated that the dendritic microsegregation pattern had been preserved during formation of the recrystallized grain as shown in Figures 110 and 111. The recrystallized grain microstructure did differ from the rest of the blade in that no sub-boundary networks were present within the recrystallized grain.

The fracture surfaces of the cracks in all four SC Alloy 3 blades were quite smooth, curved, and lightly oxidized (as shown in Figure 112). The grain boundary cracking was attributed to a combination of centrifugal and bending stresses applied to the extremely weak grain boundary that occurred during HRR testing. No indications were found on the fracture surface that were characteristic of a high-cycle-fatigue fracture.

Recrystallized grains of this type are clearly unacceptable and attributable to an improper grain etch inspection after solution heat treatment. HRR test times and temperatures were not even close to the levels required to produce recrystallization.

Following analysis of the four cracked Alloy 3 blades and the discovery of extraneous grains at the crack site, all machined blades and castings were thoroughly reinspected. This inspection included macroetching, a detailed visual review (40X magnification), a sensitive FPI using Group 7 penetrant, and another radiographic

ORIGINAL PAGE IS  
OF POOR QUALITY

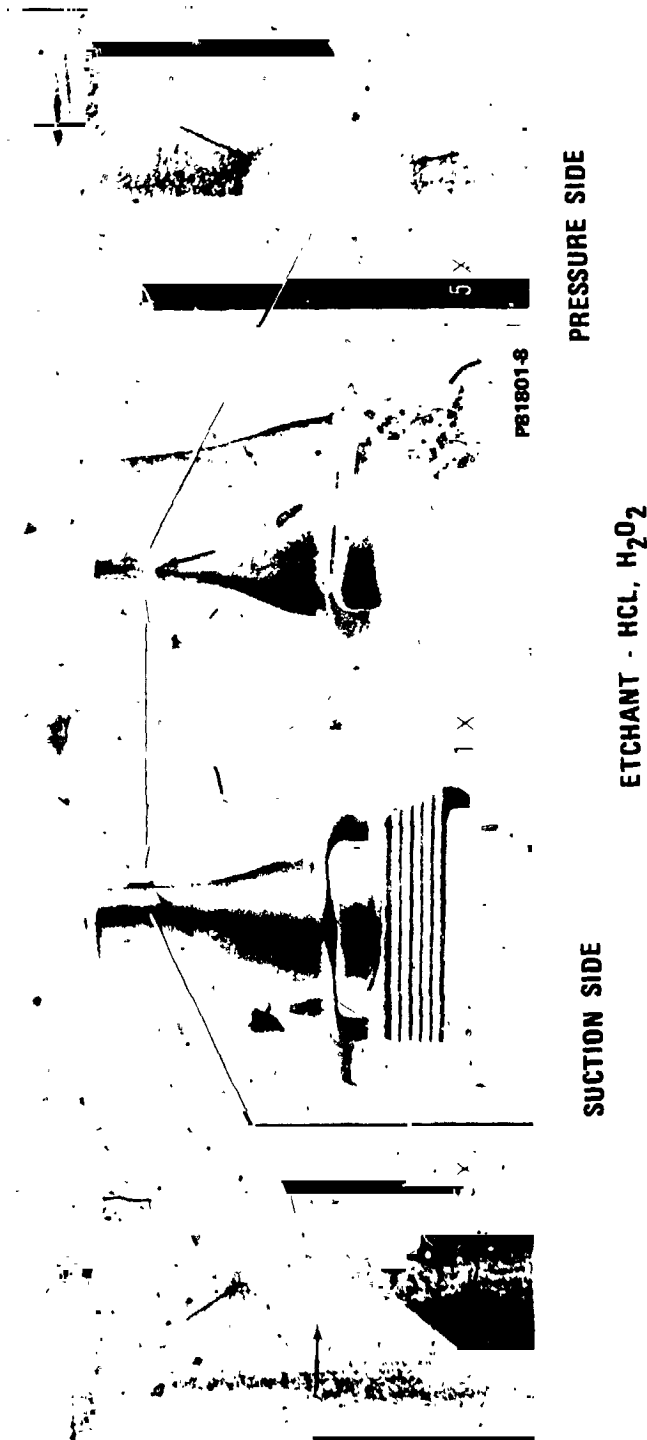


Figure 109. Macroetching Blade A41 showed that the Cracking Had propagated along the Boundary of Small Grains Located at the Leading Edge (white arrows). This Grain Appeared to Contain Several Twins and Is an Unacceptable Discontinuity in a Single-Crystal Blade.

ORIGINAL PAGE IS  
OF POOR QUALITY

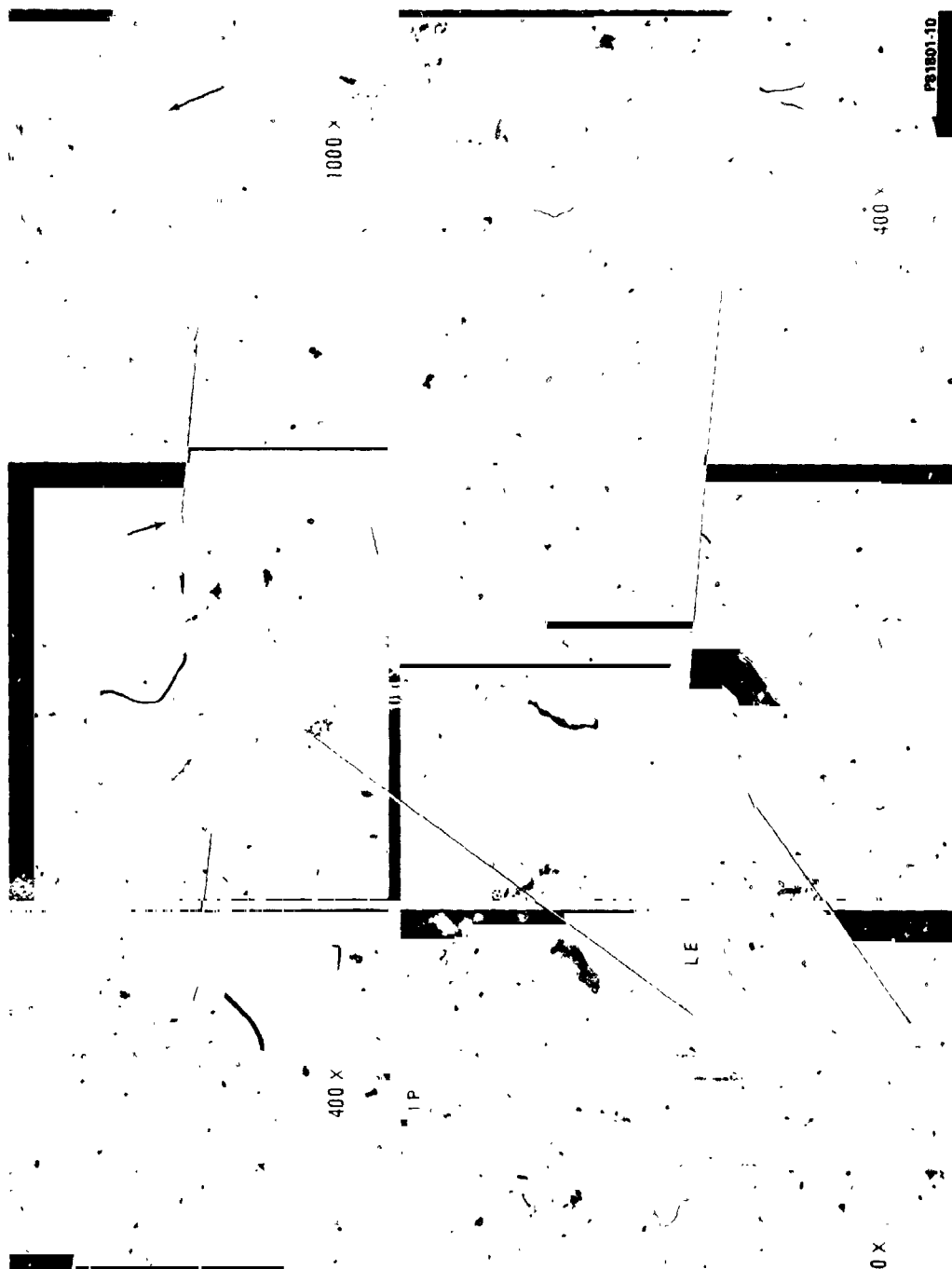


Figure 110. Microstructure of Recrystallized Grain in Leading Edge of SC Alloy 3 Blade S/N A41 Indicated that the Dendritic Microsegregation Pattern Was Preserved. The Cracks Propagated along the Boundary of the Primary and Recrystallized Secondary Grain. (Photographs are 78 percent of indicated magnifications.)



ORIGINAL PAGE IS  
OF POOR QUALITY

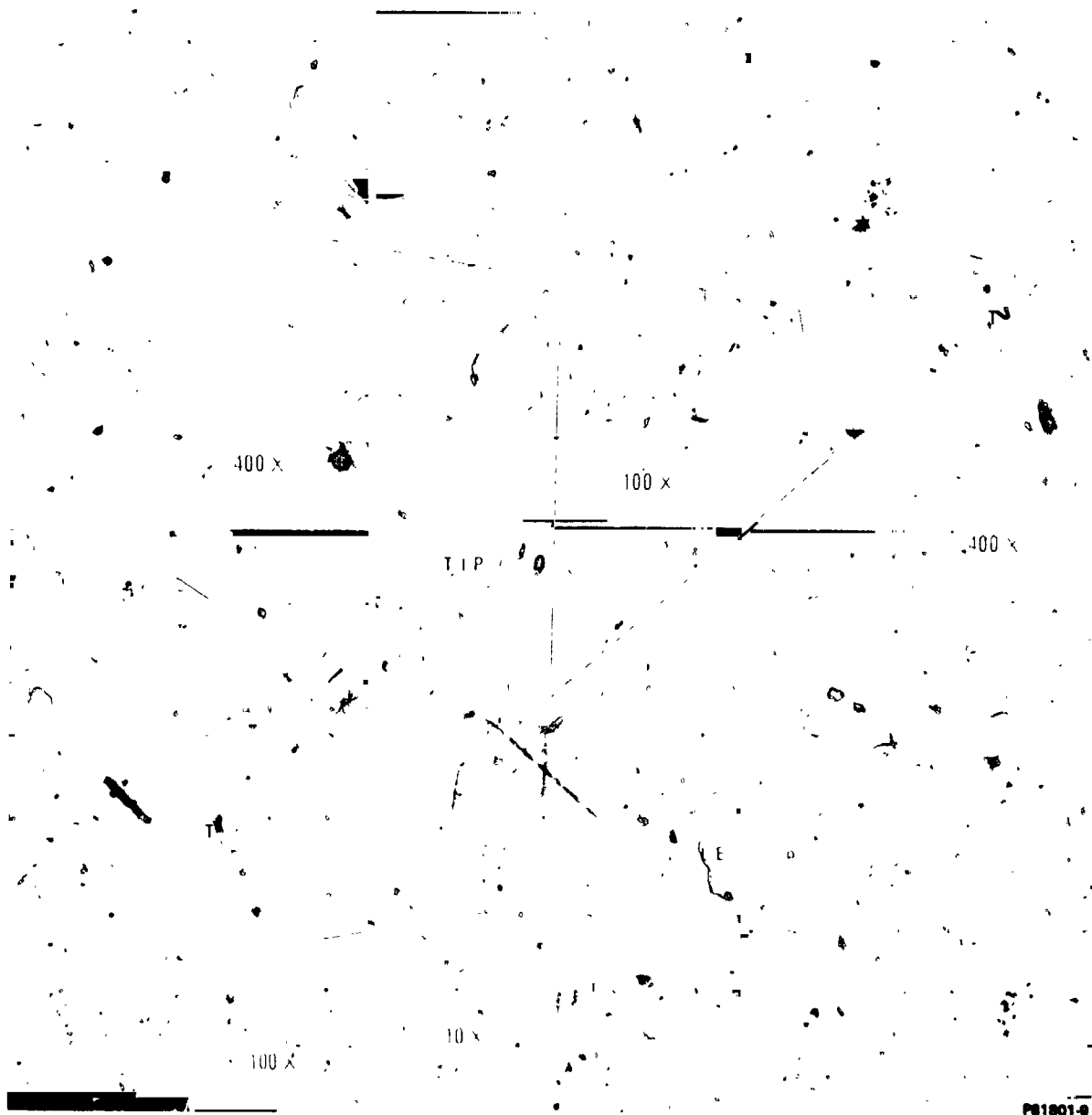


Figure 111. Microstructure of Recrystallized Grain from Edge of SC Alloy 3 Blade S/N A25. Note Presence of Twins and Absence of Sub-Boundary Network in Recrystallized Grains. (Photographs are 83 percent of indicated magnifications.)

ORIGINAL PAGE IS  
OF POOR QUALITY

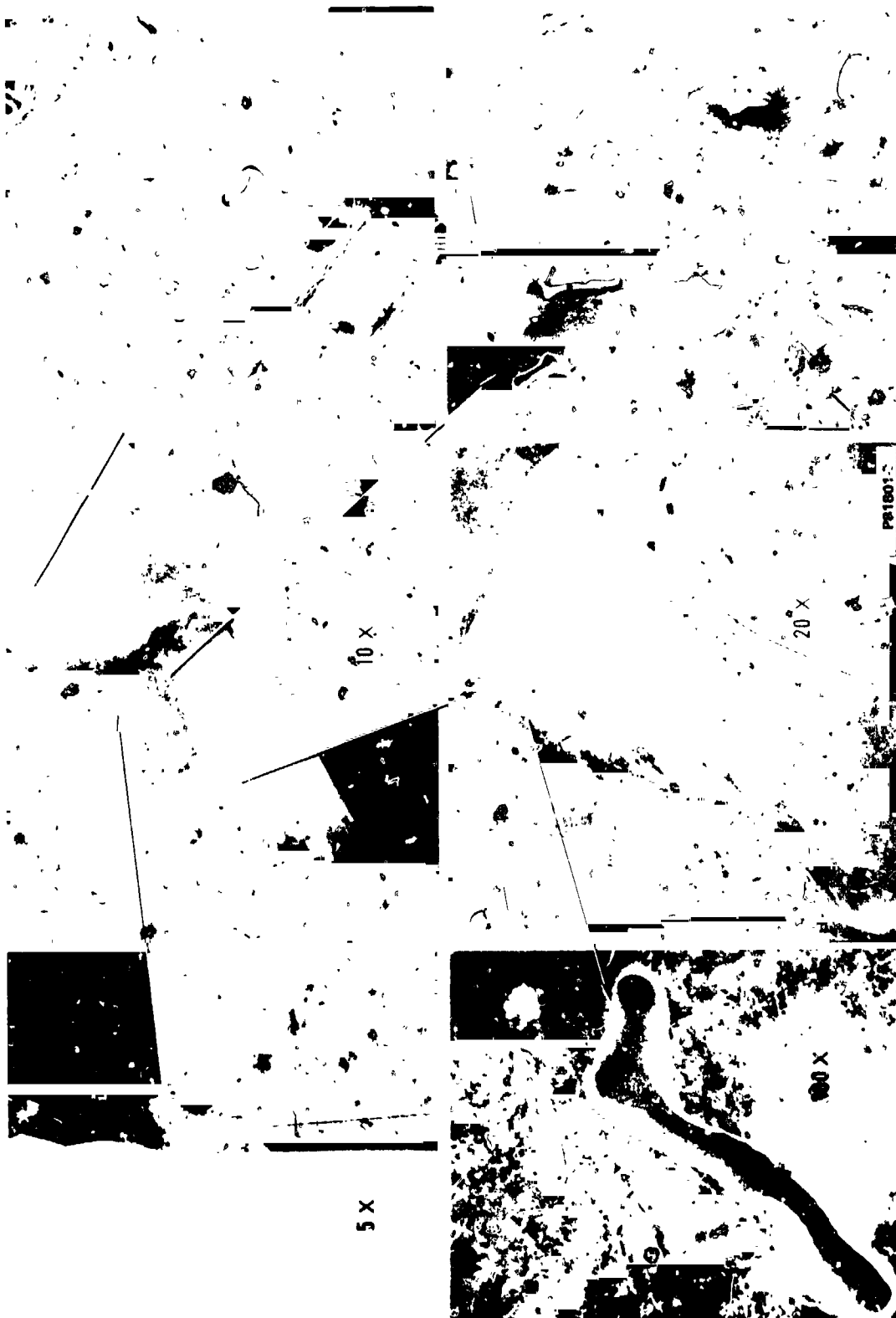


Figure 112. SEM Photographs of Crack Surface of SC Alloy 3 Blade C/N A25 after High Rotor Rig Test. The Fracture Surface Exhibited Numerous Pockets of Microporosity. (Photographs are 90 percent of indicated magnifications.)

inspection. Extraneous grains and other problems were identified in several additional machined blades and castings. The results of these inspections are shown below:

	<u>Rejected Due to Extraneous Grains</u>	<u>Rejected Due to Freckling in Critical Areas</u>	<u>Rejected Due to Major Porosity</u>
NASATR 100	16	12	10
Alloy 3	12*	2	1

\*Includes the four Alloy 3 blades cracked during HRR testing

More than 20 percent of all blades inventoried were scrapped following re-inspection. An additional 16 percent were classified as "marginal" quality. All remaining blades were approved for full-scale engine testing, which is described in Volume II of this report.

C-3

## SECTION X

### 10.0 COST ANALYSIS

It is extremely difficult to project a fair and accurate comparison of turbine blade manufacturing costs for new materials and/or configurations. Differences in raw material costs, vendors, blade configurations, economic situations, lot sizes, and timing of the order all affect the cost of a particular blade. To make this comparison more significant, Garrett historic manufacturing cost data concerning a variety of turbine blades was examined and normalized. The relative costs shown in Table 68 represent an estimate of these normalized blade costs based on production size lots of small turbine blades.

Comparing the cost of SC castings produced by the exothermic process and the withdrawal process is also difficult and can realistically only be done by a casting vendor qualified to produce SC turbine blades. These suppliers have all made substantial investments in withdrawal equipment and have all gained considerable experience in producing SC castings by the withdrawal process. Therefore, it is difficult for them to project the exothermic process to a comparable point on the learning curve and thus give an "apples-to-apples" comparison. Jetshapes has made this projection, however, and feels that an SC blade could be produced for approximately the same cost with either the exothermic or withdrawal process (assuming the automated equipment were available and the same level of experience).

Table 68 shows that the cost of an SC casting is about twice that of a DS casting for a given configuration. This increased cost is offset by the increased capabilities of the SC components. An estimate of the benefits of the SC blades to the overall engine can be calculated using a fully flexible engine cycle with variable bypass and pressure ratio. Table 69 summarizes the results of a life-cycle-cost comparison of an uncooled SC blade to an uncooled

DS blade for a typical business jet application. (For more details see Section 2.0 in Materials for Advanced Turbine Engines Program, Volume 1, Garrett Report 76-212445-1, January 10, 1977.) As shown in this study, the advantages of SC blades are quite significant in advanced engine designs that fully exploit their high temperature capability.

TABLE 68. ESTIMATED RELATIVE COSTS OF SINGLE-CRYSTAL TURBINE BLADES.

<u>BLADE TYPE</u>	<u>CASTING COST</u>	<u>TOTAL* COST</u>
EQ Cooled	1.0	1.0
DS Cooled	1.9	1.6
SC Cooled	3.5	2.7
EQ Uncooled	0.3	0.4
DS Uncooled	0.9	0.9
SC Uncooled	2.1	1.7

\*Includes machining, coating, handling, etc.

TABLE 69. RESULTS OF THE LIFE-CYCLE-COST ANALYSIS OF THE UNCOOLED SC HIGH-PRESSURE TURBINE BLADE AS COMPARED TO THE UNCOOLED DS TURBINE BLADE IN A FULLY OPTIMIZED ENGINE FOR A TYPICAL COMMERCIAL BUSINESS JET MISSION.

$$\Delta \text{TSFC} = -1.53\%$$

$$\Delta W_t = 0$$

Scaling effect (BPR) -

$$\% \Delta W_t = -6.67\%$$

Scaling effect (PR) -

$$\% \Delta W_t = 0$$

$$\text{Total } \Delta W_t = -6.67\% + 0 = -6.67\%$$

$$\Delta \text{Cost} = +0.98\%$$

Scaling effect (BPR & PR) - same as  $W_t$

$$\% \text{ Cost} = -6.67\%$$

$$\text{Total } \Delta \text{Cost} = +0.98 - 6.67 = -5.69\%$$

$$\Delta \text{Life (TBO)}^* = 20\%$$

$$\Delta \text{Reliability (MTBF)}^* = 30\%$$

#### $\Delta \text{LCC}$

$$\text{TSFC Effect:} \quad -1.571$$

$$\text{Wt. Effect:} \quad -2.868$$

$$\text{Cost Effect:} \quad -1.525$$

$$\text{TBO Effect:} \quad -0.091$$

$$\text{MTBF Effect:} \quad \underline{-0.019}$$

$$\text{Total } \Delta \text{LCC\%} \quad -6.074\%$$

$$\Delta \text{LCC, M\$} \quad 2095$$

\*Increased life and reliability may be expected due to greater integrity of a single-crystal blade (no grain boundaries).

## SECTION XI

### 11.0 CONCLUSIONS

#### Casting Process

The low-capital-cost exothermic directional solidification process was successfully modified to produce engine quality SC turbine blades.

Overall SC casting yields were not as high as expected (about 20 percent). However, since the SC grain yield was reasonably high (about 60 percent), a significant improvement in overall casting yield would be anticipated with automation of the mold construction and handling facets of the process.

#### Material Properties

SC Mar-M 247 stress-rupture capability was not significantly better than that of DS Mar-M 247.

SC derivative alloys, developed by removal of all (or most) of the grain boundary strengthening elements (Hf, B, Zr, C) from Mar-M 247, permit SC components to be optimally heat-treated and achieve significantly improved stress-rupture capabilities.

Mechanical properties (creep-rupture, tensile, LCF, and HCF) of SC NASAIR 100 and SC Alloy 3 were significantly superior to those of the DS Mar-M 247 parent alloy, with SC NASAIR 100 slightly stronger than SC Alloy 3.

SC NASAIR 100 exhibited evidence of  $\mu$  phase and  $\alpha$  tungsten in the microstructure. However, this microstructural characteristic did not produce any degradation in the alloy's mechanical proper-

ties (stress rupture and HCF) even after long-term, high-temperature exposure.

Physical property data (density, thermal conductivity, and thermal expansion) for SC NASAIR 100 were found to be equivalent to data previously obtained for DS Mar-M 247. Elastic modulus for SC NASAIR 100 was slightly lower than published data for pure nickel single crystals.

Retention of some Hf in these derivative SC alloys improves coated oxidation/hot corrosion resistance.

### Blade Design

The MATE Project 3 SC blade has significantly better fatigue and tensile capabilities and twice the stress-rupture life of the Project 1 DS blade.

Analytical techniques, modified to accept anisotropic material properties, can correctly predict the lower mode vibrational response of the single-crystal blade.

### Component Testing

No significant relationship between crystal orientation and blade vibrational response could be determined for the range of orientations examined.

Vibrational response (nodal shapes) of the Project 3 SC blade was the same as that of the Project 1 DS blade. The addition of the tip winglet to the SC blade, however, lowered the resonant frequencies.

Secondary grains with significant orientation mismatch cannot be tolerated in moderate-to-high stress areas.



The Project 3 SC blade was judged acceptable for full-scale engine testing.

#### Cost Analysis

In production quantities, the cost of the Project 3 SC blade is estimated to be about twice the cost of the Project 1 DS blade.

#### General

The increased temperature capability of the SC turbine blade will allow a significant increase in engine performance. This capability can be used through increased TIT, decreased cooling air flow, and/or increased component life.

ORIGINAL PAGE IS  
OF POOR QUALITY

# APPENDIX A

## MEASURED FREQUENCY RESPONSE OF PD SC TURBINE BLADES

TABLE 70. MEASURED FREQUENCY RESPONSE OF PD SC TURBINE BLADES  
WITH VARIOUS CRYSTALLOGRAPHIC ORIENTATIONS.

Serial No.	Crystal Orientation	First Flex	First Torsional	Torsional Complex	Second Torsional	Complex	Two Strips	Misc. Modes	Unidentified Modes
405-12	[240]-8°	4085	8453	12540			24734	26508-like 2T	19194
405-2	[100]-8.5°	4538	7977			23865	26545	28999-C	9620
408-12	[310]-8°	4097	8429			23363	26444	30365-3T	4065, 6138, 10547, 16568, 18721, 20194
343-14	[100]-6°	4953	10131				23552	26233-C 31528-3T	8570
397-8	[331]-6°	4382	8519					27105-C	26013, 30447
405-7	[100]-10°	4096	8471			24335			31424
407-8	[113]-9°	4192	8513		17544		24973	17984-C 26141-like 2T 28189-C	17191, 17357, 17517, 18279, 25211, 27597, 28180
343-10	[210]-9°	4776	8273					27124-C	18800, 19126
343-5	[100]-23°	3717	8085	13090	17597	--	21720	4475-Tip Flex 11249-Tip Flap 23683	6847, 28552, 11800
394-5	[100]-5°	4806	9441		17886		22692	29800	6.2K, 8.2K, 11.2K, 13.1K, 12.1K, 26.3K, 23.9K, 28.9K
395-8	[210]-8°	4502	9778	12672	19723	23862	28382	17.2K, 29.2K	8.2K, 11.2K, 25.4K
387-5	[100]-5°	4375	9593	13092	19685	24094		17.5K, 28.4K	12.1K, 13.5K, 29.2K
387-3	[100]-5°	4514	9446	13026	19221			12.6K	12.1K, 19.6K, 21.3K, 23.1K, 24.2K, 26.1K, 29.9K
387-8	[100]-5°	4537	9969	12372	18713	22964	24290		2756, 5104, 17K, 25.7K
344-7A	[100]-2.2°	--	9761	12427	20114	23827	--	31304	
343-5B	[100]-23°	4370	9096	13101	17817	--	--	19453, 24454, 29878	
343-13C	[110]-11°	4189	7920	12512	16412	21518	22787	20004, 34066	
343-13D	[100]-8°	4105	8565	11655	19330	21815	23923	33723	
323-5E	[100]-4°	3843	8826	--	--	21322	25380	27941, 30514	
343-16F	[110]-16°	5833	9701	15583	19481	--	22328	21691, 26481, 32721, 28601, 33635	

ORIGINAL PAGE IS  
OF POOR QUALITY

## APPENDIX B

### NASAIR 100 MATERIAL SPECIFICATION

MATERIAL SPECIFICATION		CODE IDENT NO. <b>99193</b>	SPECIFICATION NO. EMS55461	REV LTR NC																																																						
<p>1. APPLICATION</p> <p>1.1 This specification establishes the requirements for NASAIR-100.</p> <p>1.1.1 NASAIR-100 is a cast nickel-base superalloy used for single-crystal (SC) turbine vanes and blades at temperatures up to 2000°F.</p>		<p>3.3 Castings shall be poured only from remelted master heat metal.</p> <p>3.4 Blades shall be cast from every master heat and tested per EMS52501.</p> <p>3.4.1 If the configuration permits, test specimens shall also be machined from cast parts.</p> <p>3.4.1.1 Specimens may be machined from any area of the casting, unless otherwise specified.</p> <p>3.4.2 Blades shall be cast into the same type of refractory mold as the castings for which the master heat is to be used.</p>																																																								
<p>2. APPLICABLE DOCUMENTS</p> <p>2.1 The following documents form a part of this specification to the extent referenced herein.</p> <p>2.1.1 Garrett Specifications</p> <p>EMS52300 Classification and Inspection of Castings</p> <p>EMS52330 Master Heat Preparation of Nickel-Base Alloys</p> <p>EMS52501 Metallurgical Control of Directionally Solidified Single-Crystal NASAIR-100 Turbine Vanes and Blades</p> <p>2.1.2 Aerospace Materials Specification</p> <p>AMS 2280 Trace Element Control, Nickel Alloy Castings</p>		<p>3.5 Castings shall be supplied in the solution heat treated condition per EMS52501.</p> <p>4. PROCESS CONTROL</p> <p>Not applicable.</p> <p>5. INSPECTION</p> <p>5.1 All castings shall be visually, penetrant, and X-ray inspected in accordance with EMS52300.</p> <p>5.2 The supplier shall perform all testing for conformance to chemical limits.</p> <p>5.3 The supplier shall perform all mechanical-property testing.</p>																																																								
<p>3. TECHNICAL REQUIREMENTS</p> <p>3.1 Composition</p> <table border="1"> <thead> <tr> <th></th> <th>Suggested Aim</th> <th>Range</th> </tr> </thead> <tbody> <tr> <td>Carbon</td> <td>0.006</td> <td>0.006 max.</td> </tr> <tr> <td>Chromium</td> <td>9.00</td> <td>8.50-9.50</td> </tr> <tr> <td>Molybdenum</td> <td>1.00</td> <td>0.80-1.20</td> </tr> <tr> <td>Tantalum</td> <td>3.30</td> <td>3.10-3.50</td> </tr> <tr> <td>Aluminum</td> <td>5.8</td> <td>5.60-5.90</td> </tr> <tr> <td>Titanium</td> <td>1.2</td> <td>1.00-1.40</td> </tr> <tr> <td>Boron</td> <td>&lt;0.002</td> <td>0.002 max.</td> </tr> <tr> <td>Zirconium</td> <td>&lt;0.03</td> <td>0.03 max.</td> </tr> <tr> <td>Cobalt</td> <td>&lt;0.50</td> <td>0.50 max.</td> </tr> <tr> <td>Tungsten</td> <td>10.5</td> <td>10.00-11.00</td> </tr> <tr> <td>Manganese</td> <td>-</td> <td>0.20 max.</td> </tr> <tr> <td>Sulfur</td> <td>-</td> <td>0.015 max.</td> </tr> <tr> <td>Silicon</td> <td>-</td> <td>0.12 max.</td> </tr> <tr> <td>Iron</td> <td>-</td> <td>0.10 max.</td> </tr> <tr> <td>Nickel</td> <td>Remainder</td> <td>Remainder</td> </tr> <tr> <td>(O)</td> <td>&lt;10 ppm</td> <td>10 ppm max.</td> </tr> <tr> <td>(N)</td> <td>&lt;12 ppm</td> <td>12 ppm max.</td> </tr> </tbody> </table> <p>3.1.1 Trace elements shall be controlled in accordance with AMS 2280, Class 2.</p> <p>3.2 Production of master heats, remelting of master heats, and pouring of castings shall be accomplished under vacuum</p> <p>3.2.1 Master heats shall be made from 100% virgin material in accordance with EMS52330.</p> <p>3.2.2 A master heat is defined as previously refined metal from a single furnace charge.</p>			Suggested Aim	Range	Carbon	0.006	0.006 max.	Chromium	9.00	8.50-9.50	Molybdenum	1.00	0.80-1.20	Tantalum	3.30	3.10-3.50	Aluminum	5.8	5.60-5.90	Titanium	1.2	1.00-1.40	Boron	<0.002	0.002 max.	Zirconium	<0.03	0.03 max.	Cobalt	<0.50	0.50 max.	Tungsten	10.5	10.00-11.00	Manganese	-	0.20 max.	Sulfur	-	0.015 max.	Silicon	-	0.12 max.	Iron	-	0.10 max.	Nickel	Remainder	Remainder	(O)	<10 ppm	10 ppm max.	(N)	<12 ppm	12 ppm max.	<p>6. IDENTIFICATION AND PACKING</p> <p>Not applicable.</p> <p>7. APPROVAL OR PROCUREMENT</p> <p>7.1 To assure uniformity of quality, sample castings from new or reworked tooling shall be approved by the purchaser.</p> <p>7.2 Supplier shall use the same casting technique, including rate of cooling after casting, and if heat treatment is specified, the same heat-treating procedure for production castings as for approved sample castings.</p>		
	Suggested Aim	Range																																																								
Carbon	0.006	0.006 max.																																																								
Chromium	9.00	8.50-9.50																																																								
Molybdenum	1.00	0.80-1.20																																																								
Tantalum	3.30	3.10-3.50																																																								
Aluminum	5.8	5.60-5.90																																																								
Titanium	1.2	1.00-1.40																																																								
Boron	<0.002	0.002 max.																																																								
Zirconium	<0.03	0.03 max.																																																								
Cobalt	<0.50	0.50 max.																																																								
Tungsten	10.5	10.00-11.00																																																								
Manganese	-	0.20 max.																																																								
Sulfur	-	0.015 max.																																																								
Silicon	-	0.12 max.																																																								
Iron	-	0.10 max.																																																								
Nickel	Remainder	Remainder																																																								
(O)	<10 ppm	10 ppm max.																																																								
(N)	<12 ppm	12 ppm max.																																																								

ORIGINAL PAGE 15  
OF POOR QUALITY

MATERIAL SPECIFICATION	CODE IDENT NO. 99193	SPECIFICATION NO. ZMS55461	REV LTR NC
<b>8. REPORTS</b>		<b>9. QUALITY CONTROL</b>	
<p>8.1 The supplier of castings shall furnish with each shipment a report listing the results of the mechanical-property tests, results of the chemical analysis, and a statement that the castings conform to the requirements of this specification.</p>		<p>9.1 Castings shall be uniform in quality and condition, sound, and free from foreign materials and from internal and external imperfections in excess of those allowed in EMS52300 for the specific class and grade.</p>	
<p>8.1.1 This report shall include the purchase order number, master heat number and code symbol, if used, material specification number and its revision letter, part number, and quantity from each heat.</p>		<p>9.2 At the option of Garrett, a casting shall be selected from any castings received and shall be inspected in accordance with the applicable requirements for that part.</p>	
<p>8.2 The supplier of finished or semifinished parts shall furnish with each shipment a report showing the purchase order number, materials specification number, contractor or other direct supplier of castings, part number, and quantity.</p>		<p>9.3 Parts and material not conforming to the requirements of this specification shall be rejected.</p>	
<p>8.2.1 When castings for making finished or semifinished parts are produced or purchased by the parts supplier, the parts supplier shall inspect castings from each master heat or master heat lot represented and shall include in the report a statement that the castings conform, or shall include copies of laboratory reports showing the results of tests to determine conformance.</p>			

ORIGINAL PAGE IS  
OF POOR QUALITY

# APPENDIX C

## ACCEPTANCE STANDARDS FOR SINGLE-CRYSTAL TURBINE BLADES

MATERIAL SPECIFICATION	CODE IDENT NO. 99193	SPECIFICATION NO. EMS52501	REV LTR NC
1. APPLICATION			
1.1 This specification establishes the requirements for metallurgical control of turbine vanes and blades cast from NASAIR-100.			
1.1.1 NASAIR-100 is a directionally solidified single-crystal (SC) nickel-base superalloy used for said turbine components at temperatures up to 1000°F.			
1.1.2 When cast as a SC there is a significant improvement in creep-rupture properties compared to multicolumnar-grain directionally solidified (DS) and conventionally cast nickel-base alloys.			
2. APPLICABLE DOCUMENTS			
2.1 The following documents form a part of this specification to the extent referenced herein.			
2.1.1 Garrett Specifications and Forms			
EMS52300 Classification and Inspection of Castings			
EMS52309 Fluorescent Penetrant Inspection			
EMS52330 Master Heat Preparation of Nickel-Base Alloys			
EMS52332 Metallurgical Fixed Process Approval for Cast Turbine Blades (Mechanical Properties)			
EMS52348 Radiographic Inspection			
EMS55461 Nickel Alloy Castings, Investment, Corrosion- and Heat-Resistant, NASAIR-100			
Form P-5389 Quality Control-Request for Material Review Action (RMRA)			
Form P-6041 Fixed Process Form			
3. TECHNICAL REQUIREMENTS			
3.1 Composition			
3.1.1 The chemical composition shall be in accordance with EMS55461.			
3.1.2 A master heat shall be made from 100% virgin material in accordance with EMS52330.			
3.1.3 A master heat is defined as previously refined metal from a single furnace charge.			
	3.2 Master Heat Qualification		
	3.2.1 Remelting of master heats and pouring of castings shall be accomplished under vacuum.		
	3.2.2 SC turbine blades shall be cast from each master heat and tested. Testing shall consist of three 1400°F tensiles and three 1800°F stress-rupture tests.		
	3.2.3 SC turbine blades shall be cast into the same type of refractory mold as the castings for which the master heat is to be used.		
	3.2.4 If the casting configuration does not allow test specimens to be machined from it, then sample blade castings shall be cast along with the other castings and test specimens shall be machined from these sample blades.		
	3.3 Mechanical-Property Testing		
	3.3.1 SC castings used for testing to qualify the master heat may be grit blasted prior to heat treatment provided the machining of test specimens will remove sufficient material so as to clean-up all cast surfaces.		
	3.3.2 SC turbine blade castings selected for mechanical-property testing shall meet the following crystal orientation requirement:		
	Blade, [001] direction within 15° of the blade stacking axis.		
	X-ray Laue method is recommended for verification of grain orientation. Use of alternate methods for grain orientation measurement shall require written approval of Materials Engineering.		
	3.3.3 Prior to test specimen machining, SC castings shall be heat treated as follows:		
	1) Solution heat treatment - 2400 ±10°F for two hours, raise temperature to 2415 ±0-10°F, and hold for two hours followed by rapid argon-fan quench to below 1800°F. The cooling rate from the solution heat treat temperature must be sufficiently fast to meet mechanical property requirements.		
	2) Pseudo coating cycle heat treatment - 1800 ±25°F for five hours and still air cool.		
	3) Age heat treatment - 1600 ±25°F for 20 hours and air cool.		

ORIGINAL PAGE IS  
OF POOR QUALITY

MATERIAL SPECIFICATION	CODE IDENT NO. 99193	SPECIFICATION NO. ZMS52501	REV LTR NC								
<p>3.3.4 For mechanical-property testing, test specimen configuration shall be as follows:</p> <p>Blade - Test specimens machined from blades shall have a 0.070-inch diameter gauge section 0.375 inch long between radii.</p> <p>Test specimen orientation shall be parallel to the stacking axis of the blade. Figure 1 provides a sketch showing the location of the test specimen on a blade casting and a drawing of the test specimen.</p> <p>3.3.5 Tensile Testing - Tensile test specimens shall be tested at 1400 <math>\pm</math>10°F. Three specimens shall be tested with each meeting the following minimums:</p> <table><tbody><tr><td>Ultimate tensile strength (ksi)</td><td>173</td></tr><tr><td>0.2 percent yield strength (ksi)</td><td>146</td></tr><tr><td>Elongation (percent in 4D)</td><td>3.0</td></tr><tr><td>Reduction in area (percent in 4D)</td><td>3.0</td></tr></tbody></table> <p>3.3.6 Stress-Rupture Testing - Stress rupture test specimens shall be tested under a constant stress of 35,000 psi at 1800 <math>\pm</math>5°F. Three specimens shall be tested and each specimen shall have a minimum life of 47 hours.</p> <p>3.4 Qualified Master Heat</p> <p>3.4.1 Master heat material meeting mechanical-property minimums specified herein is defined as a qualified master heat.</p> <p>3.5 Metallurgical Control of SC Turbine Vanes and Blades</p> <p>3.5.1 Castings shall be poured only from remelted qualified master heat metal. The use of gates, sprues, risers, or rejected castings is not permitted.</p> <p>3.5.2 Each solution heat treat lot must be qualified.</p> <p>3.5.2.1 A solution heat treat lot is defined as a master heat/part number/solution heat treat cycle combination.</p> <p>3.5.3 The solution heat treat lot qualification may be performed in conjunction with the master heat qualification.</p> <p>3.5.3.1 All requirements for master heat qualification and mechanical-property testing apply to solution heat treat lot qualification.</p> <p>3.5.4 Metallographic Inspection</p> <p>3.5.4.1 A blade from each solution heat treat lot shall be metallographically examined for gamma prime solutioning and incipient melting. Acceptable and rejectable microstructures (100X magnification) are provided in Figures 2 and 3 respectively. A 100X photomicrograph of a representative area taken at the blade root shall be submitted to Garrett Receiving Inspection for transmittal to Materials Engineering.</p> <p>3.5.5 Surface Condition</p> <p>3.5.5.1 Production SC blade castings shall be solution heat-treated prior to any abrasive blasting operation after removal of castings from the mold.</p> <p>3.5.5.2 Blade surfaces shall show no evidence of recrystallization, alloy depletion or oxidation.</p> <p>3.5.6 Grain Orientation</p> <p>3.5.6.1 Each blade shall be chemically etched for a time sufficient to lightly reveal the grain orientation.</p> <p>3.5.6.2 The [001] crystallographic growth direction shall be within 15° of the stacking axis of the airfoil. Crystallographic orientation of all blade castings shall be determined. The orientation for each blade casting shall be documented and the results submitted to Garrett Receiving Inspection for transmittal to Materials Engineering for information purposes only. X-ray Laue method is recommended for grain orientation.</p> <p>3.5.6.3 No equiaxed grains, columnar grains, or freckles are permitted on the blade castings.</p>				Ultimate tensile strength (ksi)	173	0.2 percent yield strength (ksi)	146	Elongation (percent in 4D)	3.0	Reduction in area (percent in 4D)	3.0
Ultimate tensile strength (ksi)	173										
0.2 percent yield strength (ksi)	146										
Elongation (percent in 4D)	3.0										
Reduction in area (percent in 4D)	3.0										

ORIGINAL PAGE IS  
OF POOR QUALITY

MATERIAL SPECIFICATION	CODE IDENT NO. 99193	SPECIFICATION NO. EMS52501	REV LTR NC
<p>4. PROCESS CONTROL</p> <p>4.1 Cooling rate from solution-heat-treat temperature shall be sufficiently fast to meet mechanical properties.</p> <p>4.2 Solution heat-treat furnaces shall be qualified by the casting supplier.</p> <p>4.2.1 To qualify a furnace, the casting supplier must heat treat a minimum of 5 blades per each test condition of tensile testing and stress rupture testing specified herein in a furnace loaded to a maximum production heat treat capacity, and test to the mechanical property requirements. A simulated load by weight may be used.</p> <p>4.3 All casting processes, including metal and mold preparation methods, shall be established and documented, including controls for critical variables. Failure to meet the specified requirements shall be cause for withholding qualification of the casting process. Garrett review of the process documentation and casting evaluation shall constitute qualification of the casting process.</p> <p>4.4 After the casting process for each part number has been established, the supplier shall prepare documentation, on a Garrett supplied Fixed Process Form, of the final detailed foundry operations and processing sequences. This documentation, comprising the "fixed process," shall be submitted to Garrett for review prior to the first order of production parts.</p> <p>4.4.1 If it becomes necessary for the supplier to make any change in this fixed process, written permission shall be obtained from Garrett prior to incorporating such a change.</p> <p>4.4.2 If the supplier has made an inadvertent change in the fixed process during the production of castings, Garrett shall be immediately notified of the nature and extent of the change and quantity of parts affected, and the supplier shall obtain written permission via the normal RMRA procedure from Garrett prior to submitting the parts for acceptance.</p> <p>4.4.3 Each supplier shall keep daily records, in accordance with established procedures, of all control items in the fixed process that are recorded continuously on strip charts or circular charts, or checked and recorded by hand. All process controls shall be personally audited by the supplier's quality control section once every month, and a report filed.</p> <p>5. INSPECTION</p> <p>5.1 Subject parts shall be inspected by the casting supplier with the following methods: visual, radiographic, macro acid etch, fluorescent-penetrant, and dimensional, as applicable.</p> <p>5.2 Visual Inspection - All blades shall be inspected in accordance with EMS52300.</p> <p>5.3 Fluorescent Penetrant Inspection</p> <p>5.3.1 All blades shall be processed per EMS52309.</p> <p>5.3.2 Fluorescent penetrant indications shall be correlated with the allowable visual imperfections and the accept/reject criteria of EMS52300 as applicable.</p>			

ORIGINAL PAGE 13  
OF POOR QUALITY

MATERIAL SPECIFICATION	CODE IDENT NO. 99193	SPECIFICATION NO. EMS52501	REV LTR NC
<p>5.3.3 Evaluation of smeared or unsharp indications may be performed by wiping the indication one time only with a swab or brush dipped in solvent.</p> <p>5.4 Radiographic Inspection - All blades shall be radiographically inspected per EMS52348 and the acceptance standards defined in EMS52300 as applicable.</p> <p>5.5 Master heats shall be tested by the casting supplier for conformance to chemical limits. Chemical analysis shall be performed on a blade cast from the master heat and meet the requirements of EMS55461.</p> <p>5.5.1 Overall chemistry may be determined at any location within the blade.</p> <p>5.6 The casting supplier shall test six blades from each part number/master-heat/solution-heat-treat lot combination, three in elevated temperature tensile and three in creep-rupture per the conditions of tensile testing and stress-rupture testing specified herein, to verify conformance to the mechanical-property requirements.</p> <p>5.6.1 The specimens shall meet the mechanical property requirements of tensile testing and stress-rupture testing specified herein.</p> <p>5.6.1.1 If the mechanical properties do not meet the minimum requirements, the heat treat lot shall be retested using two more blades for each failure from the same master heat-heat treat lot combination. Any failure of a retest rejects the heat treat lot.</p> <p>5.7 A sample from each heat-treat lot received shall be inspected by Garrett for recrystallization, alloy depletion, and oxidation.</p>	<p>6. IDENTIFICATION AND PACKING</p> <p>Not applicable.</p> <p>7. APPROVAL OR PROCUREMENT</p> <p>7.1 Approval of the supplier's fixed process and process changes shall be in accordance with EMS52332. All subsequent fixed process changes shall be approved by Garrett.</p> <p>8. REPORTS</p> <p>8.1 The supplier of the castings shall furnish to Garrett Receiving Inspection with each shipment a report listing the results of the mechanical property tests for each part number/master heat/solution heat treat lot combination, the results of the chemical analysis from one casting per master heat representing the part number shipped, number of pieces per master heat/solution heat treat lot combination and statement that the castings conform to the requirements of this specification.</p> <p>8.1.1 This report shall include the purchase order number, master heat number and code symbol, if used, solution-heat-treat number, material specification number and its revision letter, part number, class and quantity from each heat.</p> <p>8.2 The supplier of finished or semifinished parts shall furnish with each shipment a report showing the purchase order number, materials specification number, contractor or other direct supplier of castings, part number, class and quantity.</p> <p>8.2.1 When castings for making finished or semifinished parts are produced or purchased by the parts supplier, the parts supplier shall inspect castings from each master heat or master heat lot represented and shall include in the report a statement that the castings conform, or shall include copies of laboratory reports showing the results of tests to determine conformance.</p>		



ORIGINAL PAGE 15  
OF POOR QUALITY

MATERIAL SPECIFICATION	CODE IDENT NO. 99193	SPECIFICATION NO. EMS52501	REV LTR NC
<p>9. QUALITY CONTROL</p> <p>9.1 Castings with indications of shrinkage in excess of Garrett Specification EMS52300 requirements shall be rejected.</p> <p>9.1.1 Castings with linear indications shall be rejected.</p> <p>9.2 Garrett shall accumulate production audit data for information only. Five blades per 5000 blades received shall be submitted to the Materials Laboratory on a CMR to study the effect of finishing on the cast blades. The blades shall be traceable by master heat number/solution heat treat lot combination.</p> <p>9.3 Parts and material not conforming to the requirements of this specification shall be rejected.</p>			

ORIGINAL PAGE 18  
OF POOR QUALITY

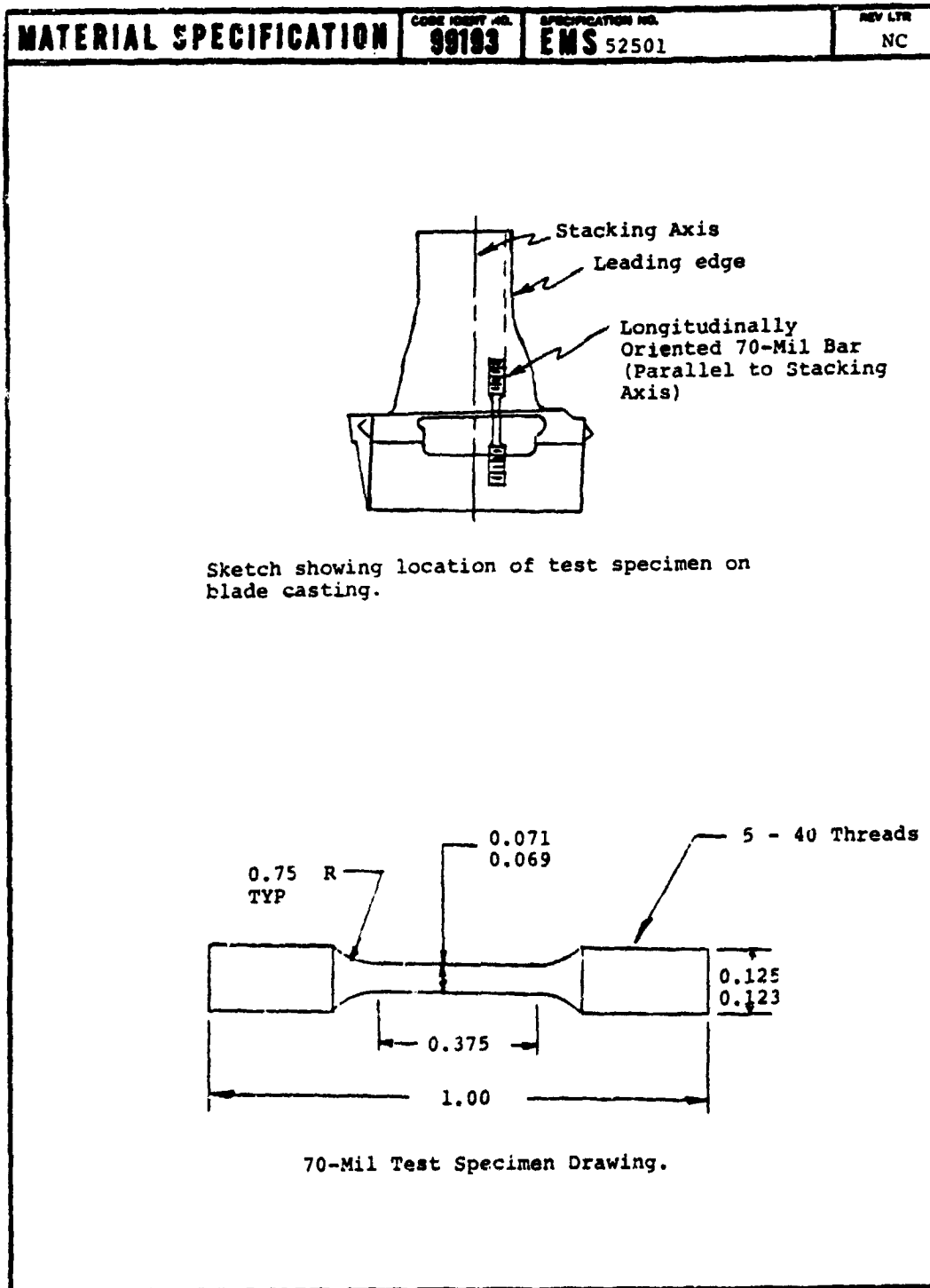
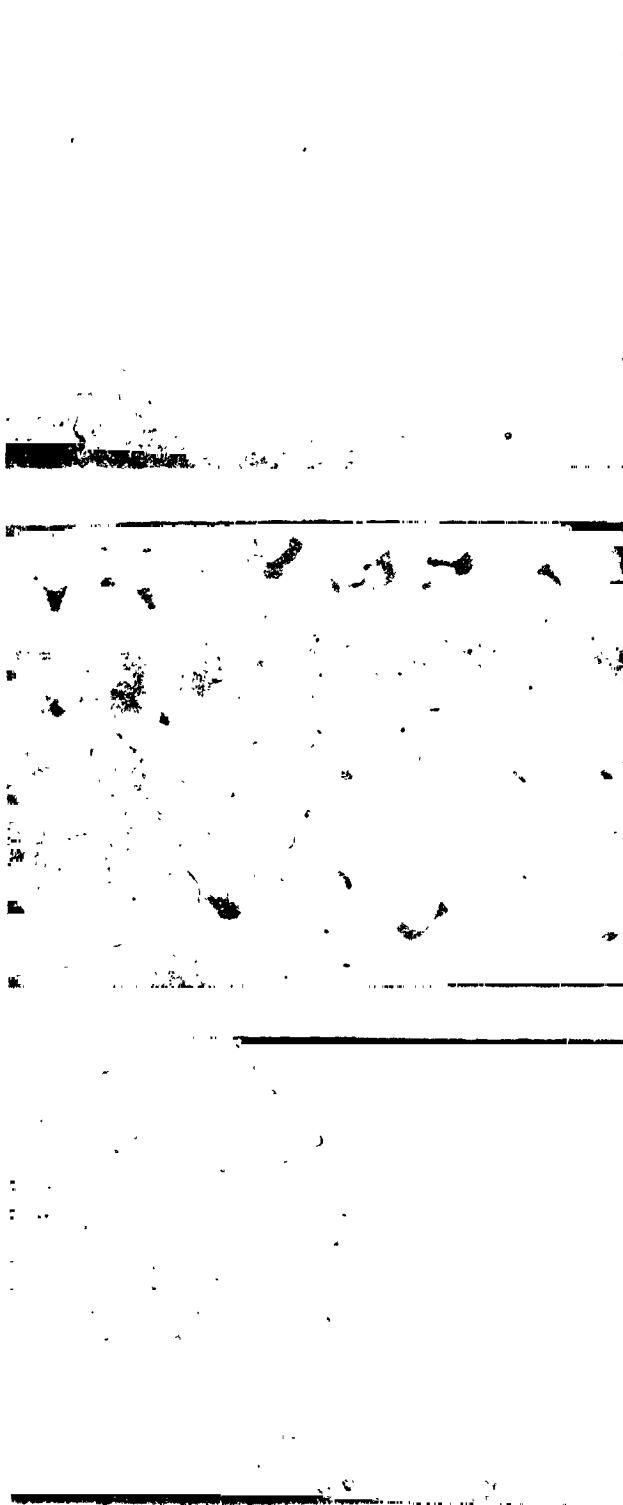


Figure 118. Location of Test Specimen and Test Specimen Drawing.

ORIGINAL PAGE 19  
OF POOR QUALITY

EMS52501  
Rev. NC

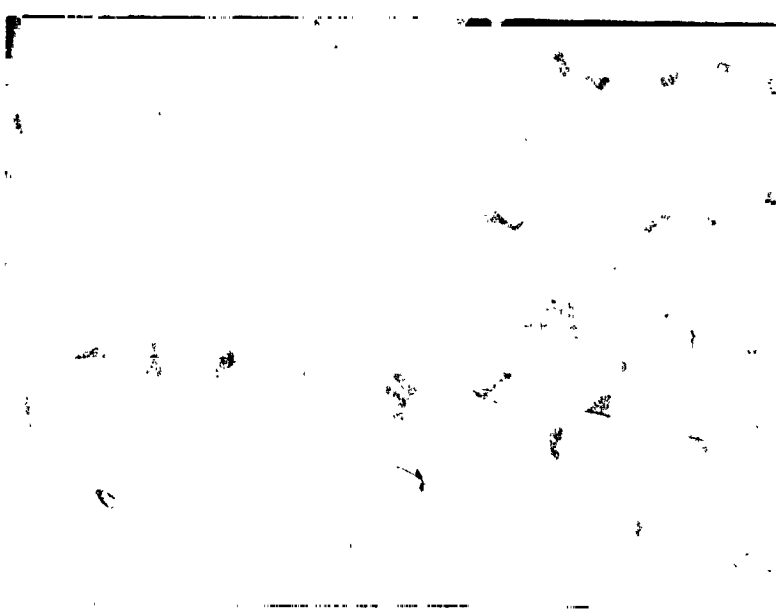
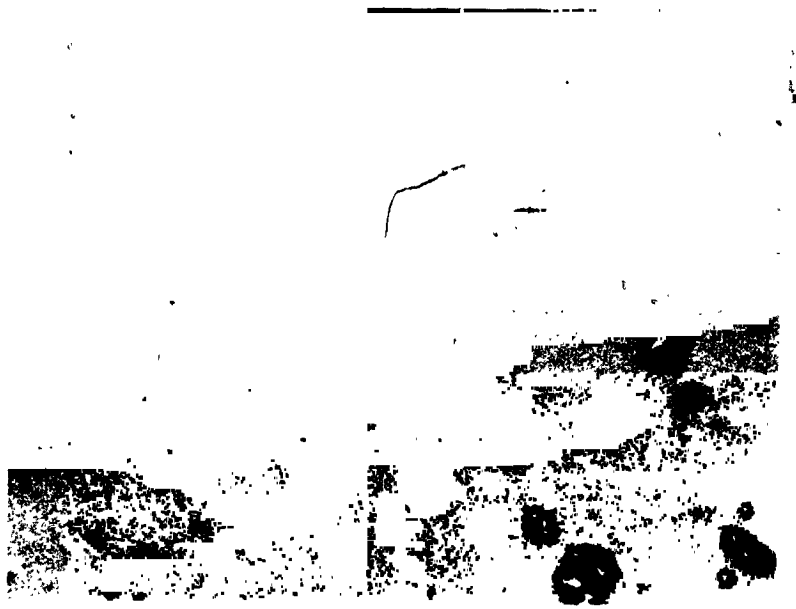


ACCEPTABLE			ACCEPTABLE			ACCEPTABLE		
o	Absence of coarse gamma-prime		o	Maximum 5 v/o coarse gamma-prime		o	Absence of coarse gamma-prime	
o	Absence of eutectic gamma-prime		o	Maximum 5 v/o eutectic gamma-prime		o	Absence of eutectic gamma-prime	
o	Absence of incipient melting		o	Absence of incipient melting		o	Maximum 1 v/o incipient melting	

Figure 119. Acceptable Solution-Heat-Treated Microstructures  
(80X Magnification).

ORIGINAL PAGE IS  
OF POOR QUALITY

EMS52501  
Rev. NC



REJECTABLE

- o >5 v/o coarse gamma-prime
- o >5 v/o eutectic gamma-prime
- o Absence of incipient melting

REJECTABLE

- o >1 v/o incipient melting

Figure 120. Rejectable Solution-Heat-Treated Microstructures  
(100X Magnification).

ORIGINAL PAGE IS  
OF POOR QUALITY

<b>MATERIAL SPECIFICATION</b>	CODE IDENT NO. <b>99193</b>	SPECIFICATION NO. EMS52501 (Appendix I)	REV LTR NC
-------------------------------	--------------------------------	--	---------------

**ACID ETCHING METHODS**

This appendix offers alternate methods for etching cast parts prior to inspection. These etching methods are utilized to accomplish two purposes, (1) to obtain an etch sufficient to expose grain boundaries or dendrites prior to macrograin inspection, and (2) to obtain a cleaning etch. When specified, the cleaning etch shall be used prior to fluorescent-penetrant inspection.

**CAUTION:** Mixing of solutions and etching of parts must be accomplished in an area with adequate exhaust ventilation, as toxic fumes are liberated from the etchants.

Method 1

**Etching Solution:**

	<u>100 gal</u>	<u>Approx 1 liter</u>
Muriatic Acid (20° Be)	80 gal	757 ml
Anhydrous Ferric Chloride, FeCl <sub>3</sub>	135 lbs	154 g
Nitric Acid (42° Be)	2 gal	19 ml
Water	11 gal	106 ml

- 1 Add ferric chloride to muriatic acid. Allow to dissolve.
- 2 Add nitric acid.
- 3 Add water.

- a) A new solution shall be prepared when a suitable etch is not obtained within 12 minutes.
- b) Do not replenish to maintain volume.

**Procedure:**

1. Load parts in etching basket, keeping level below basket rim.
2. Immerse parts basket in etching solution maintained at room temperature (75-100°F).
3. Check progress of etch after 6 minutes and every 2 minutes thereafter by removing one casting, rinsing, and visually inspecting progress of etch. Once the etch time required is established for that particular run of castings, the following loads can be run without checking. Typical etching time is 6-10 minutes.
- a) Immersion time for cleaning etch shall be 20-30 seconds.
4. Remove from etching solution and rinse in clean, cold water.
5. Immerse in alkaline cleaner solution for 3 minutes.
6. Remove from cleaner and rinse in clean, cold water.
7. Air-water nozzle scrub each individual casting clean.
8. Blow loaded basket free of excess water with air only.

Method 2

**Etching Solution:**

		<u>Approx 2 liters</u>
Muriatic acid (20° Be)	90% by vol	(1615 ml)
Glacial acetic acid	5% by vol.	(85 ml)
Nitric acid (42° Be)	5% by vol.	(85 ml)
Ferric chloride	to saturation	(12.5 lbs)

1. Add acetic acid to muriatic acid while cautiously agitating the mixture.
2. Gently heat the mixture and add sufficient ferric chloride to raise the boiling point to 150-160°F.
3. Cool saturated solution to <100°F, then cautiously add nitric acid while agitating the etchant. **CAUTION:** Never add nitric acid to the etchant when temperature is above 100°F.
- a) The etchant shall be discarded when the etching time requires more than two minutes to delineate the macrograin structure.

**Procedure:**

1. Load parts in suitable tray or basket so that airfoils do not come in contact with each other.

ORIGINAL PAGE IS  
OF POOR QUALITY

MATERIAL SPECIFICATION	CODE IDENT NO. 99193	SPECIFICATION NO. EMS52501	REV LTR NC				
<p>2. Immerse in acid etchant (150 <math>\pm</math>10°F) for a minimum length of time to bring macro-grain structure visible to unaided eye. Maximum exposure time in the etchant shall be limited to two minutes. The etchant or parts shall be agitated to aid in obtaining uniform etching and to minimize the exposure time.</p> <p>a) Immersion time for cleaning etch shall be 10-20 seconds.</p> <p>3. Rinse thoroughly in running tap water.</p> <p>4. Desmut by immersing in concentrated hydrogen peroxide (<math>H_2O_2</math>, 35 percent). Hand brush or air-water power flush surfaces of the etched parts to remove residual smut.</p> <p>5. Rinse in running tap water.</p> <p>6. Rinse in hot tap water and dry.</p> <p style="text-align: center;"><u>Method 3</u></p> <p><b>Etching Solution:</b></p> <table><tbody><tr><td>Muriatic acid (20° Be)</td><td>90% by vol.</td></tr><tr><td>Hydrogen Peroxide (30-35%)</td><td>10% by vol. (or sufficient quantity to obtain a satisfactory etch)</td></tr></tbody></table> <p>1. Add hydrogen peroxide to muriatic acid while cautiously agitating the mixture.</p> <p>a) Make up solution just prior to usage.</p> <p>b) Whenever possible, the etching solution container should be immersed in a tap water rinse tank for the purpose of dissipating the heat liberated during the etching process, so that an etching time cycle can be established.</p> <p>c) The etchant shall be discarded when the etching time requires more than five minutes to delineate the macrograin structure.</p> <p><b>Procedure:</b></p> <p>1. Load parts in suitable tray or basket so that airfoils do not come in contact with each other.</p> <p>2. Immerse in acid etchant maintained at room temperature (75-100°F) for a minimum length of time (5 min. max.) to bring macrograin structure visible to unaided eye when inspecting for grain size and casting irregularities.</p> <p>a) Immersion time for cleaning etch shall be 10-25 seconds.</p> <p>3. Rinse in running tap water. Hand brushing or air-water power flushing may be required if residual smut is not removed during the rinse cycle.</p> <p>4. Rinse in hot tap water and dry.</p>				Muriatic acid (20° Be)	90% by vol.	Hydrogen Peroxide (30-35%)	10% by vol. (or sufficient quantity to obtain a satisfactory etch)
Muriatic acid (20° Be)	90% by vol.						
Hydrogen Peroxide (30-35%)	10% by vol. (or sufficient quantity to obtain a satisfactory etch)						

## REFERENCES

1. Sink, L. W., G. S. Hoppin, III, M. Fujii: Low-Cost Directionally-Solidified Turbine Blades - Volume I, NASA CR-159464, January 1979.
2. Gell, M., D. N. Duhl, and A. F. Giamei: "The Development of Single Crystal Superalloy Turbine Blades," in Superalloys 1980 - Proceedings of the Fourth International Symposium on Superalloys, Champion, Pennsylvania, September 1980, pp. 205-214.
3. Barrett, C. A. and C. E. Lowell: "Resistance of NiCrAl Alloys to Cyclic Oxidation at 1100° and 1200°C," Oxidation of Metals, 11, 1977, pp. 199-223.
4. MacKay, R. A., R. L. Dreshfield, and R. D. Maier: "Anisotropy of Nickel-Base Superalloy Single Crystals," in Superalloys 1980 - Proceedings of the Fourth International Symposium on Superalloys, Champion, Pennsylvania, September 1980, pp. 385-394.
5. Kear, B. H. and B. J. Piarcey: "Tensile and Creep Properties of Single Crystals of the Nickel-Base Superalloy Mar-M 200," Trans. AIME, 239, 1967, pp. 1209-1215.
6. Leverant, G. R. and B. H. Kear: "The Mechanism of Creep in Gamma Prime Precipitation-Hardened Nickel-Base Alloys at Intermediate Temperatures," Metallurgical Transactions, 1, 1970, pp. 491-498.
7. Leverant, G. R., B. H. Kear, and J. M. Oblak: "Creep of Precipitation - Hardened Nickel-Base Alloy Single Crystals at High Temperatures," Metallurgical Transactions, 4, 1973, pp. 355-362.

8. Boone, D. H., D. N. Duhl, and G. W. Goward: "Nickel-Base Superalloy Resistant to Oxidation-Erosion," U.S. Patent 3,754,902, August 28, 1973.
9. Duhl, D. N. and X. Nguyen-Dinh: "Evaluation of Single-Crystal Superalloy," presented at AIME Annual Meeting, Las Vegas, February 24-28, 1980.
10. Ver Snyder, F. L. and M. Gell: "New Direction in Alloy Design for Gas Turbines," Fundamental Aspects of Structural Alloy Design, Eds. R. I. Jaffee and B. A. Wilcox, Plenum Publishing Corp., 1977, pp. 209-227.
11. Gell, M., D. N. Duhl, and A. F. Giamei: "The Development of Single Crystal Superalloy Turbine Blades," in Superalloys 1980 - Proceedings of the Fourth International Symposium on Superalloys, September 1980, Champion, Pennsylvania, pp. 205-214.
12. Jackson, J. J., M. J. Donachie, R. J. Henricks, and M. Gell: "The Effects of Volume Percent of Fine Y' on Creep in DS Mar-M 200 + Hf," Metallurgical Transactions A, 8A, 1977, pp. 1615-1620.
13. Strangman, T. E., G. S. Hoppin III, C. M. Phipps, K. Harris, and R. E. Schwer: "Development of Exothermically Cast Single-Crystal Mar-M 247 and Derivative Alloys," in Superalloys 1980 - Proceedings of the Fourth International Symposium on Superalloys, Champion, Pennsylvania, September 1980, pp. 215-224.
14. Strangman, T. E. and D. H. Boone: "Composition and Processing Considerations for the Mechanical Behavior of Coating-Superalloy Systems," in Proceedings of the Fourth Conference on Gas Turbine Materials in a Marine Environment, Annapolis, Maryland, June 1979, pp. 655-678.



15. Gell, M. and G. R. Leverant: "The Fatigue of the Nickel-Base Superalloy, Mar-M 200, in Single-Crystal and Columnar-Grained Forms at Room Temperature," Trans. AIME, 242, 1968, pp. 1869-1879.
16. Gell, M. and G. R. Leverant: "The Characteristics of Stage Fatigue Fracture in a High-Strength Nickel Alloy," ACTA MET., 16, 1968, pp. 553-561.
17. Leverant, G. R. and M. Gell: "The Influence of Temperature and Cyclic Frequency on the Fatigue of Cube Oriented Nickel-Base Superalloy Single Crystals," Metallurgical Transactions, A, 6A, 1975, pp. 367-371.
18. Puroshothaman, S. and J. K. Tien: "Slow Crystallographic Fatigue Crack Growth in a Nickel-Base Alloy," Metallurgical Transactions, 9A, 1978, pp. 351-355.
19. Sadananda, K. and P. Shahinian: "Analysis of Crystallographic High Temperature Fatigue Crack Growth in a Nickel Base Alloy," Metallurgical Transactions, 12A, 1981, pp. 343-351.
20. Strangman, T. E., E. J. Felten, and R. S. Benden: "Refinement of Promising Coating Compositions for Directionally Cast Eutectics," NASA CR-135103, October 1976.